

Studies on the Absorption of *Schisandra chinensis* and Its Pharmacological Effects on Gut Motility and Visceral Sensation

YANG, Jiaming

A Thesis Submitted in Partial Fulfilment
of the Requirements for the Degree of
Doctor of Philosophy
in
Chinese Medicine

The Chinese University of Hong Kong

September 2009

UMI Number: 3488979

All rights reserved

INFORMATION TO ALL USERS

The quality of this reproduction is dependent on the quality of the copy submitted.

In the unlikely event that the author did not send a complete manuscript and there are missing pages, these will be noted. Also, if material had to be removed, a note will indicate the deletion.



UMI 3488979

Copyright 2011 by ProQuest LLC.

All rights reserved. This edition of the work is protected against unauthorized copying under Title 17, United States Code.



ProQuest LLC.
789 East Eisenhower Parkway
P.O. Box 1346
Ann Arbor, MI 48106 - 1346

Abstract of thesis entitled:

Studies on the Absorption of *Schisandra chinensis* and Its Pharmacological Effects on Gut Motility and Visceral Sensation

Submitted by Yang Jiaming

for the Degree of Doctor of Philosophy

at The Chinese University of Hong Kong, September 2009

Abstract

Schisandra chinensis, which is named “Wu-Wei-Zi” in Chinese Pin Yin, is widely used in Chinese medicine as an astringent, tonic and sedative agent. Dibenzo[a,c]-cyclooctadiene lignans are the major components of this herb. In the present study, the chemical constituents of *S. chinensis* were first characterized. A HPLC-DAD method was developed and validated for quantitative analysis of four major Schisandra lignans, namely, schisandrin (SCH-1), gomisin A (SCH-2), deoxyschisandrin (SCH-3) and γ -schisandrin (SCH-4), in the aqueous and ethanolic extracts of *S. chinensis*. The ethanolic extract contains higher amount of lignan components than aqueous extract. The HPLC method has also been employed to obtain chromatographic fingerprintings to distinguish *S. chinensis* from a related species, *S. sphenanthera*.

With the aid of HPLC-DAD-MS for qualitative and quantitative analyses, the absorption of *S. chinensis* in the rat everted gut sac and human Caco-2 monolayer *in vitro* models have been profiled. Fifteen Schisandra lignans were identified as the major absorbable

components of *S. chinensis* in these models. Transport study on SCH-1 has shown a passive diffusion pathway with high permeability. In an *in vivo* study, metabolites of Schisandra lignans could be found in rat plasma after a single oral administration of *S. chinensis* extract. The plasma pharmacokinetics of *S. chinensis* in rats was further evaluated using simultaneous quantification of four representative Schisandra lignans (SCH-1, SCH-2, SCH-3 and SCH-4).

The modulatory effects of both *S. chinensis* extracts and four major lignans on intestinal motility were evaluated using *in vitro* intestinal motility assays. The tested compounds induced relaxation on guinea pig ileum contracted by acetylcholine, serotonin and electrical field stimulation, as well as on rat colon with spontaneous contractility. While SCH-3 was most potent in inhibiting sensorimotor response in guinea pig ileum, SCH-1 displayed the highest potency of inhibition on spontaneous contraction of rat colon.

The relaxant effect on rat colon induced by SCH-1 has been demonstrated to involve two or more non-adrenergic non-cholinergic mediators. Nitric oxide was likely to be one of the inhibitory transmitters that involved cGMP-dependent pathways, whereas the non-nitroergic component was apamin-sensitive, but probably excluded vasoactive intestinal peptide (VIP) and adenosine.

In an irritable bowel syndrome (IBS) rat model, *S. chinensis* reversed the exaggerated visceral nociceptive responses (judged by abdominal withdrawal reflex and electromyographic measurement) to colorectal distension induced by neonatal maternal

separation. Relief of visceral hypersensitivity by *S. chinensis* could be related to the decrease of elevated 5-HT level and the reduction in 5-HT₃ receptor expression in colon.

In summary, given the modulatory effects on intestinal motility and visceral sensation, *Schisandra chinensis* would be potentially useful for the treatment of relieving diarrhea and visceral pain symptoms in IBS patients. Schisandra lignans, the major absorbable components, can be regarded as the active ingredients in *S. chinensis* for the potential treatment of IBS.

論文摘要

五味子作為收斂，補益和鎮靜藥廣泛用於中醫中藥。雙苯環辛二烯類木質素是其中的主要成分。本論文先對其化學組分進行了表徵。首先建立了高效液相色譜二極體陣列檢測法定量測定五味子水提物和醇提物中的四個主要木質素的含量，包括五味子醇甲(SCH-1)，五味子醇乙(SCH-2)，五味子甲素(SCH-3)和五味子乙素(SCH-4)。結果表明醇提物中的五味子木質素含量高於水提物。此 HPLC 方法且用作指紋圖譜以區分北五味子和南五味子。

其次，以高效液相色譜質譜聯用的定性和定量分析方法，對五味子的體外和體內藥物吸收進行了研究。在大鼠外翻小腸和人 Caco-2 細胞單層體外模型中，一共鑒定了十五個五味子木質素為可吸收成分。Caco-2 細胞單層的轉運實驗表明，SCH-1 跨膜通透性良好，為被動擴散轉運途徑。與體外吸收相比，大鼠血漿的吸收譜中除了有已鑒定的可吸收木質素外，還發現了其中一些木質素的代謝產物。此外，以四個主要木質素成分 (SCH-1, SCH-2, SCH-3 和 SCH-4) 為代表進一步研究了五味子在大鼠體

內的血漿藥物動力學。

在對五味子化學成分和可吸收成分的研究基礎之上，使用體外腸肌動實驗對五味子提取物和四個主要木質素成分的腸活力調節作用進行了評價。結果表明，所用提取物和木質素成分均對由乙酰膽鹼，5-羥色氨和電場誘導的豚鼠回腸收縮具有鬆弛作用。SCH-3 對豚鼠回腸刺激誘導運動的抑制作用最好，而 SCH-1 在抑制大鼠結腸自發性收縮中效價最高。

進一步的機制研究表明，SCH-1 誘導的大鼠結腸鬆弛作用涉及了兩個或兩個以上的非腎上腺素能非膽鹼能介質。一氧化氮為其中一個主要的抑制性遞質，並通過環一磷酸鳥苷依賴性路徑發揮作用。而另外的非一氧化氮型介質部分為蜜毒明肽敏感型，但很可能不包括血管活性腸肽和腺苷。

在大腸易激症的大鼠模型中，母嬰分離作為早期應激加劇了動物對結腸直腸膨脹刺激的內臟傷害性感受反應（由腹部收縮性發射和肌電圖響應判斷），而五味子則能夠

逆轉此加劇反應。五味子這一解除內臟過敏反應作用可能與其能降低結腸 5-羥色氨水平以及減少 5-羥色氨受體 3 型表達有關。

綜上所述，基於對腸活力和內臟感覺的調節作用，五味子對解除大腸易激症病人腹瀉和內臟疼痛症狀有潛在效用。五味子木質素作為主要可吸收成分可以當作五味子用於治療大腸易激症的活性成分。

Acknowledgement

I would like to express my sincere gratitude first and foremost to Professor Chun-Tao Che, for his constant guidance and encouragement, in particular, for the generous understanding and support in the initial stage when I changed my research topic. My heartfelt gratitude

also goes to Professor John Hok Keung Yeung, who leads me to the world of pharmacology and pharmacokinetics. His scientific training is of great value for my research career. I would also like to express sincere gratitude to Professor Paul Siu Po Ip for his constant support in this project and helpful instruction.

I am also sincerely grateful to Mr. Kam Ming Chan for his expertise in isolated tissue experiments and the generous assistance, guidance and encouragement in my three-year study. The helpful assistance in Caco-2 cells and pharmacokinetic technique offered by Ms. Penelope Mei Yu Or are also deeply appreciated. Special gratitude must go to Dr. Yan Wang, who has helped me a lot during my difficult time in the study. I would also like to thank Dr. Sam Hip Tsai for his extremely helpful expertise in chemical analysis, and Ms. Yan Fang Xian for her assistance in animal experiments. Thanks also go to Professor Jiangang Shen, Dr. Ming Zhao, Dr. Yan Zhou, Ms. Yuying Zong, Mr. Yuk Wai Lee, Ms. Chartia Cheung, Mr. Yi He and all my friends who have helped me a lot.

I owe my last and deepest gratitude to my beloved mother and father for their selfless loving, constant support and encouragement. I am also greatly indebted to Ms. Yanling Zhou for her endurance and confidence on me in the past three years.

Table of Contents

	Page
Abstract (English)	i
Abstract (Chinese)	iv
Acknowledgement	vi

Table of Content	vii	
List of Figures	xiv	
List of Tables	xix	
List of Abbreviations	xxi	
Chapter 1	General Introduction	1
1.1	Chemical constituents of <i>Schisandra chinensis</i>	1
1.1.1	Introduction	1
1.1.2	Chemical constituents	3
1.1.2.1	Schisandra lignans	3
1.2	Pharmacological activities of <i>Schisandra chinensis</i> and Schisandra lignans	7
1.2.1	Antioxidant activities	7
1.2.2	Hepatoprotective effects	9
1.2.3	Effects on central nervous system	10
1.2.4	Anti-cancer effects	11
1.2.5	Effects on cardiovascular system	12
1.2.6	Other pharmacological effects	13
1.3	Pathogenesis and pathophysiology of irritable bowel syndrome	13
1.3.1	Genetic factors	14
1.3.2	Psychological factors	15
1.3.3	Gastrointestinal motility alteration	16
1.3.4	Visceral hypersensitivity	18
1.3.5	Serotonin involvement	20
1.3.5.1	Classification of serotonin receptors	21
1.3.5.2	Serotonin and gastrointestinal (GI) motility	24
1.3.5.3	Serotonin and visceral sensation	25

1.3.6	Inflammatory changes and neuro-immune interactions	27
1.3.7	Animal models for IBS	28
1.4	Therapeutic approaches for irritable bowel syndrome	31
1.4.1	Pharmacologic therapy	31
1.4.1.1	5-HT-based approaches	32
1.4.1.2	Targeting opioid receptors	33
1.4.1.3	Tachykinin antagonist	33
1.4.1.4	Other pharmacological approaches	34
1.4.2	Chinese medicine approaches	34
1.5	Objective of this study	38
Chapter 2	Analysis of Lignans in <i>Schisandra chinensis</i> by High Performance Liquid Chromatography with Photodiode Array Detection	40
2.1	Introduction	40
2.2	Materials and methods	42
2.2.1	Chemical and materials	42
2.2.2	Instrumentation	44
2.2.3	Preparation of standard solutions	44
2.2.4	Preparation of samples	44
2.2.5	HPLC-MS conditions	45
2.2.6	Method validation	46
2.2.6.1	Linearity and sensitivity	46
2.2.6.2	Accuracy and precision	46
2.2.6.3	Stability of samples	47
2.2.6.4	Recovery	47
2.3	Results	48
2.3.1	Chromatographic conditions and HPLC-MS identity conformation	48

2.3.2	Linearity, limits of detection and quantification	55
2.3.3	Reproducibility and sample stability	56
2.3.4	Recoveries of Schisandra lignans	59
2.3.5	Analysis of Schisandra extracts using the validated method	60
2.3.6	Analysis of different batches of Fructus Schisandrae	62
2.4	Discussion	64
Chapter 3	Absorption of <i>Schisandra chinensis</i> in Rat Everted Gut Sac and Human Caco-2 Cell Monolayer Model <i>In Vitro</i> and Pharmacokinetics in Rats	66
3.1	Introduction	66
3.2	Materials and methods	72
3.2.1	Materials, chemicals and reagents	72
3.2.2	Animals	73
3.2.3	Instrumentation	74
3.2.4	Preparation of Schisandra extract solutions	74
3.2.5	Preparation of standard solutions	75
3.2.6	Experimental protocols of <i>in vitro</i> absorption	75
3.2.6.1	Rat everted gut sac	75
3.2.6.2	Human Caco-2 cell monolayer model	78
3.2.7	Pharmacokinetic studies in the rat	80
3.2.8	High performance liquid chromatography and mass spectrometry (HPLC-MS)	80
3.2.8.1	Analysis of absorption profile	80
3.2.8.2	Quantification of schisandrin	81
3.2.8.3	Quantification of Schisandra lignans in rat plasma	82
3.2.8.3.1	Sample processing	82
3.2.8.3.2	HPLC-MS conditions	82

3.2.8.3.3	Method validation	83
3.2.8.3.3.1	Linearity, precision and accuracy	83
3.2.8.3.3.2	Stability	84
3.2.8.3.3.3	Recovery	84
3.2.8.3.3.4	Pharmacokinetic data analysis	84
3.3	Results	85
3.3.1	Absorption of Schisandra aqueous extract <i>in vitro</i>	85
3.3.1.1	Absorption profile of Schisandra extract in rat everted gut sac	85
3.3.1.2	Absorption profile of Schisandra extract in Caco-2 cell monolayer model	88
3.3.1.3	HPLC-DAD-APCI-MS analysis	90
3.3.1.3.1	Analysis of reference compounds of lignans	90
3.3.1.3.2	Bioanalytical method validation	108
3.3.1.3.3	Identification of absorbable components of <i>Schisandra chinensis in vitro</i>	108
3.3.1.4	Permeability of schisandrin monomer in Caco-2 cell monolayer model	126
3.3.2	Absorption of <i>Schisandra chinensis</i> in the rat	128
3.3.2.1	Absorption profile of <i>Schisandra chinensis</i> in rat plasma	128
3.3.2.2	Identification of metabolites	134
3.3.3	Pharmacokinetics of Schisandra lignans in the rat	142
3.3.3.1	Validation for simultaneous determination of Schisandra lignans in rat plasma	142
3.3.3.2	Pharmacokinetics of four Schisandra lignans in rats	149
3.4	Discussion	152
Chapter 4	Evaluation of Relaxant Effects of <i>Schisandra chinensis</i> on Intestinal Contractility <i>In Vitro</i>	162

4.1	Introduction	162
4.2	Materials and methods	164
4.2.1	Materials, chemicals and reagents	164
4.2.2	Animals	164
4.2.3	Experimental protocols of intestinal contractility <i>in vitro</i>	165
4.2.3.1	Acetylcholine (ACh) or serotonin (5-HT) induced contraction in isolated guinea pig ileums	165
4.2.3.2	Electrical field stimulated (EFS) contraction in isolated guinea pig ileum	166
4.2.3.3	Spontaneous contraction in isolated rat colon	166
4.2.4	Measurement of receptor binding of Schisandra lignans	167
4.2.5	Data analysis	167
4.3	Results	168
4.3.1	Anti cholinergic effects of <i>Schisandra chinensis</i>	168
4.3.1.1	Inhibition on acetylcholine (ACh) induced contraction in guinea pig ileum	168
4.3.1.2	Binding of Schisandra lignans to cholinergic muscarinic (M3) receptor	172
4.3.2	Inhibition on serotonin (5-HT) induced contraction in guinea pig ileum	175
4.3.3	Inhibition on electrical field stimulated (EFS) contraction in guinea pig ileum	179
4.3.4	Inhibition on spontaneous contraction in rat colon	183
4.4	Discussion	186
Chapter 5	Mechanisms of the Inhibitory Effect of Schisandrin (SCH-1) on Spontaneous Contraction of Isolated Rat Colon	190
5.1	Introduction	190

5.2	Materials and methods	192
5.2.1	Chemicals and reagents	192
5.2.2	Animals	193
5.2.3	Isolation of colon preparations	193
5.2.4	Experimental protocols	194
5.2.4.1	Measurement of contractile activity	194
5.2.4.2	Effects of blockers/inhibitors on responses to inhibitory agonists	194
5.2.4.3	Data analysis	195
5.2.5	Measurement of nitric oxide (NO) production	195
5.2.6	Measurement of cGMP production	196
5.2.7	Statistical analysis	196
5.3	Results	197
5.3.1	Effects of SCH-1 on spontaneous contraction	197
5.3.2	Evidence that SCH-1 activated non-adrenergic non-cholinergic (NANC) enteric nerves	199
5.3.3	Involvement of nitric oxide synthesis	204
5.3.4	Effect of cyclic guanosine monophosphate (cGMP)	208
5.3.5	Effects of other non-adrenergic, non-cholinergic (NANC) mediators	211
5.4	Discussion	215
Chapter 6	<i>Schisandra chinensis</i> Reverses Visceral Hypersensitivity in Neonatal Maternal Separated Rats	224
6.1	Introduction	224
6.2	Methods	226
6.2.1	Animals	226
6.2.2	Drug preparation and treatment	227
6.2.3	Behavioral testing	228
6.2.3.1	Abdominal withdrawal reflex (AWR)	228

6.2.3.2	Electromyography (EMG)	230
6.2.4	Tissue harvesting	232
6.2.5	Measurement of 5-HT content	232
6.2.6	Measurement of mRNA encoding 5-HT receptors, 5-HT transporter, and opioid receptors	233
6.2.7	Data analysis	233
6.3	Results	234
6.3.1	Effects on pain responses to colorectal distension	234
6.3.1.1	Body weight	234
6.3.1.2	Abdominal withdrawal reflex (AWR)	236
6.3.1.3	Electromyography (EMG)	239
6.3.2	5-HT content in distal colon	241
6.3.3	mRNA expression of 5-HT receptors and 5-HT transporter in distal colon	243
6.3.4	mRNA expression of opioid receptors in distal colon	246
6.4	Discussion	249
Chapter 7	General Discussion	256
References		261

List of Figures

Fig. 1-1 (a)	Original plant of <i>Schisandra chinensis</i> (Turcz.) Baill.	2
Fig. 1-1 (a)	Dried fruits of <i>S. chinensis</i> (Fructus Schisandrae)	2
Fig. 1-2	Chemical structure of schisandrin	6
Fig. 2-1	Chemical structures of the four Schisandra lignans analyzed in this	43

	study	
Fig. 2-2	Representative HPLC-DAD chromatogram of a four-lignan standard mixture	49
Fig. 2-3	Representative HPLC-DAD chromatograms of extracts of <i>S. chinensis</i> fruits	50
Fig. 2-4	Representative HPLC-MS base peak chromatogram of a four-lignan standard mixture	52
Fig. 2-5	Representative MS spectra of four lignans	53
Fig. 2-6	HPLC-DAD fingerprinting of different batches of Fructus Schisandrae	63
Fig. 3-1	Rat everted gut sac system	77
Fig. 3-2	Transwell system of Caco-2 cell monolayer model	79
Fig. 3-3	Representative HPLC-MS basic peak chromatograms of serosal fluid in rat everted gut sac	86
Fig. 3-4	Chemical structures of fifteen Schisandra lignans identified <i>in vitro</i>	87
Fig. 3-5	Representative HPLC-MS basic peak chromatograms of basolateral solution in Caco-2 monolayer model	89
Fig. 3-6	Representative HPLC-DAD-MS chromatograms of a seven-lignan standard mixture	91
Fig. 3-7	UV spectra of seven reference lignan compounds	92
Fig. 3-8	MS ⁿ spectra of schisandrin	94
Fig. 3-9	Proposed fragmentation pathway of schisandrin	95
Fig. 3-10	MS ⁿ spectra of gomisin A	97
Fig. 3-11	MS ⁿ spectra of schisantherin A	99
Fig. 3-12	MS ⁿ spectra of gomisin D	101
Fig. 3-13	MS ⁿ spectra of angeloylgomisin F	103
Fig. 3-14	MS ⁿ spectra of gomisin G	105

Fig. 3-15	MS ⁿ spectra of deoxyschisandrin	107
Fig. 3-16	MS ⁿ spectra of compound 4	114
Fig. 3-17	MS ⁿ spectra of compound 5	115
Fig. 3-18	MS ⁿ spectra of compound 6	117
Fig. 3-19	MS ⁿ spectra of compound 7	118
Fig. 3-20	MS ⁿ spectra of compound 11	120
Fig. 3-21	MS ⁿ spectra of compound 12	121
Fig. 3-22	MS ⁿ spectra of compound 8	123
Fig. 3-23	MS ⁿ spectra of compound 14	125
Fig. 3-24	Apparent permeability coefficient of schisandrin in bidirectional transport across Caco-2 cell monolayers	127
Fig. 3-25	Representative HPLC-MS extracted ion chromatograms in rat plasma after administration with aqueous extract of <i>S. chinensis</i>	129
Fig. 3-26	Representative HPLC-MS basic peak chromatograms in rat plasma after administration with 70% ethanol extract of <i>S. chinensis</i>	132
Fig. 3-27	MS ⁿ spectra of M1	135
Fig. 3-28	MS ⁿ spectra of M2	137
Fig. 3-29	MS ⁿ spectra of M3	139
Fig. 3-30	MS ⁿ spectra of M4	141
Fig. 3-31	Mass spectra of SCH-1, -2, -3 and -4, and internal standard bicyclol	143
Fig. 3-32	Selected ion monitoring mass chromatograms of SCH-1, -2, -3 and -4, and bicyclol in rat plasma	144
Fig 3-33	Plasma concentration-time curves of the four lignans	150
Fig. 4-1(a)	Effects of Schisandra extracts on ACh-induced contraction in isolated guinea-pig ileum	170
Fig. 4-1(b)	Effects of Schisandra lignans on ACh-induced contraction in isolated guinea-pig ileum	170

Fig. 4-2	Effects of atropine on ACh-induced contraction in guinea-pig ileum	171
Fig. 4-3	Concentration response of fluorescence ratio in M3 CHO-K1 DA cells to carbachol	173
Fig. 4-4	Dose-dependent inhibition of atropine on fluorescent response stimulated by carbachol in M3 CHO-K1 DA cells	173
Fig. 4-5	Effects of atropine and three Schisandra lignans on fluorescent response stimulated by carbachol in M3 CHO-K1 DA cells	174
Fig. 4-6(a)	Effects of Schisandra extracts on 5-HT-induced contraction in isolated guinea-pig ileum	176
Fig. 4-6(b)	Effects of Schisandra lignans on 5-HT-induced contraction in isolated guinea-pig ileum	176
Fig. 4-7	Effects of tropisetron on 5-HT-induced contraction in isolated guinea-pig ileum	178
Fig. 4-8(a)	Effects of Schisandra lignans on EFS-induced contraction in isolated guinea-pig ileum	180
Fig. 4-8(b)	Effects of morphine on EFS-induced contraction in isolated guinea-pig ileum	180
Fig. 4-9	Effects of naloxone on the inhibitory responses of morphine and Schisandra lignans on EFS-induced contraction in isolated guinea-pig ileum	182
Fig. 4-10(a)	Inhibitory effects of Schisandra extracts on spontaneous contraction in isolated rat colon	184
Fig. 4-10(b)	Inhibitory effects of Schisandra lignans on spontaneous contraction in isolated rat colon	184
Fig. 5-1	Effects of SCH-1 on spontaneous contraction in isolated rat colon	198
Fig. 5-2	Effects of TTX, propranolol and atropine on the inhibitory responses of SCH-1 in isolated rat colon	200

Fig. 5-3	Representative experimental records of spontaneous contraction in rat colon	201
Fig. 5-4(a)	Effects of TTX on the inhibitory responses of SCH-1 and SCH-4 in isolated rat colon	203
Fig. 5-4(b)	Effects of TTX on the inhibitory responses of Schisandra extracts in isolated rat colon	203
Fig. 5-5	Effects of L-NAME on the inhibitory responses of SCH-1	205
Fig. 5-6	Effects of SCH-1 on the NO production in isolated rat colon	206
Fig. 5-7	Effects of Ro1138452 on the inhibitory responses of SCH-1 and cicaprost	207
Fig. 5-8	Effects of ODQ on the inhibitory responses of SCH-1	209
Fig. 5-9	Effects of SCH-1 on the cGMP production in isolated rat colon	210
Fig. 5-10	Effects of apamin on the inhibitory responses of SCH-1 and SNP	212
Fig. 5-11(a)	Effects of DPCPX on the inhibitory responses of adenosine in isolated proximal rat colon	213
Fig. 5-11(b)	Effects of DPCPX on the inhibitory responses of SCH-1 in isolated distal rat colon	213
Fig. 5-12	Effects of α -chymotrypsin on the inhibitory responses of SCH-1 in isolated rat colon	214
Fig. 5-13	Proposed mechanisms of SCH-1-mediated inhibition on spontaneous contraction of isolated rat colon	222
Fig. 6-1	Scores of AWR response to graded intensity of CRD	229
Fig. 6-2	Surgery for the measurement of EMG	231
Fig. 6-3	Body weight changes in rats during treatment	235
Fig. 6-4	Pain threshold responses to the graded intensity of CRD in normal rats, NMS control rats and rats treated with <i>S. chinensis</i>	237
Fig. 6-5	AWR responses to the graded intensity of CRD in normal rats, NMS	238

	control rats and rats treated with <i>S. chinensis</i>	
Fig. 6-6	EMG responses to the graded intensity of CRD in normal rats, NMS control rats and rats treated with <i>S. chinensis</i>	240
Fig. 6-7	5-HT content in distal colon of normal rats, NMS control rats and rats treated with <i>S. chinensis</i>	242
Fig. 6-8(a)	Amount of mRNA encoding 5-HT _{3A} subunit of 5-HT ₃ receptor in distal colon of normal rats, NMS control rats and rats treated with <i>S. chinensis</i>	244
Fig. 6-8(b)	Amount of mRNA encoding 5-HT _{3B} subunit of 5-HT ₃ receptor in distal colon of normal rats, NMS control rats and rats treated with <i>S. chinensis</i>	244
Fig. 6-9(a)	Amount of mRNA encoding 5-HT ₄ receptor in distal colon of normal rats, NMS control rats and rats treated with <i>S. chinensis</i>	245
Fig. 6-9(b)	Amount of mRNA encoding 5-HT transporter in distal colon of normal rats, NMS control rats and rats treated with <i>S. chinensis</i>	245
Fig. 6-10(a)	Amount of mRNA encoding κ -opioid receptor in distal colon of normal rats, NMS control rats and rats treated with <i>S. chinensis</i>	247
Fig. 6-10(b)	Amount of mRNA encoding μ -opioid receptor in distal colon of normal rats, NMS control rats and rats treated with <i>S. chinensis</i>	247
Fig. 6-11	Amount of mRNA encoding δ -opioid receptor in distal colon of normal rats, NMS control rats and rats treated with <i>S. chinensis</i>	248

List of Tables

Table 1-1	Lignans isolated from <i>Schisandra chinensis</i> (Turc.) Baill.	4
Table 1-2	Classification of 5-HT receptors	23

Table 1-3	Category, manipulation, characterization and application of IBS animal models	29
Table 1-4	Composition of the 20-herb Chinese formula	37
Table 2-1	Retention time (t_R), UV λ_{max} and MS data of four major Schisandra lignans analyzed by HPLC-MS	54
Table 2-2	Calibration curves for the four analyzed lignans	55
Table 2-3	Accuracy and precision of the method for analysis of four Schisandra lignans	57
Table 2-4	Precision of the method for analysis of four Schisandra lignans in 70% ethanol extract of <i>S. chinensis</i> fruits	58
Table 2-5	Stability of four Schisandra lignans in 70% ethanol extract of <i>S. chinensis</i> fruits	58
Table 2-6	Recovery of four Schisandra lignans in 70% ethanol extract of <i>S. chinensis</i> fruits	59
Table 2-7	Amounts of four lignans in water extract and ethanol extracts (70% and 95%) of <i>S. chinensis</i> fruits	61
Table 3-1	Retention times of characterized peaks by EIC in HPLC-MS analysis	109
Table 3-2	LC-MS ⁿ characterization of fifteen absorbable compounds identified in rat everted gut sac and Caco-2 monolayer model	110
Table 3-3	Absorbable compounds of <i>S. chinensis</i> characterized in rat everted gut sac, Caco-2 monolayer model <i>in vitro</i> , and in rat plasma	133
Table 3-4	Calibration curves, limits of detection and quantification for the four analyzed lignans	146
Table 3-5	Accuracy and precision of the method for analysis of four Schisandra lignans in rat plasma	147
Table 3-6	Recoveries of four Schisandra lignans in rat plasma samples	148
Table 3-7	Pharmacokinetic parameters of the four Schisandra lignans in rats	151

	after single oral administration of Schisandra extract	
Table 4-1	EC ₂₀ (EC ₅₀) and E _{max} of inhibitory effects of Schisandra lignans on intestinal contractility <i>in vitro</i>	185
Table 6-1	Manipulation and drug administration of the four animal groups	227
Table 6-2	Mean AUC (area under curve) of AWR and EMG responses to graded intensity of CRD in normal, NMS control and NMS treated rats	241

List of Symbols and Abbreviations

Symbols

α	Alpha
β	Beta

δ	Delta
μ	Mu/Micro
κ	Kappa
γ	Gamma

Abbreviations

5-HT	5-Hydroxytryptamine
ACh	Acetylcholine
APCI	Atmospheric pressure chemical ionization
AUC	Area under concentration-time curve
AWR	Abdominal withdrawal reflex
BPC	Base peak chromatogram
CL	Total clearance
C_{\max}	Maximum concentration
CMC-Na	Sodium carboxymethylcellulose
CRD	Colorectal distension
CNS	Central nervous system
DMSO	Dimethyl sulfoxide
DPCPX	8-Cyclopentyl-1, 3-dipropylxanthine
EC ₅₀	Half maximal effective concentration
EFS	Electrical field stimulation
E_{\max}	Maximal effect
EMG	Electromyography
sGC	Soluble guanylyl cyclase

GI	Gastrointestine
cGMP	Cyclic guanosine monophosphate
h	Hour
HPLC-DAD-MS	High-performance liquid chromatography-diode array detector-mass spectrometry
IBS	Irritable bowel syndrome
I.S.	Internal standard
L	Liter
L-NAME	<i>N</i> _ω -nitro-L-arginine methyl ester
LOD	The limit of detection
LOQ	The limit of quantification
NANC	Non-adrenergic non-cholinergic
nm	Nanometer
NMS	Neonatal maternal separation
nNOS	Neuronal nitric oxide synthase
NO	Nitric oxide
min	Minute
<i>m/z</i>	Mass-to-charge ratio
ODQ	1 <i>H</i> -[1,2,4] oxadiazolo[4,3- α]-quinoxalin-1-one
PKG	cGMP-dependent protein kinase
<i>P</i> _{app}	Apparent permeability coefficient
R.S.D.	Relative standard deviation
SCH-1	Schisandrin

SCH-2	Gomisin A
SCH-3	Deoxyschisandrin
SCH-4	γ -Schisandrin
S.D.	Standard deviation
SERT	Serotonin reuptake transporter
S.E.M.	Standard error of the mean
SIM	Selected ion monitoring
SK _{Ca}	Small conductance Ca ²⁺ -activated K ⁺ channel
SNP	Sodium nitroprusside
T _{1/2}	Half-life
TEA	Tetraethylammonium
TIC	Total ion current
<i>t_R</i>	Retention time
TTX	Tetrodotoxin
UV	Ultraviolet
V _d	Apparent volume of distribution
VIP	Vasoactive intestinal peptide

Chapter 1 General Introduction

1.1 Chemical constituents of *Schisandra chinensis*

1.1.1 Introduction

Schisandra chinensis (Turcz.) Baill. (Magnoliaceae) is widely found in the northwest part of China (Helongjiang/Mandzuria), Korea, and the far east of Russia (Panossian and Wikman, 2008). The original plant of *Schisandra chinensis* is shown in Fig. 1-1 (a). Fructus Schisandrae (Fig. 1-1 (b)), the dried fruits of *S. chinensis*, is a famous medicinal herb in folk medicine of Eastern Asia and an important dietary complement in Western countries. In traditional Chinese medicine, *S. chinensis* is named “wu-wei-zi” (five taste fruit) and has been considered as one of the most widely used herbs. While the pharmacopoeial drug wu-wei-zi (bei-wu-wei-zi) consists of *S. chinensis* fruits cultivated and harvested from northern China, nan-wu-wei-zi is referred to the fruits of *Schisandra sphenanthera* grown in the southern provinces of China (National Committee of Chinese Pharmacopoeia, 2005). Although both herbs are available in the market, it has been reported that *S. sphenanthera* is less effective than *S. chinensis*, probably due to their different chemical compositions (Lu et al., 2009). *S. chinensis* has been intensively investigated in phytochemical and pharmacological studies.

(a)



(www.goochs.com)

(b)



(image.baidu.com)

Fig. 1-1 (a) Original plant of *Schisandra chinensis* (Turcz.) Baill.; (b) Dried fruits of *S. chinensis* (Fructus Schisandrae)

1.1.2 Chemical constituents

As classified by Opletal et al. (2004), the constituents of *S. chinensis* fruits can be divided into four classes: (i) dibenzo[a,c]cyclooctadiene lignans, such as schisandrin, schisantherins and gomisins; (ii) monpterpenes, including borneol, 1,8-cineol, citral, *p*-cymol, α - and β -pinene; (iii) sesquiterpenes, such as sesquicarene, α -ylangene, chamigrenal, α - and β -chamigrene, β -bisabolene and (iv) other compounds of various structures, such as thymoquinol, thymoquinol 5-*O*- β -glucopyranoside, kaempherol 3-*O*- β -D-rutinoside, β -sitosterol, schisandrolic acid, and citrostadienol. Dibenzo[a,c]-cyclooctadiene lignans are the most predominant components isolated from *S. chinensis* and have been considered responsible for the majority of the biological activities of this herb.

1.1.2.1 Schisandra lignans

The occurrence of dibenzo[a,c]cyclooctadiene lignan in nature is rare. In the class of Magnoliopsida, they are found in two families, Illiciaceae and Schisandraceae (Opletal et al., 2004). A series of lignans with dibenzo[a,c]cyclooctadiene structure have been isolated from *Schisandra chinensis* and chemically identified. The major Schisandra lignans are summarized in Table 1-1.

Table 1-1 Lignans isolated from *Schisandra chinensis* (Turc.) Baill.

Lignan	Synonyms	Molecular Formula	Molecular Weight (Da)
Schisandrin	schizandrin, schisandrol A, wuweizichun A	C ₂₄ H ₃₂ O ₇	432
Isoschizandrin	isoschisandrin	C ₂₄ H ₃₂ O ₇	432
Deoxyschisandrin	schisandrin A, schizandrin A, wuweizisu A	C ₂₄ H ₃₂ O ₆	416
(±)-γ-Schizandrin	schisandrin B, schizandrin B, wuweizisu B, γ-Schizandrin	C ₂₃ H ₂₈ O ₆	400
Wuweizisu C	schisandrin C, schizandrin C	C ₂₂ H ₂₄ O ₆	384
Gomisin A	schisandrol B, schizandrol B, wuweizichun B	C ₂₃ H ₂₈ O ₇	416
Gomisin B	schisantherin B, schizanthrin B, wuweizi ester B	C ₂₈ H ₃₄ O ₉	514
Gomisin C	schisantherin A, schizanthrin A, wuweizi ester A	C ₃₀ H ₃₂ O ₉	536
Gomisin D		C ₂₈ H ₃₄ O ₁₀	530
Gomisin E		C ₂₈ H ₃₄ O ₉	514
Gomisin F		C ₂₈ H ₃₄ O ₉	514
Gomisin G		C ₃₀ H ₃₂ O ₉	536
Gomisin H		C ₂₃ H ₃₀ O ₇	418
Angeloylgomisin H		C ₂₈ H ₃₆ O ₈	500
Tigloylgomisin H		C ₂₈ H ₃₆ O ₈	500
Benzoylgomisin H		C ₃₀ H ₃₄ O ₈	522
Gomisin J		C ₂₂ H ₂₈ O ₆	388
Gomisin K1		C ₂₃ H ₃₀ O ₆	402
Gomisin K2		C ₂₃ H ₃₀ O ₆	402
(+)-Gomisin K3	gomisin K3, schisanhenol, schizanthrin	C ₂₃ H ₃₀ O ₆	402

Table 1-1 (continued)

Lignan	Synonyms	Molecular Formula	Molecular Weight (Da)
Gomisin N	(-)-gomisin N	C ₂₃ H ₂₈ O ₆	400
Gomisin O		C ₂₃ H ₂₈ O ₇	416
Angeloylgomisin O		C ₂₈ H ₃₄ O ₈	498
Angeloylisogomisin O		C ₂₈ H ₃₄ O ₈	498
Benzoylgomisin O		C ₃₀ H ₃₂ O ₈	520
Benzoylisogomisin O		C ₃₀ H ₃₂ O ₈	520
Epigomisin O		C ₂₃ H ₂₈ O ₇	416
Gomisin P		C ₂₃ H ₂₈ O ₈	432
Angeloylgomisin P	schisantherin C	C ₂₈ H ₃₄ O ₉	514
Tigloylgomisin P		C ₂₈ H ₃₄ O ₉	514
Angeloylgomisin Q		C ₂₉ H ₃₈ O ₉	530
Tigloylgomisin Q		C ₂₉ H ₃₈ O ₉	530
Gomisin R		C ₂₂ H ₂₄ O ₇	400
Gomisin S		C ₂₃ H ₃₀ O ₇	418
Gomisin T		C ₂₃ H ₃₀ O ₇	418
Pregomisin		C ₂₂ H ₃₀ O ₆	390
Schisantherin D	schizanthrin D	C ₂₉ H ₂₈ O ₉	520

Information taken from Opletal et al. (2004) and Lu and Chen (2009).

The first dibenzo[a,c]cyclooctadiene lignan isolated from *S. chinensis* is schisandrin (also named schizandin, schisandrol A or wuweizichun A) (Kochetkov et al., 1979). As shown in Fig. 1-2, the skeleton of the chemical structure of schisandrin comprises of a cyclooctane ring (B) and two benzene rings (A and C). The substituents (methyl and hydroxyl) at C-7 and C-8 position are in *cis*-disposition. Most of the lignans found in *S. chinensis* are derivatives from schisandrin bearing different substitutions in rings A, B and C. In ring B, substitution at C-7 and C-8 could form a pairs of stereoisomers when the substituents are different at each site, such as γ -schisandrin and gomisin N. There are also a variety of substitutions at C-6 and C-9 in ring B, usually with an ester substituent, thereby forming a schisantherin compound, such as schisantherin A or angeloylgomisin H. Substituents in ring A and C usually include methoxy and methylenedioxy groups. The occurrence of methylenedioxy substitution appears to be in favour of C-2 and C-3 or C-12 and C-13 rather than C-1 or C-14 in currently identified *Schisandra* lignans.

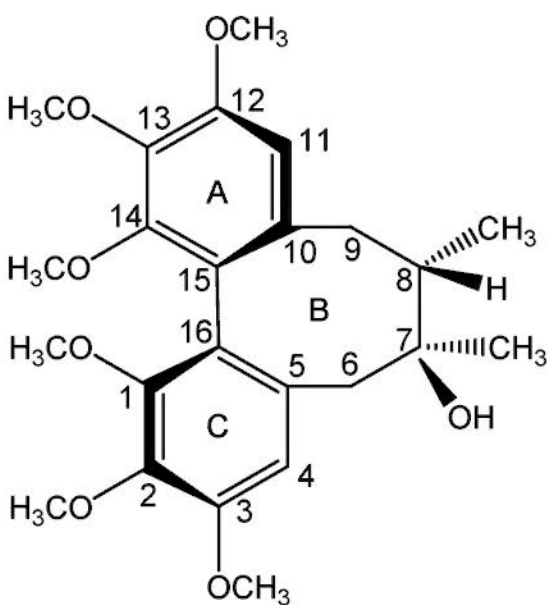


Fig. 1-2 Chemical structure of schisandrin

1.2 Pharmacological activities of *Schisandra chinensis* and Schisandra lignans

In traditional Chinese medicine, *Schisandra chinensis* is widely used as a tonic, astringent and sedative agent to treat sexual weakness, enuresis, protracted diarrhea, night sweating and body weakness (National Committee of Chinese Pharmacopoeia, 2005). A number of recent investigations using animals, isolated tissues and cultured cells have demonstrated that *Schisandra chinensis* possesses anti-oxidant, hepatic detoxifying, neuroprotective, anti-cancer and cardiovascular-protective properties. Dibenzo[a,c]cyclooctadiene lignans, the major component in *S. chinensis*, have been considered the major active ingredients responsible for the biological and pharmacological activities of *S. chinensis*, as reviewed in the following sections.

1.2.1 Antioxidant activities

Liu and Lesca (1982) reported the antioxidant properties of dibenzo[a,c]cyclooctadiene derivatives isolated from *S. chinensis* fruits. This study revealed that Schisandra lignans exhibit inhibitory effects on carbon tetrachloride-induced lipid peroxidation and metabolism, as well as covalent binding of carbon tetrachloride to lipids. The antioxidant activities of a series of Schisandra lignans have been further investigated. It was reported that seven of the nine tested lignans inhibited iron/cysteine-induced lipid peroxidation (malondialdehyde formation) of rat liver microsomes as well as superoxide anion production in the xanthine/xanthine oxidase system, showing much higher potency than vitamin E (Lu and Liu, 1992). Among these active compounds, schisanhenol was the

most potent which also prevented the decrease of membrane fluidity of liver microsomes. Liu (1992) also stated that the antioxidant action of dibenzo[a,c]cyclooctadiene lignans included two major mechanisms, which involved inhibition on lipid peroxidation of biomembranes through scavenging active oxygen radicals and enhancement of the ability to eliminate active oxygen radicals by inducing the activity of superoxide dismutase and catalase. In addition to studies on hepatocyte, Schisandra lignans have been shown to protect against peroxidant damage of aging and ischemic rat brain (Xue et al., 1992) and oxidation of human low density lipoprotein (Yu et al., 2004).

Effects of Schisandra lignans on oxidative status under pathological conditions in animals have also been investigated (Ip et al., 1995). It has been reported that schisandrin B protected against carbon tetrachloride-induced hepatotoxicity and stated the hepatoprotection of schisandrin B might be mainly attributed to the enhancement in the functioning of the hepatic glutathione antioxidant system. It has also been demonstrated that schisandrin B exerted protective effects against ischemia-reperfusion injury in isolated rat hearts, which could be at least partly attributed to the modulation on changes in non-enzymatic antioxidant levels (Ko and Yiu, 2001). Moreover, findings in recent studies have revealed that the protection of schisandrin B against stress damage in brain and kidney were associated with the enhancement in mitochondrial antioxidant status as well as improvement of mitochondrial functional and structural integrity (Chiu et al., 2008; Chen et al., 2008).

1.2.2 Hepatoprotective effects

In China, *Schisandra chinensis* fruits have been widely used to improve the liver function of patients with virus hepatitis B (Liu, 1977). The great demand of Schisandra drugs has facilitated the pharmacological investigations on *S. chinensis* and chemical synthesis of novel hepatoprotective agents on the basis of the active compounds found in *S. chinensis*. A synthetic lignan analogue known as DDB (bifendate) is potent antihepatotoxic compound which is used for the treatment of hepatitis B (Liu, 1989). As suggested by Liu (1985), the detoxifying effect of Schisandra lignans is due to the antioxidant activity and their interactions with hepatic enzymes. Recent studies confirmed the connection between antioxidant activity and hepatoprotective effect of *S. chinensis*. Ip et al. (1996) reported that the protective effects of *S. chinensis* against aflatoxin B1 and cadmium chloride-induced hepatotoxicity in rats were associated with an enhancement of hepatic antioxidant/ detoxification system, including increases in hepatic reduced glutathione level and the activities of hepatic glutathione reductase and glutathione S-transferase. The anti-hepatotoxin effect of *S. chinensis* has also been demonstrated by its ability to restore hepatic drug metabolism in carbon tetrachloride damaged liver (Zhu et al., 1998). Moreover, it has been shown that schisandrin B can decrease hepatic total cholesterol and triglyceride levels, and increase liver weight in a mouse model of hypercholesterolemia, indicating this lignan compound could be potentially useful for the treatment of adiposis hepatica (Pan et al., 2008).

1.2.3 Effects on central nervous system

Neuropharmacology of *S. chinensis* has attracted much interest in last few decades. Schisandrol A (Schisandrin) was shown to affect the presence of monoamine neurotransmitters and their metabolites in different regions of the brain in rats, including dopaminergic, adrenergic and serotonergic systems (Zhang and Niu, 1991). It was proposed that the modulatory effects on neurotransmitters could contribute to the sedative effect of *S. chinensis*. A recent study has demonstrated that deoxyschisandrin decreases spontaneous and synchronous intracellular calcium oscillations in cultured hippocampal neural networks, and suggested deoxyschisandrin might be able to maintain neural networks in homeostasis in case of perturbations caused by pathological events (Fu et al., 2008). A similar study has evaluated the effects of four Schisandra lignans on the membrane potential in C6 glioma cells, and found that wuweizisu C was the most potent one to decrease the membrane potential with modulation of intracellular $[Ca^{2+}]$ (Choi et al., 2008). Moreover, schisandrin and gomisin A have been shown to reverse scopolamine-induced cognitive impairment in rodents (Kim et al., 2006; Egashira et al., 2008). These central actions of Schisandra lignans may be related to the enhanced activity of cholinergic nervous system, as suggested by the inhibitory effects of a number of lignans on acetylcholinesterase activity *in vitro* (Kim et al, 2006; Hung et al., 2007). In addition, a number of dibenzocyclooctadiene lignans isolated from *S. chinensis* have shown protective effects against glutamate-induced neurotoxicity, as indicated by improvements in antioxidant status such as an inhibition on the formation of cellular peroxide (Kim et al., 2004). Among the tested compounds, wuweizisu C possessed the

highest potency of protection, followed by gomisin N, deoxyschisandrin and gomisin A, while schisandrin had little effects.

1.2.4 Anti-cancer effects

A number of recent studies have suggested an adjuvant role of dibenzocyclooctadiene lignans in cancer treatment. This potential application is related to their capability to reverse multidrug resistance in cancer cells. Pan et al. (2005) showed that schisandrin B is a relatively potent P-glycoprotein inhibitor, as suggested by the effect of reversing P-glycoprotein-mediated cancer multidrug resistance (MDR) with a comparable potency to verapamil. This research group further proved that the lignan could reverse the cancer drug resistance mediated by multidrug resistance-associated protein 1 (MRP1) (Sun et al., 2006). In addition, schisandrin B enhanced anticancer drug-induced apoptosis in cancer cells but not in normal cells, through a mechanism not associated with P-glycoprotein or MRP1, but related to an enhanced activation of mitochondrial apoptotic pathways (Li et al., 2006). Furthermore, five major dibenzocyclooctadiene lignans present in *Schisandra chinensis* displayed similar potency to reverse MRP1-mediated drug resistance in cancer cells (Li et al., 2007). In a recent study, it was demonstrated that the crude extract of *Fructus Schizandrae* and five lignan components displayed reversal activity to multidrug resistance *in vitro* and *in vivo* (Huang et al., 2008). The activity was associated with the influence on expression of P-glycoprotein, mdr1 gene and protein kinase C. The structure-activity relationship has also been analyzed, and it appeared that the presence of a dimethoxyl group rather than a methylenedioxy ring on the benzene ring could enhance

the MDR reversal activity (Huang et al., 2008). Apart from the MDR reversal activity, antiproliferative effects of Schisandra lignans on human cancer cells have also been reported, and schisantherin C was found to be the most potent one among ten tested compounds (Min et al., 2007).

1.2.5 Effects on cardiovascular system

As described in 1.2.1, schisandrin B has shown protective effects against ischemia-reperfusion injury in isolated rat hearts, which may be attributed to its antioxidant activity. In addition, *S. chinensis* and Schisandra lignans also exhibit beneficial effects on cardiovascular system through vasodilatory actions. Recent studies have demonstrated the vasodilatory effects of *S. chinensis* extracts on isolated rat thoracic aorta (Lee et al., 2004; Rhyu et al, 2006; Park et al., 2009). The mechanisms of the vasorelaxant effects have been found to involve endothelium-dependent (nitric oxide) and endothelium-independent (calcium influx and dephosphorylation of myosin light chain) pathways (Rhyu et al, 2006; Park et al., 2009). The vasodilatory action of *S. chinensis* extracts was also suggestive of a role as weak phytoestrogen (Lee et al., 2004). Moreover, a pure substance gomisin A has also been shown to induce endothelium-dependent and direct relaxation in rat thoracic aorta, indicating dibenzocyclooctadiene lignans could count for the vasodilatory effects of *S. chinensis* (Park et al., 2007).

The most common subdivision of IBS is based on alterations in bowel habit. IBS is most often classified as constipation-predominant (C-IBS), diarrhea-predominant (D-IBS) and alternating forms. The balance of diarrhea versus constipation varies in regions, but approximately one third of the patients fit the D-IBS subtype and one-third C-IBS; the remainder tends to report normal or alternating stools without significant urgency, and a primary complaint of abdominal pain or discomfort (Ragnarsson and Bodemar, 1999). Overall, altered gastrointestinal motility and visceral hypersensitivity have been conventionally included in the most important pathophysiological factor of IBS. However, the pathogenetic and pathophysiological mechanisms of IBS are complex and incompletely understood, leading to the limited therapeutic options available for IBS patients. During the last years, the steadily increasing interest in this topic has improved the current understanding of IBS pathogenesis, with new areas including the brain-gut axis, immunity and genetics. The major pathophysiological factors of IBS have been reviewed below.

1.3.1 Genetic factors

There have been reports suggesting that genetic component is involved in IBS. It has been found that family members of IBS patients would usually experience similar symptoms, and IBS clusters in families (Kalantar et al., 2003; Kanazawa et al., 2004). The aggregation of IBS in family is also suggested by the finding that the concordance of IBS is twice as great in monozygotic compared with dizygotic twins (Levy et al., 2001). Moreover, a number of studies have examined the DNA sequences of IBS subjects to

explore the genetic variants that could increase the risk of having IBS. One of strongest evidences for a link between polymorphism and IBS has been found on serotonin-transporter (Camilleri et al., 2002). Polymorphisms of genes controlling down-regulation of inflammation, such as IL-10 and transforming growth factor- β_1 (Gonsalkorale et al., 2003), and cytokine gene (Gonsalkorale et al., 2003) have also been reported to be related to IBS in some case studies. Nevertheless, it is unlikely that genetic factors alone are the cause of IBS. They could interact most with environmental factors to fully express the disease. Further studies in larger samples are needed to clarify the contributions of genetic and environmental factor to IBS (Saito et al., 2005).

1.3.2 Psychological factors

The role of psychological factors in IBS has been largely investigated for the past few decades. A variety of studies supported an association between psychosocial factors and the aggravation of IBS symptoms. Affective disorders, including anxiety, hostility and phobia, are common in comorbidity with IBS (Irwin et al., 1996). The IBS patients also frequently have a history of emotional, physical and sexual abuse. Salmon et al. (2003) proposed a model in which childhood abuse is associated with IBS because it causes a tendency to dissociate, and thereby a general increase in physical symptoms. New findings in the studies with high numbers of IBS patients also suggested the involvement of abuse such as somatisation in the development of IBS, even though the explanations are unlikely well established (North et al., 2004; Spiegel et al., 2005). Further to the view that psychological factors influence the severity of the symptoms and the health care

seeking behavior of the patients, recent population-based studies have suggested that psychological factors, such as psychological distress, fatigue, health anxiety and illness behavior, may be involved in the etiopathogenesis of IBS (Weinryb et al., 2003).

Psychological factors (particularly stress) have also been found to influence gastrointestinal motor function and visceral perception (Welgan et al., 1988; Mayer et al., 2001), although this was demonstrated in acute stress, while chronic stress remained less explored in human. Studies in animals have suggested that acute stress may activate the mucosal inflammatory cells, especially mast cells, leading to alteration in bowel physiology and symptom generation. Stress-induced release of corticotrophin-releasing factor (CRF) may be responsible for mast cell activation and inflammatory mediator release (Eutamene et al., 2003). Moreover, recent studies have demonstrated that early life stress, such as neonatal maternal separation, induced permanent alterations in gastrointestinal tract and central nervous system, resulting in the dysregulation of gut motility and enhancement of visceral sensation in laboratory animals (Lopes et al., 2008).

1.3.3 Gastrointestinal motility alteration

Abnormalities of gastrointestinal motility have been commonly found in IBS at different regions of GI tract, including colon and small bowel (Chey et al., 2001; Portincasa et al., 2003). Meal ingestion, stress, mechanical stimulation, cytokinin and corticotrophin-releasing factor infusion have been shown to exaggerate GI motor responses (Camilleri et al., 1998). However, it is still difficult to clarify the relationship between GI motor

changes and different symptom generations of IBS, since the majority of current studies include small numbers of patients and a variety of protocols and methodologies. Nevertheless, an association between pain episodes in IBS patients and colonic high-amplitude propagating contractions has been demonstrated (Clemens et al., 2003). Corsetti et al. (2004) reported rectal hyperreactivity to distension in IBS patients was associated with enhanced pain, further suggesting a combination of sensory and motor abnormalities in IBS. To summarize, GI motor abnormalities are present in the bowel habit symptoms in IBS, but its relevance for other symptoms requires further elucidation.

Bloating and abdominal distension are frequent complaints accompanied with motor abnormalities in IBS patients (Houghton and Whorwell, 2005). It has been reported that in normal subjects, gas experimentally infused in the small bowel was propelled rapidly through the bowel and consequently expelled. In contrast, a high proportion of IBS patients retained a significant amount of the infused gas (Serra et al., 1998; Serra et al., 2003). The retained excessive gas thereby reproduced patients' symptoms. Importantly, the gas-related symptoms can be modulated by nutrients such as dietary lipids (Serra et al., 2002), physical activity (Dainese et al., 2004), body posture (Dainese et al., 2003) and pharmacological agents (Caldarella et al., 2002). Taken together, the difficulty in expelling intestinal gas in IBS patients may be ascribed to abnormal intestinal motility and poor tolerance to intestinal gas, and it could be relevant to different symptoms in IBS.

1.3.4 Visceral hypersensitivity

Visceral hypersensitivity is one of the most common pathophysiological alterations characterized in IBS and other functional gastrointestinal disorders (Camilleri et al., 2001). Since the first report by Ritche (1973) describing that IBS patients had poor tolerance to rectal balloon distension, hypersensitivity to rectal distension in IBS patients has been demonstrated by a number of research groups (Whitehead et al., 1990; Mertz et al., 1995; Naliboff 1997), suggesting the rectal hypersensitivity can be a useful biological marker of IBS to confirm the diagnosis of IBS and to discriminate IBS from other causes of abdominal pain (Whitehead et al., 1990; Bouin et al., 2002). Nevertheless, there are still some discussions on the persistence (Faure et al., 2007) and subtype-discrepancy (Prior et al., 1990) of rectal hypersensitivity in IBS patients. It has been reported that the lower sensation threshold could be more frequently found in diarrhea-predominant IBS patients as opposed to constipation-predominant patients, in whom discomfort may be perceived at higher distension pressures than healthy controls (Prior et al., 1990; Simrén et al., 2001a). Besides, increased perception of visceral stimuli also affects other regions of the gastrointestinal tract, including ileum, duodenum and oesophagus (Accarino et al., 1995; Trimble et al., 1995). Although the cause and consequence of the altered sensory processing is debatable, a number of factors have contributed to the generation and development of visceral hypersensation, including nutrients, stress, psychological and hormonal factors.

Postprandial worsening of symptoms and adverse reactions to food consumption is common in IBS patients (Simrén et al., 2001b). It has been demonstrated that lipid administration enhances the colonic sensitivity in IBS patients compared to healthy controls (Simrén et al., 2007a). The enhancement of visceral sensitivity has also been reported in IBS patients with intraduodenal administration of lipids (Distrutti et al., 2000). Moreover, the dietary composition seems to be important for IBS patients, since a fatty meal had more pronounced effects on rectal sensitivity in IBS patients than a meal rich in carbohydrates as compared with control subjects (Simrén et al., 2007b). The underlying mechanisms of the enhancement of visceral sensitivity in IBS patients after nutrient delivery into the gastrointestinal tract are far from being understood; both central and peripheral factors could be involved (Simrén et al., 2003).

A correlation between visceral sensitivity and stress and psychological factors has usually been described by patients with IBS. A number of studies demonstrate an altered visceral perceptual response in IBS patients relative to health controls after or during stress, including auditory, mental and acute psychological stress (Dickhaus et al., 2003; Murray et al., 2004; Posserud et al., 2004). In a study of veterans, it was shown that participation in war, as a form of severe stress, could result in visceral as well as cutaneous hypersensitivity, and the significant variation in the pain measures is in concordance with psychological measures, suggesting the roles of stress and psychological factors in modulating visceral sensation (Dunphy et al., 2003). On the other hand, findings from studies of physical and sexual abuse seem to be somewhat controversial (Ringel et al., 2004; Coretti et al., 2005). Stress and psychological factors therefore seem to play a role

in modulating visceral hypersensitivity, but the effects could greatly vary from the underlying factors.

1.3.5 Serotonin involvement

Serotonin (5-HT) is one of the key neurotransmitters in the gastrointestinal (GI) tract, where about 95% of the serotonin in the body is found. The majority of enteric serotonin (~90%) is synthesized and stored in enterochromaffin (EC) cells, and released in response to different luminal stimuli (Mawe et al., 2006). 5-HT plays a crucial role in regulating the motility, secretion, absorption and sensory events in GI tract via the activation of a number of 5-HT receptors distributed widely on smooth muscle, enteric nerves and sensory afferents (De Ponti and Tonini, 2001). The effect of 5-HT is terminated by the serotonin reuptake transporter (SERT). The role of 5-HT as a mediator in enteric nervous system has been extensively investigated. Changes in 5-HT content and release, 5-HT receptor expression or changes in SERT expression/activity could contribute to the alterations of sensorimotor function and visceral perception in IBS. A number of recent studies have demonstrated altered 5-HT availability and signaling in IBS patients, and drug development during the last few years has focused on the drugs interacting with 5-HT signaling in the gut, which is further described in section 1.4. Taken together, the studies assessing 5-HT levels in platelet depleted plasma have suggested increased release of 5-HT postprandially and/or reduced 5-HT reuptake in diarrhea-predominant IBS patients (Bearcroft et al., 1998; Houghton et al., 2003; Atkinson et al., 2006) and patients with post-infectious IBS (Dunlop et al., 2005),

whereas impaired release seems to be a feature of constipation- predominant IBS patients (Dunlop et al., 2005; Atkinson et al., 2006). Moreover, recent finding has revealed that the mucosal 5-HT was reduced in IBS patients, probably resulting from the decreased level of tryptophan hydroxylase, the rate limiting enzyme in 5-HT synthesis, but SERT mRNA was also reduced, which could increase the availability of 5-HT (Coates et al., 2004). The number of EC cells in the rectal mucosa was normal in this study, but in specific assessment of patients with post-infectious IBS, the number of EC cells was found to be upregulated (Dunlop et al., 2003). Although evidence for altered 5-HT signaling in IBS patients exists, further studies are needed to evaluate the link to specific symptoms, and to clarify the subsequent 5-HT signaling in motor functions and sensory events in IBS.

1.3.5.1 Classification of serotonin receptors

5-HT receptors in the GI tract are present on enteric neurons, enterochromaffin cells, GI smooth muscle, and possibly on enterocytes and immune cells. Kim et al. (2000) has summarized the classification of 5-HT receptors and the relevant effects in the GI tract, as presented in Table 1-2. General overviews that cover various aspects of 5-HT receptors are also available (Barnes and Sharp, 1999).

Seven types or families (5-HT₁ – 5-HT₇) and multiple subtypes of 5-HT receptors have been identified and characterized by a combination of pharmacological techniques and molecular approaches (Barnes and Sharp, 1999), as indicated in Table 1-2. Except for the

5-HT₃ receptor, a ligand-gated ion channel, all other serotonin receptors are G-protein-coupled receptors that activate an intracellular secondary messenger cascade to produce an excitatory or inhibitory response. Among the seven types or families of receptors, 5-HT₃ and 5-HT₄ receptors have been demonstrated to be critically involved in the endogenous modulation of GI motility and bowel sensation, and 5-HT₁, 5-HT₂ and 5-HT₇ receptors could also play a role. The significance of these receptors in 5-HT signaling in GI tract is further elucidated in the following sections.

Table 1-2 Classification of 5-HT receptors (Kim et al., 2000)

	Location		GI Effect
	GI tract	Brain	
5-HT _{1A}	Enteric nerves	Hippocampus	Neuronal inhibition
5-HT _{1B}	Sympathetic nerves	Substantia nigra, Basal ganglia	Neuronal inhibition
5-HT _{1D}		Substantia nigra, Basal ganglia	Neuronal inhibition
5-HT _{1E}		Substantia nigra, Basal ganglia	
5-HT _{1F}		Dorsal raphe, Hippocampus, Cortex	
5-HT _{1P}	Enteric neurons		Neuronal depolarization
5-HT _{2A}	Guinea pig ileum	Cortex, Caudate nucleus	Contract muscle, neuronal depolarization
5-HT _{2B}	Rat stomach fundus	Cerebellum	
5-HT _{2C}		Choroid plexus	
5-HT ₃	Vagus, sympathetic, enteric nerves	Area postrema	Neuronal depolarization
5-HT ₄	Myenteric plexus	Hippocampus	Contract muscle, Facilitate cholinergic transmission
5-HT ₅		Mouse cerebellum or whole brain	
5-HT ₆		Caudate nucleus	
5-HT ₇		Thalamus, Hypothalamus, Hippocampus	

1.3.5.2 Serotonin and gastrointestinal (GI) motility

It is now accepted that local mucosal stimulation, such as pressure and acid, induces the release of 5-HT from EC cells and initiates the peristaltic reflex. 5-HT stimulates the submucosal intrinsic, primary, afferent neurons (IPANs) by acting on 5-HT_{1p} and 5-HT₇ receptors. The activated submucosal IPANs release acetylcholine (ACh) and calcitonin gene-related peptide (CGRP), which is presynaptically amplified by 5-HT₄ receptor. The subsequent synapse in the myenteric plexus with ascending and descending interneurons thereby induces excitatory and inhibitory responses locally (Pan and Gershon, 2000, Gershon, 2005). Ascending interneurons activate excitatory motor neurons by releasing substance P and ACh onto myocytes leading to circular muscle contraction. Descending cholinergic neurons stimulate inhibitory motor neurons to release nitric oxide, vasoactive intestinal peptide and adenosine triphosphate, resulting in circular muscle relaxation. The resulting peristaltic reflex is mainly responsible for the propulsion of intestinal materials from proximal sites to distal sites (Goyal and Hirano, 1996). In addition to the neurotransmission initiated at submucosal IPANs, myoenteric IPANs, activated by 5-HT₃ receptor, may be involved in a gut reflex that increases intestinal motility and secretion (Houghton et al., 2000; Gershon, 2005).

Given the significance of 5-HT receptors in neuromuscular activity, coordinated intestinal contractions and transit appear to be modulated by pharmacological agents acting specifically on receptor subtypes. Since activation of 5-HT₃ or 5-HT₄ receptors enhances gastrointestinal transit, they have been the potential targets for pharmacological therapies

of IBS to relieve symptoms related to GI motor abnormality. It has been suggested that antagonizing 5-HT₃ receptor slows the intestinal transit while agonizing the 5-HT₄ receptor accelerates GI transit. Alosetron, a highly potent and specific 5-HT₃ antagonist, has been shown to delay colonic transit in both healthy volunteers and patients with diarrhea-predominant IBS (Houghton et al., 2000). On the other hand, 5-HT₄ receptor agonists, such as tegaserod and prucalopride, accelerate gastrointestinal transit (Bouras et al., 1999; Degen et al., 2001). These observations have led to the efforts to develop and evaluate the clinical use of the agents targeting 5-HT receptors in IBS patients with abnormal bowel function. It will be further discussed in the pharmacological therapies for IBS (Section 1.4).

1.3.5.3 Serotonin and visceral sensation

5-HT plays an important role in visceral pain transmission. Intraluminal stimuli induce the release of 5-HT from EC cells with mucosal crypts. 5-HT activates extrinsic primary afferent nerves via 5-HT₃ and 5-HT₄ receptors, thereby conveying sensory responses to the central nervous system (Mazzia et al., 2003; Berthoud et al., 2004). Nociceptive signals are transmitted from the viscera to specific site of the dorsal horn. Synaptic input activates specific subsets of second-order projection neurons leading to activation of specific brain stem and thalamic regions, the sensation and perception of pain, and subsequently evaluative and discriminative processes in higher brain regions. Bulbosplinal pathways activated by nociception send descending projections from the periaqueductal gray and raphe nuclei to neurons in the dorsal horn, utilizing serotonergic, noradrenergic

and opiate transmitters to result in inhibition or facilitation of nociceptive inputs (Crowell, 2001)

IBS patients have demonstrated visceral hypersensitivity compared to healthy controls, although there is difference in sensory threshold to colorectal distension between D-IBS and C-IBS, as described in Section 1.3.4. The enhanced visceral perception could involve increased availability of 5-HT (induced by the increased release or reduced reuptake of 5-HT), or dysregulation of expression and/or activity of relevant 5-HT receptors responsible for the sensory transmission, but the underlying mechanism remains unknown. Nevertheless, it has been shown that pharmacological agents acting on 5-HT₃ or 5-HT₄ receptors are able to modulate the visceral sensation in animal models and human subjects. Kozłowski et al. (2000) demonstrated that the 5-HT₃ receptor antagonist, alosetron, inhibits the depressor response and Fos-like immunoreactivity in the spinal cord following noxious colorectal distention in rats. A recent study using alosetron in a rat model of delayed stress-induced visceral hyperalgesia demonstrated the dual role of 5-HT₃ receptor in modulating pain pathways, and suggested that 5-HT₃ receptors on vagal afferents are involved in a tonic inhibitory control of visceral nociception, independent of stress sensitization, whereas 5-HT₃ receptors on central terminals of spinal afferents are engaged in the facilitatory effect of stress on visceral sensory perception (Bradesi et al., 2007). On the other hand, tegaserod, a highly selective partial agonist of 5-HT₄ receptor, has been suggested to directly inhibit mechanosensitive afferents in response to rectal balloon distension in the rat (Schikowski et al., 2002). The pain modulatory effect of tegaserod was proposed to possibly result from the competitive antagonism with

endogenous 5-HT at periphery 5-HT₄ receptors, thereby reducing afferent transmission (Grundy, 2002). Although the roles of 5-HT₃ and 5-HT₄ receptors in modulating visceral sensation pathways are now unclear, the corresponding pharmacological agonists or antagonists have been widely used to relieve visceral pain in IBS patients.

1.3.6 Inflammatory changes and neuro-immune interactions

Although IBS has been discriminated from inflammatory bowel disease (IBD), evidence from literatures suggests that transient and chronic inflammation in low-grade may play a role in the pathogenesis of IBS. As addressed by Barbara et al. (2004), there are three main lines of evidence supporting this hypothesis. Firstly, patients in remission from IBD develop IBS symptoms with a higher prevalence than normal population (Simrén et al., 2002). Secondly, approximately 15-30% IBS patients report onset of disease after an acute episode of infectious gastroenteritis (Parry et al., 2003). Third, increased populations of inflammatory cells, including mast cells, T lymphocytes and macrophages, have been detected in the colonic and ileal mucosa as well as in muscularis externa of jejunum of IBS patients (O'Sullivan et al., 2000; Chadwick et al., 2002; Tornblom et al., 2002; Barbara et al., 2004). In addition, the increased inflammatory cells have been found to be activated, in proximity to the enteric nerves, and to release a number of mediators, including interleukins, nitric oxide, histamine and proteases (Gwee et al., 2003; Barbara et al., 2004), which could in turn affect the functions of enteric nerves, leading to the altered bowel function and enhanced visceral sensory perception (Barbara et al., 2002). However, the relationship between low-grade inflammation and IBS, particularly

subgroups other than post-infectious IBS, remains elusive. The unsuccessful attempt to inhibit intestinal inflammation with steroids in post-infectious IBS (Dunlop et al., 2003) implies that long-term changes in function and structures of nerves within the GI tract or sensory afferent system, such as dorsal horn of spinal cord, could occur under the chronic inflammatory conditions.

1.3.7 Animal models for IBS

IBS is a gastrointestinal disorder characterized by chronic abdominal pain and discomfort associated with altered bowel habits in the absence of a demonstrable pathology. While alterations in bowel habits are likely related to altered gut motility caused by dysregulation of enteric innervation, symptoms of abdominal pain and discomfort are regarded as a form of visceral hypersensation involving changes of transmission in visceral sensory events. Progress in the development of more effective therapies has been hampered partially by the lack of satisfactory animal models that mimics the features of IBS, in particular the enhanced visceral perception. Currently established animal models for IBS can be divided into two broad categories based on their primary pathogenetic mechanisms: models triggered by centrally targeted stimuli, such as neonatal stress and post-traumatic stress, and those triggered by peripherally targeted stimuli, such as intestinal infection and inflammation. The manipulation, characterization and application of both categories of IBS animal models are summarized in Table 1-3.

Table 1-3 Category, manipulation, characterization and application of IBS animal models

Category	Stimulus	Manipulation	Model validation	Altered sensory events in CNS	Alterations in GI tract	Application in Pharmacology	Reference
Centrally targeted	Neonatal stress	Neonatal maternal separation, 180 min daily for 14-21 days	Enhanced colonic motility: increased defecation in response to acute stressor (WA)	Hypersecretion of CRF	Increase of 5-HT content at post-CRD in colon;	20-herb formula (personal communication)	Ren et al., 2007; Elaine et al., 2007; Al-Chaer et al., 2000; Liang et al., 2005; O'Mahony et al., 2008;
		Neonatal CRD on a daily basis from postnatal day 8 to 21	Visceral hypersensitivity: increased responses to CRD measured by AWR and/or EMG	Increased activity and sensitivity of central NE systems	Induction of contraction related protein in myenteric plexus and longitudinal muscles	Tegaserod (5-HT ₄ receptor agonist)	Lopesa et al., 2008; Coutinho et al., 2002
	Adult stress	Movement restraint	Increased fecal output	Enhanced central 5-HT response	Altered expression of alpha subunits of G protein in the brain		Zou et al., 2008
		Overnight illumination. hot environment. water and food deprivation, level vibration	Increased pain response (EMG) to CRD		Altered colonic mucosal physiology		

Table 1-3 (continued)

Category	Stimulus	Manipulation	Model validation	Altered sensory events in CNS	Alterations in GI tract	Application in Pharmacology	Reference
	Intestinal infection	Transient infection with the nematode parasite <i>Tricbinella spiralis</i>	Altered smooth muscle function		Increased substance P in myenteric nerves		Swain et al., 1992; Vallance and Collins, 1998
Peripherally targeted	Intestinal irritation (non-infection)	Intracolonic instillation of acetic acid Injection of pH 4.0 sterile saline into the gastrocnemius muscle	Increased fecal output in response to restrain stress or WA Visceral hypersensitivity: increased responses to CRD measured by AWR and/or EMG		Increased degranulation rate of mucosal mast cell in colon	Ginseng total saponins Alosetron (5-HT ₃ receptor antagonist)	La et al., 2003, 2004; Xu et al., 2006; Kim et al., 2005; Miranda et al., 2006

CRD, colorectal distension; WA, water avoidance; AWR, abdominal withdrawal reflex; EMG, electromyography; NE, norepinephrine; CRF, corticotrophin-releasing factor; 5-HT, serotonin; NO, nitric oxide.

Given that the enhanced visceral perception has been demonstrated in IBS patients (Section 1.3.4), visceral hypersensitivity has been a critical criteria to evaluate the validity of an animal model for IBS. However, quantitative assessment of pain in animal model has been a challenge in the research of IBS. To date, there are two validated methods of measurement of visceral pain. Both methods utilize abdominal muscle contraction in response to noxious stimuli (visceromotor reflex). The conventional method employs electromyography (EMG) as a form of myoelectric activity of abdominal muscle by implanting recording electrodes and wires in the abdominal muscles. The extent of pain perception is assessed by the amplitude of EMG signal. The other method is a semiquantitative measurement assessing abdominal withdrawal reflex (AWR). This is an involuntary motor reflex that is quantified by a numerical scoring system to the graded intensity of the stimulus. As a semiquantitative method, AWR may include a larger variance caused by subjective observation, as compared to EMG. Meanwhile, the advantage of the AWR over EMG is that the latter requires additional surgery to implant recording electrodes and wires in the abdominal muscles, which might induce sensitization to visceral pain.

1.4 Therapeutic approaches for irritable bowel syndrome

1.4.1 Pharmacologic therapy

One of the major problems in developing therapeutic regimens for IBS patients is that the disease comprises a group of functional intestinal disorders in which there are no unique

targets for pharmacotherapy (De Ponti and Malagelada, 1998). As describe in section 1.3, IBS involves central and peripheral physiological changes together with psychological factors. Despite the unclear physiologic mechanism of IBS, a number of pharmacologic therapies have been developed for the management of IBS symptoms on the basis of the important pathophysiologic factors, including altered bowel motility, visceral hypersensitivity, and imbalance in neurotransmitters, in particular serotonin (5-HT).

1.4.1.1 5-HT-based approaches

5-HT based approaches have played an important role in conventional pharmacologic therapies for IBS. Two relevant 5-HT receptor, 5-HT₃ and 5-HT₄, have been popularly targeted using antagonists and agonists, respectively. Several 5-HT₃ receptor antagonists, such as granisetron and ondansetron, have shown beneficial effects to patients with IBS (Hammer et al., 1993; Prior and Read, 1993), in particular diarrhea-predominant IBS. Alosetron, a selective 5-HT₃ receptor antagonist, has been shown to decrease colonic transit time, increase compliance of colon distension and increase sodium absorption from the jejunal lumen (Camilleri et al., 2001). Unfortunately, the drug is now withdrawn from the market due to a severe side effect of ischemic colitis. 5-HT₄ receptor agonists have been recognized as prokinetic agents for constipation-predominant IBS patients. Tegaserod, a selective 5-HT₄ receptor partial agonist, shows prokinetic effects by virtue of stimulating peristalsis and increasing intestinal transit, and also by modulating sensory pathways (Camilleri, 2001). Moreover, 5-HT_{2B}, 5-HT_{1P} and 5-HT₇ receptor subtypes, as

well as 5-HT transporters could be potential therapeutic targets for developing novel treatment for IBS (McLean et al., 2006).

1.4.1.2 Targeting opioid receptors

Opioid receptors (μ , κ and δ) are present in GI tract located particularly in the myenteric and submucosal plexus, as well as on the nociceptive pathways to the brain. Opioids have been well known for their effects on pain perception and GI functions. Asimadoline, a novel and highly selective κ opioid agonist, has shown to decrease pain perception in response to colonic distension and decreased satiation and postprandial symptoms after a liquid meal (Delgado-Aros et al., 2003). Loperamide, an μ and δ opioid agonist that can not cross blood-brain barrier, acts peripherally to reduce acetylcholine and tachykinin release from the enteric neurons, and thereby relieves the diarrhea symptoms.

1.4.1.3 Tachykinin antagonist

Tachykinins (also known as neurokinins), such as substance P, neurokinin A and B, are distributed in both the central and peripheral nervous systems, with a dominant location in the peripheral endings of capsaicin-sensitive primary afferent neurons that innervate many regions including GI tract. There are three known neurokinin receptors, designated as NK-1, NK-2 and NK-3, involved in the mediation of neurokinins. NK-1 receptor plays an important role in the transmission and modulation of visceral afferent information. In a pilot study, treatment of IBS patients with a NK-1 receptor antagonist, ezlopitant, reduced

the emotional response to rectal distension and produced a trend towards decreased rectal sensitivity (Oh-Young et al., 2000)

1.4.1.4 Other pharmacological approaches

Tricyclic antidepressants have shown clinical benefits in IBS patients with severe abdominal pain, but the side effects have largely limited their use. A similar situation occurs in the application of anticholinergic agents in IBS patients. However, novel pharmacological agents acting more specifically on muscarinic receptor subtype have been shown to reduce colonic motility in IBS patients (Houghton et al., 1997). Other novel approaches of pharmacotherapies for IBS include modulation of corticotrophin-releasing factor receptor, proteinase-activated receptor and nerve growth factor (Bueno, 2005; Giorgio et al., 2007).

1.4.2 Chinese medicine approach

Although there are a number of therapeutic agents available for IBS patients, the conventional pharmacologic regimens are not effective for all IBS patients. Further, the benefit of the synthetic drugs has been found to be usually associated with various side effects. On the other hand, a number of studies revealed that herbal drugs may have beneficial effects in IBS patients (Bensoussan et al., 1998; Chen and Zhang, 1999; Madishch et al., 2004). The search for useful drug regimen from traditional Chinese medicine is therefore considered a logical alternative. As a matter of fact, herbal remedies

have been used for many IBS patients not only in China but also in other countries where herbal treatment is considered an important part of complementary and alternative medicine.

In Traditional Chinese Medicine, there are two classical herbal prescriptions for treating IBS-like symptoms. The prototype is recorded in *Jin Yue Chuan Shu* (“Collected Treatises of Zhang Jin-Yue”, 1624AD) dated back in the Ming Dynasty. The formula, known as the “Important Prescription for Abdominal Pain and Diarrhea” (Tong Xie Yao Fang), includes four components herbs, namely, dried rhizome of largehead *Atractylodes* (*Atractylodes macrocephala* Koidz.), dried peeled root of peony (*Paeonia lactiflora* Pall.), dried pericarp of tangerine (*Citrus reticulata* Blanco), and dried root of *Saposhnikovia divaricata* (Turcz.) Schischk. The second herbal formula useful for relieving IBS-like conditions is the *Zhong Man Fen Xiao Wan*, first appearing in the book entitled *Lan Shi Mi Cang* (Secrets from the Orchid Chamber, 1336AD). The formula is composed of seventeen herbs which are usually prescribed for patients with IBS-like symptoms, including abdominal distension, a sensation of fullness, bursting pain in the epigastrium and abdomen, irritability, fever and a bitter taste in the mouth.

In recent Chinese medical literatures, there are a large number of reports describing the therapeutic effects of herbal formulas in the treatment of IBS. However, the major concerns raised from most of the reports include a lack of viable control groups (placebo), variable entry criteria, and poor validation of clinical outcome measurements. Nevertheless, a randomized, double-blind, placebo-control trial has been performed on a

Chinese herbal formula prescribed for IBS patients, as reported by Bensoussan et al. (1998). The study has demonstrated that this formula appears to offer improvements in symptoms of some patients with IBS (~70%). Based on the positive clinical observations, the biological potentials have been further evaluated in our group. In the previous studies, it has been demonstrated that decoction of the formula inhibits the sensorimotor activity of guinea pig ileum *in vitro*, and relieves the visceral hypersensitivity in an IBS rat model induced by neonatal maternal separation. These results indicated the clinical effects of the herbal formula on IBS patients could be related to its modulatory effects on GI motility and visceral perception. The formula is composed of twenty component herbs, which are summarized in Table 1-4. In this formula, *Schisandra chinensis* (fruit) accounts for 7% of component herbs by weight. In Chinese medicine, the fruits of *S. chinensis* have been used for the treatment of exhaustion, spermatorrhoea, cough, frequent urination, protracted diarrhea, night sweating, palpitation and insomnia (State Administration of Traditional Chinese Medicine of China and Editorial Committee of Chinese Materia Medica, 1999). The astringent and sedative properties of *S. chinensis* fruits may be useful for the relief of IBS symptoms such as diarrhea and visceral pain.

Table 1-4 Composition of the 20-herb Chinese formula

No.	Pharmaceutical name	Used part of original plant	Percentage in weight (%)	No.	Pharmaceutical name	Used part of original plant	Percentage in weight (%)
1	Radix Codonopsis (黨參)	Root	7	11	Cortex Fraxini (秦皮)	Bark of branch or stem	4.5
2	Radix Paeoniae Alba (白芍)	Root	3	12	Radix Bupleuri (柴胡)	Root	4.5
3	Radix Aucklandiae (木香)	Root	3	13	Herba Pogostemonis (廣藿香)	Aerial part	4.5
4	Radix Saposhnikoviae (防風)	Root	3	14	Poria (茯苓)	Sclerotium	4.5
5	Cortex Phellodendri Chinensis (* 柏)	Bark	4.5	15	Semen Plantaginis (車前子)	Ripe seed	4.5
6	Rhizoma Coptidis (* 連)	Rhizome	3	16	Rhizoma Atractylodis Macrocephalae (白術)	Rhizome	9
7	Cortex Magnoliae Officinalis (厚樸)	Bark of root, branch, Stem	4.5	17	Rhizoma Zingiberis Praeparatum (炮薑)	Rhizome	4.5
8	Radix Glycyrrhizae Preparata (炙甘草)	Root and Rhizome	4.5	18	Fructus Schisandrae Chinensis (五味子)	Ripe fruit	7
9	Radix Angelicae Dahuricae (白芷)	Root	2	19	Pericarpium Citri Reticulatae (陳皮)	Pericarp	3
10	Herba Artemisiae Scopariae (茵陳)	Aerial Part	3	20	Semen Coicis (薏苡仁)	Ripe kernel	7

1.5 Objective of this study

Schisandra chinensis is widely used in Chinese medicine as an astringent, tonic and sedative agent. Dibenzo[a,c]-cyclooctadiene lignans are the predominant components isolated from *S. chinensis* and have been recognized to be the major active ingredients of this herb, but the absorption, metabolism and pharmacokinetics of *S. chinensis* are less understood. Despite a number of pharmacological and biological activities of *S. chinensis*, the modulatory effects on gastrointestinal motility and pain perception are seldom documented. Recently, a Chinese herbal formula has been shown to offer improvement of symptoms in IBS patients based on a randomized, double-blind, placebo-control trial, and *S. chinensis* is one of the component herbs (Bensoussan et al., 1998). This study therefore aims to evaluate the related pharmacological activities of *S. chinensis* which are potentially useful for treatment of IBS, as well as to determine the absorption and pharmacokinetics of *S. chinensis*.

In the present work, the chemical constituents of *S. chinensis* extracts are first characterized by a validated HPLC-MS method before pharmacological studies. To determine the bioavailability of *S. chinensis*, the *in vitro* and *in vivo* absorption of this herb are analyzed with the aid of HPLC-MS method. The plasma pharmacokinetics of *S. chinensis* in the rat has been further evaluated. In pharmacological studies, the effects of *S. chinensis* extracts and four major Schisandra lignans on gut motility are evaluated toward intestinal motor response *in vitro*. The mechanisms of relaxation on isolated rat colon induced by schisandrin (SCH-1) are then further investigated. In an IBS rat model,

the effect of *S. chinensis* on reversal of the visceral hypersensitivity is demonstrated, and the related neurophysiological factors are also examined.

Chapter 2

High Performance Liquid Chromatographic Analysis of Lignans in

Schisandra chinensis

2.1 Introduction

The major constituents of *Schisandra chinensis* are dibenzocyclooctadiene lignans, which are commonly known as Schisandra lignans. More than 40 lignans have been isolated from various parts of this plant (Chen et al., 2001; Opletal et al., 2004). As discussed in Chapter 1, Schisandra lignans exhibit a variety of bioactivities. There is increasing interest in using pure isolated substances as well as the standardized extracts as drugs and health supplements. Therefore, quality control for the lignan components in Schisandra extracts is indispensable for further pharmacological investigation of this commonly used herb.

Schisandra lignans have been qualitatively or quantitatively analyzed by a great number of methods, including thin layer chromatography (Zhao et al., 1995; Mu et al., 2005; Li et al., 2007), high performance liquid chromatography with ultraviolet detection (HPLC-UV) (Avula et al., 2005; Halstead et al., 2007; Zhu et al., 2007; Zhang et al., 2008), high performance liquid chromatography coupled with mass spectrography (HPLC-MS) (He et al., 1997; Huang et al., 2007; Deng et al., 2008; Huang et al., 2008b), gas chromatography couple with mass spectrography (GC-MS) (Schwarzinger et al., 2004), high counter current chromatography (Huang et al., 2005), capillary electrophoresis

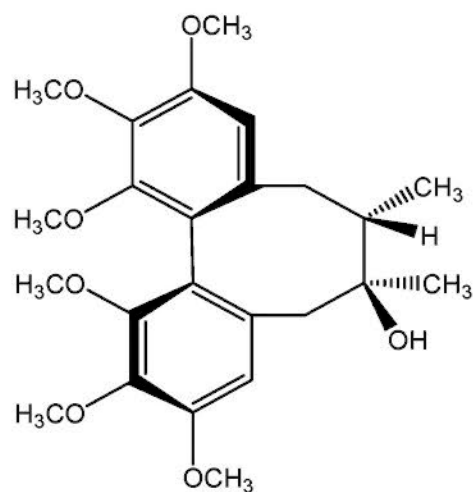
(Kvasnickova et al., 2001) and micellar electrokinetic capillary chromatography (Sterbova et al., 2002). In this study, a high performance liquid chromatography with photodiode array detection (HPLC-DAD) method has been developed for quantitative analysis of four major Schisandra lignans, schisandrin, gomisin A, deoxyschisandrin and γ -schisandrin. These lignan compounds have been chosen based on the abundance at which they are found in most samples of *S. chinensis* (Halstead et al., 2007; Zhang et al., 2009) and the potential bioactivities as suggested in the literatures.

By comprehensively validating the detection parameters, such as linearity, detection and quantification limits, precision, accuracy, stability and recovery, the HPLC-DAD method is useful in quantifying the contents of the four lignan compounds in water extract and ethanolic extracts of *S. chinensis*, and analyzing different batches as a form of fingerprinting. This determination will provide important information for the chemical composition of Schisandra extracts used in the studies.

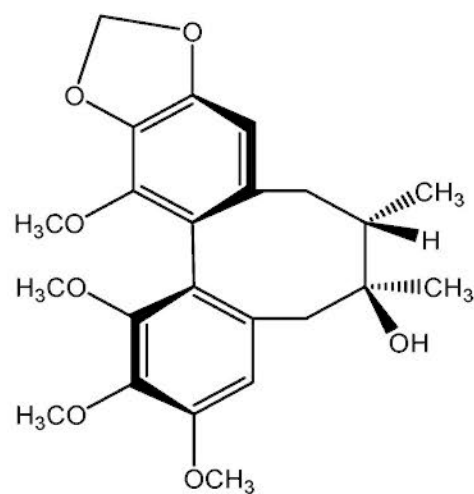
2.2 Materials and methods

2.2.1 Chemical and materials

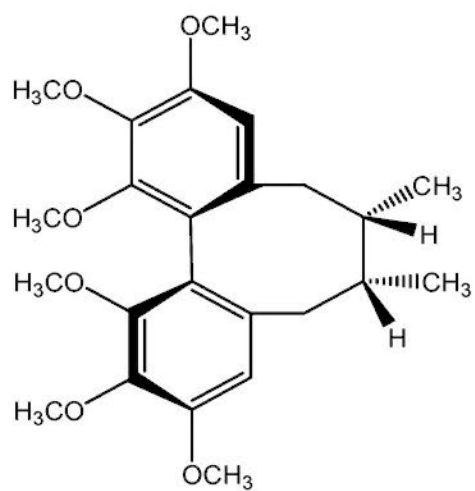
Dried berries of *Schisandra chinensis* and *Schisandra sphenanthera* were provided by Zhixin Pharmaceutical Company (Guangdong, China), identified and authenticated by Ms. Zong Yuying, School of Chinese Medicine, The Chinese University of Hong Kong. The voucher specimens were deposited in a temperature-control warehouse. Reference compounds, schisandrin (SCH-1), deoxyschisandrin (SCH-3), γ -schisandrin (SCH-4) and schisantherin A were purchased from National Institute for the Control of Pharmaceutical and Biological Products (Beijing, China) and were of purity >98%. Gomisin A was obtained from the Hong Kong Jockey Club Institute of Chinese Medicine with purity >97%. The chemical structures are presented in Fig. 2-1. HPLC grade acetonitrile (Fisher, Fair Lawn, NJ, USA) and trifluoroacetic acid were used for chromatography. Water was purified by Milli-Q academic purification system (Millipore, USA).



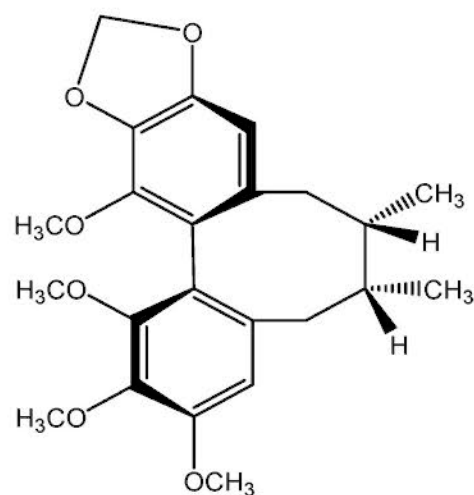
Schisandrin (SCH-1)



Gomisin A (SCH-2)



Deoxyschisandrin (SCH-3)



γ -Schisandrin (SCH-4)

Fig. 2-1 Chemical structures of the four Schisandra lignans analyzed in this study

2.2.2 Instrumentation

An Agilent 1100 LC-MSD-Trap-SL system (Agilent Technologies, Palo Alto, CA, USA) consisted of a degasser, an autosampler, a column compartment, a quaternary pump, a diode-array detector, and an atmospheric pressure chemical ionization (APCI) ion trap mass spectrometer. The HPLC analysis was performed on a Prevail C18 column (250mm×4.6mm I.D., 5 µm, Alltech) with a guard column (12.5mm×4.6mm I.D., 5 µm, Alltech).

2.2.3 Preparation of standard solutions

A standard stock solution for each Schisandra lignan was prepared in methanol at a concentration of 1 mg/mL, and the mixed standard stock solution for four Schisandra lignans was prepared in methanol at concentrations of 200 µg/mL for SCH-1, 50 µg/mL for SCH-2, 25 µg/mL for SCH-3 and 50 µg/mL for SCH-4, respectively. A serial dilution with methanol was performed for calibration plotting of the four Schisandra lignans. The stock solutions were stored at -20 °C and the calibrators were fresh prepared for each determination.

2.2.4 Preparation of samples

Dried *S. chinensis* fruits (500 g) were soaked in 4 liters of distilled water for 30 min at

room temperature. Then, the fruits were boiled three times for one hour with 4 L, 3 L and 3 L of distilled water, successively. The combined decoction was filtered and condensed by rotor evaporation under reduced pressure. Finally, the concentrate was freeze-dried to obtain the aqueous extract powder with the yield of 35.2%. Ethanol extracts were obtained by 70% or 95% ethanol extraction following the procedures described above and the extract yields were 30.4% and 27.6% respectively. The dry powder was placed in a desiccator at room temperature for further use.

For quantitative assays, approximate 200 mg of samples (water and ethanol extracts) were weighed and dissolved in 10 mL methanol by sonication for 30 min. Supernatant was obtained by centrifugation at $10000 \times g$ for 10 min and passed through a $0.45 \mu\text{m}$ RCF filter. For ethanol extract samples, ten-fold dilution with methanol was performed before HPLC analysis. Twenty microliters of the sample solution was injected into HPLC system and separated under the chromatographic conditions described below.

2.2.5 HPLC-MS conditions

The samples were separated by HPLC at a flow rate of 0.8 mL/min. The mobile phase consisted of 0.1% trifluoroacetic acid water (A) and acetonitrile (B) with a gradient elution of 20% B at 0 – 5 min; 45% B at 6 – 35 min; 45 – 60% at 35 – 50 min; 60 – 100% B at 50 – 60 min. The column temperature was 25 °C. The injection volume was 20 μl and the detection wavelength was set at 230 nm. The effluent was directly introduced to the APCI-MS.

The APCI-MS analysis was divided into two time segments. The first four minutes was set as waste to avoid the influx of inorganic ions into the mass analyzer and the other segment was set for sample analysis with the following optimized conditions: positive ion mode; nebulizer (N₂), 60 psi; dry gas (N₂), 5 L/min; drying gas temperature, 325 °C; corona current, 4000 nA; target mass, 500 *m/z*; compound stability, 80%; trap drive level, 80%, full scan range, 140 – 1100 *m/z*.

2.2.6 Method validation

2.2.6.1 Linearity and sensitivity

Calibration curve for each analyte was constructed by plotting the peak area against the corresponding concentration of standard solution. Quantification was performed upon six levels of external standards. The limit of quantification (LOQ) was determined as the concentration with a signal-to-noise ratio of more than ten. The lower limit of detection (LOD) was defined as the concentration that could be detected with a signal-to-noise ratio of more than three.

2.2.6.2 Accuracy and precision

The accuracy and precision of the method were evaluated by analyzing spiked samples of mixed reference standard at high concentrations of 100, 25, 12.5 and 25 µg/mL, and low

concentrations of 10, 2.5, 1.25 and 2.5 µg/mL for SCH-1, SCH-2, SCH-3 and SCH-4, respectively. Accuracy was determined by comparing the calculated concentration to the known concentration. The intra-day variance was determined by assaying six replicates in a single day and inter-day variance was assayed at 12, 24, 48, 72 and 96 h in four consecutive days.

Precision of sample determination was evaluated within-batch and between-batch. Within-batch precision was determined by the analysis of the same sample (70% ethanol extract) six times within one day. Between-batch precision was obtained by analyzing six independent preparations of 70% ethanol extract at the same concentration within one day. All precision was expressed as the relative standard deviation (R.S.D.).

2.2.6.3 Stability of samples

Stability of samples was tested by analyzing the same sample (70% ethanol extract) solution at 12, 24, 48, 72 and 96 h in four consecutive days. Variation was expressed as the relative standard deviation (R.S.D.).

2.2.6.4 Recovery

The extraction recovery was evaluated by spiking assays. Approximately 100 mg of 70% ethanol Schisandra extract (dried powder) with known amount for each analyte was spiked with about 80% of the amount for each analyte in the sample. Four replicates were

performed and the recoveries were determined by the comparison between amount added and measured.

2.3 Results

2.3.1 Chromatographic conditions and HPLC-MS identity conformation

Acetonitrile-water was selected as mobile phase due to its better separation and shorter analysis time than methanol-water. Trifluoroacetic acid (TFA) with final content of 0.1% in aqueous phase was added to improve separation of lignans. Considering the balance between analysis time and peak separation, gradient elution program was applied. The detection wavelength was set as 230 nm, since Schisandra lignans exhibited higher absorbance with less matrix disturbance at this wavelength, which could improve sensitivity and specificity of the method. All the analytes (SCH-1 to SCH-4) were well separated in a mixture of standards (Fig. 2-2) as well as in Schisandra extracts (Fig. 2-3), Resolution factors for all the analytes were over 2.0.

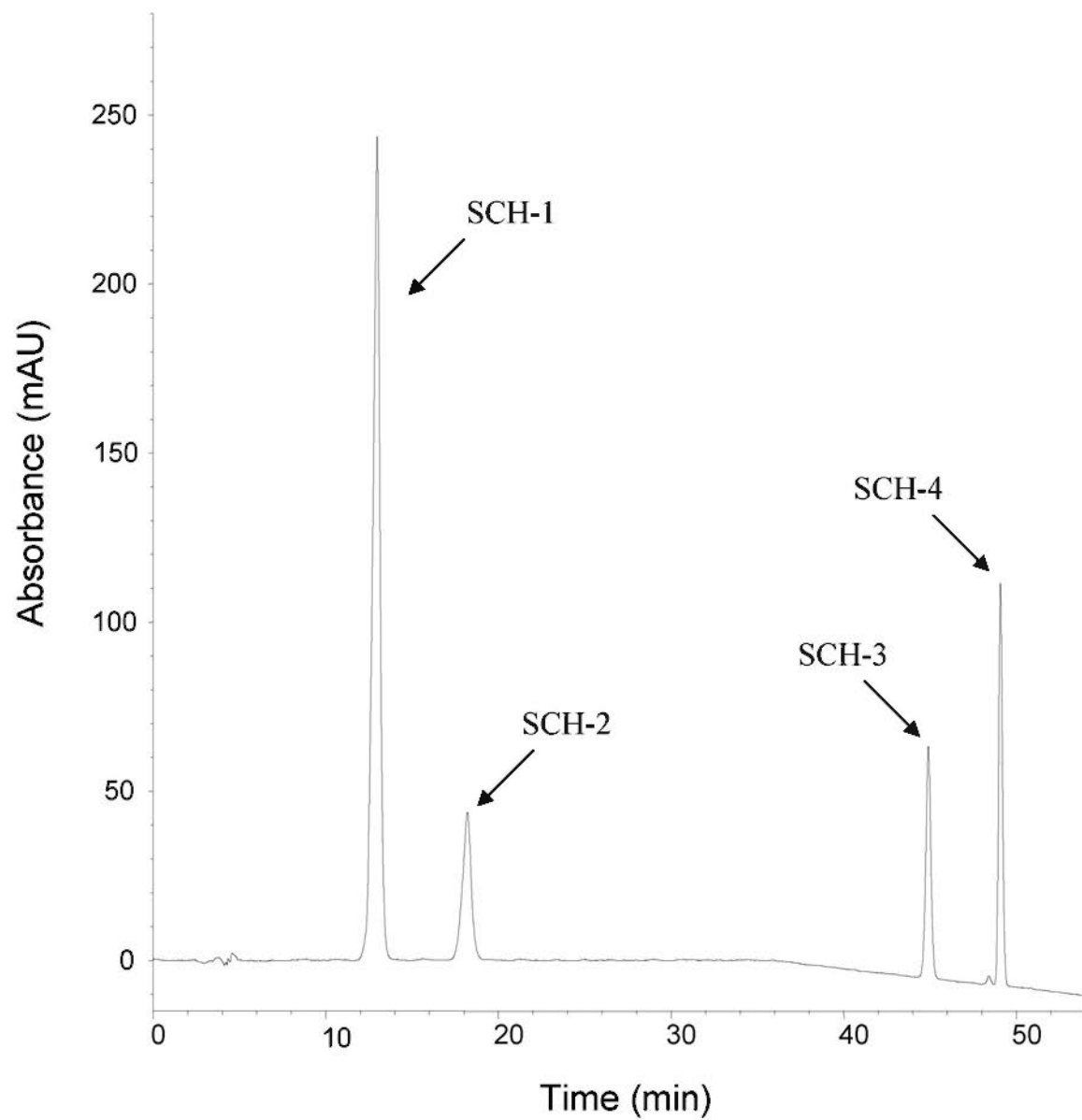


Fig. 2-2 Representative HPLC-DAD chromatogram of a pure standard mixture of schisandrin (SCH-1), gomisin A (SCH-2), deoxyschisandrin (SCH-3), γ -schisandrin (SCH-4). The detection wavelength was set at 230 nm.

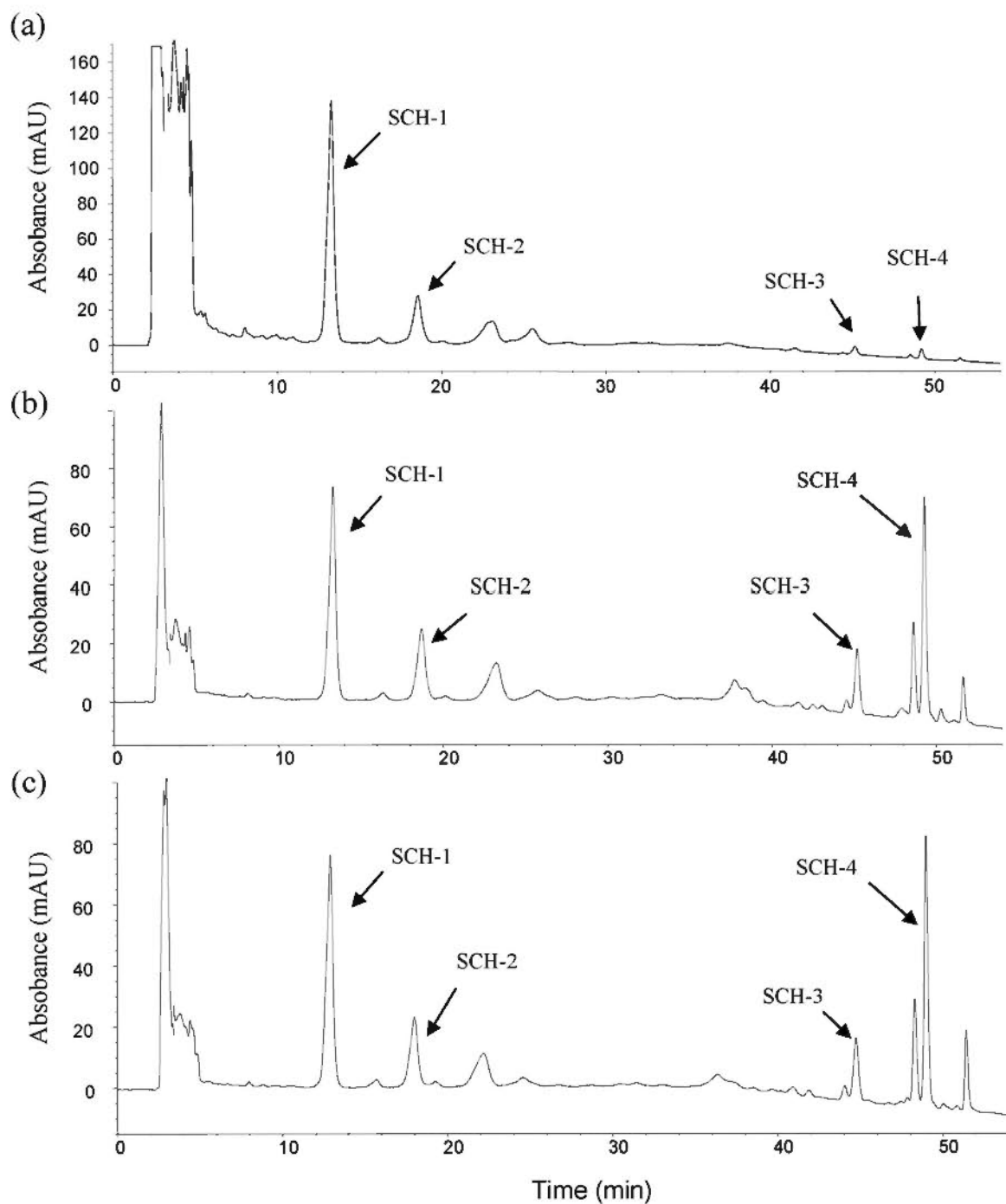


Fig. 2-3 Representative HPLC-DAD chromatograms of (a) water extract, (b) 70% ethanol extract and (c) 95% ethanol extract of *Schisandra chinensis* fruits. The detection wavelength was set at 230 nm. SCH-1 to SCH-4 denoted schisandrin, gomisin A, deoxyschisandrin and γ -schisandrin, respectively.

HPLC-MS experiments were also performed to confirm the identities of the four Schisandra lignans (SCH-1 to SCH-4). As shown in Fig. 2-4, the base peak chromatogram (BPC) of a standard mixture was comparable to the UV chromatogram using sequential analysis of DAD and MS (APCI in positive mode). The response of SCH-4 in MS analysis was lower than that of SCH-1 as compared to those in DAD analysis. This could be explained by the decrease in the polarity of SCH-4 that could render it difficult ionization in APCI source. MS spectra of the four Schisandra lignans are presented in Fig. 2-5. The base peak for SCH-1 and SCH-2 was the adduct ion $[M+H-H_2O]^+$ at m/z 415 and 399 respectively, whereas a protonated ion $[M+H]^+$ at m/z 433 with low intensity was also observed in the MS spectra of SCH-1. SCH-3 and SCH-4 exhibited the protonated ion $[M+H]^+$ at m/z 417 and 401 as their base peak, respectively. All the MS spectra of the analytes obtained from Schisandra extracts were identical to those obtained from the standards, thus confirming their identities. Retention time (t_R), UV λ_{max} and MS data of the four analyzed Schisandra lignans are summarized in Table 2-1.

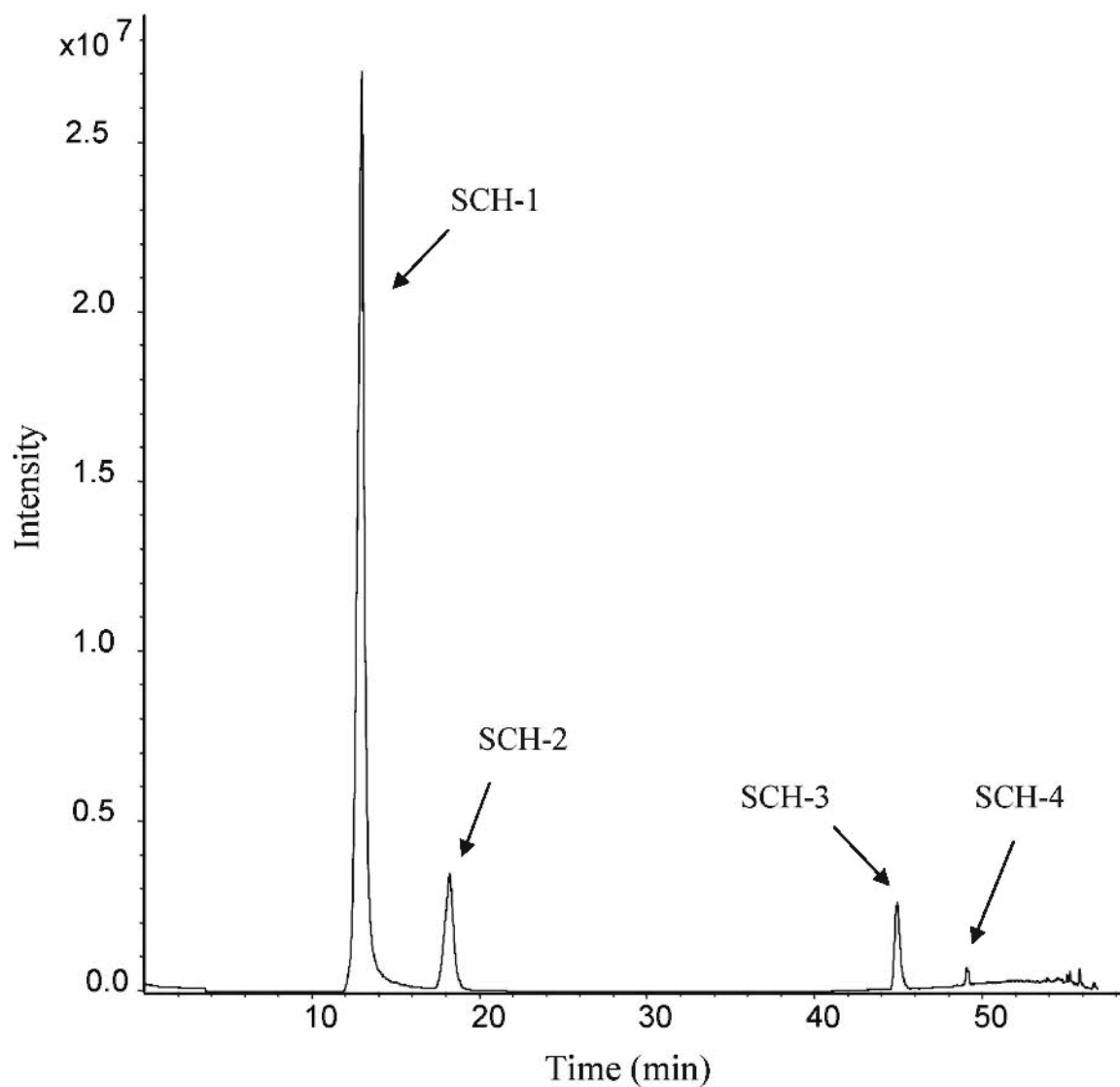


Fig. 2-4 Representative HPLC-MS base peak chromatogram (BPC) of a pure standard mixture of schisandrin (SCH-1), gomisin A (SCH-2), deoxyschisandrin (SCH-3), γ -schisandrin (SCH-4) using positive ionization mode with an APCI source.

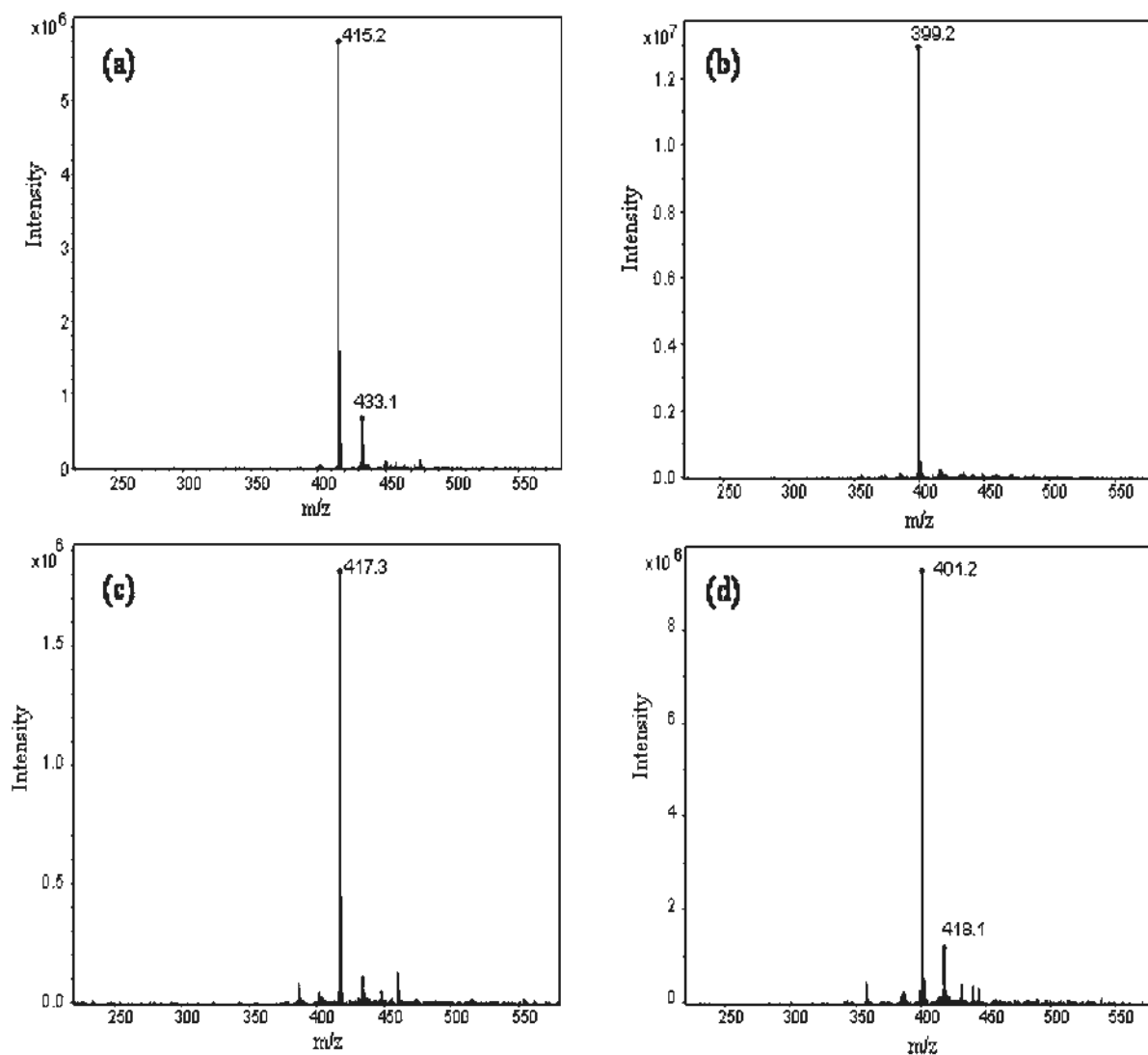


Fig. 2-5 Representative MS spectra of (a) schisandrin (SCH-1), (b) gomisin A (SCH-2), (c) deoxyschisandrin (SCH-3) and (d) γ -schisandrin (SCH-4) obtained from HPLC-DAD-MS analysis using positive ionization mode with an APCI source.

Table 2-1 Retention time (t_R), UV λ_{\max} and MS data of four major Schisandra lignans analyzed by HPLC-MS

Compounds	Retention time (min)	UV λ_{\max} (nm)	Molecular weight	Detected ion (m/z)
SCH-1	12.8	217, 252, 286	432	415 [M+H-H ₂ O] ⁺
SCH-2	17.9	218, 254, 286	416	399 [M+H-H ₂ O] ⁺
SCH-3	44.7	217, 252, 287	416	417 [M+H] ⁺
SCH-4	48.9	217, 255, 282	400	401 [M+H] ⁺

2.3.2 Linearity, limits of detection and quantification

Representative regression equations for the calibration plots, limits of detection (LOD) and quantification (LOQ) are listed in Table 2-2. For the four Schisandra lignans, calibration curves showed good linear correlations ($r^2 > 0.999$). The LOD for SCH 1-4 determined as a signal-to-noise ratio of more than three were 0.4, 0.4, 0.2 and 0.2 $\mu\text{g/mL}$, respectively. The LOQ for SCH 1-4 determined as a signal-to-noise ratio of more than ten were 0.1, 0.1, 0.05 and 0.05 $\mu\text{g/mL}$, respectively.

Table 2-2 Calibration curves for the four analyzed lignans

Analyte	Regression equation	r^2	Linear range ($\mu\text{g/mL}$)	LOD ($\mu\text{g/mL}$)	LOQ ($\mu\text{g/mL}$)
SCH-1	$y = 66.98x - 20.68$	0.9997	10–200	0.1	0.4
SCH-2	$y = 58.245x - 6.2792$	0.9995	2.5–50	0.1	0.4
SCH-3	$y = 97.827x + 0.7894$	0.9999	0.25–25	0.05	0.2
SCH-4	$y = 70.916x + 4.0622$	0.9999	0.5–25	0.05	0.2

2.3.3 Reproducibility and sample stability

Two levels of concentrations (low and high) for each analyte were used to evaluate the precision and accuracy of the method. As presented in Table 2-3, the intra-day precision of the measured concentrations for each concentration was <1.9% R.S.D. (n = 6) while the inter-day precision was within 4.3% R.S.D. (n = 6). The accuracy for each concentration was within the range from 100% to 114 % (comparing the calculated concentration to the known concentration) in both intra-day and inter-day assays. Precision for analyzing the four Schisandra lignans in 70% ethanol extract is presented in Table 2-4. The within batch precision for each analyte was <1.7% R.S.D. (n = 6), and the between-batch precision was within 2.2% R.S.D. (n = 6). Most of the R.S.D. values in the validation were less than 3% (<4.3% for all), suggesting good reproducibility of the method.

Stability of the four Schisandra lignans in sample solutions was tested by the analysis of one sample at different time in three days (n = 5). As listed in Table 2-5, precision of the determination for each analyte in 70% ethanol extract of *S. chinensis* fruits was <2.9% R.S.D. (n = 5), demonstrating that the sample solutions were stable for at least 72 h after preparation when stored at room temperature.

Table 2-3 Accuracy and precision of the method for analysis of four Schisandra lignans

Analyte	Concentration ($\mu\text{g/mL}$)	Intra-day (n = 6)			Inter-day (n = 6)		
		Mean \pm S.D. ($\mu\text{g/mL}$)	Accuracy (%)	Precision (R.S.D., %)	Mean \pm S.D. ($\mu\text{g/mL}$)	Accuracy (%)	Precision (R.S.D., %)
SCH-1	10	10.82 \pm 0.10	108.15	0.91	10.88	108.77	1.43
	100	102.74 \pm 1.44	102.74	1.40	105.24	105.23	2.97
SCH-2	2.5	2.85 \pm 0.05	113.89	1.86	2.84	113.60	3.63
	25	25.75 \pm 0.40	102.98	1.56	26.71	106.83	3.21
SCH-3	1.25	1.34 \pm 0.02	107.67	1.68	1.42	114.00	4.29
	12.5	12.77 \pm 0.20	102.15	1.57	13.86	110.90	4.12
SCH-4	2.5	2.68 \pm 0.04	107.27	1.52	2.68	107.34	3.62
	25	25.55 \pm 0.32	102.21	1.27	25.88	103.52	2.30

Table 2-4 Precision of the method for analysis of four *Schisandra* lignans in 70% ethanol extract of *Schisandra chinensis* fruits

Analyte	Within-batch (n = 6)		Between-batch (n = 6)	
	Mean ± S.D. (mg/g)	Precision (R.S.D., %)	Mean ± S.D. (mg/g)	Precision (R.S.D., %)
SCH-1	15.84 ± 0.12	0.80	15.48 ± 0.34	2.20
SCH-2	7.36 ± 0.12	1.62	7.20 ± 0.15	2.03
SCH-3	2.37 ± 0.01	0.60	2.32 ± 0.04	1.88
SCH-4	8.97 ± 0.08	0.87	8.53 ± 0.18	2.15

Table 2-5 Stability of four *Schisandra* lignans in 70% ethanol extract of *Schisandra chinensis* fruits (n = 5)

Analyte	SCH-1	SCH-2	SCH-3	SCH-4
Mean ± S.D. (mg/g)	16.20 ± 0.44	7.47 ± 0.21	2.42 ± 0.04	9.09 ± 0.18
Precision (R.S.D., %)	2.74	2.86	1.67	1.93

2.3.4 Recoveries of Schisandra lignans

Recoveries for the four Schisandra lignans determined by spiking assays were presented in Table 2-6. The recovery of each analyte was within the range of 96.5 – 108.9%. The R.S.D. of each recovery analysis was less than 3.8%. These results suggest that the analytical method was of good accuracy.

Table 2-6 Recovery of four *Schisandra* lignans in 70% ethanol extract of *Schisandra chinensis* fruits (n = 4)

Analyte	Amount in 100 mg sample (mg)	Amount added (mg)	Amount measured (mg)	Recovery (%)	R.S.D. (%)
SCH-1	1.68	1.20	2.78	96.53	3.60
SCH-2	0.78	0.50	1.35	105.45	2.43
SCH-3	0.25	0.20	0.49	108.89	3.13
SCH-4	0.93	0.80	1.73	100.32	3.77

$$\text{Recovery} = [(\text{measured amount} - \text{amount in sample})/\text{amount added}] \times 100\%$$

2.3.5 Analysis of Schisandra extracts using the validated method

Determined by the validated method, the quantities of four Schisandra lignans (SCH 1-4) in water extract, 70% and 95% ethanol extracts were presented in Table 2-7. SCH-1 was found to be the most abundant lignan, covering 75.4%, 46.2% and 46.6% of total amount of the four analyzed lignans in water extract, 70% and 95% ethanol extracts, respectively. In water extract, the amounts of SCH-1 ($2960 \pm 28 \mu\text{g/g}$) and SCH-2 ($852 \pm 16 \mu\text{g/g}$) were considerable while only a small quantity of SCH-3 ($49 \pm 2 \mu\text{g/g}$) and SCH-4 ($60 \pm 2 \mu\text{g/g}$) was found. When determined in ethanol extracts, higher contents of all lignan compounds were found as compared to water extract. SCH-1 and SCH-2 increased by 4-8 folds, whereas the increases of SCH-3 and SCH-4 amount were more dramatic with 50 folds and 190 folds higher in 95% ethanol extract, respectively. This could be explained by the increasing lipophilicity of SCH-1, SCH-2, SCH-3 and SCH-4. Compounds with high lipophilicity, such as SCH-3 and SCH-4, favor the organic solvent extraction like ethanol. Comparatively, the lignan amount and composition were comparable in 70% and 95% ethanol extracts. The total contents of four analyzed lignans found in water, 70% and 95% ethanol extracts were 3,921, 33,521 and 40,797 $\mu\text{g/g}$, respectively, approximately in the proportion of 1:8.5:10.4.

Table 2-7 Amounts of four lignans in water extract and ethanol extracts (70% and 95%) of *Schisandra chinensis* fruits (n = 5)

Analyte	Water extract		70% Ethanol extract		95% Ethanol extract	
	Mean ± S.D. (µg/g)	R.S.D. (%)	Mean ± S.D. (µg/g)	R.S.D. (%)	Mean ± S.D. (µg/g)	R.S.D. (%)
SCH-1	2960 ± 28	0.96	15475 ± 341	2.20	19024 ± 275	1.45
SCH-2	852 ± 16	1.86	7199 ± 146	2.03	7501 ± 151	2.01
SCH-3	49 ± 2	3.77	2314 ± 44	1.88	2684 ± 35	1.30
SCH-4	60 ± 2	2.83	8533 ± 183	2.14	11588 ± 177	1.52

2.3.6 Analysis of different batches of Fructus Schisandrae

The validated HPLC-DAD method was used to analyze different batches of Fructus Schisandrae as a form of chemical fingerprinting. As shown in Fig. 2-6, the HPLC-DAD chromatograms of methanolic extract of *Schisandra chinensis* from different batches were comparable in terms of the major lignan components. In contrast, the fingerprinting of *Schisandra sphenanthera* was markedly different, with the major lignan of schisantherin A identified by comparing with standard, and the lignan components present in *S. chinensis*, such as SCH-1, SCH-2, SCH-3 and SCH-4, were absent or present in much less amount in *S. sphenanthera*.

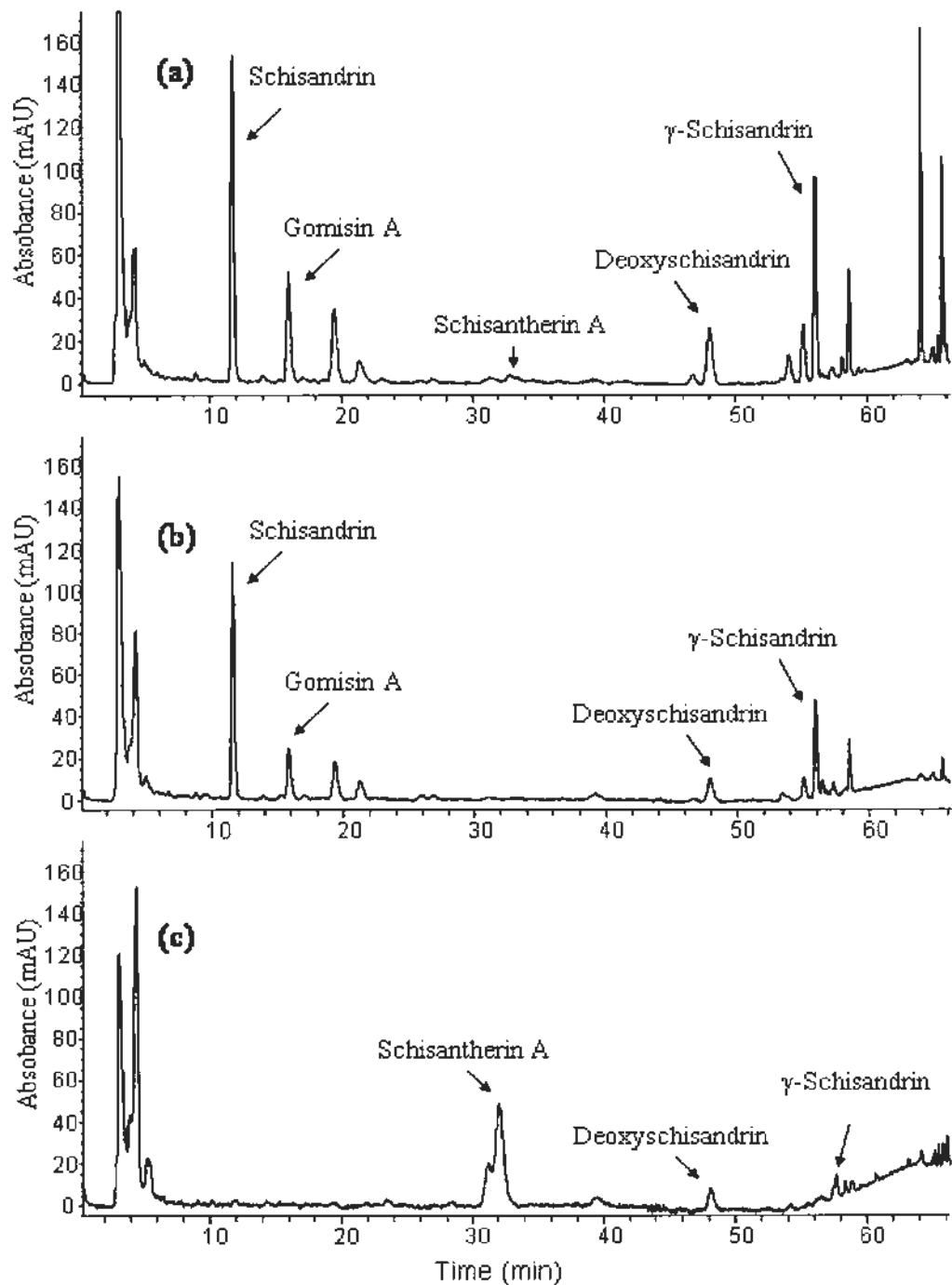


Fig. 2-6 HPLC-DAD fingerprinting of different batches of Fructus Schisandrae provided by Zhixin Pharmaceutical Company (Guangdong, China) detected at 230 nm. (a) *Schisandra chinensis* (obtained in 2006). (b) *Schisandra chinensis* (obtained in 2008). (c) *Schisandra sphenanthera* (obtained in 2008).

2.4 Discussion

Schisandra chinensis is rich in lignan components (Opletal et al., 2004). Owing to the importance of lignans, a variety of HPLC-DAD or HPLC-DAD-MS methods have been developed for quantitative or qualitative analysis of lignan components in *S. chinensis* (Huang et al., 2007; Deng et al., 2008; Huang et al., 2008b). Among the lignan compounds isolated in *S. chinensis*, schisandrin (SCH-1), gomisin A (SCH-2), deoxyschisandrin (SCH-3) and γ -schisandrin (SCH-4) are the dominant ones. Therefore, a HPLC-DAD method has been developed for quantitative analysis of these four lignan components in three kinds of extracts of *S. chinensis* fruits before pharmacological investigations of Schisandra extracts *in vitro* (Chapter 4) and *in vivo* (Chapter 6). Validation of the HPLC method in this study demonstrated accuracy, precision and reproducibility with sufficient sensitivity and selectivity for quantitative analysis of the four Schisandra lignans.

Compared to the previous methods, the composition of mobile phase in this study was simple, which allowed the effluent directly analyzed by mass spectrometry. In addition to the DAD detection, MS analysis can provide more useful information on the identities of analytes thereby improving the specificity of the method. Thus, the HPLC condition with modifications of MS determination has been applied in the absorption profiling of *S. chinensis* in rat everted gut sac and Caco-2 cell monolayer model (Chapter 3). Moreover, samples of *Schisandra sphenanthera* fruits were also analyzed using this method as a form of chemical fingerprinting for analyzing different batches of Fructus Schisandrae

available in the market. It was found that many of the lignans present in *S. chinensis* fruits were absent in *S. sphenanthera* fruits. SCH-1, SCH-2, SCH-3 and SCH-4, amounts of which were substantial in *S. chinensis*, were much lower in *S. sphenanthera*, whereas schisantherin A was the major component in *S. sphenanthera*. These results were in accordance with previous findings (Yu et al., 2007; Zhu et al., 2007; Deng et al., 2008; Huang et al., 2008b) and further confirmed the authentication of *S. chinensis* fruits used. As it is generally accepted that *S. chinensis* is superior to *S. sphenanthera* in quality, it is important to distinguish these two species before use. The HPLC-DAD-MS method in this study could thus be useful for quality control of *S. chinensis*.

Schisandra lignans have been reported to be rich in organic solvent extracts such ethanol and hexane (Opletal et al., 2004). The results in this study support this point of view. Total contents of four Schisandra lignans in the 95% ethanol extract was ten times more than that in the water extract. In terms of pharmacological studies, Schisandra water extract is commonly used in traditional Chinese Medicine while ethanol extract has been investigated more extensively in current studies. Both water extract and ethanol extract have been employed in the following pharmacokinetic (Chapter 3) and pharmacological studies (Chapter 4 & 6).

The comprehensively validated HPLC-DAD method in this study has ensured the quality of *S. chinensis* used and provided essential information on the chemical constituents of Schisandra extracts used in the following studies.

Chapter 3

Absorption of *Schisandra chinensis* in Rat Everted Gut Sac and Human Caco-2 Cell Monolayer Model *In Vitro* and Pharmacokinetics in Rats

3.1 Introduction

Optimized bioavailability is one of the determining factors for the development phase of orally administered drugs in pharmaceutical industry. Bioavailability represents the quantity and rate of transfer of the active compound from pharmaceutical form into blood circulation and further to the drug target sites. A variety of approaches, including *in silico* methods, dissolution test and *in vitro* culture-based cell models, have been adopted for preclinical prediction of oral drug availability. In the evaluation of bioavailability, determination of intestinal permeability using *in vitro* and *in vivo* techniques is among the most important steps.

Gastrointestinal permeability is one of the fundamental parameters in controlling the rate and extent of drug bioavailability. Although high-throughput techniques and computational prediction approaches have been rapidly developed in recent years, laboratory measurements of drug permeability across intestinal barriers are still essential for evaluating drug absorption and bioavailability. Currently, several *in vitro* models are used to determine the intestinal absorption of a drug candidate and the mechanisms of absorption. The everted gut sac model was developed by Wilson and Wiseman (1954) to study the transport of sugars and amino acids. Considering the claim that sac viability

was poor in simple buffer (Bridges et al., 1978), this gut sac model had been improved by using a complex tissue culture medium (TC 199) to replace the buffer salt solution (Bridges et al., 1978; Barthe et al., 1998). In this oxygenated, temperature-controlled medium system, the tissue viability can be maintained for up to 120 min, as demonstrated by oxygen consumption, glucose and amino acid uptake, as well as histological observation at light and electron levels (Bridges et al., 1978; Plumb et al., 1987; Barthe et al., 1998). The improved everted gut sac has been used to study oral drug absorption and metabolism, and the mechanisms of absorption. The sac system has previously been used to study the uptake of macromolecules with orally absorption potential, such as liposome (Rowland and Woodley, 1981). Using the everted sac technique, it is possible to identify the mechanisms of a drug's passage through the intestinal epithelial wall. Barthe et al. (1998) measured the transport of mannitol in everted gut sac and demonstrated the applicability of the sac system in studying paracellular transport across the small intestine. Furthermore, the everted gut sac model can be applied to study the action of intestinal efflux system on intestinal drug absorption, such as P-glycoprotein (Barthe et al., 1998). Given the presence of a number of metabolic enzymes in the intestine including uridine diphosphate glucuronyltransferases, sulfotransferases, esterases and cytochromes P450 (Peters et al., 1989; Capiello et al. 1991; Prueksaritonont et al., 1996; Watkins et al., 1997; Prueksaritonont et al., 1998), first-pass metabolism during intestinal drug absorption can be also studied using the system (Arellano et al., 2005; Chan et al., 2006). Thus, the improved everted gut sac can offer more information on the physiological process like first-pass metabolism, and it is simple, quick and inexpensive. However, there are some disadvantages which limit its applications. Firstly, it is an animal model, thus the

absorption results obtained by the sac model may not be extrapolated to human. Secondly, no acceptable and standardized parameters measured in the sac system have been established to evaluate the intestinal drug permeability. The absorption results may also vary between laboratories, owing to the handling procedure of everted gut sac.

The most commonly used methods for studies of intestinal drug permeability, mechanisms of absorption and interactions with epithelial proteins, such as transporters and enzymes, are the cultured cell models, including Caco-2, HT-29 and T84 cells originating from human colon carcinoma, and MDCK cells originating from Madin-Darby canine kidney. Among these cell lines, Caco-2 cell line has been the most widely used for preclinical prediction of oral drug absorption in pharmaceutical industry, and mechanistic studies of drug absorption in laboratory research (Artursson et al., 2001; Sun et al., 2008). The main reasons for the popularity of Caco-2 cell line are that the cells are easy to maintain in culture, and spontaneously differentiate under standard culture conditions to a confluent monolayer on porous support, forming tight junctions between the cells and expressing typical brush-border enzymes (hydrolases) on the apical face that are found in normal small intestines, such as alkaline phosphatase, sucrase and amino peptidases (Hauri et al., 1985). The polarized Caco-2 cell monolayer structurally and functionally resembles the intestinal epithelium, permitting the studies of drug permeability and mechanisms of drug transport across the intestinal barriers. Coupled with suitable analytical methods, such as high performance liquid chromatography with UV or mass spectrometry detection, a great number of research groups have studied the intestinal transport of various drug candidates in Caco-2 cell monolayer model, including

synthetic compounds, antibiotics, cholesterol and natural substances (Wang et al., 2000; Takashi et al., 2005; Boisset et al., 2000; Tian et al., 2006; Palmgrén et al., 2005). Moreover, given the expression of ATP-binding cassette efflux transporters such as P-glycoprotein, multidrug resistance-associated protein 2, and the breast cancer-resistant protein on the mucosal membrane (Hunter et al., 1993; Hirohashi et al., 2000), as well as multidrug resistance-associated protein 3 and organic solute transporters α and β on the serosal membrane in Caco-2 cell monolayer (Hirohashi et al., 2000; Okuwaki et al., 2007), the mechanisms of drug transport across intestinal barriers and interactions with epithelial proteins have been extensively studied using Caco-2 cell monolayer model (Leung et al., 2006; Yoo et al., 2007; Zhang et al., 2007). In addition, multiple types of metabolic enzymes such as sulfotransferases, uridine diphosphate glucuronyltransferases, glutathione *S*-transferases and cytochrome P450 isoenzymes have been found in the Caco-2 cells, even though some of them may be subjected to induction (Peters and Roelofs, 1989; Lampen et al., 1998; Munzel et al., 1999; Cummins et al., 2001, Sun et al., 2002). Thus the first-pass metabolisms of drugs could also be studied using this cell model (Zhou et al., 2005; Zhang et al., 2007). Compared to everted gut sac model, the major advantage of Caco-2 cells is that they are a human cell line, and therefore should not display interspecies differences in morphological and physiological characteristics of enterocytes. Further, Caco-2 cell model can provide comparative information on the intestinal drug absorption by quantitatively determining a standardized permeability parameter, which is expressed as the apparent permeability coefficient, permitting the prediction and evaluation of oral drug absorption potential. However, a major disadvantage of Caco-2 cell model is the long cell culture period of at least 21 days. It

was also reported that owing to the tight cell junction, the paracellular transport rate was much lower than that in small intestine (Artursson et al., 1993; Delie et al., 1997). Nevertheless, the Caco-2 cell monolayer model is currently the most popular *in vitro* model adopted by pharmaceutical industry and research laboratories for the investigations of intestinal drug absorption.

In using *in vitro* systems as described above, the impact of physiological parameters such as intestine transit, stomach emptying, intestinal juice secretion and microenvironment on drug absorption can not be evaluated. Indeed, *in vivo* studies on intestinal drug absorption and bioavailability are crucial in the development of a potent oral drug. For research purposes, a variety of animal models have been used to investigate the intestinal absorption and bioavailability, including radiolabel, *in situ* perfusion and *in vivo* pharmacokinetic modeling (Barthe et al., 1999). Pharmacokinetic modeling of drug absorption using plasma concentrations as a function of time has been largely used. Although this type of model provides less information on mechanistic phenomenon, it has been considered adequate to make descriptions of plasma concentrations in different situations of drug administration (single dosing, multiple dosing and cassette dosing) by measuring pharmacokinetic parameters, such as time at maximum plasma concentration (T_{max}), half life ($T_{1/2}$), and the area under the curve (AUC). The data obtained with animal pharmacokinetic modeling can be valuable for the prediction of intestinal drug absorption in human.

Traditional Chinese Medicine has been successfully applied for thousands of years.

Recent investigations have demonstrated the biological and pharmacological effects of a large number of Chinese medicines. However, the bioavailability and pharmacokinetic of Chinese medicines are much less studied, which, at least partially, limits the modernization and globalization of Chinese Medicine. *Schisandra chinensis*, the herb used in this study, has shown a large number of bioactivities (Chapter 1). With increasing interest in pharmacological studies on *Schisandra* lignans, the pharmacokinetics of some of the active ingredients such as schisandrin and γ -schisandrin has been studied using animals (Cui and Wang, 1992; Hiromasa et al., 1995; Xu et al., 2005; Chen et al., 2007). There were also literature reports on the intestinal absorption of active ingredients in *S. chinensis* extracts, which focused on one or several major lignans (Chen et al., 2007; Madgula et al., 2008; Xu et al., 2008; Wang et al., 2008). Few report on the whole absorption profile of *S. chinensis* extract is available, despite the whole aqueous extract of the herb was commonly used in the traditional way.

Liquid chromatography coupled with mass spectrometry (LC-MS) has been used for rapid identification of chemical constituents in herbal extracts and drugs in biological specimens. The high sensitivity and selectivity of MS facilitate the discovery of the constituents in complex specimens. The chromatographic characters and mass spectrometric fragmentation behaviors of *Schisandra* lignans have been investigated in recent years (He et al., 1997; Zhang et al., 2008). Simultaneous LC-MS quantification of fifteen *Schisandra* lignans has been performed by Deng et al. (Deng et al., 2008), while Huang et al. analyzed the lignan constituents of a methanol extract of *S. chinensis* fruits and identified fifteen peaks including position isomers and *cis-trans* isomers (Huang et al.,

2007; Huang et al., 2008b).

In the present work, the intestinal absorption of *Schisandra chinensis* is studied using two *in vitro* models, the rat everted gut sac and the human Caco-2 cell monolayer model. As determined by HPLC-DAD-APCI-MS method, fifteen lignans are unambiguously or tentatively identified in the *in vitro* absorption profile of *S. chinensis* aqueous extract. Further, the bidirectional transport of schisandrin in Caco-2 cell model is determined. In support of *in vivo* studies, the absorbable components of *S. chinensis* and the related metabolites were also analyzed in rat plasma. Moreover, using a selective, sensitive and comprehensively validated HPLC-MS quantitative method, the pharmacokinetics of *S. chinensis* was studied with rat plasma concentrations of four major Schisandra lignans as a function of time after oral administration of an 70% ethanol extract of this herb.

3.2 Materials and methods

3.2.1 Materials, chemicals and reagents

Reference compounds, schisandrin, schisantherin A and deoxyschisandrin were purchased from National Institute for the Control of Pharmaceutical and Biological Products (Beijing, China) and were of purity >98%. Gomisin A was obtained from the Hong Kong Jockey Club Institute of Chinese Medicine with purity >97%; gomisin D, angeloylgomisin F and gomisin G (purity >95%) were gifts from Dr. Zhou Yan from the Hong Kong Jockey Club Institute of Chinese Medicine. Bicyclol (>99%) was a product

of the Beijing Union Pharmaceutical Factory. Dried berries of *Schisandra chinensis* were provided by Zhixin Pharmaceutical Co. Ltd. (Guangzhou, China), and authenticated by Ms. Zong Yuying. The voucher specimens were deposited in the temperature-control warehouse. HPLC grade acetonitrile (Fisher, Fair Lawn, NJ, USA) and trifluoroacetic acid were used for chromatography. Water was purified by Milli-Q academic purification system (Millipore, USA).

Caco-2 cells were purchased from the American Type Culture Collection (ATCC, Manassas, USA). Medium 199 powder (Gibco; with Earle's salts and L-glutamine, without NaHCO₃), Dulbecco's modified Eagle's medium (DMEM), fetal bovine serum (FBS), non-essential amino acid, antibiotics, Trypsin-EDTA (1mM) and Hank's buffer salt solution (HBSS) were obtained from Invitrogen (Carlsbad, CA). The following chemicals were purchased from Sigma Chemical Co. (St. Louis, MO): dimethylsulfoxide (DMSO), *N*-2-hydroxyethylpiperazine-*N'*-2-ethanesulfonic acid (HEPES), sodium carboxymethyl cellulose (CMC-Na) and heparin. The other chemicals for buffer solutions were analytical grade for common laboratory use. Transwells were obtained from Corning Costar (Cambridge, MA)

3.2.2 Animals

Male Sprague-Dawley rats (250–280 g) were bred and housed by the Laboratory Animal Services Centre of the Chinese University of Hong Kong. All experiments were approved by the Animal Research Ethics Committee, The Chinese University of Hong Kong. The

animals were kept in a temperature controlled room (23 ± 2 °C) with a 12-hr light-dark cycle, with free access to food and water.

3.2.3 Instrumentation

An Agilent 1100 LC-MSD-Trap-SL system (Agilent Technologies, Palo Alto, CA, USA) consisted of a degasser, an autosampler, a column compartment, a quaternary pump, a diode-array detector, and an atmospheric pressure chemical ionization (APCI) ion trap mass spectrometer. The HPLC analysis was performed on a Prevail C18 column (250mm×4.6mm I.D., 5 µm, Alltech) with a guard column (12.5mm×4.6mm I.D., 5 µm, Alltech).

3.2.4 Preparation of Schisandra extract solutions

Dried extracts of *Schisandra chinensis* were prepared as described in Chapter 2 and they were stored in a desiccator at room temperature. Solutions of *S. chinensis* water extract for *in vitro* absorption study in rat everted gut sac and Caco-2 monolayer model were prepared in Medium 199 solution and Hank's buffer salt solution at the concentrations of 10 mg/mL and 1.5 mg/mL, respectively. In the animal studies, the sample solutions were prepared by suspending the required amount of dried extract of *S. chinensis* in 0.5% sodium carboxymethyl cellulose. All solutions were freshly prepared on the day of performing experiments.

3.2.5 Preparation of standard solutions

Stock solution of schisandrin for transport study in Caco-2 cell monolayer model was prepared in 100% DMSO at a concentration of 20 mM. Working solutions were obtained by spiking the required amount of stock solution in Hank's buffer salt solution (pH 7.4, DMSO \leq 1%), giving the concentrations of 40 and 200 μ M, respectively.

In the rat pharmacokinetic study, a mixed standard stock solution for four Schisandra lignans was prepared in methanol at the concentrations of 25 μ g/mL for schisandrin (SCH-1), 12.5 μ g/mL for gomisin A (SCH-2), 5 μ g/mL for deoxyschisandrin (SCH-3) and 5 μ g/mL for γ -schisandrin (SCH-4), respectively. A serial dilution with methanol was performed and the working standards were prepared by spiking blank plasma (180 μ L) with corresponding methanolic diluents (20 μ L) and bicyclol solution (10 μ L, 10 μ g/mL). The stock solutions were stored at -20 °C and the calibrators were freshly prepared for each determination.

3.2.6 Experimental protocols of *in vitro* absorption

3.2.6.1 Rat everted gut sac

Six adult male Sprague-Dawley rats (250–300g) were fasted overnight, sacrificed by cervical dislocation, and the small intestine, except for the duodenum section, was removed and flushed three times with normal saline at room temperature. The intestine

was then immediately placed in 37 °C and oxygenated (O₂/CO₂, 95%:5%) medium TC 199 solution. With the aid of a smooth glass rod, the intestine was everted gently and sealed with silk braided sutures in one end before the gac sac was filled with 20 mL fresh medium TC199. After the other end was sealed, two small gut sacs (3 – 4 cm in length) were tied with sutures. Each sac was placed in a 50 mL Erlenmeyer flask containing 10 mL medium with or without *S. chinensis* extract (10 mg of powder per mL); they were the treatment group and control group, respectively. The sacs were incubated at 37 °C in an oscillating water bath (50 cycles / min) for 90 min, bubbled by gas (O₂/CO₂, 95:5%). Afterwards, the sacs were taken out, washed with saline and blotted dry. Then, the sacs were cut open and the serosal side solution, which should contain the absorbable components of *S. chinensis* extract, as well as the mucosal side solution, was harvested for analysis. The rat everted gut sac system is described in Fig. 3-1. The viability of the sacs was monitored by glucose uptake experiments by measuring the glucose concentrations in serosal and mucosal solutions with glucose assay kit (Sigma, St. Louis, MO). All samples were stored at -20 °C in a medical freezer until HPLC-MS analysis.

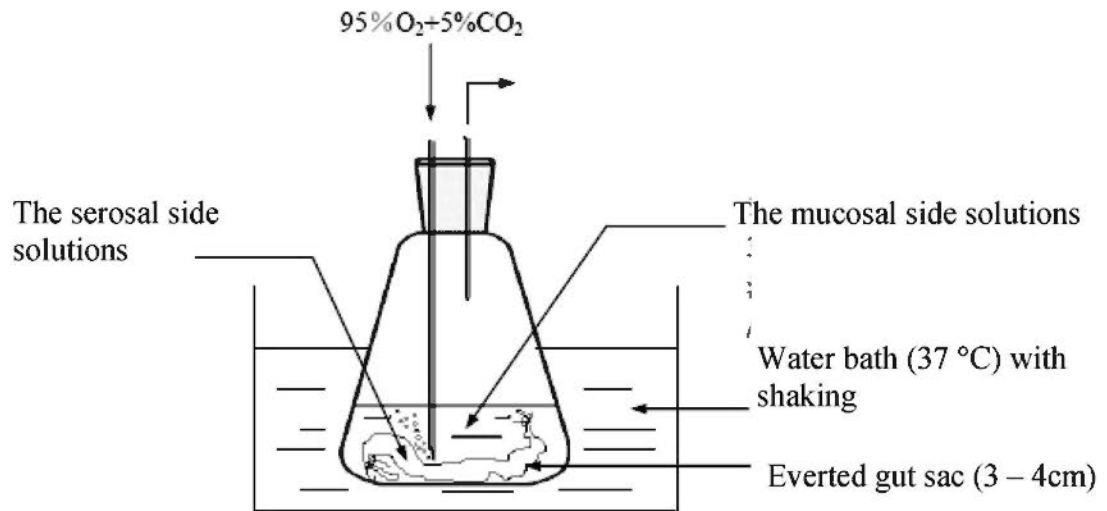


Fig. 3-1 The rat everted gut sac system. A rat everted gut sac was incubated with M199 medium solution containing Schisandra water extract at 37 °C gassed with 95% O₂ and 5% CO₂. The absorption direction was referred to as being from the mucosal side to the serosal side.

3.2.6.2 Human Caco-2 cell monolayer model

Human colonic adenocarcinoma (Caco-2) cells were cultured in DMEM medium supplemented with 10% fetal bovine serum (FBS), 1% non-essential amino acid, and 1% penicillin-streptomycin at 37 °C in a humidified air – 5% CO₂ atmosphere. Cells were seeded in Transwell inserts coated with collagen at a density of 3×10⁵ cells / well and cultured for 21 days prior to the transport experiments. The medium (1.5 mL in the apical side and 2.6 mL in the basolateral side) was changed every other day. Cytotoxic effects of the test drugs on Caco-2 cells were pre-evaluated using MTT assay with 180 min co-incubation. The integrity of cell monolayer was monitored by measurement of transepithelial electrical resistance (TEER) value before and after transport study using the Millicell-ERS system from Millipore Corp. (Bedford, MA); the ones showing less than 800 Ω•cm² were not used.

The monolayers were washed with the transport buffer, Hank's buffer saline (HBS) solution containing 10 mM HEPES (pH 7.4), and were preincubated for 25 min at 37 °C. In the absorption study of *S. chinensis* aqueous extract, after removal of the solutions, 1.5 mL of fresh transfer buffer with or without the extract at a concentration of 2 mg/mL extract powder, corresponding to the treatment group and control group respectively, was added to the apical chamber and incubated at 37 °C. Aliquots (500 µL) were taken from the basolateral chamber at 60, 120, 180 min and replaced with equal volume of transfer buffer after each sampling. At the end of transport study, samples of both sides were

collected for analysis.

In the transport study of schisandrin, bidirectional studies were initiated by the addition of transfer buffer containing schisandrin (40 μM or 200 μM in $\leq 1\%$ DMSO) to the apical chamber in apical (A) to basolateral (B) studies or to the basolateral chamber in basolateral to apical studies, respectively. Aliquots were taken from the receiver chamber at different time intervals (20, 40, 60, 90, 120, 180 min). Samples in both chambers were collected for the analysis of permeability and recovery at the end of transport. All samples were stored at $-20\text{ }^{\circ}\text{C}$ until analysis. The transwell system of Caco-2 cell monolayer model is described in Fig. 3-2.

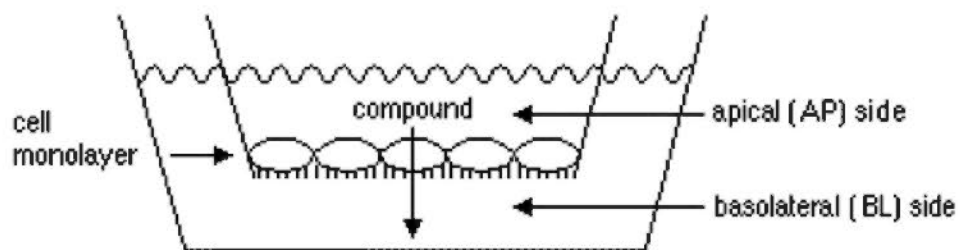


Fig. 3-2 The transwell system of Caco-2 cell monolayer model. The transport direction of compound is referred to as being from the apical side (donor) to basolateral side

(receiver).

3.2.7 Pharmacokinetic study in the rat

Male SD rats (250 – 280 g) were fasted overnight before the pharmacokinetic study. The sample solution was prepared by suspending the required amount of dried extract of *S. chinensis* in 0.5% sodium carboxymethyl cellulose (CMC-Na). Rats were given a single oral administration of Schisandra extract at the dosage of 2 g/kg for 70% ethanol extract (equivalent to 30.95 mg/kg for schisandrin, 14.40 mg/kg for gomisin A, 4.63 mg/kg for deoxyschisandrin, 17.06 mg/kg for γ -schisandrin) and 4 g/kg for water extract (equivalent to 11.84 mg/kg for schisandrin, 3.4 mg/kg for gomisin A, 0.20 mg/kg for deoxyschisandrin, 0.24 mg/kg for γ -schisandrin). Plasma pharmacokinetics was performed at the intervals of 0, 0.25, 0.5, 1, 1.5, 2, 3, 4, 6, 8, 10, 12, 24 hour. Blood samples of about 0.3 mL were collected by orbital bleeding via heparinized capillary tubes under anesthetizing with isoflurane, and centrifuged at 7000 \times g for 10 min at room temperature. Plasma (about 0.15 mL) was obtained and frozen at -20 °C prior to HPLC-MS analysis.

3.2.8 High performance liquid chromatography and mass spectrometry (HPLC-MS)

3.2.8.1 Analysis of absorption profile

The samples were separated by HPLC at a flow rate of 0.8 mL/min after filtration through 0.45 μ m filter. The mobile phase consisted of 0.1% trifluoroacetic acid water (A)

and acetonitrile (B) with a gradient elution of 20% B at 0 – 5 min; 45% B at 6 – 35 min; 45 – 60% at 35 – 50 min; 60 – 100% B at 50–60 min. The column temperature was 25 °C. The injection volume was 60 µL and the detection wavelengths were set at 210, 230, 254 and 280 nm. The effluent was directly introduced to the APCI-MS.

The APCI-MS analysis was divided into two time segments. The first four minutes was set as waste to avoid the influx of inorganic ions into the mass analyzer and the other segment was set for sample analysis with the following optimized conditions: positive ion mode; nebulizer (N₂), 60 psi; dry gas (N₂), 5 L/min; drying gas temperature, 325 °C; corona current, 4000 nA; target mass, 500 *m/z*; compound stability, 80%; trap drive level, 80%, full scan range, 140–1100 *m/z*. Two precursor ions were selected for MSⁿ experiments in automatic mode with active exclusion (after 2 spectra). The fragmentation amplitude was 1.20 V. Collected data were processed by Agilent 1100 Chemstation version 09.03, and LC/MSD Trap software version 4.2 (Agilent Technologies).

3.2.8.2 Quantification of schisandrin

Separation of schisandrin was achieved by an isocratic elution HPLC system using a mobile phase of water (0.1% trifluoroacetic acid) and 50% acetonitrile at a flow rate of 0.8 mL/min. The injection volume was 60 µL and detection wavelength of DAD was set at 230 nm. Quantitative analysis of schisandrin was performed on six levels of external standards. Method validation covered the linearity of calibration curve, limits of detection

and quantification, precision, accuracy and stability. The retention time of schisandrin was 8.9 min. The calibration curves showed good linear correlation ($r^2 = 0.9998$) between peak area and concentration in the range of 5 – 250 μM . Precision of the method was in the acceptable limits with R.S.D. <0.5%. Samples were stable within 48 h at room temperature (R.S.D. <3%). Adequate detection limit (0.4 μM) and quantification limit (1 μM) enabled the quantitative analysis of schisandrin in the transport study.

3.2.8.3 Quantification of Schisandra lignans in rat plasma

3.2.8.3.1 Sample processing

Frozen plasma was allowed to thaw at room temperature. Fibrin deposits were removed by centrifugation at $10000 \times g$ for 2 min. Aliquot of each sample (100 μl) was spiked with 5 μl internal standard bicyclol (10 $\mu\text{g}/\text{mL}$ in methanol). Acetonitrile (150 μl) was added for protein precipitation and analyte extraction. The mixture was vortex-mixed for 30 s and centrifuged at $10000 \times g$ for 15 min at room temperature. The supernatant was removed and 80 μl was injected into the HPLC-MS system.

3.2.8.3.2 HPLC-MS conditions

The samples were separated at a flow rate of 0.8 mL/min with an operating temperature of 25 °C. The mobile phase consisted of 0.1% trifluoroacetic acid water (A) and acetonitrile (B) programmed to a gradient elution of 50 – 70% B at 0 – 25 min; 70 –

100% at 25 – 30 min. The effluent was introduced to APCI-MS ion trap with positive mode. The Schisandra lignans were analyzed in selected ion monitoring (SIM) mode at m/z 415 for schisandrin (SCH-1), m/z 399 for gomisin A (SCH-2), m/z 417 for deoxyschisandrin (SCH-3), m/z 401 for γ -schisandrin (SCH-4) and m/z 373 for bicyclol (internal standard), respectively. MS conditions were optimized as follow: nebulizer (N_2), 60 psi; dry gas (N_2), 5 l/min; drying gas temperature, 325 °C; corona current, 4000 nA; compound stability, 80%; trap drive level, 80%.

3.2.8.3.3 Method validation

3.2.8.3.3.1 Linearity, precision and accuracy

The linearity of the method was evaluated by construction of calibration curves at a concentration range of 0.025–2.5 $\mu\text{g/mL}$ for SCH-1, 0.0125–1.25 $\mu\text{g/mL}$ for SCH-2, 0.005–0.5 $\mu\text{g/mL}$ for SCH-3 and 0.005–0.5 $\mu\text{g/mL}$ for SCH-4. Calibration curve for each analyte was obtained by plotting the peak-area ratio (analyte versus internal standard) against the corresponding analyte concentration. Quantification was performed upon seven levels of external standards.

The precision and accuracy were evaluated by analyzing samples of mixed reference standard at high concentrations of 2, 1, 0.4 and 0.4 $\mu\text{g/mL}$, medium concentrations of 0.5, 0.25, 0.1 and 0.1 $\mu\text{g/mL}$, and low concentrations of 0.125, 0.0625, 0.0025 and 0.0025

µg/mL for SCH-1, SCH-2, SCH-3 and SCH-4, respectively. The intra-day variance was determined by assaying six replicates in a single day and inter-day variance was assayed at 12, 24, 48 and 72 h in three consecutive days. Accuracy was determined by comparing the calculated concentration to the known concentration.

3.2.8.3.3.2 Stability

Stability of samples was tested by analyzing spiked samples of mixed reference standard at three concentration levels at 12, 24, 48 and 72 h in three consecutive days. Variation was expressed as the relative standard deviation (R.S.D.).

3.2.8.3.3.3 Recovery

The recovery of each analyte was obtained by comparing the peak area ratio determined in the spiked plasma solution with that in methanol solution. Three concentration levels of standard solutions at three replicate were determined to calculate the recoveries.

3.2.8.3.3.4 Pharmacokinetic data analysis

Data fitting and pharmacokinetic parameter calculation were performed by PK solutions version 2. Plasma concentration-time curves were plotted using a single compartment module. Values were expressed as mean \pm S.E.M..

3.3 Results

3.3.1 Absorption of Schisandra aqueous extract *in vitro*

3.3.1.1 Absorption profile of Schisandra extract in rat everted gut sac

The viability of everted sacs was maintained for up to 120 min, as suggested by the glucose concentrations in the serosal solution increasing gradually from 0.30 to 0.58 mg/mL during this period of time. Figure 3-3 shows the base peak chromatograms of samples detected in positive mode. On the basis of experimental data, including retention time, UV spectra (if available) and MSⁿ fragmentation data, fifteen peaks were unambiguously identified or tentatively characterized in the serosal solution of the rat everted gut sac model. All fifteen compounds were identified to be Schisandra lignans, denoted as schisandrin (C1), gomisin D (C2), gomisin A (C3), angeloylgomisin H (C4 or C5), tigloylgomisin H (C4 or C5), angeloylgomisin Q (C6 or C7), tigloylgomisin Q (C6 or C7), tigloylgomisin F (C8), angeloylgomisin F (C9), gomisin G (C10), schisantherin B (C11 or C12), schisantherin C (C11 or C12), schisantherin A (C13), gomisin E (C14) and deoxyschisandrin (C15). Their chemical structures are shown in Figure 3-4.

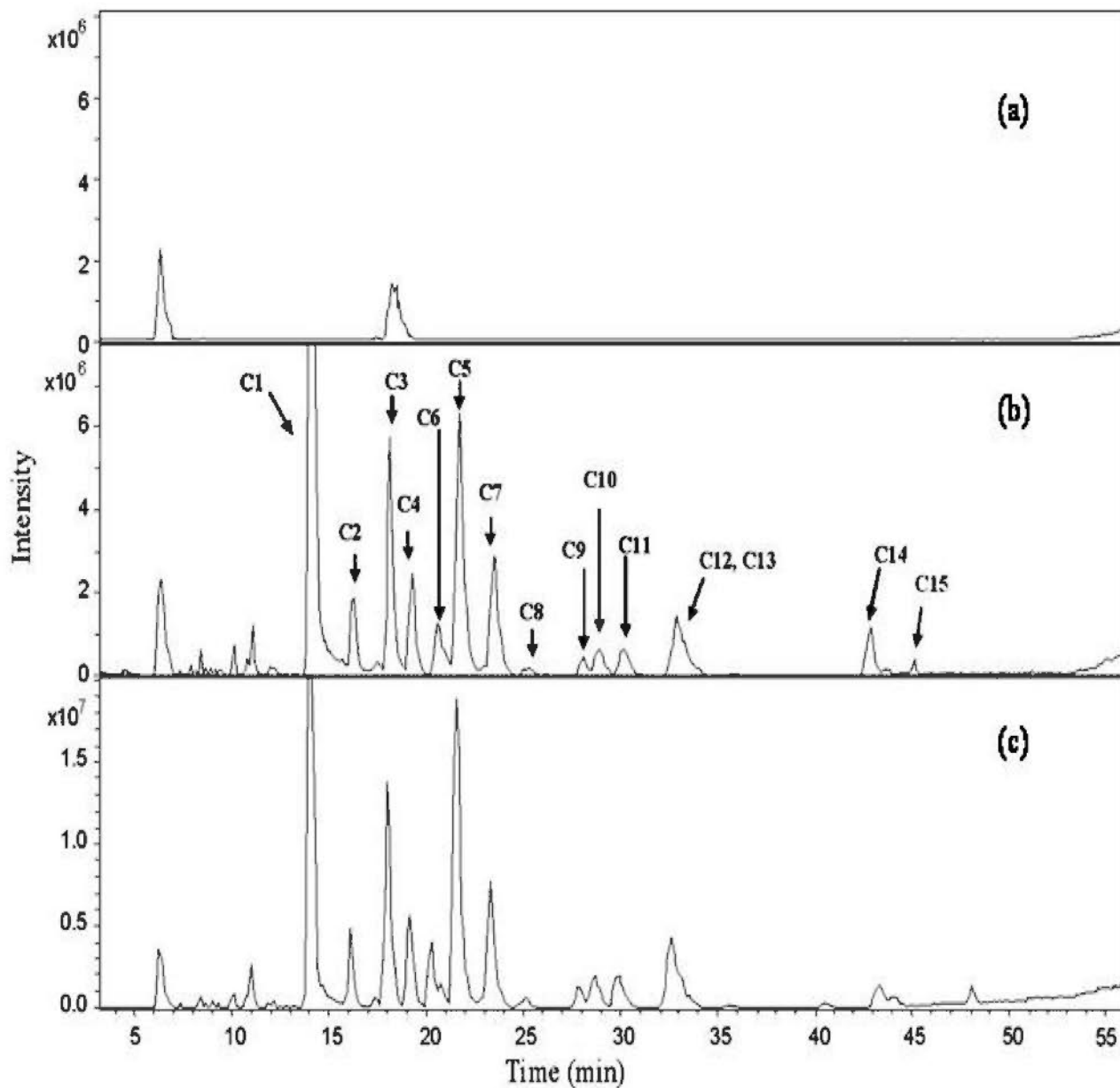


Fig. 3-3 Representative HPLC-MS basic peak chromatograms (BPC) in positive mode of serosal fluid after 90 min incubation in the rat everted gut sac. (a) Control serosal solution, (b) Serosal solution and (c) Mucosal solution incubated with medium containing Schisandra water extract at a concentration of 10 mg/mL. C1 to C15 denote compounds 1-15.

Compound	Structure	R1	R2	R3	R4	R5	R6	R7
Schisandrins		-	-	MeO	MeO	MeO	OH	-
Gomisin A		-	-	MeO	-OCH ₂ O-		OH	-
Angeloylgomisin H		-	-	OAng	MeO	MeO	OH	-
Tigloylgomisin H		-	-	OTig	MeO	MeO	OH	-
Deoxyschisandrins		-	-	MeO	MeO	MeO	H	-
Angeloylgomisin Q		MeO	MeO	MeO	MeO	MeO	OH	OAng
Tigloylgomisin Q		MeO	MeO	MeO	MeO	MeO	OH	OTig
Angeloylgomisin F		-OCH ₂ O-		MeO	MeO	MeO	OH	OAng
Tigloylgomisin F		-OCH ₂ O-		MeO	MeO	MeO	OH	OTig
Gomisin G		-OCH ₂ O-		MeO	MeO	MeO	OH	OBen
Schisantherin B		MeO	MeO	MeO	-OCH ₂ O-		OH	OAng
Schisantherin C		MeO	MeO	MeO	-OCH ₂ O-		OH	OTig
Schisantherin A		MeO	MeO	MeO	-OCH ₂ O-		OH	OBen
Gomisin D			-	-	-	-	-	OH
Gomisin E	-		-	-	-	-	MeO	H

Fig. 3-4 Chemical structures of fifteen Schisandra lignans characterized in the rat everted gut sac and Caco-2 cell monolayer model *in vitro*.

3.3.1.2 Absorption profile of Schisandra extract in Caco-2 cell monolayer model

The cytotoxic effect of Schisandra aqueous extract on Caco-2 cells was pre-evaluated using MTT assay. There was no viability reduction observed at concentration below 2 mg/mL, while cell viability decreased about 80% when the extract concentration was higher than 4 mg/mL. Thus the Schisandra aqueous extract for transport studies was prepared at the concentration of 1.5 mg/mL. The integrity of cell monolayer was also monitored by measuring transepithelial electrical resistance (TEER) value before and after transport study, and the ones showing resistance below $800 \Omega \cdot \text{cm}^2$ were rejected.

Figure 3-5 shows the base peak chromatograms of the samples detected in positive mode. As analyzed using HPLC-MS method, the fifteen peaks (C1–C15, denoting compounds 1–15) previously identified in the serosal solution of rat everted gut sac model could also be found in the basolateral solution of the Caco-2 cell monolayer model. They could be regarded as the major absorbable components of the Schisandra aqueous extract. The lower intensity of C14 and C15 found in the Caco-2 cell model than in the rat everted gut sac could be explained by the low concentration of extract used in the cell model. The chemical structures of identified compounds are shown in Figure 3-4.

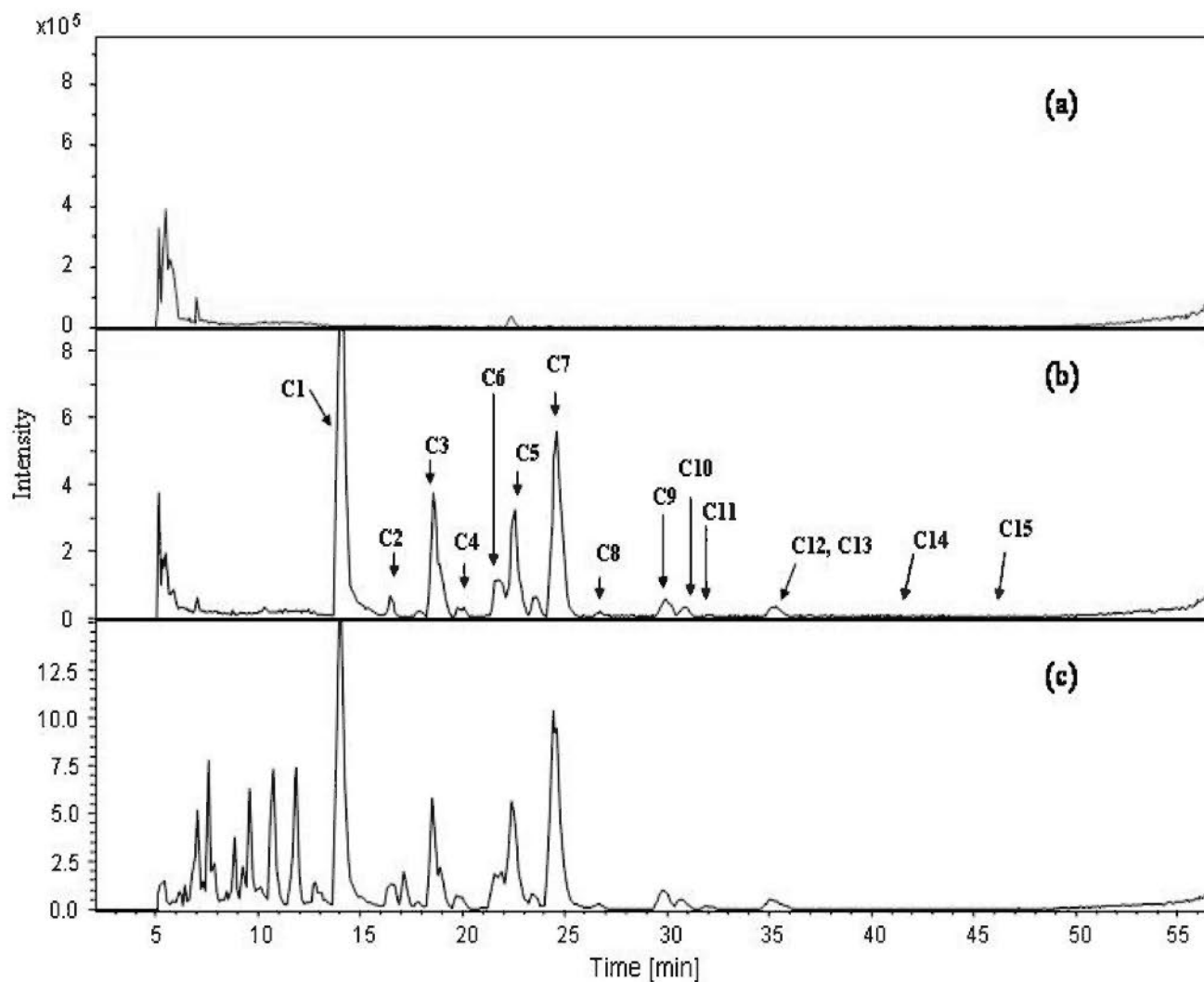


Fig. 3-5 Representative HPLC-MS basic peak chromatograms (BPC) in positive mode of samples obtained from the Caco-2 cell monolayer model after 180 min incubation. (a) Control basolateral solution. (b) Basolateral solution and (c) Apical solution incubated with Hank's buffer containing *S. chinensis* aqueous extract at a concentration of 1.5 mg/mL. C1 to C15 denote compounds 1–15.

3.3.1.3 HPLC-DAD-APCI-MS analysis

3.3.1.3.1 Analysis of reference compounds

Fig. 3-6 shows the chromatogram of seven reference compounds, namely, schisandrin, gomisin D, gomisin A, angeloylgomisin F, gomisin G, schisantherin A, deoxyschisandrin, each of which was characterized by retention time, UV spectral and APCI-MSⁿ spectral data. UV spectra of the reference compounds are presented in Fig. 3-7. The above information was useful for comparison with the data obtained from the compounds present in the experimental specimen. Positive ion mode was selected for the determination in this study as the extensive structural information via collision-induced dissociation (CID) could be obtained.

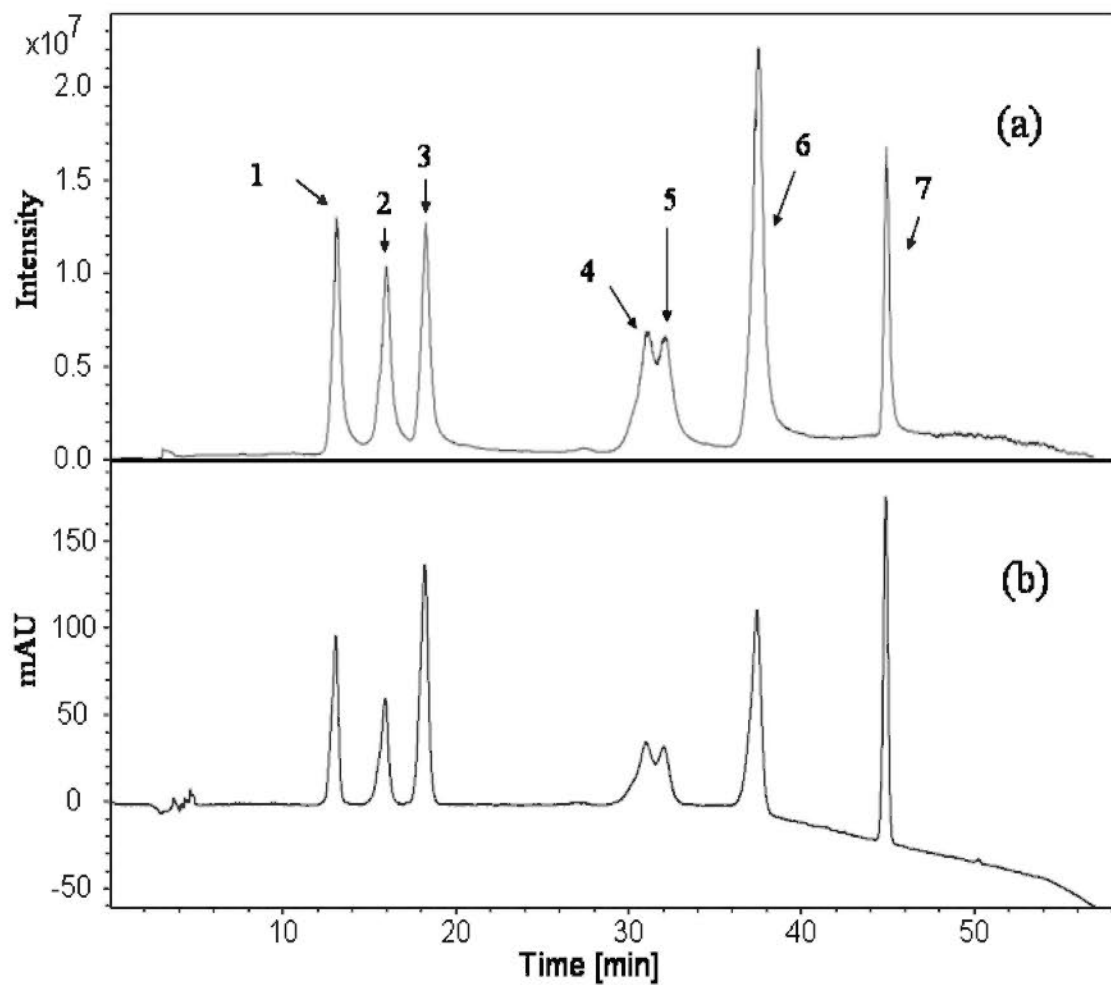


Fig. 3-6 Representative HPLC-DAD-APCI-MS chromatograms of reference compounds. (a) Total ion chromatogram (TIC) at positive mode. (b) UV chromatogram at 230nm. 1-7 denote schisandrin, gomisin D, gomisin A, angeloylgomisin F, gomisin G, schisantherin A, and deoxyschisandrin.

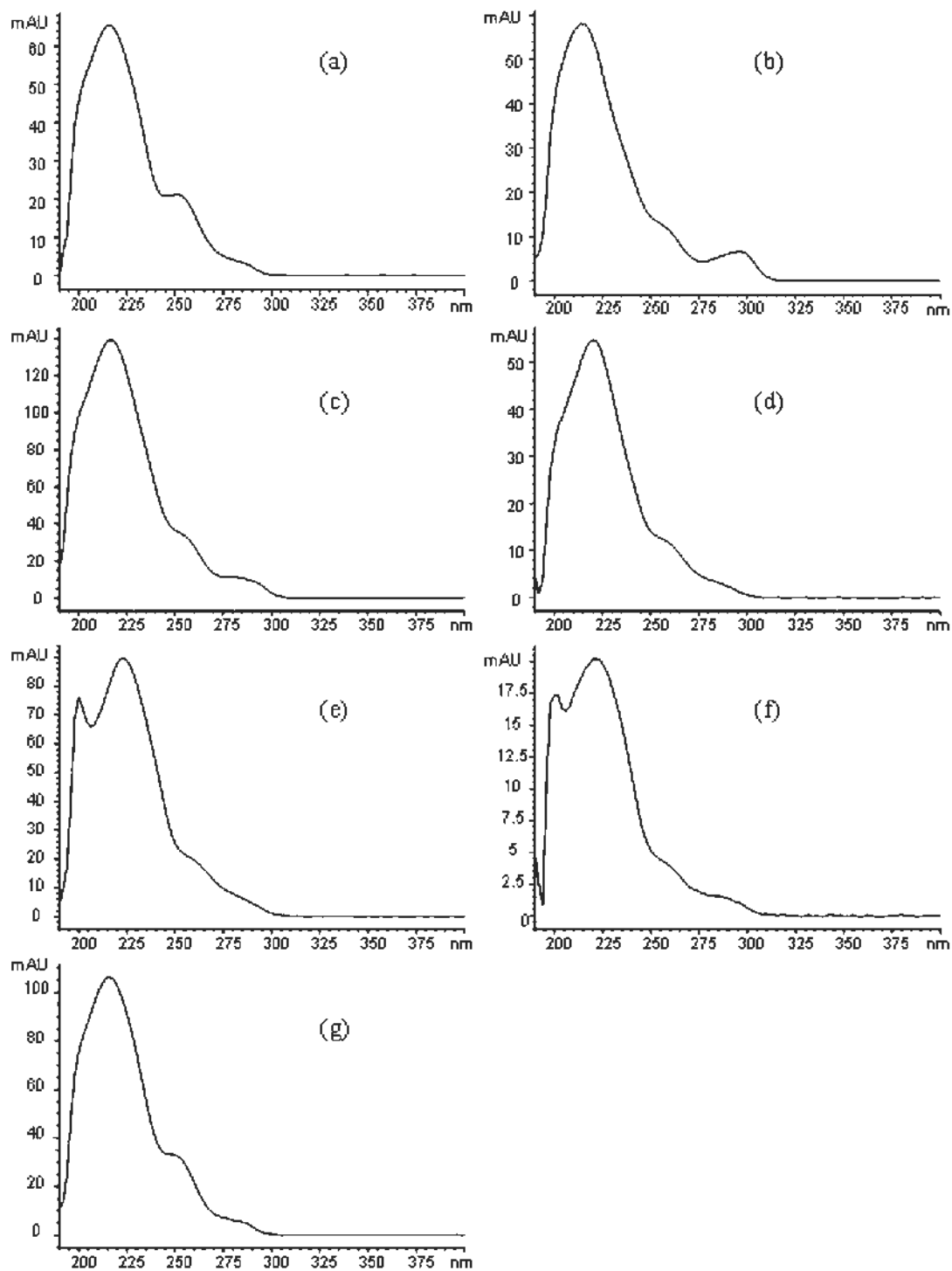


Fig. 3-7 UV spectra of reference compounds (a) schisandrin, (b) gomisin D, (c) gomisin A, (d) angeloylgomisin F, (e) gomisin G, (f) schisantherin A, (g) deoxyschisandrin.

The retention time of schisandrin was 13.2 min, with UV λ_{max} at 217, 252 and 286 nm. The MS spectrum (Fig. 3-8) showed two ions with high abundance. The protonated ion $[\text{M}+\text{H}]^+$ at m/z 433 and the adduct ion $[\text{M}+\text{H}-\text{H}_2\text{O}]^+$ at m/z 415 resulted from the loss of a molecule of water to form a double bond between C-7 and C-8. In the MS² spectrum, the m/z 433 ion yielded the only product ion at m/z 415. The MS² spectrum of the m/z 415 ion further showed product ions at m/z 400, 384, 373 and 359, presumably formed by the elimination of CH₃, CH₃O, C₃H₆ and C₄H₈, respectively. The fragment ions at m/z 369 and 353 from the precursor ion at m/z 384 were formed by the loss of CH₃ and CH₃O group respectively. The suggested fragmentation pathway of schisandrin is proposed in Fig. 3-9, which was consistent with the previous report (Huang et al., 2007).

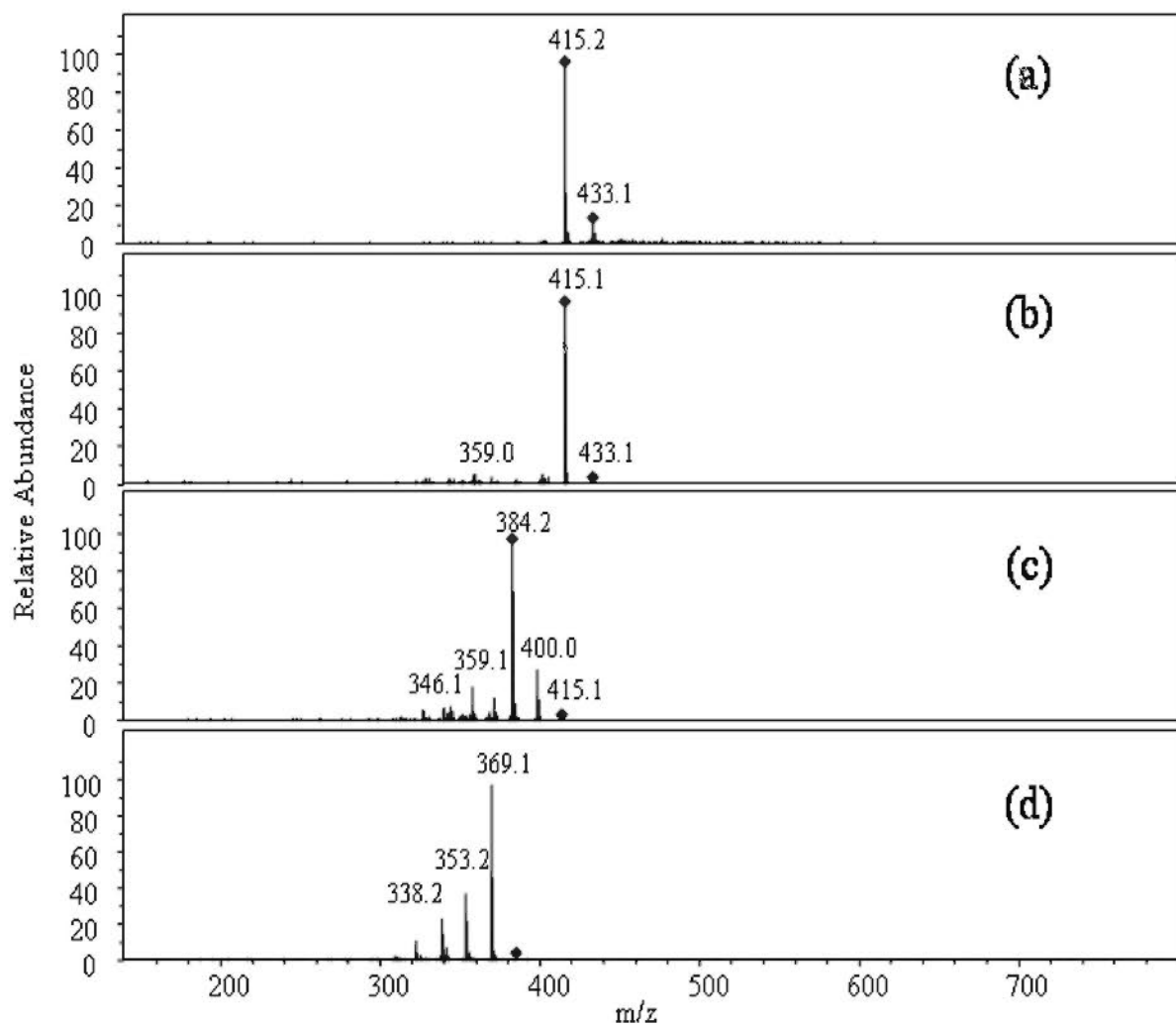


Fig. 3-8 MSⁿ spectra of schisandrin. (a) MS spectrum of schisandrin. (b) MS² spectrum of the $[M+H]^+$ ion at m/z 433. (c) MS² spectrum of the $[M+H-H_2O]^+$ ion at m/z 415. (d) MS³ spectrum of the ion at m/z 384.

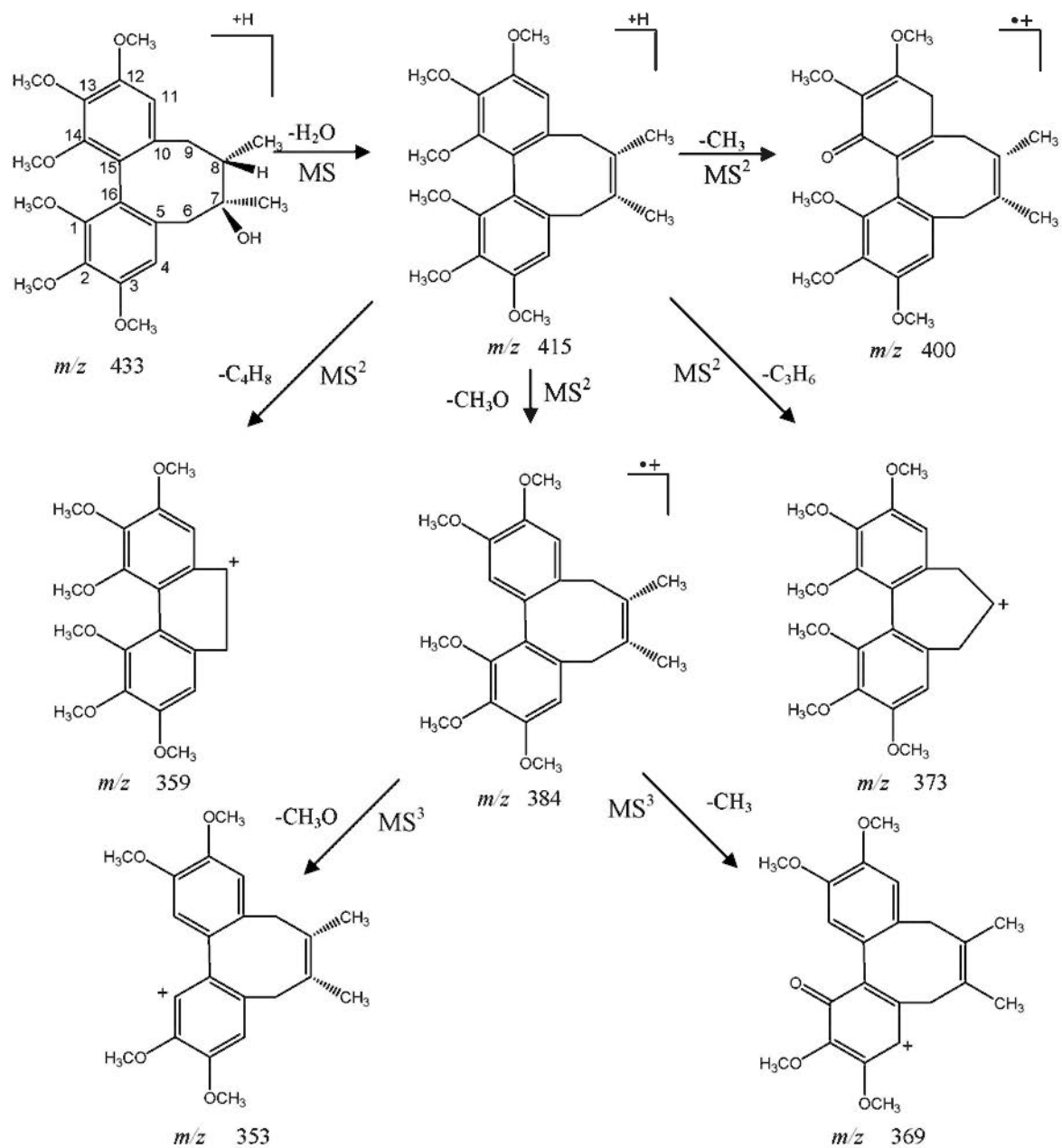


Fig. 3-9 Proposed fragmentation pathway of schisandrin

The retention time of gomisin A was 16.1 min with UV λ_{max} at 218, 256 and 286 nm. As shown in Fig. 3-10, it exhibited an intense ion $[\text{M}+\text{H}-\text{H}_2\text{O}]^+$ at m/z 399 as the base peak. In the MS^2 spectrum of the m/z 399 ion, fragment product ions at m/z 384, 369, 368, 357, 343 and 337 were found, and the m/z 368 ion was further fragmented to ions at m/z , 353 and 337 in MS^3 experiment. The mass difference between them was 15, 30, 31, 42, 56 and 62 Da, respectively. These daughter ions were presumably formed via analogous fragmentation route as the m/z 415 ion in schisandrin, except for the distinguishing ion at m/z 369 which was produced by the loss of CH_2O , indicating the presence of methylenedioxy group in gomisin A. In the MS^3 experiment, the m/z 368 ion produced product ions at m/z 353 and 337 by the elimination of CH_3 and CH_3O respectively.

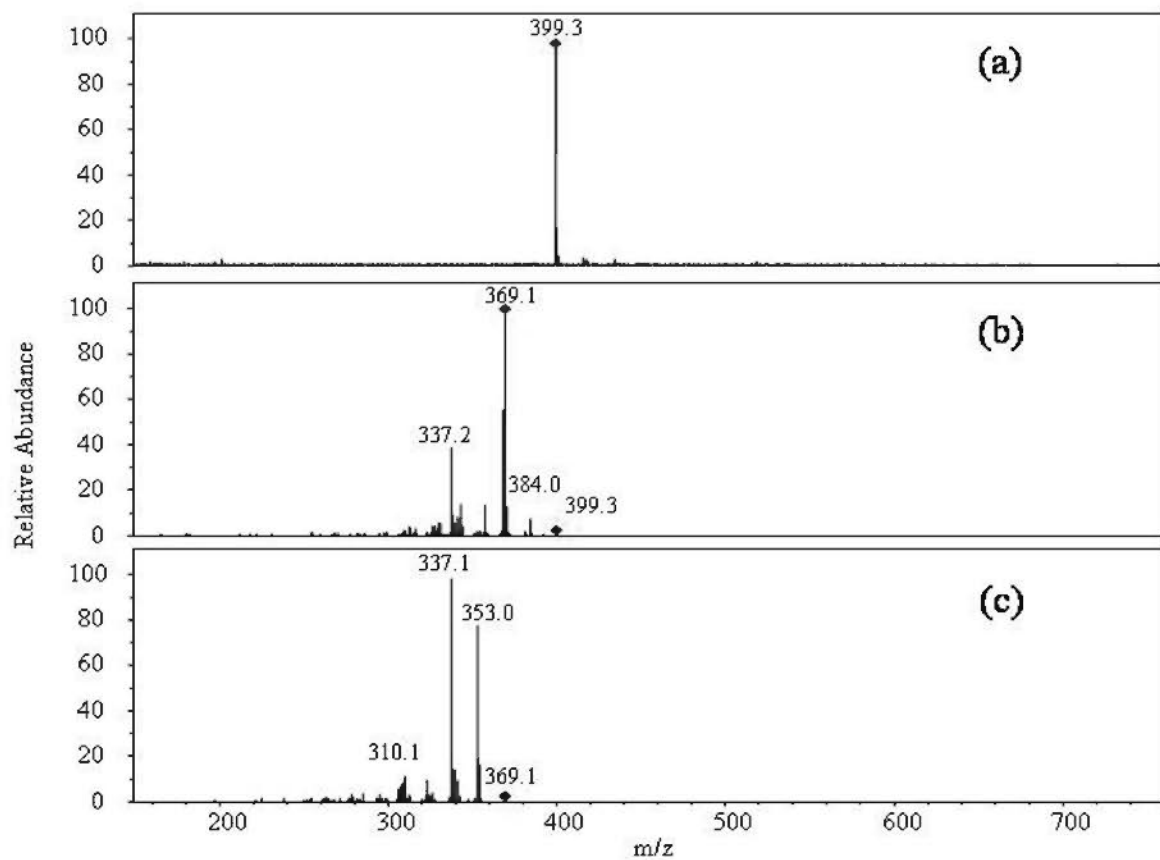


Fig. 3-10 MSⁿ spectra of gomisin A. (a) MS spectrum of gomisin A. (b) MS² spectrum of the [M+H-H₂O]⁺ ion at *m/z* 399. (c) MS³ spectrum of the ion at *m/z* 369.

The retention time of schisantherin A was 37.8 min and the UV λ_{\max} was at 202, 224, 260 and 290 nm. As presented in Fig. 3-11, it exhibited an adduct ion at m/z 554 as its base peak. Since the presence of ester bond in the structure of schisantherin A may facilitate formation of an adduct ion $[M+H_2O]^{+\bullet}$, the m/z 554 ion was likely generated by addition of $H_2O^{+\bullet}$. The other significant ion at m/z 415, which was also the only product ion of the m/z 554 ion, was likely formed by losing a molecule of benzoic acid ($\Delta m = 122u$) and a radical group of OH. In MS^2 spectrum of the m/z 415 ion, it gave rise to the product ions at m/z 397 $[M+H-C_6H_5COOH-H_2O]^+$, 385 $[M+H-C_6H_5COOH-CH_2O]^+$, 373 $[M+H-C_6H_5COOH-C_3H_6]^+$ and 371 $[M+H-C_6H_5COOH-C_2H_4O]^+$. The abundant m/z 371 ion further produced fragment ions at m/z 356 $[M+H-C_6H_5COOH-C_2H_4O-CH_3]^{+\bullet}$, 341 $[M+H-C_6H_5COOH-C_2H_4O-CH_2O]^+$, 340 $[M+H-C_6H_5COOH-C_2H_4O-CH_3O]^{+\bullet}$ in its MS^3 spectrum. A similar fragmentation pattern has been reported in the literature (Huang et al., 2007).

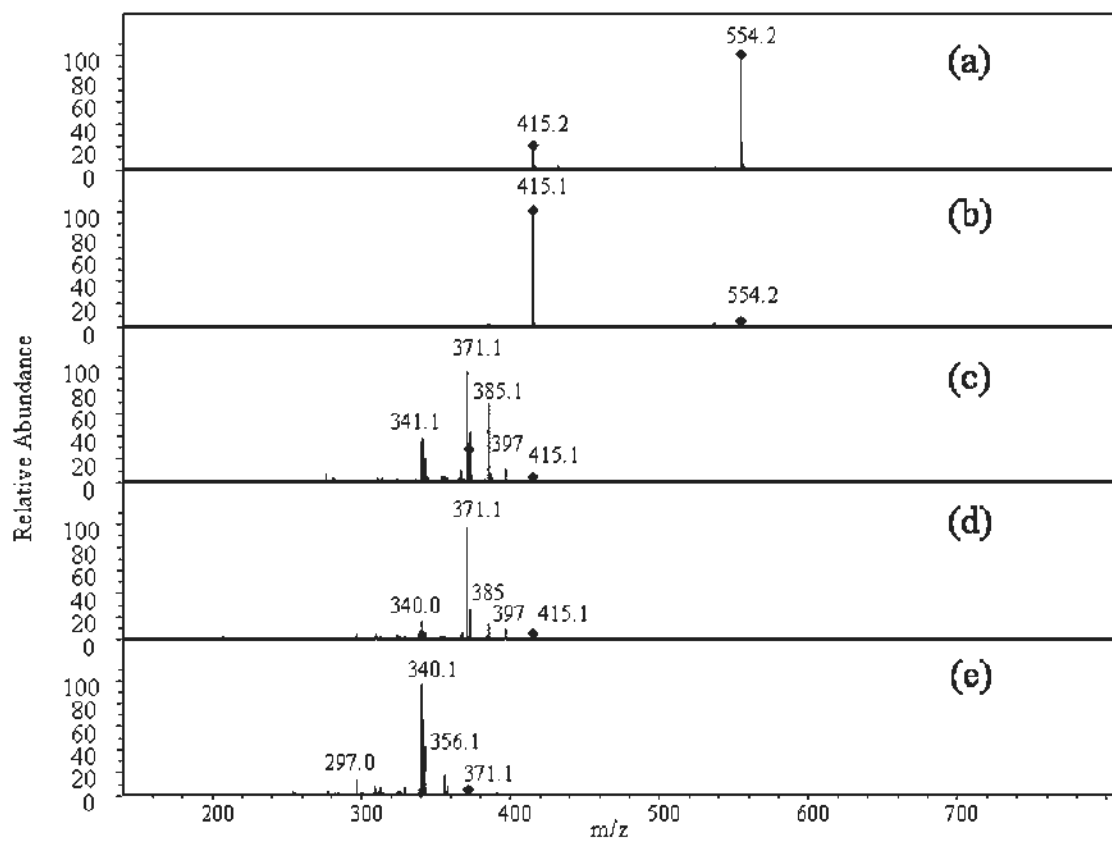


Fig. 3-11 MSⁿ spectra of schisantherin A. (a) MS spectrum of schisantherin A. (b) MS² spectrum of the ion at m/z 554. (c) MS² spectrum of the ion at m/z 415. (d) MS³ spectrum of the ion at m/z 415. (e) MS³ spectrum of the ion at m/z 371.

The retention time of gomisin D was 14.0 min with UV λ_{max} at 216, 258 and 298 nm. It gave a protonated ion at m/z 531 and an intense adduct ion $[M+H_2O]^+$ at m/z 548, like schisantherin A. Fig. 3-12 shows that the m/z 548 ion formed product ions at m/z 531, 485 and 401 in the MS² fragmentation. In the MS² spectrum of the m/z 531 ion, it further gave fragment ions at m/z 485, 401 and 383. According to the structure of gomisin D, the m/z 485 ion likely resulted from the neutral loss of HCOOH from the precursor ion at m/z 531, and the ion at m/z 401 was formed by the elimination of a molecule of 2-hydroxyl-2,3-dimethyl-3-butenoic acid ($\Delta m = 130u$). This proposed fragmentation pathway was supported by the MS³ spectrum of the m/z 401 ion, which produced an abundant fragment ion at m/z 383 through the loss of H₂O, similar to the MS² data of the m/z 433 ion of schisandrin. In addition, the MS³ experiment of the m/z 401 ion also gave rise to notable product ions at m/z 353 and 341, presumably formed by subsequent loss of CH₂O and C₃H₆ following the elimination of H₂O, respectively.

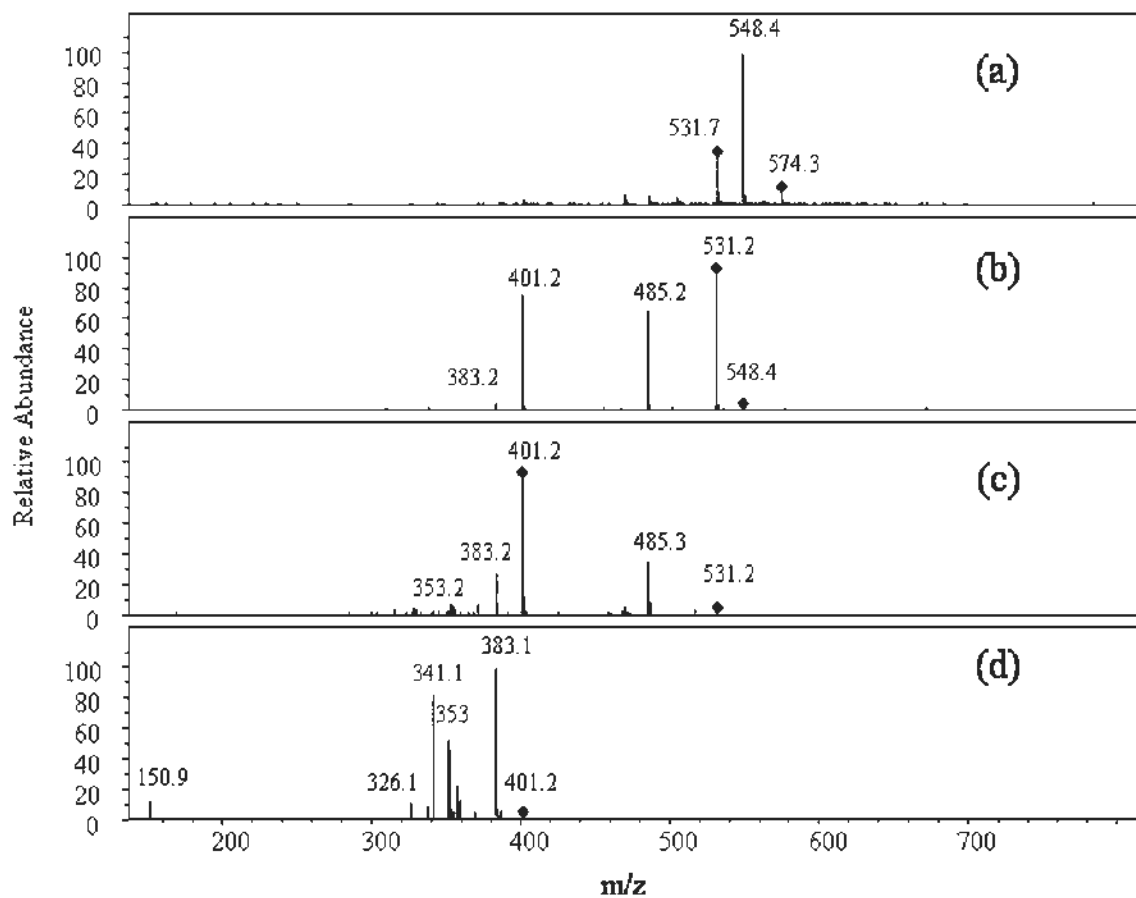


Fig. 3-12 MSⁿ spectra of gomisin D. (a) MS spectrum of gomisin D. (b) MS² spectrum of the ion at m/z 548. (c) MS² spectrum of the ion at m/z 531. (d) MS³ spectrum of the ion at m/z 401.

The retention time of angeloylgomisin F was 31.4 min with UV λ_{max} at 222, 258 and 285 nm. As presented in Fig. 3-13, it showed an adduct ion $[M+H_2O]^{+\bullet}$ at m/z 532 as the base peak and a significant ion $[M+H-C_5H_8O_2]^+$ at m/z 415. Also, the ion at m/z 532 yielded the only product ion at m/z 415, which was presumably generated by the loss of 2-methyl-2-butenic acid ($\Delta m = 100u$) and OH group. In the MS² spectrum of the m/z 415 ion, product ions at m/z 397, 383, 373, 371, 356 and 341 were found, which was similar to the fragmentation of the m/z 415 ion of schisantherin A, except for the diagnostic ions at m/z 383 and 341 in fragmentation of angeloylgomisin F due to the different substitution site of methylenedioxy group. The m/z 383 ion was derived from the loss of CH₃OH and the ion at m/z 341 arose from the loss of C₂H₄O and CH₂O. In the MS³ experiment, the precursor ion at m/z 371 gave rise to product ions at m/z 341 and 340 by losing CH₂O and CH₃O group, respectively.

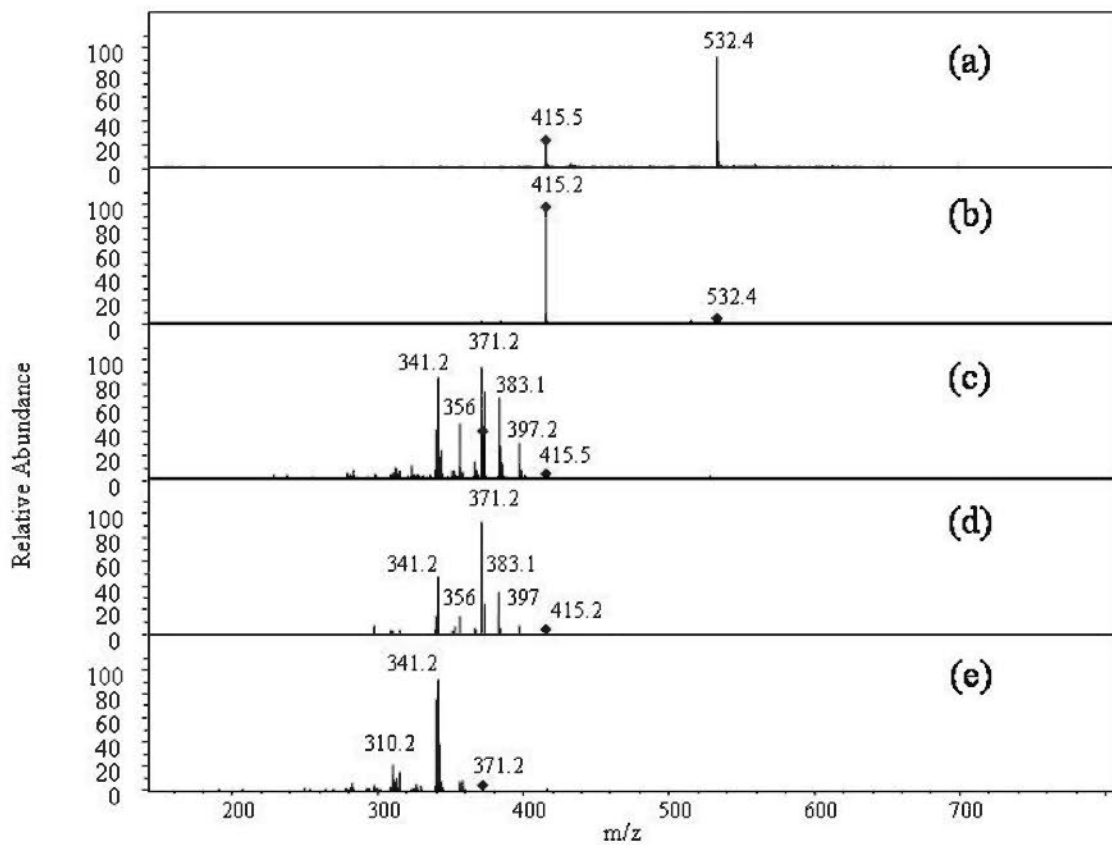


Fig. 3-13 MSⁿ spectra of angeloylgomisin F. (a) MS spectrum of angeloylgomisin F. (b) MS² spectrum of the ion at *m/z* 532. (c) MS² spectrum of the ion at *m/z* 415. (d) MS³ spectrum of the ion at *m/z* 415. (e) MS³ spectrum of the ion at *m/z* 371.

The retention time of gomisin G was 32.5 min and its UV λ_{\max} was observed at 202, 225, 260 and 280 nm. Fig. 3-14 showed that the adduct ion $[M+H_2O]^+$ at m/z 554 was the base peak and an intense ion at m/z 415 was also observed, which was identical with the MS data of schisantherin A. According to the structure of gomisin G, the m/z 415 ion could have been derived from the loss of a molecule of benzoic acid at C6. In the MS² spectrum of the m/z 415 ion, however, it gave rise to product ions at m/z 397, 383, 373, 371, 356, 341 and 340, which was identical with that of angeloylgomisin F while distinguished from schisantherin A by the diagnostic ions at m/z 383 and 341 of gomisin G. This observation was due to the identical skeleton owned by these three compounds except for the different substitution sites of methylenedioxy group at C12-13 (for schisantherin A) and C2-3 (for angeloylgomisin F and gomisin G), resulting in different fragmentations of the m/z 415 ions. The MS³ spectrum of the m/z 371 ion, which was identical with that of angeloylgomisin F, further confirmed the proposed fragmentation pathways.

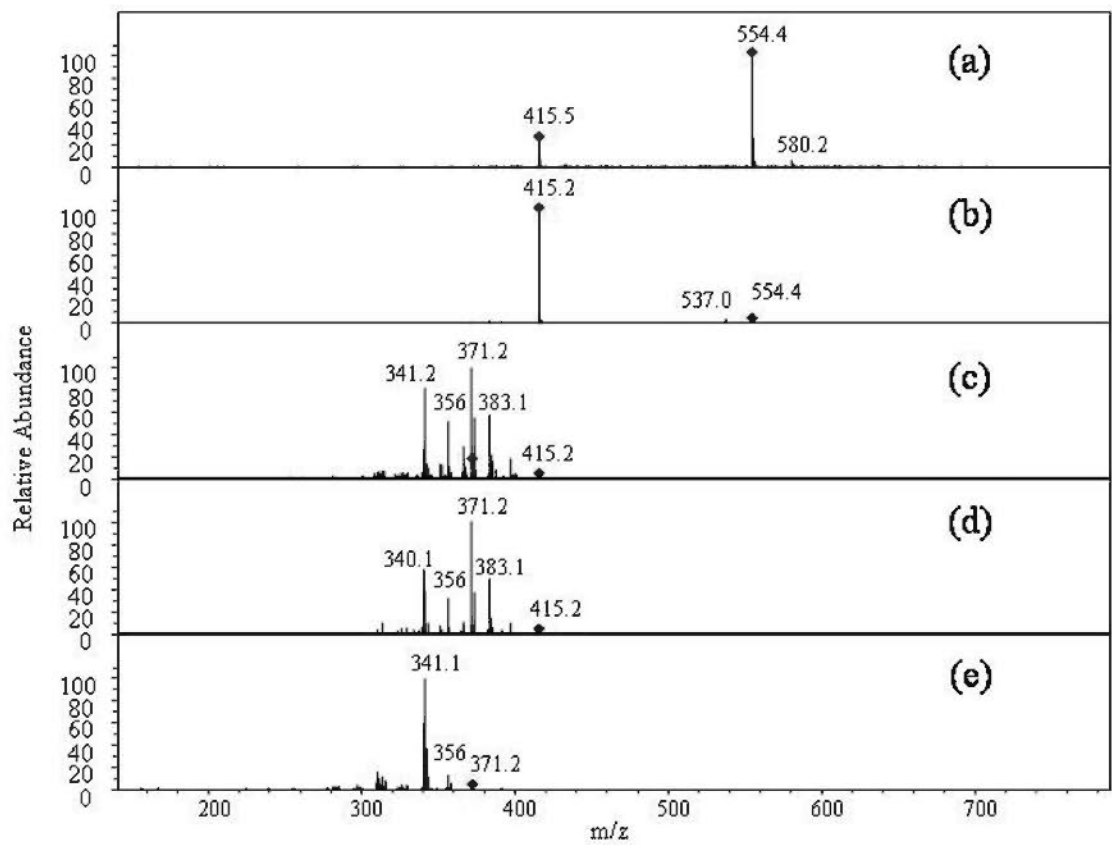


Fig. 3-14 MSⁿ spectra of gomisin G. (a) MS spectrum of gomisin G. (b) MS² spectrum of the ion at *m/z* 554. (c) MS² spectrum of the ion at *m/z* 415. (d) MS³ spectrum of the ion at *m/z* 415. (e) MS³ spectrum of the ion at *m/z* 371.

The retention time of deoxyschisandrin was 45.1 min, with UV λ_{max} at 217, 252 and 287 nm. As shown in Fig. 3-15, the protonated ion $[M+H]^+$ at m/z 417 was found to be the base peak. It also exhibited an adduct ion $[M+H_2O]^{+\bullet}$ at m/z 434, which produced the only fragment ion at m/z 417 in its MS^2 spectrum. In the MS^2 experiment, the m/z 417 ion gave rise to product ions at m/z 402 $[M+H-CH_3]^{+\bullet}$, 386 $[M+H-CH_3O]^{+\bullet}$, 370 $[M+H-CH_3OH-CH_3]^{+\bullet}$, 347 $[M+H-C_5H_{10}]^+$ and 316 $[M+H-C_5H_{10}-CH_3O]^+$. In the MS^3 experiment, the precursor ions at m/z 347 and 316 yielded product ions at m/z 332, 316, and m/z 301, 285, corresponding to the elimination of CH_3 and CH_3O group, respectively. This proposed fragmentation was consistent with the reported data (Huang et al., 2007).

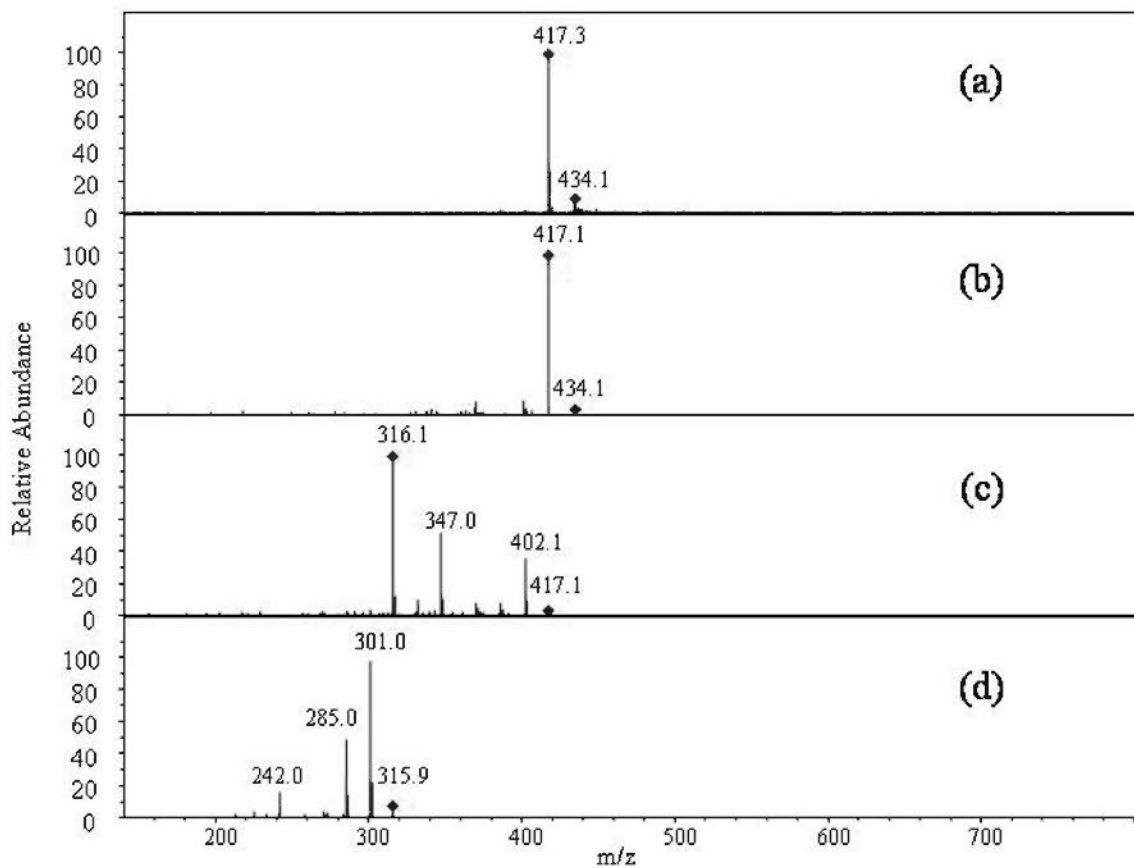


Fig. 3-15 MSⁿ spectra of deoxyschisandrin. (a) MS spectrum of deoxyschisandrin. (b) MS² spectrum of the ion at m/z 434. (c) MS² spectrum of the $[M+H]^+$ ion at m/z 417. (d) MS³ spectrum of the ion at m/z 316.

3.3.1.3.2 Bioanalytical method validation

As shown in Table 3-1, the R.S.D. of retention times of fifteen peaks identified in the basolateral solution obtained from Caco-2 cell model were used to evaluate the precision, repeatability and stability of the method. The R.S.D. of retention times from six consecutive determination of the same sample was less than 1.2%. By analyzing six independently prepared samples, the R.S.D. of retention times were less than 1%. When the same sample was analyzed within 2 days, retention time R.S.D. were less than 2.5%, indicating that the sample remained stable at room temperature for at least 2 days. These findings suggest that the present method is specific, reliable and reproducible.

3.3.1.3.3 Identification of absorbable components of *Schisandra chinensis in vitro*

Characterization of HPLC peaks using chromatographic and mass spectrometric characteristics can be employed for the identification of compound structure. In the present study, the identities of absorbable components of *Schisandra chinensis* were elucidated by comparing the retention time, UV spectra and MSⁿ data with those of reference compounds or the data reported in literatures. Altogether, the chromatographic and mass spectrometric characteristics and elucidation of individual peaks in the *in vitro* absorption profile are summarized in Table 3-2.

Table 3-1 Retention times of characterized peaks in HPLC-MS analysis

No.	Precision (n = 6)		Repeatability (n = 6)		Stability (n = 4)	
	Mean \pm S.D. (min)	R.S.D. (%)	Mean \pm S.D. (min)	R.S.D. (%)	Mean \pm S.D. (min)	R.S.D. (%)
1	13.23 \pm 0.12	0.90	13.13 \pm 0.09	0.70	13.42 \pm 0.18	1.37
2	16.11 \pm 0.16	0.96	16.00 \pm 0.12	0.76	16.40 \pm 0.26	1.57
3	18.49 \pm 0.17	0.92	18.32 \pm 0.13	0.72	18.76 \pm 0.28	1.50
4	19.91 \pm 0.20	0.99	19.69 \pm 0.15	0.77	20.25 \pm 0.38	1.90
5	23.03 \pm 0.23	0.99	22.79 \pm 0.20	0.87	23.41 \pm 0.43	1.82
6	21.99 \pm 0.23	1.06	21.79 \pm 0.17	0.76	22.38 \pm 0.38	1.72
7	25.36 \pm 0.27	1.07	25.09 \pm 0.22	0.89	25.85 \pm 0.49	1.91
8	27.74 \pm 0.28	1.00	27.42 \pm 0.20	0.73	28.33 \pm 0.68	2.41
9	31.43 \pm 0.33	1.06	31.07 \pm 0.21	0.69	32.06 \pm 0.65	2.03
10	32.52 \pm 0.38	1.15	32.17 \pm 0.23	0.72	33.16 \pm 0.63	1.91
11	34.07 \pm 0.39	1.13	33.72 \pm 0.21	0.63	34.82 \pm 0.77	2.20
12	37.17 \pm 0.27	0.73	36.86 \pm 0.18	0.50	37.68 \pm 0.55	1.46
13	37.84 \pm 0.30	0.80	37.52 \pm 0.20	0.52	38.29 \pm 0.50	1.30
14	41.30 \pm 0.19	0.46	41.22 \pm 0.14	0.33	41.67 \pm 0.35	0.85
15	45.10 \pm 0.11	0.25	44.97 \pm 0.07	0.15	45.29 \pm 0.24	0.54

Table 3-2 LC-MSⁿ characterization of fifteen absorbable compounds identified in the rat everted gut sac and human Caco-2 monolayer model

Code	<i>t_R</i> (min)	MS ⁿ (<i>m/z</i>) and relative abundance (%)	Identification
C1	13.23	MS: 433(11), 415(100) MS ² [433]: 415(100) MS ² [415]: 400(28), 384(100), 373(12), 359(18.4) MS ³ [384]: 369(100), 353(38), 338(23), 322(10)	Schisandrin
C2	16.11	MS: 548(100), 531(34) MS ² [548]: 531(100), 485(72), 401(84), 383(4) MS ² [531]: 485(38), 401(100), 383(29), 371(6), 353(6) MS ³ [401]: 383(100), 371(7), 353(14), 341(7)	GomisinD
C3	18.49	MS: 399(100) MS ² [399]: 384(13), 369(100), 368(60), 357(14), 343(14), 337(42) MS ³ [368]: 353(84), 337(100), 323(10)	Gomisin A
C4	19.91	MS: 501(9), 483(100), 401(6) MS ² [501]: 483(100), 401(55) MS ² [483]: 451(72), 436(10), 427(21), 409(15), 401(100), 399(50), 395(21), 369(65) MS ³ [401]: 386(16), 370(52), 369(100), 359(17), 337(21)	Angeloylgomisin H / Tigloylgomisin H
C5	23.03	MS: 501(5), 483(100), 401(6) MS ² [501]: 483(100), 401(55) MS ² [483]: 451(52), 436(8), 427(15), 409(12), 401(100), 399(43), 395(19), 369(44) MS ³ [401]: 386(10), 370(68), 369(100), 359(17), 337(25)	Angeloylgomisin H / Tigloylgomisin H
C6	21.99	MS: 548(100), 431(43) MS ² [548]: 431(100) MS ² [431]: 413(10), 399(36), 389(30), 387(100), 372(30), 356(39) MS ³ [387]: 372(17), 356(100)	Angeloylgomisin Q / Tigloylgomisin Q
C7	25.36	MS: 548(100), 431(45) MS ² [548]: 431(100) MS ² [431]: 413(12), 399(39), 389(35), 387(100), 372(34), 356(43) MS ³ [387]: 372(21), 356(100)	Angeloylgomisin Q / Tigloylgomisin Q

Table 3-2 (continued)

C8	27.74	MS: 532(100), 415(30) MS ² [532]: 415(100) MS ² [415]: 397(31), 383(73), 373(78), 371(100), 356(49), 341(91), 340(44) MS ³ [371]: 341(100), 340(82)	Tigloylgomisin F
C9	31.43	MS: 532(100), 415(32) MS ² [532]: 415(100) MS ² [415]: 397(33), 383(74), 373(80), 371(100), 356(51), 341(90), 340(38) MS ³ [371]: 341(100), 340(80)	Angeloylgomisin F
C10	32.52	MS: 554(100), 415(23) MS ² [554]: 415(100) MS ² [415]: 397(17), 383(57), 373(54), 371(100), 356(51), 341(81), 340(26) MS ³ [371]: 341(100), 340(59)	Gomisin G
C11	34.07	MS: 532(100), 415(26) MS ² [532]: 415(100) MS ² [415]: 397(4), 385(22), 373(18), 371(100), 341(10), 340(14) MS ³ [371]: 356(19), 341(41), 340(100)	Schisantherin B / Schisantherin C
C12	37.17	MS: 532(100), 415(27) MS ² [532]: 415(100) MS ² [415]: 397(6), 385(32), 373(25), 371(100), 341(10), 340(16) MS ³ [371]: 356(25), 341(50), 340(100)	Schisantherin B / Schisantherin C
C13	37.84	MS: 554(17), 415(100) MS ² [532]: 415(100) MS ² [415]: 397(12), 385(71), 373(45), 371(100), 341(39), 340(36) MS ³ [371]: 356(17), 341(69), 340(100)	Schisantherin A
C14	41.30	MS: 515(100) MS ² [515]: 469(22), 385(100), 355(30), 343(3), 323(10) MS ³ [385]: 367(5), 355(100), 353(16), 343(13), 323(30)	Gomisin E
C15	45.10	MS: 417(100) MS ² [417]: 402(36), 386(8), 370(8), 347(53), 332(10), 316(100) MS ³ [316]: 301(100), 285(50)	Deoxyschisandrin

By comparing retention time, UV spectra (if available) and APCI-MSⁿ data with those of reference compounds, compounds 1, 2, 3, 9, 10, 13 and 15 were unambiguously identified as schisandrin, gomisin D, gomisin A, angeloylgomisin F, gomisin G, schisantherin A, deoxyschisandrin, respectively.

Compound 4 ($t_R = 19.9$ min) and compound 5 ($t_R = 23.0$ min) exhibited identical MSⁿ spectra. As shown in Fig. 3-16 and Fig 3-17, both compounds gave an intense adduct ion $[M+H-H_2O]^+$ at m/z 483 and a weak protonated ion $[M+H]^+$ at m/z 501. In the MS² spectrum (Fig. 3-8), the m/z 501 ion yielded product ions at m/z 483 and 401, and the m/z 401 ion also arose from the fragmentation of the m/z 483 ion. The formation of m/z 483 ion could be explained by the loss of water as in schisandrin, and the m/z 401 ion was produced by successive loss of H₂O and C₅H₆O ($\Delta m = 82u$, a derivative from 2-methyl-2-butenoic acid), indicating the presence of a hydroxyl group and an ester (angeloyl or tigloyl) group. In addition, the simultaneous presence of the m/z 483 and 401 ions in the LC/MS spectra indicated that the ester group and hydroxyl group were not vicinal to each other. Such evidence pointed to the structure of angeloylgomisin H or tigloylgomisin H, in which the OH group is at C-7 position while the ester group is at C-14 position. In the MS² spectrum of the ion at m/z 401, it produced ions at m/z 386, 369 and 337 corresponding to the loss of CH₃, CH₃OH, and 2CH₃OH, which could be distinguished from the MS² spectrum of the m/z 415 ion in angeloylgomisin F. Such difference probably resulted from the different substitution sites of ester group between angeloylgomisin H (or tigloylgomisin H) and angeloylgomisin F. Since angeloylgomisin H and tigloylgomisin H are *cis*- and *trans*- isomers, the exact discrimination between

these compounds can not be fully achieved by MSⁿ analysis. Nevertheless, the difference in t_R values implied different chromatographic behaviors between compound 4 and compound 5. This was consistent with the report that tigloylgomisin H was eluted followed by angeloylgomisin H under acetic mobile phase (Deng et al., 2008). Thus, Compound 4 and 5 were tentatively identified as tigloylgomisin H or angeloylgomisin H.

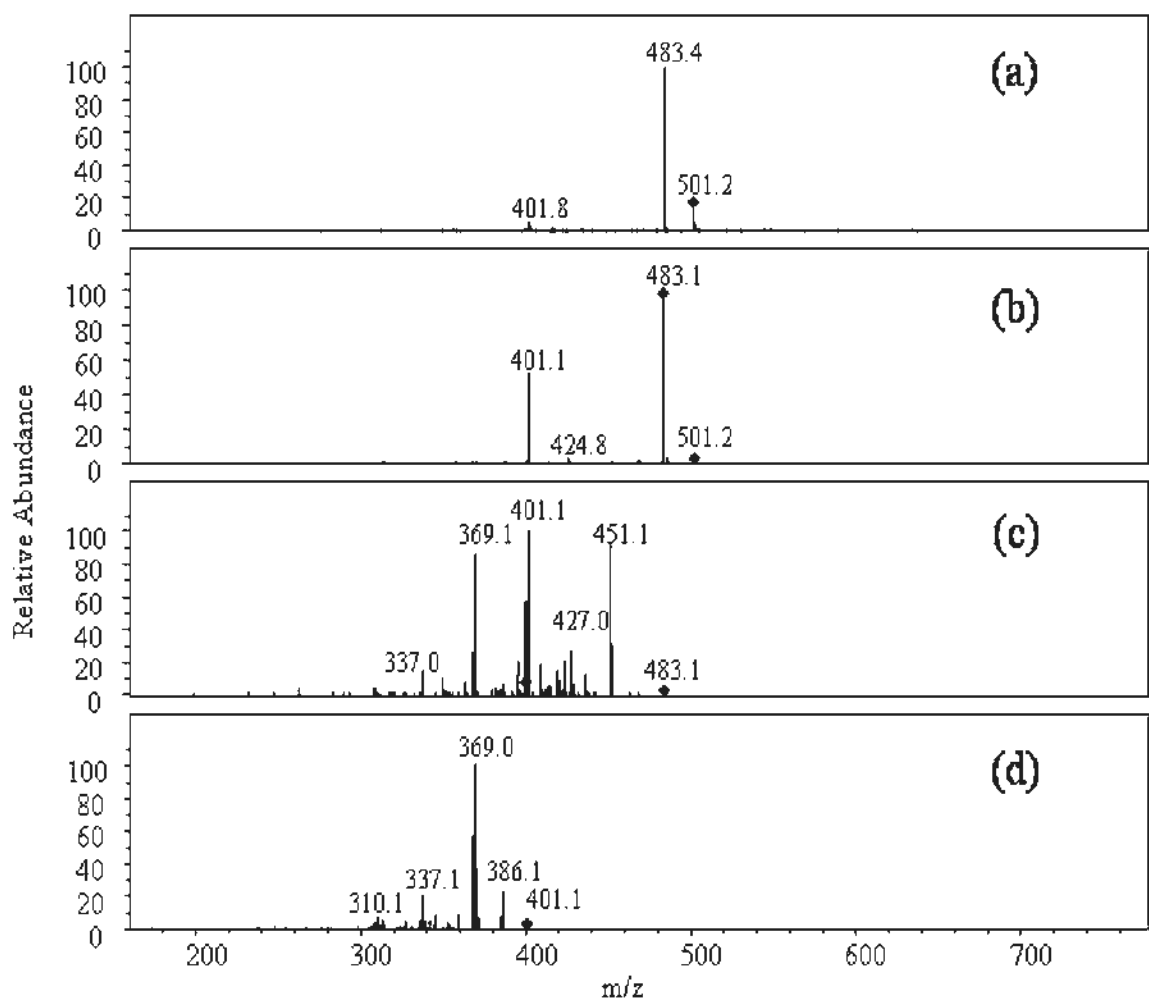


Fig. 3-16 MSⁿ spectra of compound 4. (a) MS spectrum. (b) MS² spectrum of the $[M+H]^+$ ion at m/z 501. (c) MS² spectrum of the ion at m/z 483. (d) MS³ spectrum of the ion at m/z 401.

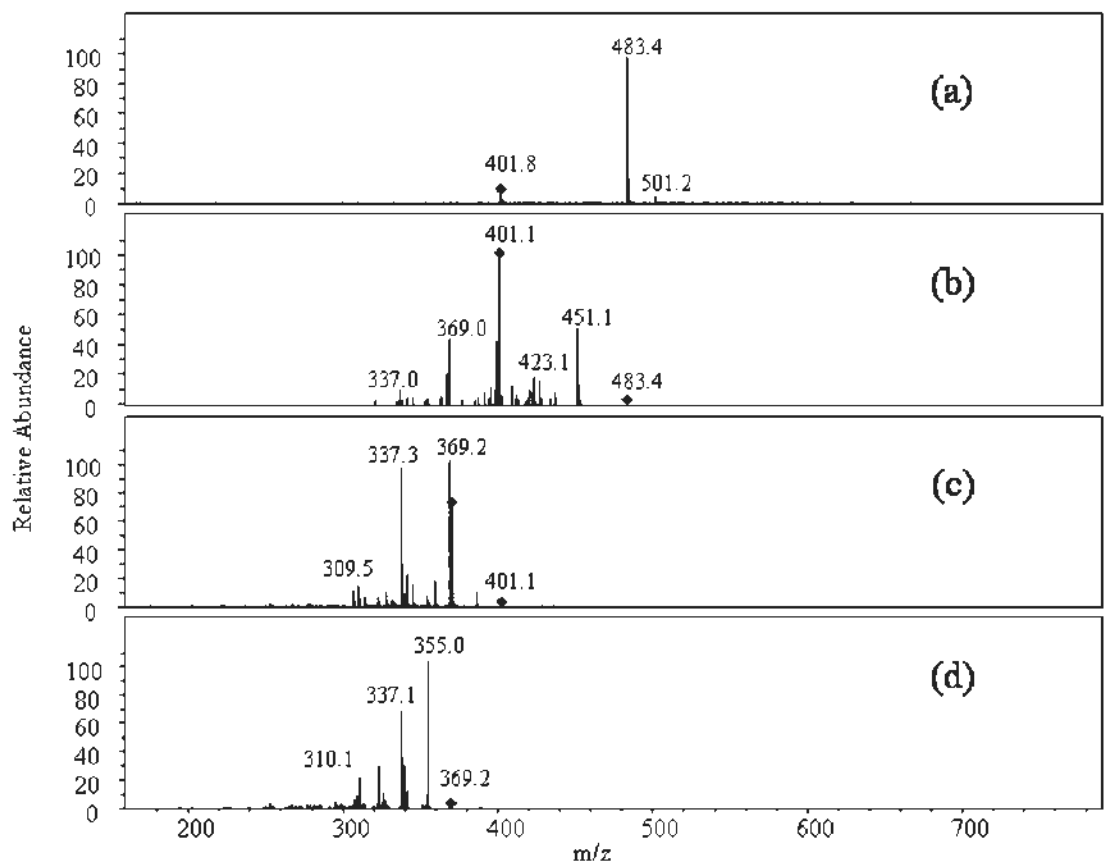


Fig. 3-17 MSⁿ spectra of compound 5. (a) MS spectrum. (b) MS² spectrum of the ion at m/z 483. (c) MS³ spectrum of the ion at m/z 401. (d) MS³ spectrum of the ion at m/z 369.

The MSⁿ spectra of Compound 6 ($t_R = 22.0$ min) and compound 7 ($t_R = 25.4$ min) are presented in Fig. 3-18 and Fig. 3-19. They both gave an adduct ion $[M+H_2O]^{+\bullet}$ at m/z 548 as their base peak and a notable ion at m/z 431. In the MS² experiment of the m/z 548 ion, it yielded the only product ion at m/z 431 via the loss of 2-methyl-2-butenoic acid and OH group. The precursor ion at m/z 431 gave rise to product ions at m/z 413, 399, 389 and 387. The mass difference between them was 18, 32, 42 and 44, corresponding to the loss of H₂O, CH₃OH, C₃H₆ and C₂H₄O, respectively, which was analogous to schisantherin except for the loss of CH₃OH instead of CH₂O. This implied the absence of methylenedioxy group in compound 6 and 7. In the MS³ spectrum of the m/z 387 ion, it produced ions at m/z 372 and 356 via loss of CH₃ and CH₃O group respectively. The above MSⁿ data pointed to the structure of angeloylgomisin Q or tigloylgomisin Q, which are *cis*- and *trans*- isomers. Thus, compound 6 and compound 7 were tentatively identified as angeloylgomisin Q or tigloylgomisin Q.

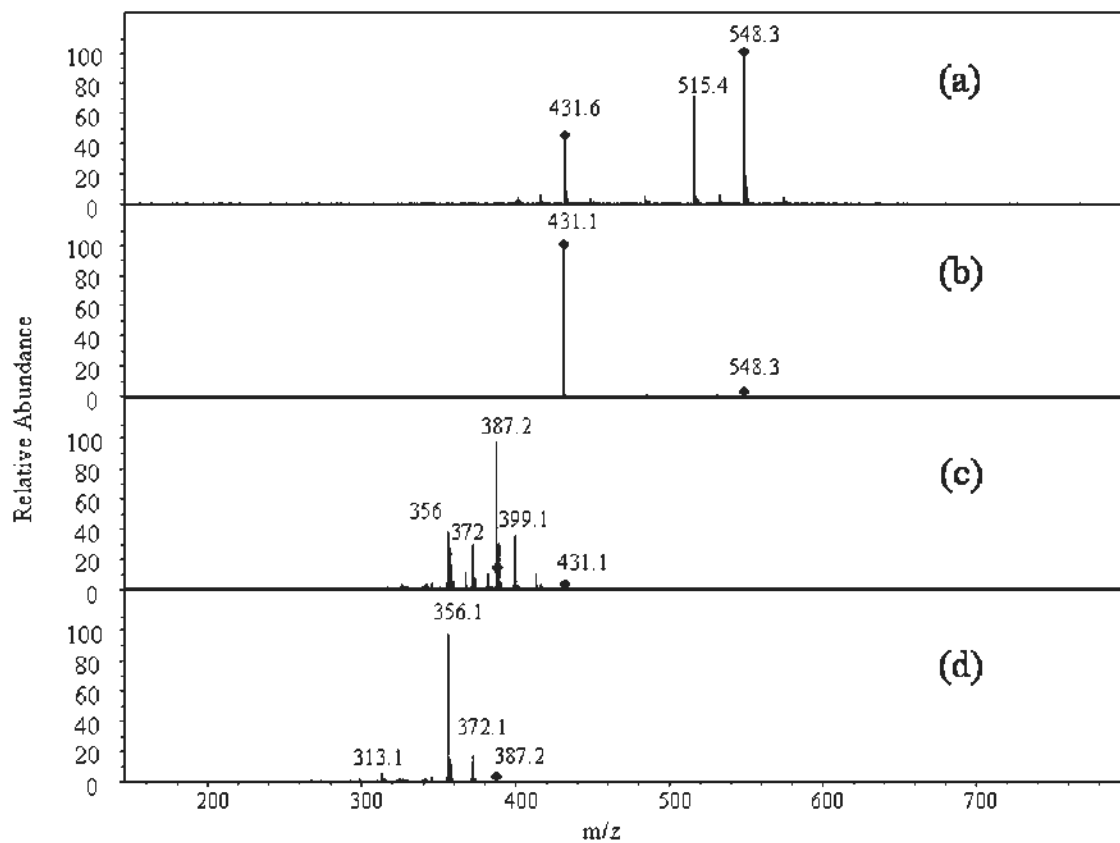


Fig. 3-18 MSⁿ spectra of compound 6. (a) MS spectrum. (b) MS² spectrum of the ion at m/z 548. (c) MS² spectrum of the ion at m/z 431. (d) MS³ spectrum of the ion at m/z 387.

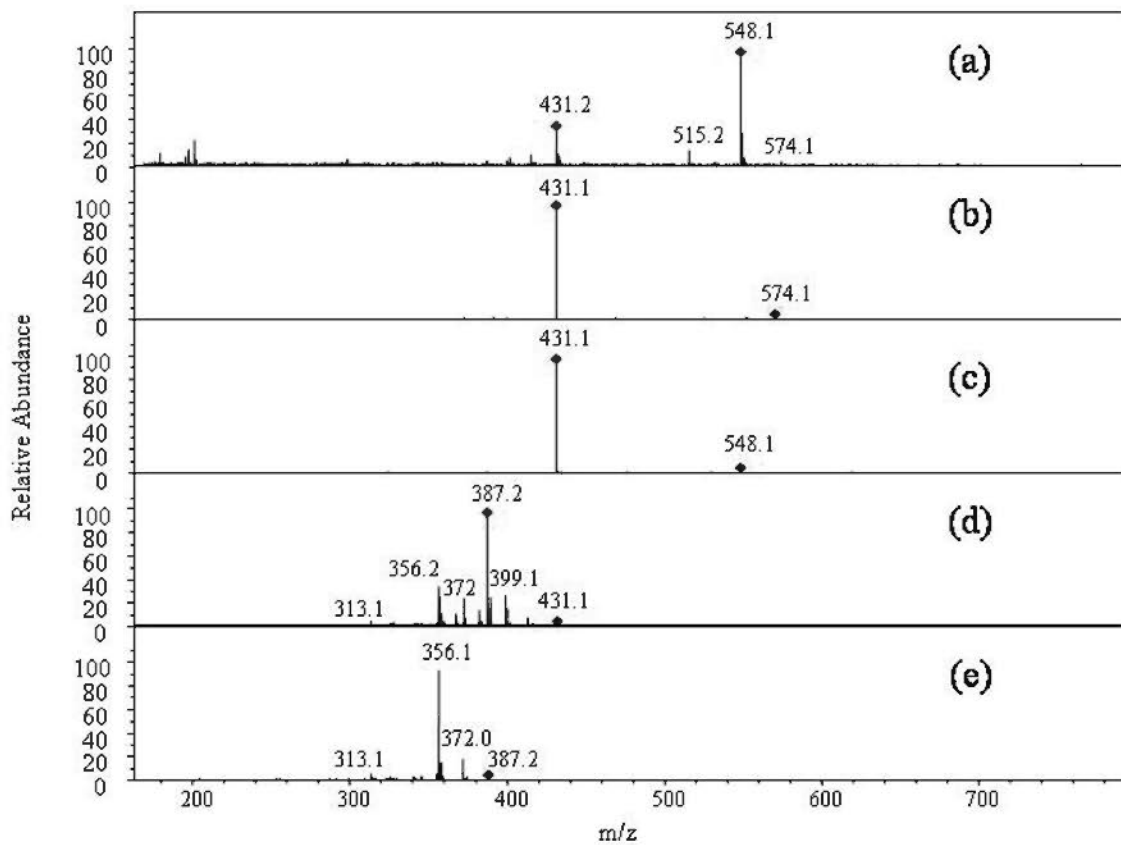


Fig. 3-19 MSⁿ spectra of compound 7. (a) MS spectrum. (b) MS² spectrum of the ion at *m/z* 574. (c) MS² spectrum of the ion at *m/z* 548. (d) MS² spectrum of the ion at *m/z* 431. (e) MS³ spectrum of the ion at *m/z* 387.

Compound 11 and compound 12 both exhibited an adduct ion $[M+H_2O]^+$ at m/z 532 as the base peak and a significant ion at m/z 415, implying that an ester group is present (Fig. 3-20 and Fig. 3-21). Also, in the MS^2 experiment of the m/z 532 ion, it yielded the only fragment ion at m/z 415, corresponding to the combined loss of 2-methyl-2-butenoic acid ($\Delta m = 100u$) and OH group. As in the case of schisantherin A, the MS^3 spectrum of the ion at m/z 415 gave rise to product ions at m/z 397, 385, 373 and 371 through the loss of H_2O , CH_2O , C_3H_6 , and C_2H_4O , respectively. Compounds 11 and 12 were probably schisantherin B or schisantherin C, which are also *cis*- and *trans*- isomers.

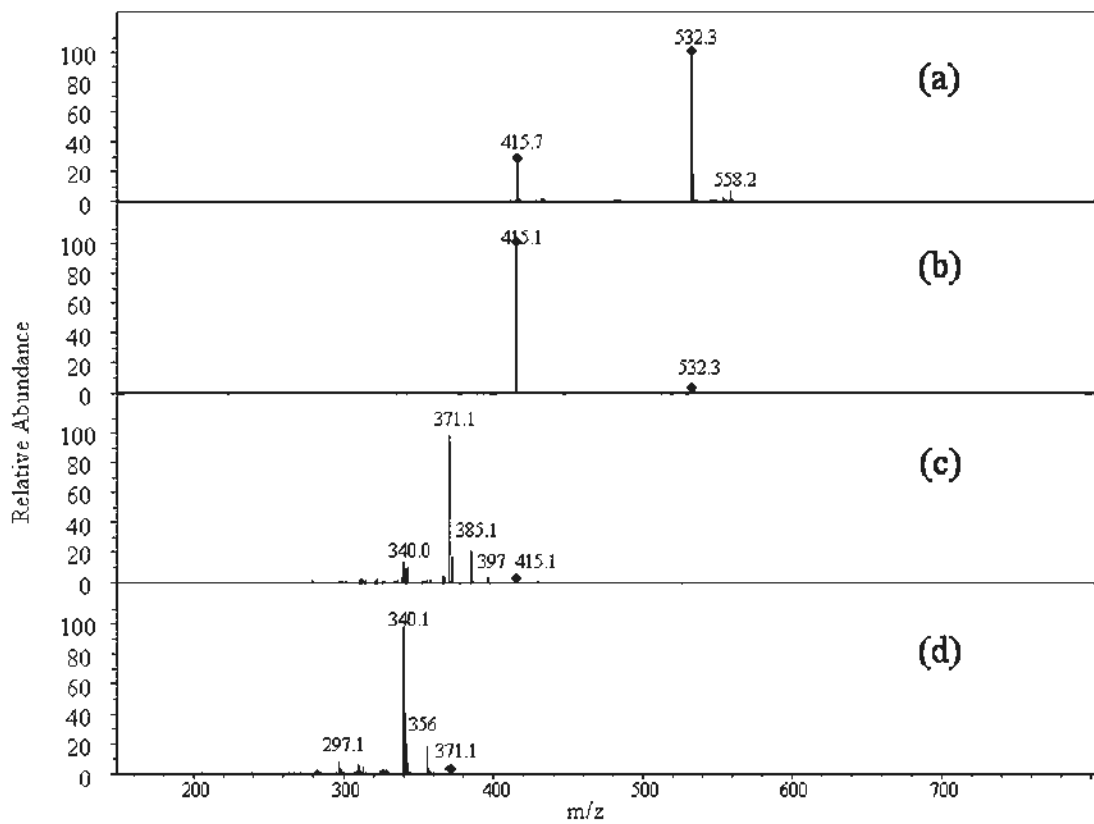


Fig. 3-20 MSⁿ spectra of compound 11. (a) MS spectrum. (b) MS² spectrum of the ion at *m/z* 532. (c) MS² spectrum of the ion at *m/z* 415. (d) MS³ spectrum of the ion at *m/z* 371.

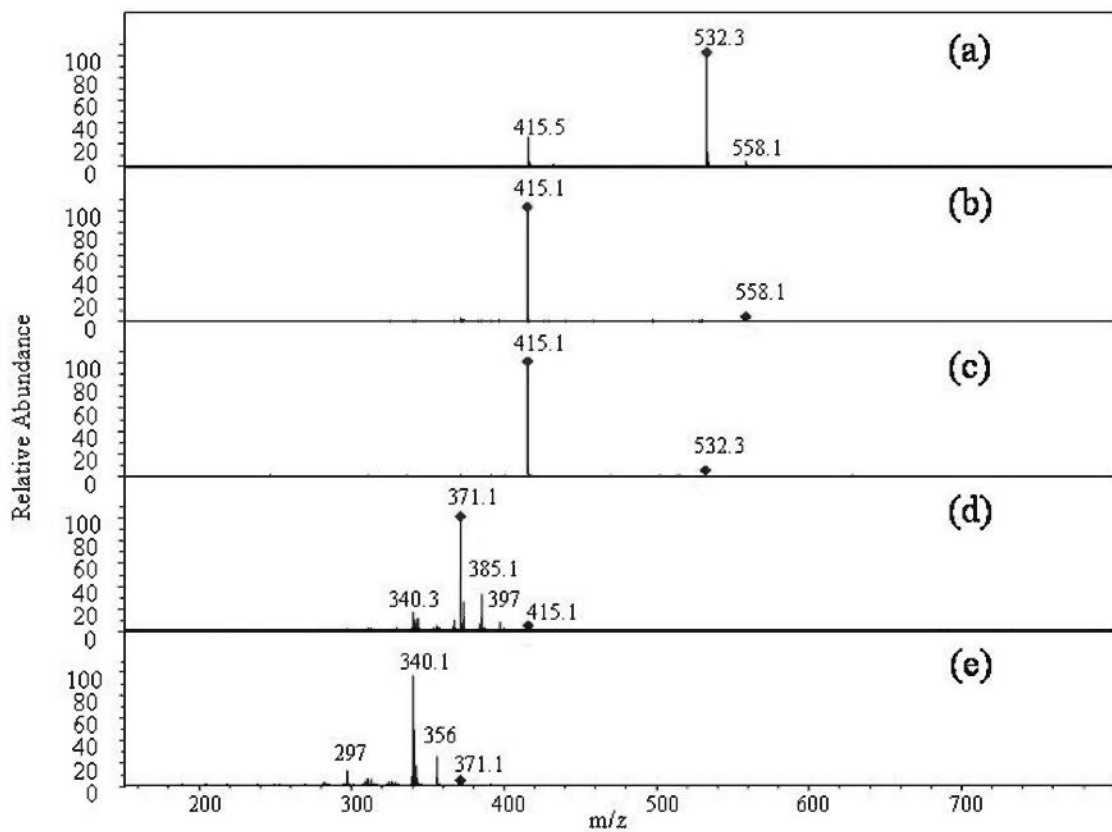


Fig. 3-21 MSⁿ spectra of compound 12. (a) MS spectrum. (b) MS² spectrum of the ion at m/z 558. (c) MS² spectrum of the ion at m/z 532. (d) MS² spectrum of the ion at m/z 415. (e) MS³ spectrum of the ion at m/z 371.

As shown in Fig. 3-22, compound 8 also gave an adduct ion $[M+H_2O]^+$ at m/z 532 and an intense ion at m/z 415, which was identical to compounds 11 and 12. In the MS² experiment of the m/z 415 ion, it gave rise to product ions at m/z 397, 383, 373, 371, 356 and 341. The MS² fragmentation pattern was similar to compounds 11 and 12, except for the diagnostic ion at m/z 383 of compound 8. This can be explained by the involvement of positional isomerism at the substitution site of methylenedioxy group as discussed above. Furthermore, the MSⁿ data of compound 8 was identical with those of angeloylgomisin F, indicating they were likely a pair of stereoisomers. Taken together, compound 8 was thus tentatively identified as tigloylgomisin F.

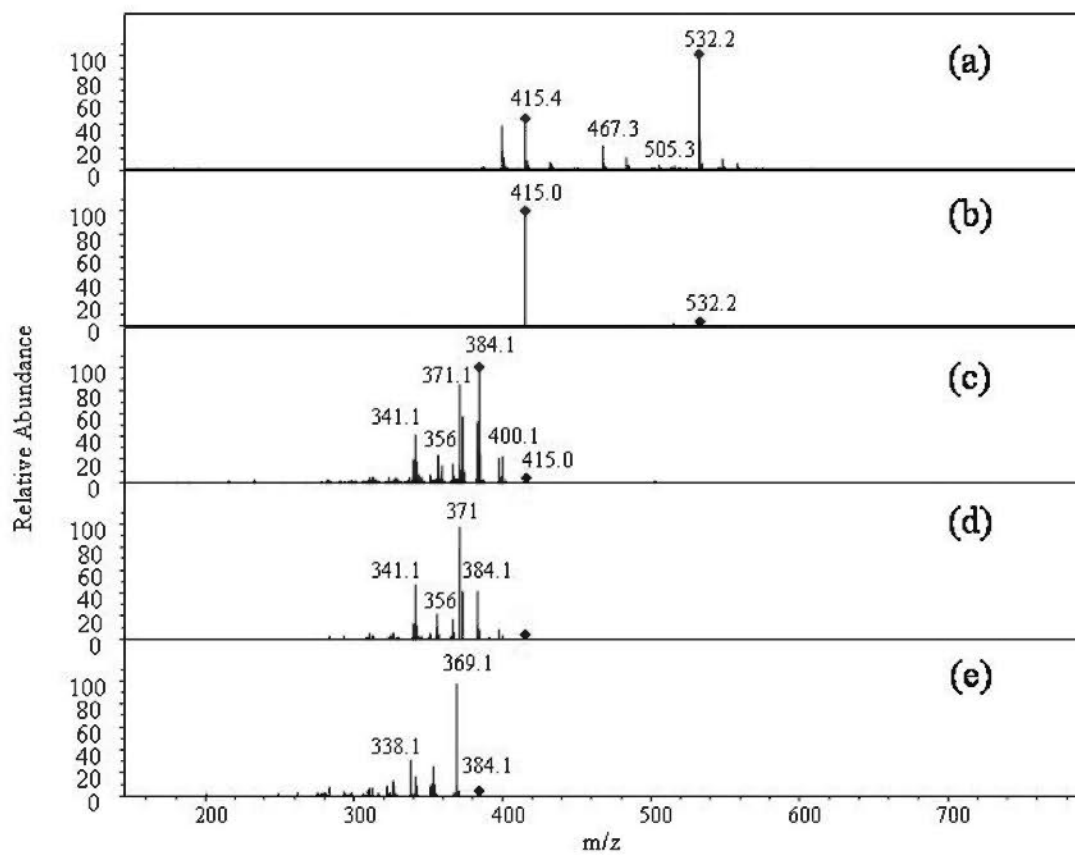


Fig. 3-22 MSⁿ spectra of compound 8. (a) MS spectrum. (b) MS² spectrum of the ion at *m/z* 532. (c) MS² spectrum of the ion at *m/z* 415. (d) MS³ spectrum of the ion at *m/z* 415. (e) MS³ spectrum of the ion at *m/z* 384.

Fig. 3-23 shows that compound 14 ($t_R = 41.3$ min) exhibited a protonated ion $[M+H]^+$ at m/z 515 and a weak adduct ion at m/z 532, demonstrating a molar mass of 514. In the MS^2 experiment of the m/z 515 ion, it gave rise to ions at m/z 469, 385, 355 and 323. The m/z 469 and 385 ions, as in the case of gomisin D, arose from the loss of formic acid ($\Delta m = 46u$) and 2-hydroxyl-2,3-dimethyl-3-butenoic acid ($\Delta m = 130u$) respectively. These data matched the structure of gomisin E. Further, the MS^3 data of the m/z 385 ion showed daughter ions at m/z 367, 355, 353, 343 and 323, corresponding to the loss of H_2O , CH_2O , CH_3OH , C_3H_6 , CH_2O and CH_3OH , respectively. The base peak in the MS^3 spectrum was the m/z 353 ion arising from the loss of CH_2O . In contrast, the MS^3 experiment of gomisin D showed the abundant fragment ion at m/z 383 through the loss of H_2O . Such evidence further pointed to the structure of gomisin E, which possesses the identical skeleton to gomisin D, except for the absence of hydroxyl group on the cyclooctadiene ring in gomisin E. Furthermore, the t_R value of compound 14 was between those of schisantherin A (C13) and deoxyschisandrin (C15), consistent with the chromatographic behavior of gomisin E reported in previous study (Huang et al., 2007). Compound 14, therefore, was tentatively identified as gomisin E.

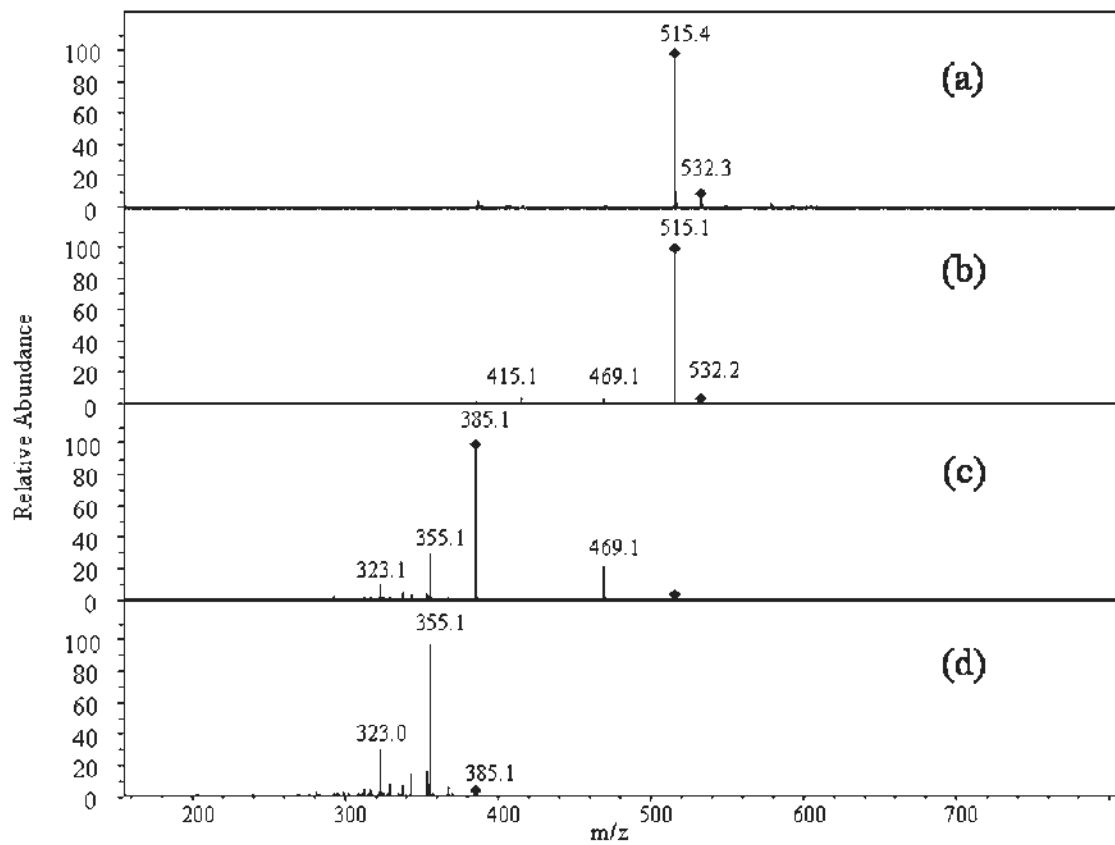


Fig. 3-23 MSⁿ spectra of compound 14. (a) MS spectrum. (b) MS² spectrum of the ion at m/z 532. (c) MS² spectrum of the ion at m/z 515. (d) MS³ spectrum of the ion at m/z 385.

3.3.1.4 Permeability of schisandrin monomer in Caco-2 cell monolayer model

Drug transport in the Caco-2 cell model is evaluated by the apparent permeability coefficient (P_{app}), which is determined by the equation of P_{app} (cm/s) = $dQ/dt/AC_0$, where dQ/dt is the rate of appearance of schisandrin in apical or basolateral chamber, C_0 is the initial concentration of schisandrin, and A is the surface area across which transport proceeded. Drug candidates with higher P_{app} would have good oral bioavailability in human. Transport from apical to basolateral chambers (A to B) is referred to as being absorption from human lumen to blood fluid whereas the one from basolateral to apical (B to A) mimics secretory process.

In the bidirectional transport studies, the result (Fig. 3-24) showed that there was no significant difference between the apparent permeability of A to B transport ($P_{app(AB)} = 18.8 \pm 0.8 \times 10^{-6}$ cm/sec) and B to A transport ($P_{app(BA)} = 20.6 \pm 0.6 \times 10^{-6}$ cm/sec) when the initial concentration was 40 μ M ($P > 0.05$, Mann-Whitney test). In studies using a high concentration (200 μ M), there was a significant decrease in permeability of A to B transport ($P_{app(AB)} = 14.9 \pm 0.4 \times 10^{-6}$ cm/sec) as compared to B to A transport ($P_{app(BA)} = 18.8 \pm 0.6 \times 10^{-6}$ cm/sec, $P < 0.01$, Mann-Whitney test). Since it was reported that schisandrin exhibited inhibitory effect on P-glycoprotein-mediated efflux (Yoo et al., 2007), schisandrin could be also a potent P-glycoprotein substrate, indicating the decreased permeability of schisandrin in A to B transport at high concentration might be attributed to the involvement of P-glycoprotein-mediated drug efflux. Nevertheless, the efflux ratio ($P_{app(BA)} : P_{app(AB)}$) at low and high concentrations were 1.09 and 1.26

respectively, suggesting the absorption was mainly via passive transcellular diffusion.

Compared with the reported permeability of high absorbable drug, propranolol ($P_{app(AB)} = 14.80 \times 10^{-6}$ cm/sec) and medium absorbable compound, ranitidine ($P_{app(AB)} = 4.59 \times 10^{-6}$ cm/sec) (Leung et al., 2005), schisandrin was found to exhibit high intestinal absorption. By comparing peak area of other absorbable components with schisandrin present in the absorption profile of *Schisandra chinensis* (Fig. 3-5), those compounds were speculated to exhibit medium to high intestinal absorption.

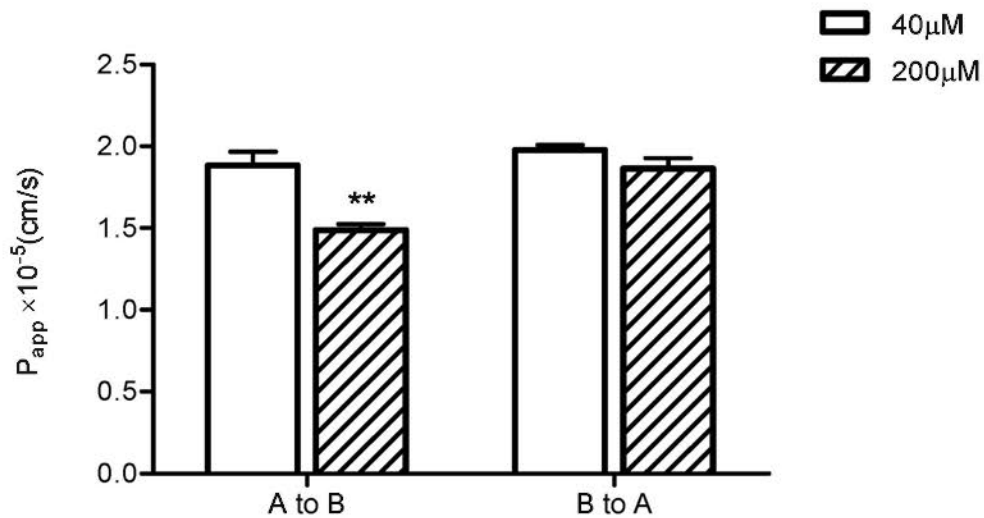


Fig. 3-24 Apparent permeability coefficient of schisandrin obtained in transports from apical to basolateral chamber (A to B) and from basolateral to apical chamber (B to A) using two initial concentrations (40 μM and 200 μM). Data are expressed as mean \pm S.E.M. (n = 5–6). Permeability in A to B transport was compared with B to A transport

using Mann-Whitney test. Significance was set as $P < 0.01$.

3.3.2 Absorption of *Schisandra chinensis* in the rat

3.3.2.1 Absorption profile of *Schisandra chinensis* in rat plasma

Absorption of *Schisandra chinensis* was assessed in plasma of the rats following oral administration of Schisandra extracts. The HPLC-MS method described in Section 3.3.1 has been used for analyzing the absorbable components and the related metabolites. Fig. 3-25 shows a representative HPLC-MS chromatogram of rat plasma obtained at 2 h after oral administration of Schisandra aqueous extract. Owing to the relatively low intensity of analytes and interference of matrix, extracted ion chromatograms (EIC) were used for presentation. By analysis of chromatographic characteristics and MSⁿ data as described in Section 3.3.1, schisandrin (C1), gomisin D (C2), gomisin A (C3), angeloylgomisin H / tigloylgomisin H (C5), schisantherin B/schisantherin C (C11, C12) and schisantherin A (C13) were identified. The absence of C4, C6, C7, C8, C9, C10, C14 and C15 could be explained by their low concentrations in the aqueous extract (2.96 mg/g for schisandrin) or relatively poor absorption *in vivo*. Moreover, four new peaks (M1–M4) that were not included in the Schisandra extract were observed at the early retention time range from 5 min to 10 min. As the first-phase metabolism such as hydroxylation and demethylation would usually increase the polarity of the parent drugs, M1–M4 could be metabolites generated from the absorbable components of *S. chinensis*.

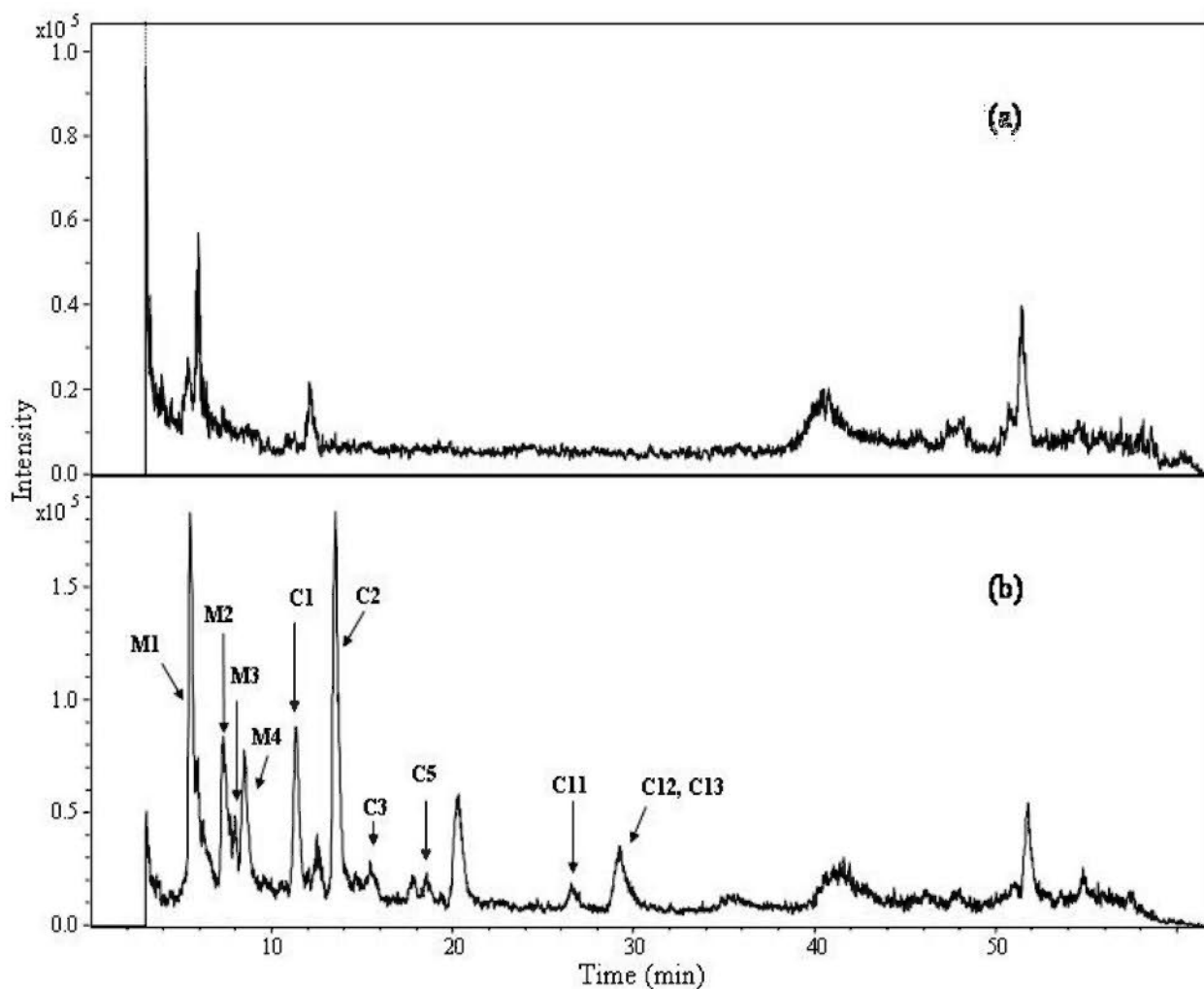


Fig. 3-25 Representative HPLC-MS extracted ion chromatograms (EIC) at m/z 415, 548, 399, 483, 532, 554, 417, 431 and 401 in positive mode. Plasma was obtained from the rat orally treated with an aqueous extract of *Schisandra chinensis* (3.5 g/kg) at time intervals of (a) 0 min, (b) 2 h. C1 to C13 denote compounds 1–13. M1 to M4 denote metabolites 1

–4.

Fig. 3-26 shows the absorption profiles in rat plasma obtained at different time intervals of 0, 0.25, 2, 4, 6 h after oral administration of 70% ethanol extract of *Schisandra chinensis*. On the basis of the chromatographic characteristics and MSⁿ data obtained with HPLC-MS analysis, schisandrin (C1), gomisins D (C2), gomisins A (C3), angeloylgomisin H / tigloylgomisin H (C4, C5), gomisins G (C10), schisantherin B/schisantherin C (C11, C12), schisantherin A (C13), gomisins E (C14) and deoxyschisandrin (C15) were identified. γ -Schisandrin (C16) was also identified by comparing with standard reference. The absence of C6, C8 and C9 could be explained by their low concentrations in the extract, but interestingly, although C7 (angeloylgomisin Q/tigloylgomisin Q) was markedly absorbed in the *in vitro* models (Section 3.3.1), it was not found in rat plasma, implying a poor bioavailability of C7. In the chemical structure of C7, there is a tigloyl or angeloyl substitution group on the cyclooctadiene ring. Given the ester bond could be hydrolyzed by the abundant hydrolase in small intestinal wall, enteric bacteria, plasma and liver, the poor bioavailability of C7 could be due to degradation caused by first-pass metabolism or rapid clearance after absorption. This could also explain the absence of C6, C8 and C9 in rat plasma, whose chemical structures also include tigloyl or angeloyl substitution group on the cyclooctadiene ring.

As presented in Fig. 3-26 (b), the major absorbable components, such as schisandrin (C1), gomisins D (C2) and gomisins A (C3), could be found at 15 min after oral administration, indicating the entrance of the absorbable lignan compounds across intestinal barriers was fast. Comparing the peak area of each analyte at different time intervals, most of the

absorbable components reached their maximum concentrations at approximately 4 h after administration.

Similar to the observation for Schisandra aqueous extract, new peaks (M1–M4) were found in plasma from the rats administered with an ethanol extract. As addressed above, these new peaks could represent metabolites of the absorbable components. In addition to the evidence of retention time, the time-dependent increase in peak area of these compounds suggested the new compounds of metabolites. In Section 3.3.2.2, these new peaks were further identified by comparing the MSⁿ data with those of absorbable Schisandra lignans and the data in previous reports on the metabolism of Schisandra lignans. The absorbable components and related metabolites identified in the *in vitro* models and rat plasma are summarized in Table 3-3.

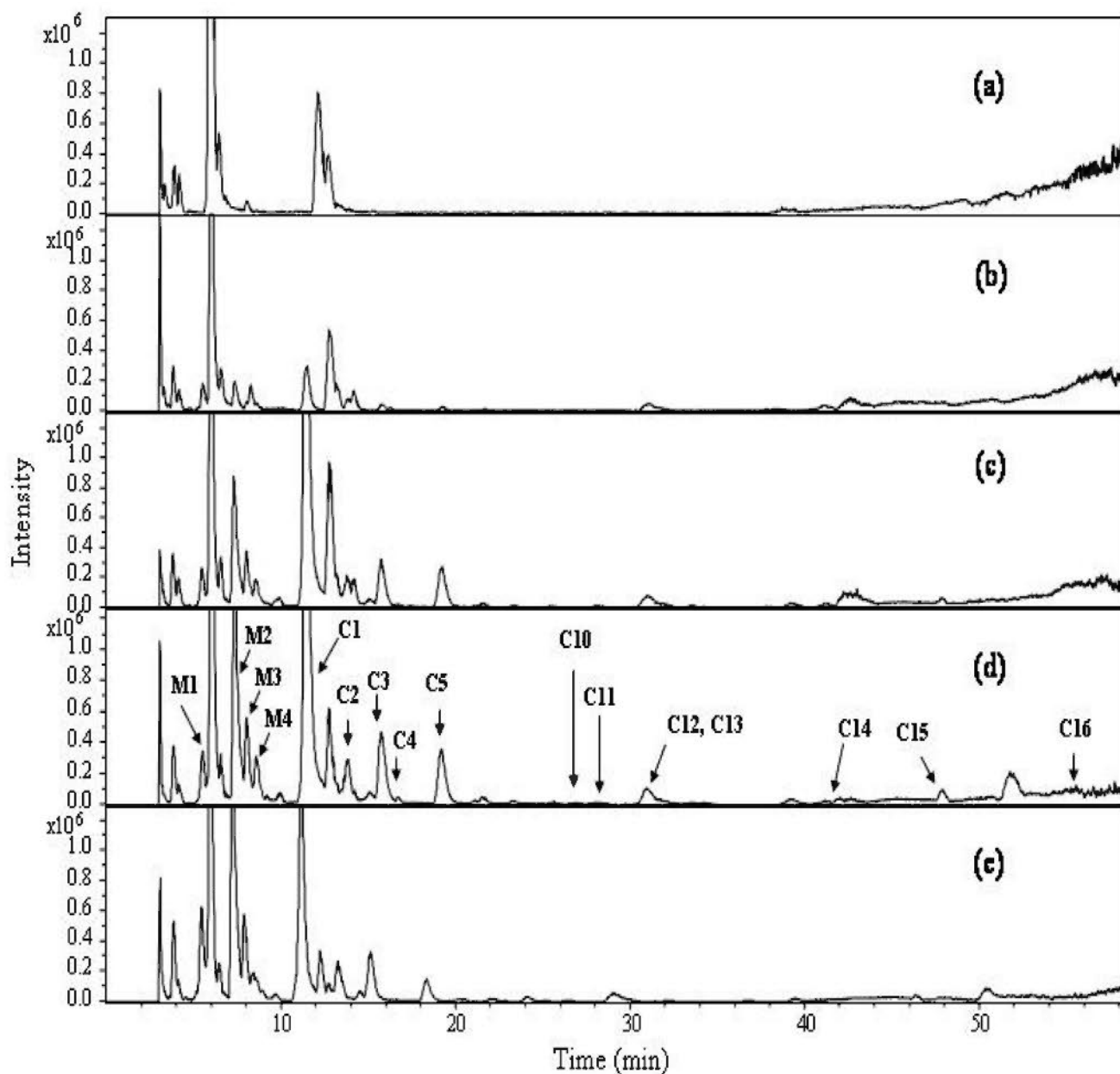


Fig. 3-26 Representative HPLC-MS basic peak chromatograms (BPC) in positive mode. Plasma was obtained from the rat orally treated with a 70% ethanol extract of *Schisandra chinensis* (2g/kg) at the time intervals of (a) 0 h, (b) 0.25 h, (c) 2 h, (d) 4 h and (e) 6 h. C1 to C16 denote compounds 1–16. M1 to M4 denote metabolite metabolites 1–4.

Table 3-3 Absorbable compounds of *Schisandra chinensis* characterized in rat everted gut sac, Caco-2 monolayer model *in vitro*, and in rat plasma.

Code	Compound	Aqueous extract			Ethanol extract
		Rat everted gut sac	Caco-2 cell monolayer	Rat plasma	Rat plasma
C1	Schisandrin	√	√	√	√
C2	Gomisin D	√	√	√	√
C3	Gomisin A	√	√	√	√
C4	Angeloylgomisin H / Tigloylgomisin H	√	√		√
C5	Angeloylgomisin H / Tigloylgomisin H	√	√	√	√
C6	Angeloylgomisin Q / Tigloylgomisin Q	√	√		
C7	Angeloylgomisin Q / Tigloylgomisin Q	√	√		
C8	Tigloylgomisin F	√	√		
C9	Angeloylgomisin F	√	√		
C10	Gomisin G	√	√		√
C11	Schisantherin B / Schisantherin C	√	√	√	√
C12	Schisantherin B / Schisantherin C	√	√	√	√
C13	Schisantherin A	√	√	√	√
C14	Gomisin E	√	√		√
C15	Deoxyschisanrin	√	√		√
C16	γ-Schisandrin				√
M1				√	√
M2				√	√
M3				√	√
M4				√	√

3.3.2.2 Identification of metabolites

In the MS spectrum shown in Fig 3-27, M1 exhibited an adduct ion $[M+H-H_2O]^+$ at m/z 417 as the base peak and a notable protonated ion at m/z 435, suggesting a molecular weight of 434. The mass difference between M1 and schisandrin was 2 Da. Given schisandrin was the dominant absorbable compound, M1 could be yielded from schisandrin through hydroxylation ($\Delta m = 16$) and demethylation ($\Delta m = 14$). Cui and Wang (1993) reported the isolation and structure determination of metabolites of schisandrin co-cultured with rat live microsomal fraction, and stated that schisandrin could be hydroxylated at the C-8 position following demethylation of methoxyl group at C-2 and C-3 position. Moreover, in the MS² spectrum of the ion at m/z 417, it gave rise to an abundant fragment ion at m/z 359 by neutral loss of C₃H₆O, indicating the presence of hydroxyl group at the cyclooctadiene ring. Thus M1 could be tentatively identified as 6,7,8,9-tetrahydro-1,(2 or 3),12,13,14-pentamethoxy-7,8-dimethyl-2,7,8-dibenzo[a,c]-cycloactenetriol.

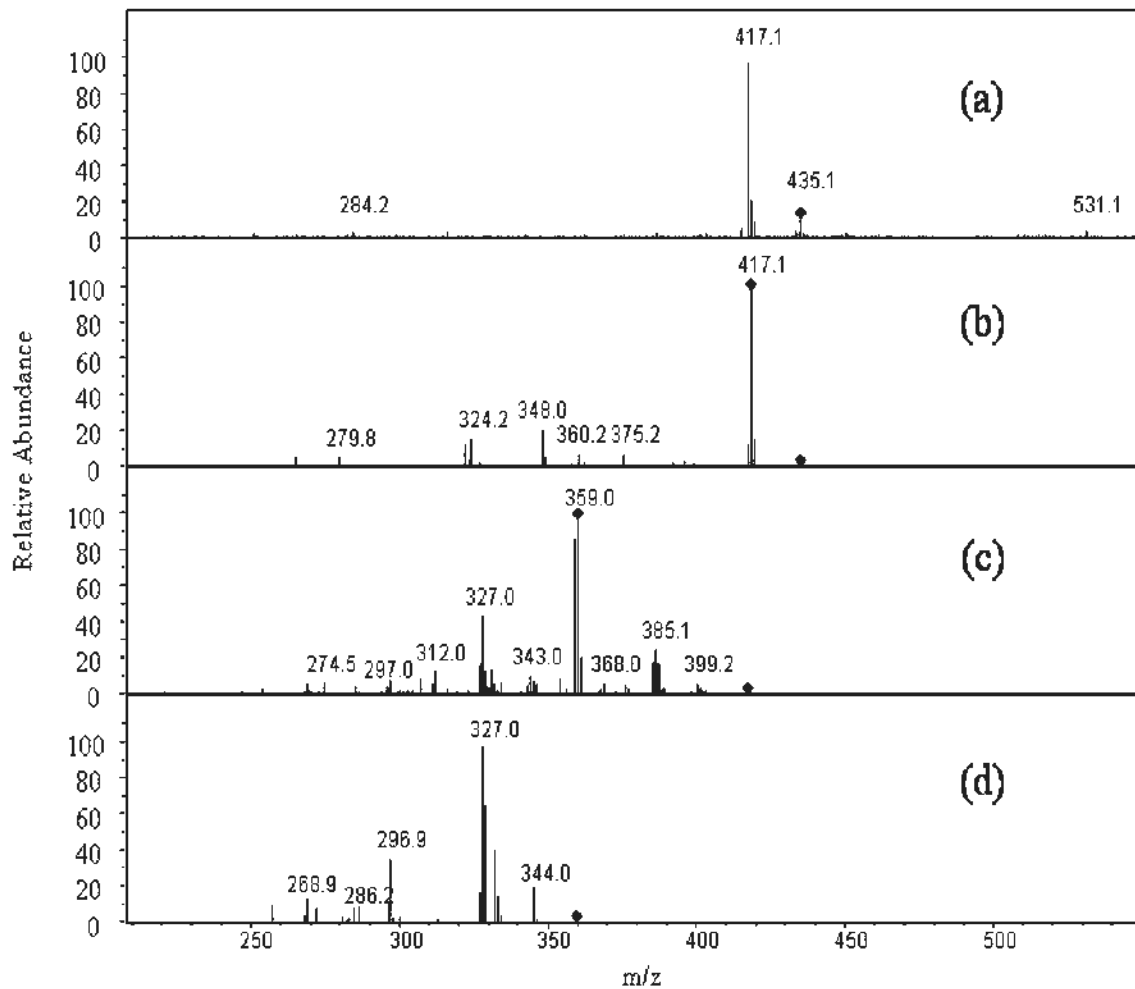


Fig. 3-27 MSⁿ spectra of M1. (a) MS spectrum of M1. (b) MS² spectrum of the ion at m/z 435. (c) MS² spectrum of the $[M+H-H_2O]^+$ ion at m/z 417. (d) MS³ spectrum of the ion at m/z 359.

As shown in Fig. 3-28, M2 gave an adduct ion $[M+H-H_2O]^+$ at m/z 431 as the base peak and a protonated ion at m/z 449. Neural loss of C_3H_6O was observed in the MS^2 spectrum of the m/z 431 ion, similar to the case in M1. Given hydroxylation produces mass addition of 16 Da, M2 could be generated from schisandrin (M.W. = 432) with hydroxylation at C-8 position. This metabolite of schisandrin has been isolated and determined in rat liver microsomal fraction, as well as in rat and dog bile treated with β -glucuronidase and arylsulfatase (Cui and Wang, 1993; Ikeya et al., 1995). Thus M2 was tentatively determined as 6,7,8,9-tetrahydro-1,2,3,12,13,14-hexamethoxy-7,8-dimethyl-7,8-dibenzo[a,c]cycloactenediol.

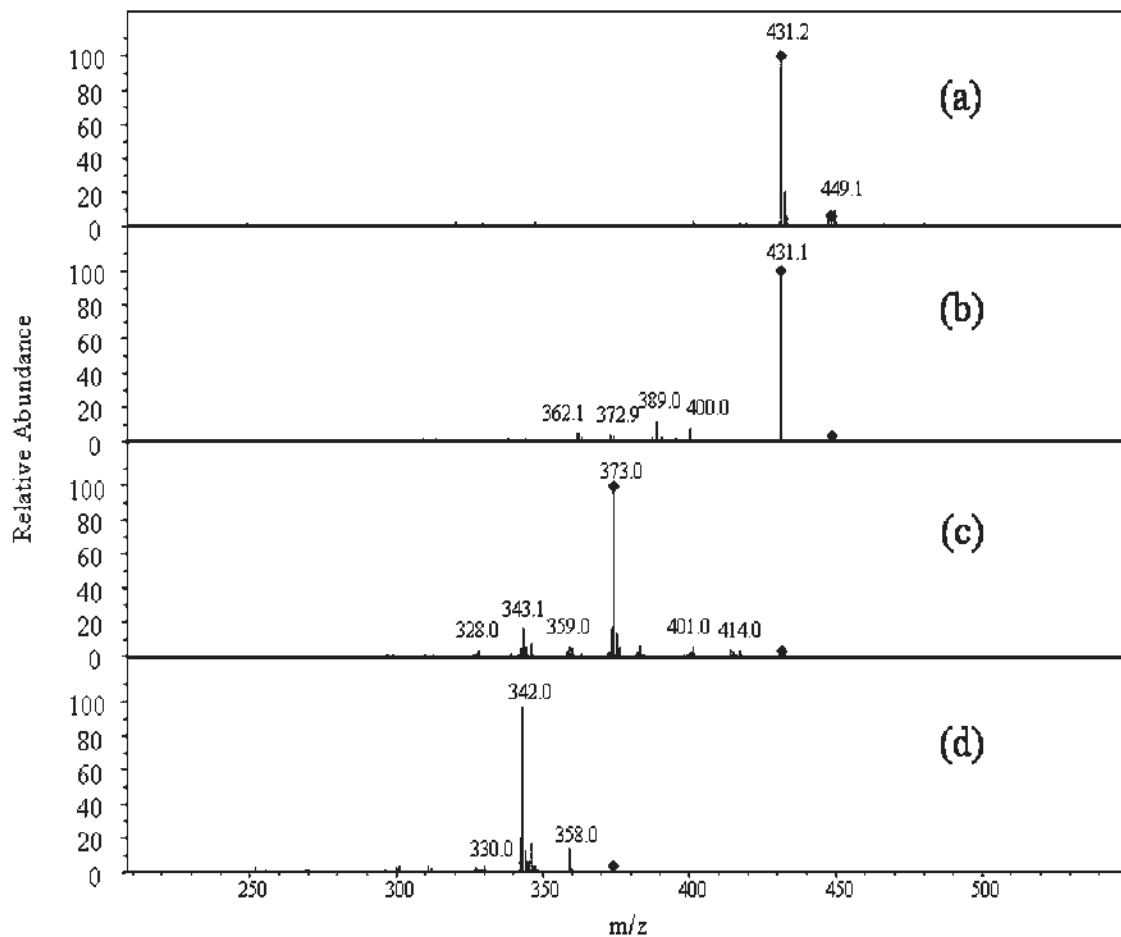


Fig. 3-28 MSⁿ spectra of M2. (a) MS spectrum of M2. (b) MS² spectrum of the $[M+H]^+$ ion at m/z 449. (c) MS² spectrum of the $[M+H-H_2O]^+$ ion at m/z 431. (d) MS³ spectrum of the ion at m/z 373.

In the MS spectrum of M3 (Fig. 3-29), the base peak was an adduct ion $[M+H-H_2O]^+$ at m/z 401. In the MS² experiment, the precursor ion at m/z 401 gave rise to product ions at m/z 386 $[M+H-H_2O-CH_3]^+$, m/z 370 $[M+H-H_2O-CH_3O]^+$ and m/z 338 $[M+H-H_2O-CH_3O-CH_4O]^+$. The abundant ion at m/z 370 further yielded fragment ions at m/z 355, 338, 324 and 313 by elimination of CH₃, CH₄O, CH₃ and CH₃O, CH₃ and C₃H₆, respectively. The fragmentation pathway of M3 was analogous to that of schisandrin, indicating a correlation of their chemical structures. As the mass difference between M3 and schisandrin was 14 Da, M3 could be formed by demethylation of schisandrin. Four demethylated forms of schisandrin at C-2, C-3, C-12, C-13 position had been isolated from rat and dog bile treated with β -glucuronidase and arylsulfatase (Ikeya et al., 1995). Therefore, M3 was tentatively identified as 6,7,8,9-tetrahydro-(2, 3, 12 or 13)-hydroxy-pentamethoxy-7,8-dimethyl-8-dibenzo[a,c]cycloactenol. Moreover, among the three metabolites deriving from schisandrin, M1 exhibited the shortest retention time, followed by M2 and M3, indicating the polarity of M1 being the most polar, M3 being the least, and M2 in between. This observation likely agreed with the number of hydroxyl group in the elucidated structures of M1, M2 and M3 showing decreasing number of hydroxyl substitution on the cyclooctadiene ring. Such evidence further supported the identification of M1, M2 and M3.

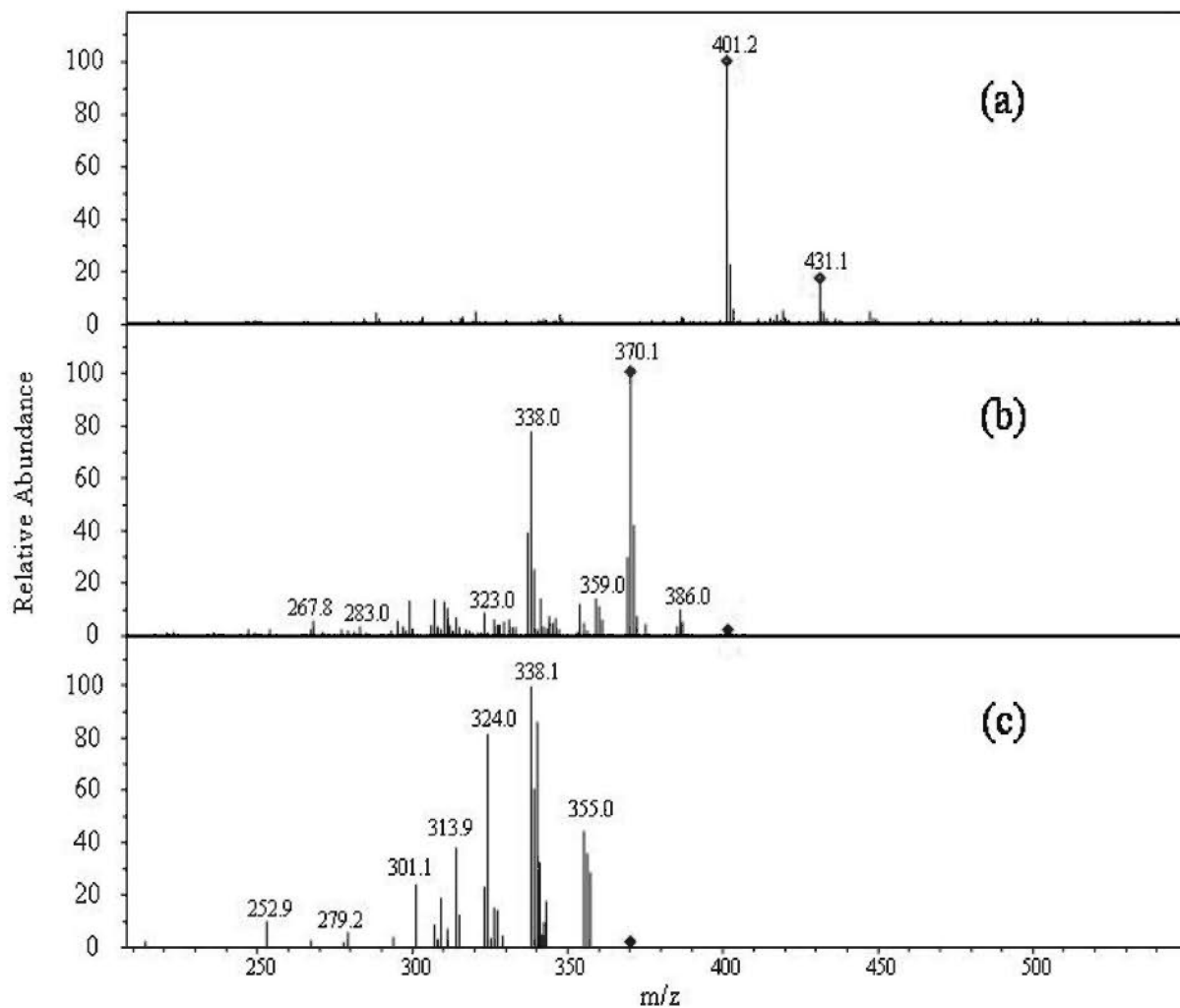


Fig. 3-29 MSⁿ spectra of M3. (a) MS spectrum of M3. (b) MS² spectrum of the [M+H-H₂O]⁺ ion at *m/z* 401. (c) MS³ spectrum of the ion at *m/z* 370.

Fig. 3-30 shows that M4 gave an adduct ion $[M+H-H_2O]^+$ at m/z 431 in the MS spectrum, which was identical with M1. However, in the MS² spectrum of M4, the precursor ion at m/z 431 gave entirely different product ions at m/z 413, 399, 389 and 387. The mass difference between them was 18, 32, 42 and 44, corresponding to the loss of H₂O, CH₃OH, C₃H₆ and C₂H₄O, respectively. In the MS³ spectrum of the m/z 387 ion, it produced daughter ions at m/z 372 and 356 via the loss of CH₃ and CH₃O group respectively. Interestingly, angeloylgomisin Q and tigloylgomisin Q (C6 and C7) also exhibited the adduct ion at m/z 431 (Fig. 3-18 and Fig. 3-19, Section 3.3.1.3.3) that gave the identical MSⁿ fragmentation with the m/z 431 ion of M4. As stated above, the poor bioavailability of C6 and C7 in rat plasma could be due to rapid hydrolysis of enzymes in the small intestine, blood or liver. Thus M4 could be hydrolyzed product of angeloylgomisin Q or tigloylgomisin Q. Owing to the substitution site of angeloyl or tigloyl group, M4 may be hydrolyzed at C-6 position, which could be distinguished from the C-8 hydroxylation of M1. This could explain the different MSⁿ fragmentation pattern between them. Therefore, M4 could be identified as 6,7,8,9-tetrahydro-1,2,3,12,13,14-hexamethoxy-7,8-dimethyl-6,7-dibenzo[a,c]cycloactenediol.

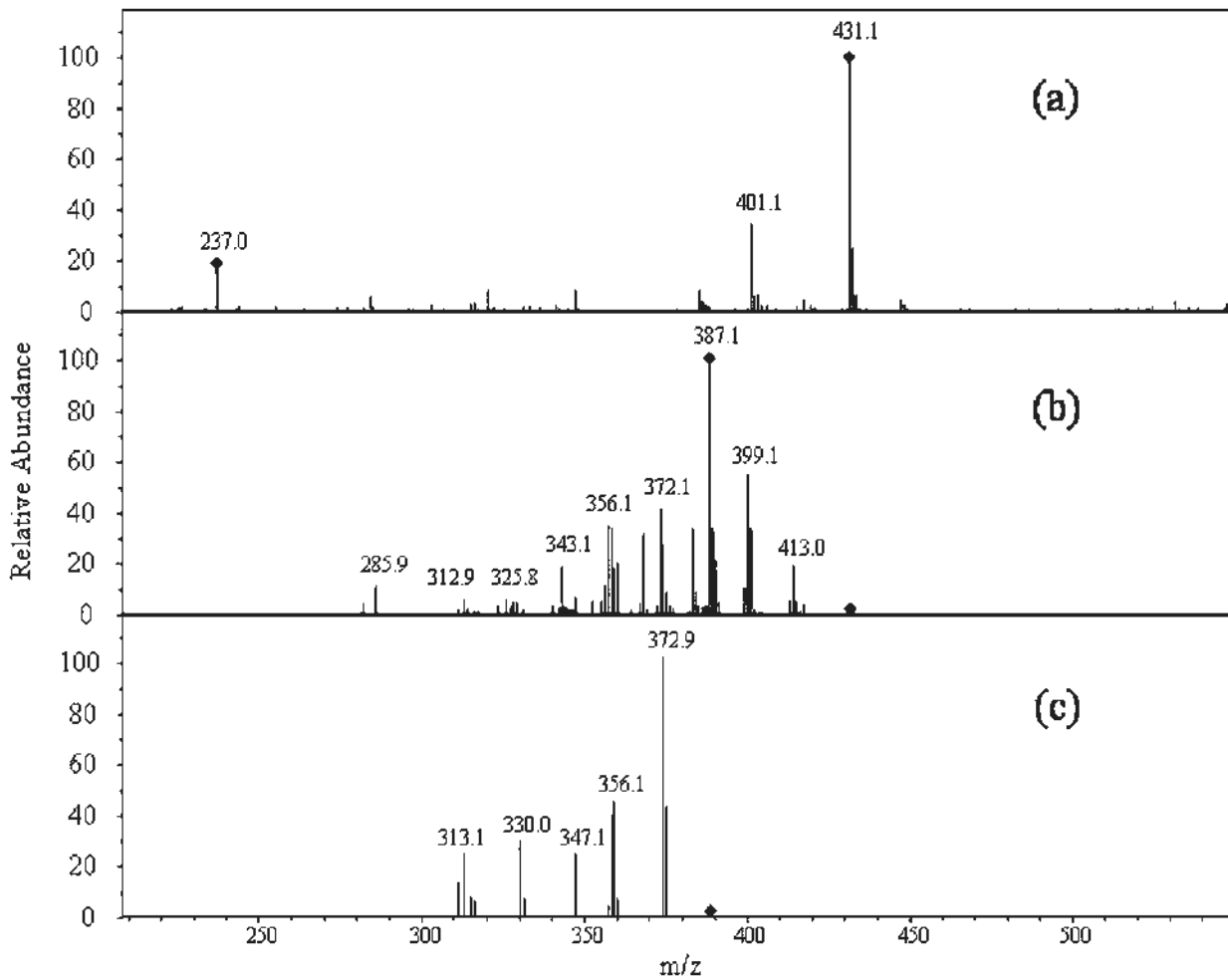


Fig. 3-30 MSⁿ spectra of M4. (a) MS spectrum of M4. (b) MS² spectrum of the [M+H-H₂O]⁺ ion at *m/z* 431. (c) MS³ spectrum of the ion at *m/z* 387.

3.3.3 Pharmacokinetics of Schisandra lignans in the rat

3.3.3.1 Validation for simultaneous determination of Schisandra lignans in rat plasma

The HPLC-MS method described in this section has high sensitivity and specificity that enabled simultaneous determination of four Schisandra lignans in rat plasma. In the MS spectra, schisandrin (SCH-1), gomisin A (SCH-2) and the internal standard (I.S.) bicyclol formed dominant adduct ion by elimination of a molecular of water at m/z 415, 399 and 373, respectively, whereas deoxyschisandrin (SCH-3) and γ -schisandrin (SCH-4) exhibited protonated ion at m/z 417 and 401 as the base peak respectively, as shown in Fig. 3-31. Under the described HPLC condition, the retention times of SCH-1, SCH-2, SCH-3, SCH-4 and I.S. were 8.6, 10.2, 19.3, 23.2 and 6.4 min, respectively. As presented in Fig. 3-32, the resolution of the method is sufficient and no interfering peak was observed in rat plasma samples under selected ion monitoring (SIM) detection mode. The overall analysis time was 30 min, which is suitable for the simultaneous determination of four analytes.

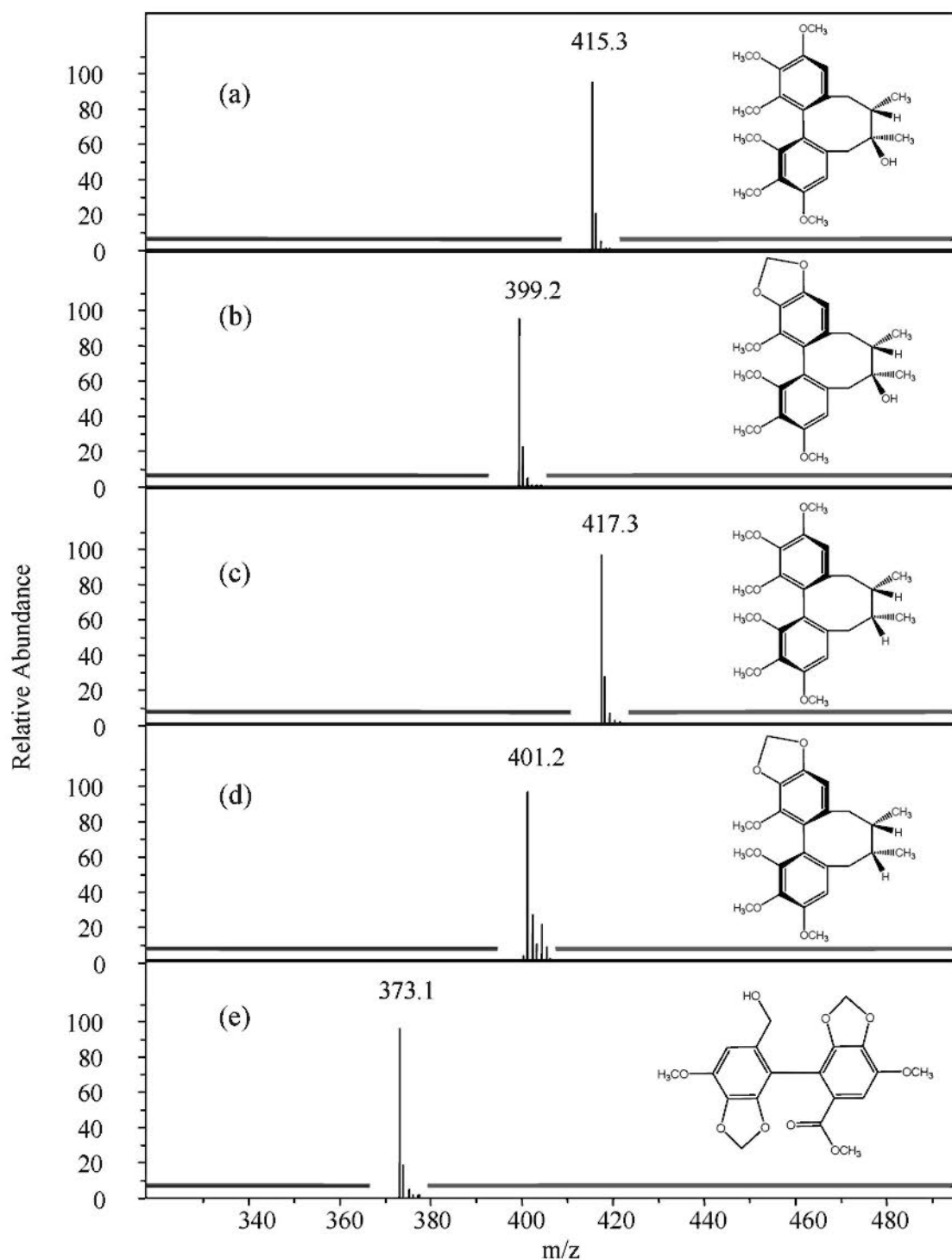


Fig. 3-31 Mass spectra of schisandrin (SCH-1), gomisin A (SCH-2), deoxyschisandrin (SCH-3), γ -schisandrin (SCH-4) and internal standard bicyclol (I.S.) obtained by selected ion monitoring (SIM). The compound structures are also shown.

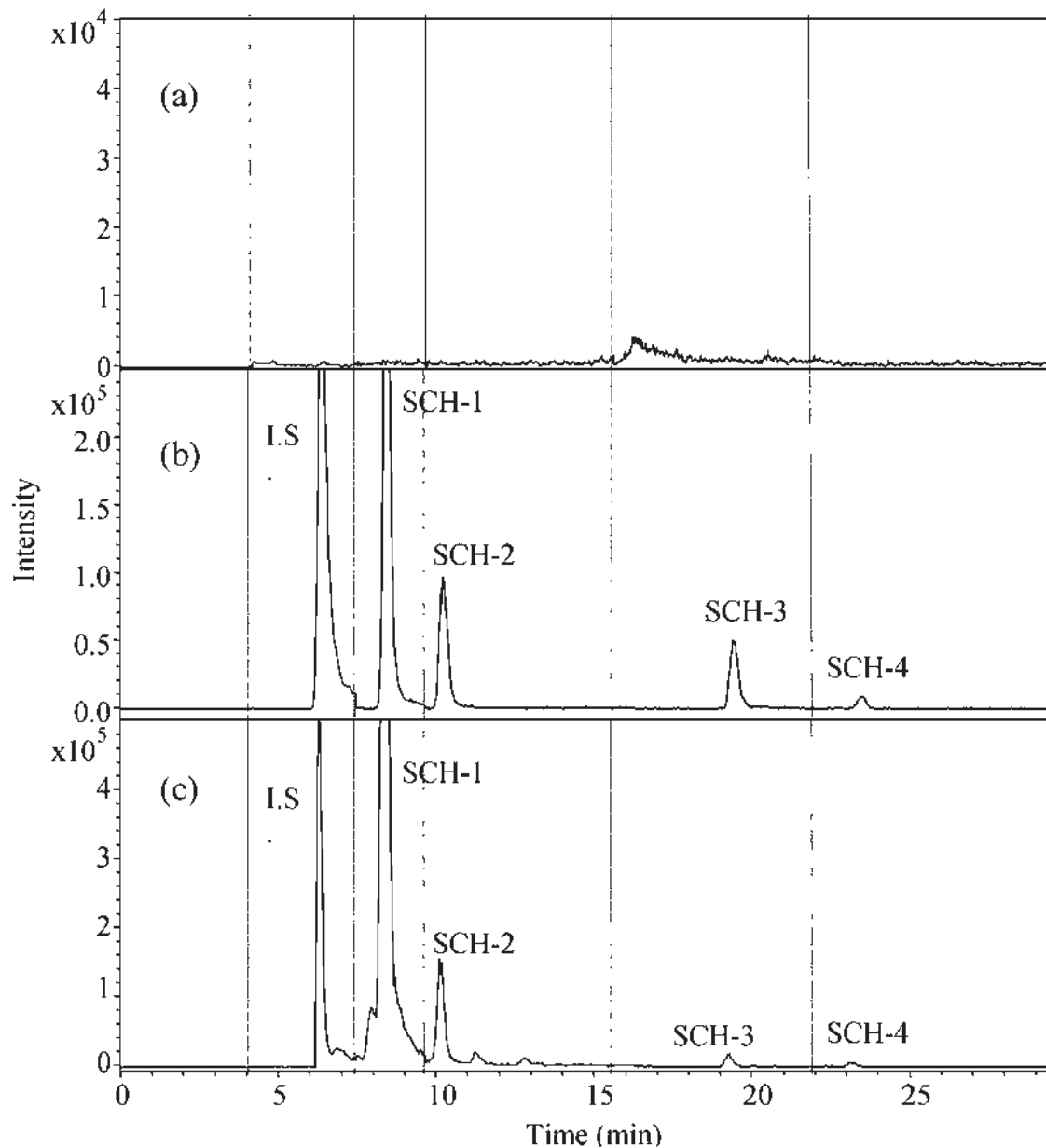


Fig. 3-32 Selected ion monitoring (SIM) mass chromatograms obtained by HPLC-APCI-MS with positive mode, giving target ions of schisandrin (SCH-1, m/z 415), gomisin A (SCH-2, m/z 399), deoxyschisandrin (SCH-3, m/z 417), γ -schisandrin (SCH-4, m/z 401) and bicyclol (I.S., m/z 373) in (a) blank plasma, (b) blank plasma spiked with four Schisandra lignans and bicyclol and (c) a plasma sample at 4 h after oral administration of a 70% ethanol extract of *S. chinensis* at the dosage of 2 g/kg.

As listed in Table 3-4, calibration curves for the Schisandra lignans showed good linear correlations ($r^2 > 0.99$). The LOD for SCH 1-4 determined by signal-to-noise ratio of more than five were 0.5, 1, 2 and 2 ng/mL, respectively. The LOQ for SCH 1-4 determined as a signal-to-noise ratio of more than ten were 1, 3, 5 and 5 ng/mL, respectively. The low limits of detection and quantification guarantee high sensitivity that permits analyzing biological specimen with low drug concentrations.

Three levels of concentrations (low, medium and high) for each analyte were used to evaluate the precision, accuracy and recovery of the method. As presented in Table 3-5, the intra-day precision of the measured concentrations for each concentration level was <15% R.S.D. ($n = 5$) while the inter-day precision was within 18% R.S.D. ($n = 6$). The accuracy for each concentration level was within the range from 80% to 110 % (comparing the calculated concentration to the known concentration) in both intra-day and inter-day assays. Compared to the HPLC-DAD method established in Chapter 2 (precision <4.3% R.S.D. and accuracy within the range from 100% to 114%), the variance of precision and accuracy of the HPLC-MS method was larger, which was reported in the literature using HPLC-MS method for quantitative analysis (Deng et al., 2007; Wang et al., 2008). Nevertheless, this range of precision and accuracy is acceptable for simultaneous determination of four analytes in complex samples such as rat plasma in this study. Recoveries of the four Schisandra lignans determined by comparing peak area ratios measured in plasma with those in methanol are presented in Table 3-6. The recovery of each analyte at each concentration level was within the range of 80–110%. These findings suggest that the analytical method has good recovery for all analytes.

Table 3-4 Calibration curves, limits of detection and quantification for the four analyzed lignans

Analyte	Regression equation ^a	r^2	Linear range ($\mu\text{g/mL}$)	LOD (ng/mL)	LOQ (ng/mL)
SCH-1	$y = 1.6603x - 0.0326$	0.9987	0.025–2.5	0.5	1
SCH-2	$y = 1.1522x - 0.0273$	0.9950	0.0125–1.25	1	3
SCH-3	$y = 1.6674x - 0.0181$	0.9951	0.005–0.5	2	5
SCH-4	$y = 0.2147x + 0.0002$	0.9963	0.005–0.5	2	5

Table 3-5 Accuracy and precision of the method for analysis of four Schisandra lignans in rat plasma

Analyte	Concentration ($\mu\text{g/mL}$)	Intra-day (n = 5)			Inter-day (n = 5)		
		Mean \pm S.D. ($\mu\text{g/mL}$)	Accuracy (%)	Precision (R.S.D., %)	Mean \pm S.D. ($\mu\text{g/mL}$)	Accuracy (%)	Precision (R.S.D., %)
SCH-1	0.125	0.107 \pm 0.004	85.2	3.8	0.105 \pm 0.011	85.4	10.2
	0.50	0.451 \pm 0.030	90.2	6.7	0.457 \pm 0.078	91.4	17.0
	2.0	1.689 \pm 0.250	84.4	15.0	1.776 \pm 0.180	88.8	10.1
SCH-2	0.0625	0.063 \pm 0.004	100.2	6.7	0.064 \pm 0.009	102.9	13.7
	0.25	0.205 \pm 0.011	81.6	5.2	0.202 \pm 0.018	80.7	8.9
	1.0	0.863 \pm 0.090	86.3	10.4	0.863 \pm 0.111	86.3	12.9
SCH-3	0.025	0.025 \pm 0.004	100.4	3.3	0.027 \pm 0.003	108.9	10.8
	0.10	0.085 \pm 0.005	84.8	5.8	0.094 \pm 0.014	93.9	14.9
	0.4	0.363 \pm 0.030	90.67	8.3	0.401 \pm 0.058	100.2	14.4
SCH-4	0.025	0.021 \pm 0.002	85.2	7.5	0.022 \pm 0.003	87.3	14.9
	0.10	0.096 \pm 0.004	95.6	3.9	0.104 \pm 0.015	104.2	14.8
	0.4	0.390 \pm 0.055	97.4	14.1	0.428 \pm 0.071	107.0	16.7

Table 3-6 Recoveries of four Schisandra lignans in rat plasma samples (n = 3)

Analyte	Concentration ($\mu\text{g/mL}$)	Peak area ratio measured in plasma	Peak area ratio measured in methanol	Recovery (%)
SCH-1	0.125	0.137 ± 0.016	0.171 ± 0.025	80.5
	0.50	0.716 ± 0.050	0.842 ± 0.109	85.0
	2.0	2.645 ± 0.461	2.806 ± 0.097	94.2
SCH-2	0.0625	0.045 ± 0.004	0.047 ± 0.002	94.7
	0.25	0.208 ± 0.012	0.243 ± 0.008	85.5
	1.0	0.967 ± 0.104	0.878 ± 0.052	110.2
SCH-3	0.025	0.024 ± 0.001	0.029 ± 0.002	82.0
	0.10	0.123 ± 0.008	0.125 ± 0.009	98.8
	0.4	0.587 ± 0.050	0.591 ± 0.053	99.2
SCH-4	0.025	0.005 ± 0.001	0.005 ± 0.000	100.6
	0.10	0.021 ± 0.001	0.019 ± 0.002	107.6
	0.4	0.080 ± 0.013	0.076 ± 0.008	105.1

Recovery = (Peak area ratio measured in plasma/Peak area ratio measured in methanol) \times 100%

3.3.3.2 Pharmacokinetics of four Schisandra lignans in rats

The validated HPLC-MS method has been utilized for the quantitative analysis of four lignans in rat plasma in support of *in vivo* pharmacokinetic studies of *Schisandra chinensis*. Plasma concentrations versus time profiles of the four lignans after a single oral dose of *S. chinensis* ethanol extract are shown in Fig 3-33., and the main pharmacokinetic parameters are summarized in Table 3-7. The plasma concentrations of four lignans were detectable at 0.25 h after oral administration, and reached maximum concentrations at 3.29 ± 0.42 , 4.07 ± 0.86 , 3.85 ± 0.77 and 4.71 ± 0.99 h for SCH-1, SCH-2, SCH-3 and SCH-4, respectively, which suggested the transport of these lignans across intestinal barrier was fast. Comparing the C_{max} and $AUC_{\infty}(\text{expo})$ of each analyte, SCH-1 exhibited the largest absorptive fraction, followed by SCH-2, SCH-4 and SCH-3. In addition, considering the equivalent dosage of the four lignans (30.95 mg/kg for SCH-1, 14.40 mg/kg for SCH-2, 4.63 mg/kg for SCH-3 and 17.06 mg/kg for SCH-4), it was suggested that the bioavailability of SCH-1 was higher than the other three, while SCH-3 and SCH-4 were comparable but poorer than SCH-1 and SCH-2. Further, V_d values revealed that the tissue distribution of SCH-4 was the most extensive among the four lignans. The results also demonstrated SCH-1 was rapidly eliminated whereas clearance of SCH-4 was the slowest as indicated by the $T_{1/2}$ and CL values.

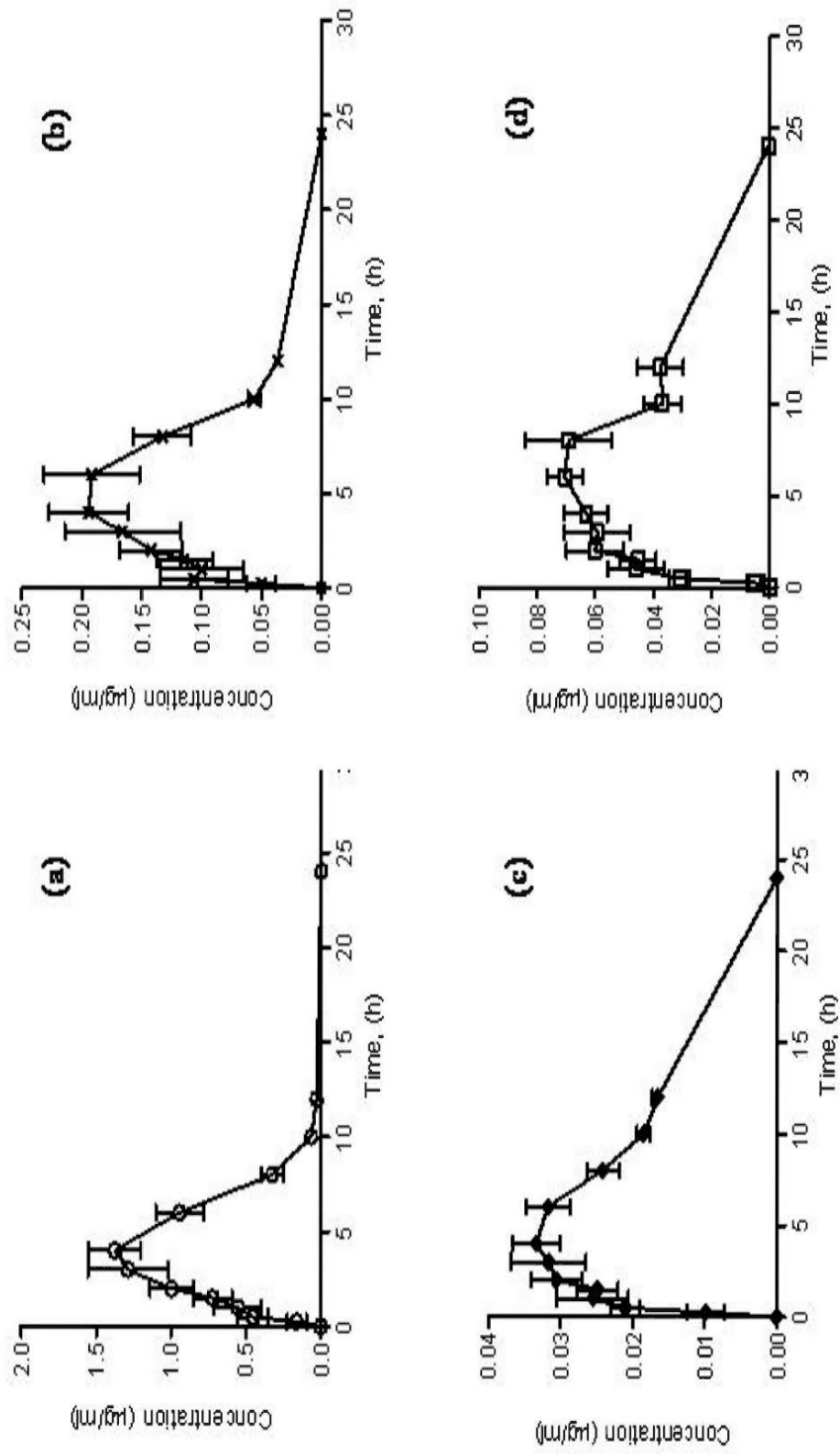


Fig 3-33 Plasma concentration-time curves of the four lignans, (a) SCH-1, (b) SCH-2, (c) SCH-3 and (d) SCH-4, after oral administration of a 70% ethanol extract of *S. chinensis* at a dose of 2 g/kg to rats. Values are expressed as mean \pm S.E.M. (n = 7).

Table 3-7 Pharmacokinetic parameters of the four Schisandra lignans in rats after a single oral administration of Schisandra 70% ethanol extract at 2g/kg. Values are expressed as mean \pm S.E.M. (n = 7).

	SCH-1	SCH-2	SCH-3	SCH-4
$T_{1,2}$ (h)	1.30 \pm 0.07	2.52 \pm 0.29	6.16 \pm 0.79	6.04 \pm 1.96
C_{max} (μ g/mL)	1.531 \pm 0.236	0.226 \pm 0.038	0.040 \pm 0.003	0.099 \pm 0.009
T_{max} (h)	3.29 \pm 0.42	4.07 \pm 0.86	3.85 \pm 0.77	4.71 \pm 0.99
AUC_r (expo) (μ g·min/mL)	35.62 \pm 5.01	5.15 \pm 1.46	0.59 \pm 0.04	1.88 \pm 0.52
Vd (L/kg)	9.16 \pm 2.4	35.84 \pm 6.10	89.48 \pm 8.25	129.3 \pm 25.1
CL (L/min/kg)	4.64 \pm 0.84	9.62 \pm 1.09	10.46 \pm 0.77	18.42 \pm 2.45

3.4 Discussion

A number of investigations have demonstrated the biological and pharmacological effects of a huge number of Chinese medicines using a variety of *in vitro* and *in vivo* models. However, the behaviors of active ingredients in the body system are less studied. Recently, more investigations on the absorption and metabolism of isolated pure substances, including flavonoids, isoflavones, polyphenols, alkaloids, quinines and saponins, have been carried out (Walle, 2004; Williamson and Manach, 2005; Hao et al., 2006; Han et al., 2006; Zhang et al., 2006). Considering the multiple active ingredients in Chinese medicine, pharmacokinetic studies on single compound are far from sufficient. Owing to the importance of bioavailability of modern drug development, the lack of absorption study on Chinese Medicine, at least partially, limits its modernization and globalization. The highly sensitive, selective and efficient HPLC-MS method enables the analysis of multiple active principles in the complex biological specimens. In the present work, a HPLC-DAD-MS method has been employed as a useful tool for profiling the absorption of *Schisandra chinensis* in rat everted gut sac and Caco-2 cell monolayer *in vitro* models. Absorption and metabolism of *S. chinensis* were also analyzed in rat plasma. Further to the qualitative analysis, a validated HPLC-MS method was used for simultaneously determining the plasma pharmacokinetics of four major Schisandra lignans in the rat.

Everted gut sac has long been used as an *in vitro* tissue system to study intestinal drug absorption, but its application is limited by the lack of standardized permeability coefficient. Caco-2 cell is a human colon cancer cell line, and the monolayer model has

been recognized by American Food and Drug Administration (FDA) as a useful tool to clarify the intestinal transport of drug candidates. In the present work, these two *in vitro* models have been utilized to examine the intestinal absorption of *S. chinensis*. Fifteen lignans were identified as the absorbable compounds from a Schisandra aqueous extract based on HPLC-MSⁿ data. The attempt to use ethanol extract of *S. chinensis* was unsuccessful due to the poor dissolution of lipophilic components (such as γ -schisandrin) in the transport solutions. It has been reported that different intestinal absorption profiles of Astragali Radix decoction were observed in rat everted gut sac and Caco-2 cell monolayer models, and glycosides were less permeable in the cells than in the gut sac (Xu et al., 2006). However, in this study, there was little difference between the absorption profiles of *S. chinensis* in rat everted gut sac and human Caco-2 cell monolayer models, except for the lower signal intensity in the cell model than the sac system, which could be explained by the low concentration used in Caco-2 cells. This suggested that the absorbable lignans identified could exhibit high intestinal absorption potential in both rat and human.

Further to the profiling studies, quantitative analysis of intestinal permeability in the Caco-2 cell monolayer model revealed that schisandrin, the major absorbable compound, exhibited high intestinal absorption potential with an apparent permeability coefficient (P_{app}) in the range of $14\text{-}19 \times 10^{-6}$ cm/sec (apical to basolateral), and the transport across intestinal mucosa proceeded mainly via passive diffusion as indicated by the efflux ratio in the range of 1.0 – 1.3 in bidirectional transport. By comparing the peak area of the other absorbable lignan compounds with schisandrin in the profiles obtained from Caco-2

cell model, it has been shown that these lignans would exhibit medium to high intestinal absorption potential. This is in accordance with the findings that gomsin A, which was also present in the absorbable components in this study, displayed high intestinal permeability with P_{app} values in the range of $25 - 29 \times 10^{-6}$ cm/sec (Madgula, 2007).

Intracellular accumulation of the absorbable lignans in Caco-2 cells was also determined after transport studies. There was no significant amount of the fifteen lignans found in the cell extraction, indicating these absorbable components could be predominantly transported across intestinal mucosa to enter body fluid circulation with little accumulation in the enterocytes. The mass balance, which was determined by comparing the sum of the cumulative amount transported and the amount remaining in both chambers with the initial amount added in the donor, was more than 92% for each assay. The overall recovery of schisandrin was more than 95% and no degradation and metabolism was observed. Similarly, during the transport of Schisandra aqueous extract, no metabolite was detected in the rat everted gut sac and human Caco-2 cell monolayer models, indicating first-pass metabolism did not take place during intestinal absorption.

The *in vitro* models enable rapid profiling of the intestinal absorption of Schisandra aqueous extract and provide information on the absorption mechanisms of absorbable compounds, but the pharmacokinetic behaviors of absorbable lignans should be clarified *in vivo*. The absorption profile of *Schisandra chinensis in vivo* was examined in rat plasma at different time intervals. It appeared that the absorption extent of aqueous extract was lower than that of ethanol extract, which could be due to the lower

concentrations of lignan compounds and the abundance of saccharide interfering lignan absorption of the aqueous extract. Nevertheless, both absorption profiles shared similar characters. In relation to the *in vitro* studies, Schisandra lignans were also identified as the major absorbable components *in vivo*. Meanwhile, the metabolites that were not found during *in vitro* absorption were present in rat plasma. Four major metabolites have been identified as the derivatives of absorbable compounds probably from the first-phase metabolic transformation including hydrolysis, hydroxylation and demethylation.

M1, M2 and M3 were identified as the hydroxylated and demethylated forms of schisandrin, one of major absorbable components of *S. chinensis*, according to the MSⁿ data and previous studies. The present results were in agreement with previous work reporting 7,8-dihydroxy-schisandrin (M2), 7,8-dihydroxy-2-demethyl-schisandrin (M1) and 7,8-dihydroxy-3-demethyl-schisandrin were the major metabolites isolated from the culture containing rat liver microsomal fraction (Cui et al., 1992; 1993). In the hepatic clearance system, cytochrome P450 (CYP) enzymes play a predominant role in drug metabolism and toxicity elimination by performing a variety of oxidation reaction, including aromatic and aliphatic hydroxylation, N-/O-/S- dealkylation, N-/S- oxidation, epoxidation and so on (Smith et al., 1992; Lewis et al., 1998; Smith et al., 2006). Xu et al. (2007) demonstrated the possible involvement of CYP3A and CYP2C isoforms in schisandrin metabolism using selective inhibitors of CYP enzymes and stated that the gender difference of schisandrin metabolism could be due to the difference of corresponding metabolic enzymes in rat liver. Despite the uncertainty of specific metabolic enzymes responsible for the biotransformation of schisandrin, CYP enzymes

for sure play a key role. On the other hand, no significant metabolism was observed in the *in vitro* absorption despite the presence of P450 isoenzymes in rat small intestine (Zhang et al., 1996). Given the marked difference in expression and function of P450 isoenzymes between small intestine and liver, these results were not surprising (Zhang et al., 1999; Lindell et al., 2003). It has been reported that the expression of CYP3A4 in the intestinal wall was rather poor without induction or transfection (Cummins et al., 2001). It was also possible that the expression and function of the P450 enzymes responsible for the biotransformation of schisandrin was too weak in the small intestine to carry out metabolism of schisandrin.

Moreover, as suggested by Xu et al. (2007) and Ono (2001), 7,8-dihydroxy-2-demethyl-schisandrin (M1) was the major metabolite of schisandrin in rat plasma as well as in the culture treated with hepatic microsomes *in vitro*. As presented in Fig 3-25 and Fig 3-26, a noticeable difference of metabolite concentrations (by peak area comparison) was observed when different extracts were used, 7,8-dihydroxy-2-demethyl-schisandrin (M1) being the major metabolite in aqueous extract and 7,8-dihydroxy-schisandrin (M2) in ethanolic extract. One possible explanation could be the difference in drug-drug interaction caused by the various contents of lignan compounds in the extracts, as suggested in Chapter 2. In the aqueous extract, schisandrin was the predominant lignan that accounted for more than 70% of four major lignans, thus metabolic transformation of schisandrin in aqueous extract could be similar to the isolated form, with M1 being the major metabolite. On the other hand, the amounts of other lignans were considerable in the ethanolic extract (schisandrin : gomsin A : deoxyschisandrin : γ -schisandrin = 15.5 :

7.2 : 2.3 : 8.5), thus drug-drug interaction on the metabolism of schisandrin should be taken into account. In previous studies, *Schisandra chinensis* extracts and the isolated lignan components had been found to inhibit rat and human cytochrome P450 activity (Liu et al., 1982; Iwata et al., 2004). Recent study had pinpointed the inhibitory effects of Schisandra lignans on various human P450 activities, including CYP1A2, CYP2C9, CYP2C19, CYP2D6 and CYP3A4, using marker substrate assays (Iwata et al., 2004). It was suggested that gomisins B, C and G inhibited CYP3A4 more specifically than the other isomers while gomisins A and N exhibited comparable inhibition on CYP2C19 and CYP3A4. Among the examined Schisandrin lignans, gomisins A, B (schisantherin B), C (schisantherin A) and G have been identified as the absorbable components of *S. chinensis* in this study. Thus, these absorbable lignans might specifically inhibit CYP3A4 isoform possibly responsible for O-demethylation of schisandrin, resulting in the concentration decrease of 7,8-dihydroxy-2-demethyl-schisandrin (M1) in rat plasma.

In addition to the P450-mediated metabolism, the hydrolysis of absorbable lignans has been observed in rat plasma. On the basis of MSⁿ data, M4 was identified as the hydrolyzed form at carbon-6 position of angeloylgomisin H (C6) and/or tigloylgomisin H (C7). Since this metabolite was not found in the rat everted gut sac or Caco-2 cell monolayer model, hydrolysis of the parent compounds could take place before or after absorption. Although there were reports on the intestinal bacterial communities mediated dietary lignan metabolism in human (Clavel et al., 2005), the bacterial function was unlikely to contribute to the rapid and dramatic degradation of angeloylgomisin H and tigloylgomisin H in rat plasma. Therefore, the rapid clearance could be predominantly

mediated by the blood where the erythrocyte surface has high contents of non-specific esterases responsible for hydrolysis of ester molecules. Furthermore, rodent blood has very high esterase amount, thus angeloylgomisin H and tigloylgomisin H could be rapidly hydrolyzed once entering blood stream to form metabolite M4. The hydrolytic reaction could also happen to C8 and C9 that possess an aliphatic ester bond at carbon-6 position (Fig. 3-4). In contrast, angeloylgomisin and tigloylgomisin H (C4 and C5) were still detected despite the presence of ester in their structures (Fig. 3-4). One possible explanation is that the phenolic ester in C4 and C5 required hydrolysis of arylesterases, whose content could be lower than aliesterases in rat blood. Besides, gomisin G, schisantherin B, schisantherin C and schisantherin A (aliphatic ester molecules) also underwent less clearance as indicated by their presence in rat plasma. This could have been stabilized by benzoyl group (rather than O-angeloyl or O-tigloyl group) that can presumably prevent close approach of the attacking nucleophile to the ester bond (Smith et al., 2006). Similarly, steric effects have been utilized to stabilize a variety of antimuscarinic compounds by the incorporation of hydroxyethyl side chain or a cyclic ring system at a position surrounding the ester function (Smith et al., 2006).

Four major Schisandra lignans, including schisandrin, gomisin A, deoxyschisandrin and γ -schisandrin, have been chosen as representatives of active principles for studying the pharmacokinetic characteristics of *Schisandra chinensis*. Compared to the HPLC-DAD method (Chapter 2), the HPLC-MS in this part of study showed much higher sensitivity with 400-, 133-, 40- and 40-fold of LOQ for SCH-1, 2, 3, 4, respectively. The higher sensitivity and selectivity enabled simultaneous quantification of four lignans in the rat

plasma. At 15 min after single dose administration, plasma concentrations of all the analytes were detectable, indicating their transport across intestinal epithelium could be fast. On the other hand, AUC and C_{max} values of the analytes varied dramatically with the range of 1.88 – 35.62 $\mu\text{g}\cdot\text{min}/\text{mL}$ and 0.04 – 1.53 $\mu\text{g}/\text{mL}$ respectively. Out of these four lignans, SCH-3 and SCH-4 tended to exhibit much lower bioavailability than SCH-1 and SCH-2. Considering the decreasing solubility of SCH-1, 2, 3, 4 in aqueous solutions (log P of 4.18, 4.77, 5.87 and 6.46, respectively), the results were not surprising. Although the high lipophilicity of hydrophobic compounds such as SCH-3 and 4 can facilitate the penetration across apical membrane of enterocytes, it also strongly interferes with the compound dissolution in lumen for contacting intestinal epithelium and the release from enterocytes at the basolateral side into systemic circulation. Similar low bioavailability has been observed for other highly lipophilic compounds such as amphotericin B (Wasan et al., 1998) and tanshinone IIA (Hao et al., 2006).

SCH-1 represented the largest fraction absorbed in rats among the four lignans, which was in agreement with its high bioavailability, as suggested in the literatures (One, 2001, Xu et al., 2005). Combining these results with permeability across Caco-2 cell monolayers and the physicochemical properties (log P, 4.18; mass solubility, 0.005 mg/mL), SCH-1 would be classified into the high permeability-low solubility group according to the biopharmaceutical classification system (Amisdon et al., 1995; Pade et al., 1998). On the other hand, SCH-1 also underwent the most rapid metabolic clearance as indicated by the shortest $T_{1/2}$ and CL values among the four lignans. This was further supported by the observation that the metabolites (M1, M2 and M3) of schisandrin were

detectable as the major metabolites as soon as 15 min after administration (Fig. 3-26). It is arguable that the $T_{1/2}$ value in this study was shorter than the reported range of 1.5 - 4.5 h (Xu et al., 2007; Wang et al., 2008). However, owing to the variance of experimental conditions, the $T_{1/2}$ difference could result from the various levels of metabolic enzymes in animals influenced by age, diet and living conditions, as well as the different compositions of *Schisandra* extracts that could affect enzymatic metabolism of schisandrin. Moreover, with the increasing lipophilicity, systemic clearance of SCH-1, 2, 3 and 4 slowed down correspondingly. In parallel, the V_d values increased in the order of SCH-1, 2, 3 and 4. Since larger V_d value indicates higher potential of tissue distribution, SCH-4 was speculated to be widely distributed in organs as suggested by the rather large volume of distribution (18.4 L/kg), about 32-fold of the total body water volume of rats. Although the experimental data about tissue distribution was not available in this study to clarify the underlining mechanisms, the high lipophilicity of SCH-4 (log P, 6.46) might be the main contributor causing extensive binding to the tissues. Similarly, extensive tissue distribution was also observed for other highly lipophilic compounds such as tanshinone IIA (Hao et al., 2006). In terms of the slower clearance and wider tissue distribution, SCH-4 can maintain an effective concentration for a longer period and more sufficient contact with potential targets despite the lower bioavailability. Therefore, the lipid-soluble components in *Schisandra chinensis*, such as SCH-3 and 4, can also make important contributions to the pharmacological effects for the concerning disease (irritable bowel syndrome) in this study, in complement with those highly absorbed, but rapidly eliminated and weakly distributed components, such as SCH-1 and 2.

In summary, with the aid of HPLC-DAD-MS for qualitative and quantitative analysis, the absorption of *Schisandra chinensis* in the rat everted gut sac and human Caco-2 monolayer *in vitro* models have been profiled. Schisandra lignans have been identified as the major absorbable components in these models, suggesting their high intestinal absorption potentials both in the rat and human. Besides, transport studies on schisandrin in Caco-2 cell monolayers have shown a passive diffusion pathway with high permeability, which provides quantitative evidence on the intestinal absorption of Schisandra lignans in addition to the profiling analysis. Further to the *in vitro* studies, the absorption, metabolism and plasma pharmacokinetics of *Schisandra chinensis* have been investigated in rats. Compared to the *in vitro* studies, remarkable first-phase metabolites deriving from absorbable components have been found in rat plasma. The plasma pharmacokinetics of four representative Schisandra lignans in the rat was further evaluated, and their pharmacokinetic characteristics have been recorded. As demonstrated above, bioavailability study using *in vitro* models, such as rat everted gut sac and human Caco-2 cell monolayer, and animal models *in vivo* subsequently coupled to HPLC-MS analysis, would be a useful approach to investigate the absorption, metabolism and pharmacokinetics of herbal medicines, despite the complexity of constituents. Since it has been shown that Schisandra lignans are the major absorbable components of *Schisandra chinensis*, the findings in this study also provide useful information for understanding the roles of Schisandra lignans in the pharmacological actions of the plant drug.

Chapter 4

Evaluation of Relaxant Effects of *Schisandra chinensis* on Intestinal Contractility *In Vitro*

4.1 Introduction

Irritable bowel syndrome (IBS) is a complex disease that comprises of a group of functional gastrointestinal disorders in which no unique target receptor for pharmacotherapy is currently available (Parons and Garner, 1995; De Ponti and Malagelada, 1998). In spite of the yet unclear mechanisms of IBS, alteration of bowel motility caused by psychological or physical stress and ingestion of food has been regarded as one of the crucial pathophysiological factors in the development of IBS (Azpiroz, 2002; Camilleri, 2002). Based on alterations of bowel habit, IBS is often classified as diarrhea-predominant (D-IBS), constipation predominant (C-IBS) and alternating forms. Approximately one third of IBS patients fit the D-IBS subtype (Ragnarsson and Bodemar, 1999). Pharmacological agents that can modulate gut motility have been or are being developed for the clinical treatment of IBS (Gattuso and Kamm, 1994; Fioramonti and Buéno, 1995; Baker and Sandle, 1996; Camilleri and Choi, 1997; Vandeplassche et al., 1997).

Previous study showed that lignans isolated from *Schisandra* fruits exhibited relaxant activities in isolated trachea and ileum of guinea pigs, mesenteric artery of dogs (Mamoru et al., 1987). More recently, gomisin A and *Schisandra* extracts were found to cause

relaxation on both endothelium-intact and endothelium-denuded aortas of rats, indicating the relaxant effects of Schisandra lignans on smooth muscle contraction (Park et al., 2007; Park et al., 2009). Previous studies in our laboratory have determined the modulatory effects of a 20-herb formula on agonists (acetylcholine and serotonin) induced contraction in isolated guinea pig ileum. *S. chinensis* was one of the composite herbs found to be one of the potent components.

This part of study aims to evaluate the *in vitro* sensorimotor-modulatory effects of Schisandra extracts and four dominant Schisandra lignans. As discussed in Chapter 1, apart from the conventional cholinergic antagonism (which have antispasmodic effect with antidiarrhea potential), new pharmacologic approaches for IBS treatment include serotonin antagonism (which slows small bowel and colonic transit, as well as reduces colonic tonic response to feeding and sensation of volume of distentions) and opioid agonism (which increases threshold for visceral pain nociception). Therefore, the modulatory effects of *Schisandra chinensis* were determined by performing *in vitro* assays on guinea pig ileum contracted by acetylcholine, serotonin and electrical field stimulation (for measurement of opioid effects), as well as on rat colon with spontaneous contractility (for measurement of effects on rat colonic transit).

4.2 Materials and methods

4.2.1 Materials, chemicals and reagents

All the herbal extracts were prepared as described in the previous Chapter 2. Schisandrin (SCH-1), deoxyschisandrin (SCH-3) and γ -schisandrin (SCH-4) were obtained from National Institute for the Control of Pharmaceutical and Biological Products (Beijing, China), and Gomisin A (SCH-2) was from the Hong Kong Jockey Club Institute of Chinese Medicine. Serotonin, acetylcholine, morphine, atropine, tropisetron and naloxone were purchased from Sigma Co. (USA). The chemicals for buffer solution were analytical grade for common laboratory use. Stock solutions of water and ethanol extracts of *S. chinensis* were prepared with distilled water and dimethyl sulfoxide (DMSO) respectively. Schisandra lignans were dissolved in 100% DMSO at 100 μ M as stock. All the stock solutions were stored at -20 °C. Appropriate diluents were prepared before use. Each drug administration was between 0.5 to 30 μ l, and in each experiment, the volume of drug working solution added to the organ bath was no more than 0.3% of the bath volume.

4.2.2 Animals

Male guinea pigs (350-500g) and Sprague-Dawley rats (250-300 g) were bred and housed by the Laboratory Animal Services Centre of the Chinese University of Hong Kong. All experiments were performed with approval from the Animal Research Ethics Committee,

The Chinese University of Hong Kong. The animals were kept in a temperature controlled room (23 ± 2 °C) with a 12-hr light-dark cycle, with free access to food and water.

4.2.3 Experimental protocols of intestinal contractility *in vitro*

4.2.3.1 Acetylcholine (ACh) or serotonin (5-HT) induced contraction in isolated guinea pig ileums

Male guinea pigs were fasted overnight and sacrificed by cervical dislocation and exsanguination. A 20 cm length of ileum was removed and placed in Krebs-Henseleit solution: NaCl 118, KCl 4.7, CaCl₂ 2.5, MgSO₄ 1.2, KH₂PO₄ 1.18, NaHCO₃ 25, glucose 10 mM. After cleaning of mesenteric tissues, the ileum was cut into segments of 2 cm length and suspended in 10 mL organ bath filled with Krebs solution. The bathing solution was maintained at constant temperature 37 °C and aerated with 95%O₂/5%CO₂. Washout of the organ bath was performed by solution upward displacement and overflow. Contractions of the longitudinal muscle of guinea-pig ileum were measured with Grass FT03 isometric transducers connected to Powerlab data acquisition system (ADInstruments Pty Ltd, Australia). Initially, a basal tension of 0.8 g was applied. After equilibration for about 1 h, with frequent washes, the resting tension remained steady at approximately 0.4 g. An appropriate agonist (ACh or 5-HT) at the final concentration of 10 μM was tested on each preparation to ensure a steady and acceptable level of tension (about 3.0 g) had been reached before the experimental procedures began. After washout with Krebs solution, the isolated ileum was allowed to rest for 7 min and 10 μM ACh or

5-HT was added again to produce reference tone. Concentration-response curves of Schisandra extracts and Schisandra lignans were obtained by non-cumulative pre-incubation of these inhibitory agonists for 15 min before addition of ACh or 5-HT. After 3 min treatment, a standard procedure with washout for 3 min and resting for 7 min was allowed in between each drug administration.

4.2.3.2 Electrical field stimulated (EFS) contraction in isolated guinea pig ileum

Ileums from male guinea pigs were isolated and mounted onto the organ bath as described in Section 4.2.3.2. After equilibration for about an hour, the preparations were pre-contracted by electrical pulse with Grass S88 stimulator (Grasstechnologies, West Warwick, U.S.A.) under the following condition: 30 V of voltage, 2 ms of duration, and 0.04 TPS of rate. When the maximal contracted force reached steady at about 2.5 g, concentration-response curves of tested drugs were obtained by cumulative addition of these agonists at 5 min intervals. At the end of last dose, 200 nM naloxone was added for 3 min treatment to determine the reversal effects.

4.2.3.3 Spontaneous contraction in isolated rat colon

Male Sprague-Dawley rats were fasted overnight and sacrificed by cervical dislocation and exsanguination. Colon segments, proximal and distal, were isolated and mounted as described in Section 4.2.3.1. A basal tension of 0.5 g was applied and the basal tone remained steady at about 0.3 g after equilibration. Concentration-response curves of

Schisandra extracts and Schisandra lignans were obtained by non-cumulative incubation of these inhibitory agonists for 5 min. A standard procedure with washout for 3 min and resting for 10 min was allowed in between each drug administration.

4.2.4 Measurement of receptor binding of Schisandra lignans

Binding of Schisandra lignans to cholinergic muscarinic (M3) receptor was analyzed by a commercially available cell-based assay in GeneBLAzer M3 CHO-K1 DA cells according to the manufacturer's notes (Invitrogen, Carlsbad, C.A.). Binding was evaluated by the dual-color (blue/green) fluorescence ratio with carbachol as agonist. Effects of SCH-1, SCH-3 and SCH-4 were expressed as compared to DMSO (vehicle blank), and atropine was used as positive control. SCH-2 was not included in this binding assay due to the unavailability of reference compound when this assay was carried out.

4.2.5 Data analysis

Inhibitory responses of Schisandra extracts and lignans on the contractility of isolated guinea pig ileum were measure as the reduction of maximum tension (in grams over baseline) induced by the corresponding agonists (ACh, 5-HT) or electrical field stimulation. Values were taken as the percentage change from reference tension (e.g. -100% corresponds to the abolition of contraction). In EFS experiments, the maximum tension (in grams over baseline) was taken as the average of the last three peak values before the next treatment. Spontaneous contractility of isolated rat colon was measured as

the average contractile force (in grams over baseline) for a 4 min period. Relaxant responses of the tested drugs were taken as the percentage change from the resting spontaneous contraction before addition of inhibitory agonists. All values were expressed as mean \pm S.E.M., where n was the number of preparations from different animals used, which was at least five for all experiments. GraphPad Prism software was used to fit sigmoidal curves (variable slope) and to determine the E_{\max} and EC_{20} (or EC_{50}) values from the concentration-response curves. Results from the controls and treatments were compared by unpaired Student's t test or two-way ANOVA followed by Bonferroni post test, as appropriate. All tests were two-tailed and the significance was set at $P < 0.05$.

4.3 Results

4.3.1 Anti-cholinergic effects of *Schisandra chinensis*

4.3.1.1 Inhibition on acetylcholine (ACh) induced contraction in guinea pig ileum

As shown in Fig. 4-1(a), all *Schisandra* extracts exhibited concentration-dependent relaxant effects on ACh-induced contraction in isolated guinea pig ileum. Ethanol extracts were much more potent than water extract ($P < 0.001$) while there was no significant difference between the potency of 70% and 95% ethanol extracts ($P > 0.05$).

As determined by HPLC in Chapter 2 and 3, *Schisandra* lignans are the major chemical and absorbable components in *Schisandra* extracts and schisandrin (SCH-1), gomisin A

(SCH-2), deoxyschisandrin (SCH-3) and γ -schisandrin (SCH-4) are the four dominant ones. Fig. 4-1(b) showed that these four lignans displayed concentration-dependent inhibition on ACh-induced contraction in isolated guinea pig ileums, while DMSO (vehicle blank) had no significant effect. Regarding potency, SCH-3 was the most potent followed by SCH-4, SCH-2 and SCH-1, with their EC_{20} values of 2.2 ± 0.4 , 3.1 ± 0.6 , 3.5 ± 0.7 , $13.2 \pm 4.7 \mu\text{M}$, and the E_{max} values of $-94.5 \pm 6.5 \%$, $-98.3 \pm 13.6 \%$, $-47.0 \pm 3.9 \%$, $-34.6 \pm 5.1 \%$, respectively. Compared to vehicle, SCH-3 showed significant inhibitory response at concentrations from $1 \mu\text{M}$ to $100 \mu\text{M}$, but there was no significant difference between SCH-3 and SCH-4. SCH-1 caused significant inhibition when the concentration was up to $30 \mu\text{M}$ and was less potent than the other three. As presented in Fig. 4-2, atropine, a well known nonselective antagonist for muscarinic receptors, concentration-dependently inhibited ACh-induced contraction in isolated guinea pig ileum and abolished the contractile response ($> 90\%$) at the concentration of $1 \mu\text{M}$. Given an EC_{50} value of $25.0 \pm 0.3 \text{ nM}$, the potency of atropine was much higher than that of Schisandra lignans for at least two orders. In addition, the E_{max} value of atropine ($-94.6 \pm 2.0 \%$) was comparable to SCH-3 ($-94.5 \pm 6.5 \%$) and SCH-4 (-98.3 ± 13.6) while markedly higher than SCH-1 ($-34.6 \pm 5.1 \%$) and SCH-2 ($-47.0 \pm 3.9 \%$).

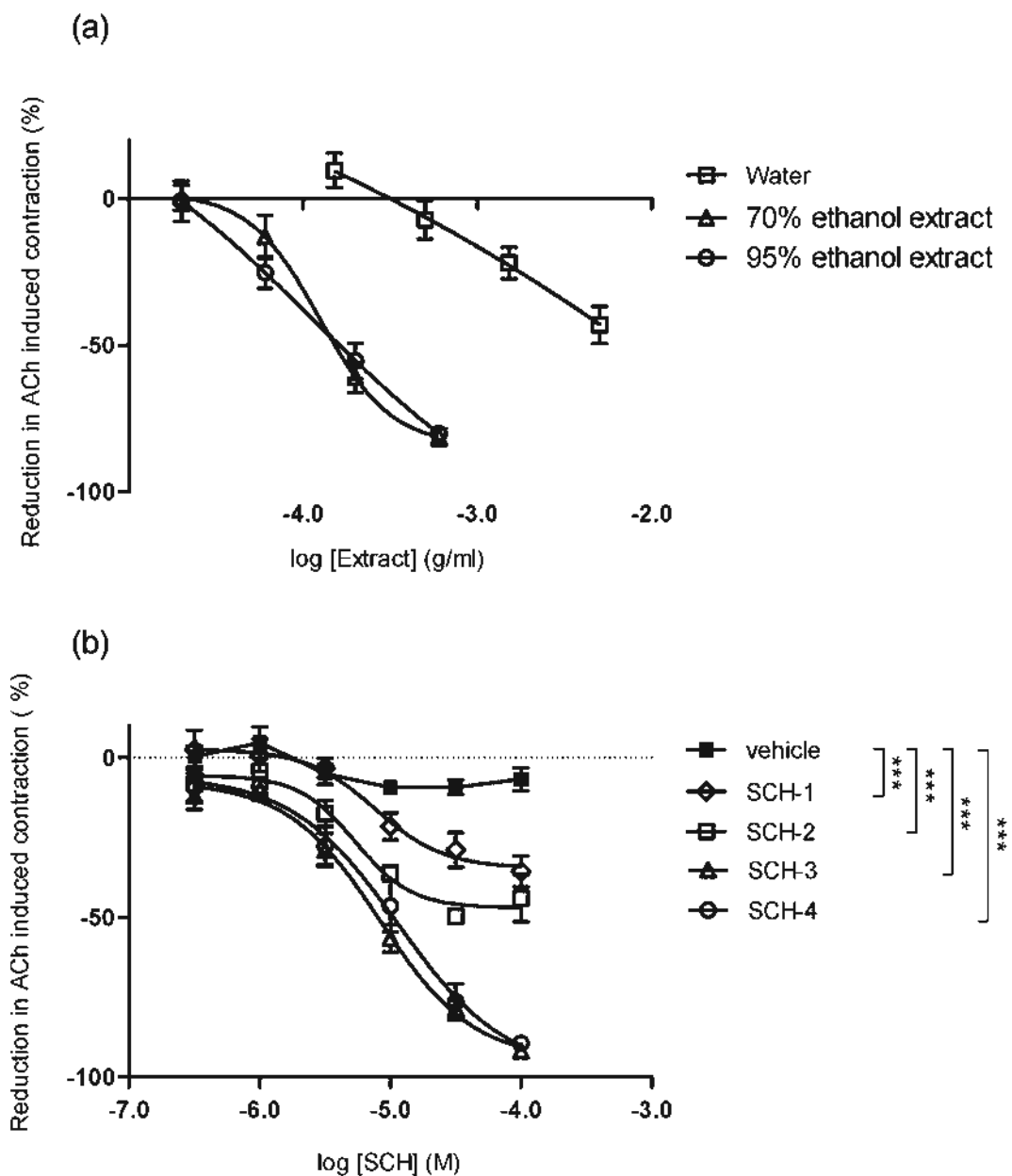


Fig. 4-1 Effects of Schisandra extracts (a) and Schisandra lignans (b) on ACh (10 μ M) induced contraction in isolated guinea pig ileums with DMSO as the vehicle blank. Isolated tissues were pre-incubated with drugs (or vehicle) for 15 min before addition of ACh. Values are expressed as mean \pm S.E.M. (n = 5-6). *** P <0.001 compared to vehicle using one-way or two-way ANOVA.

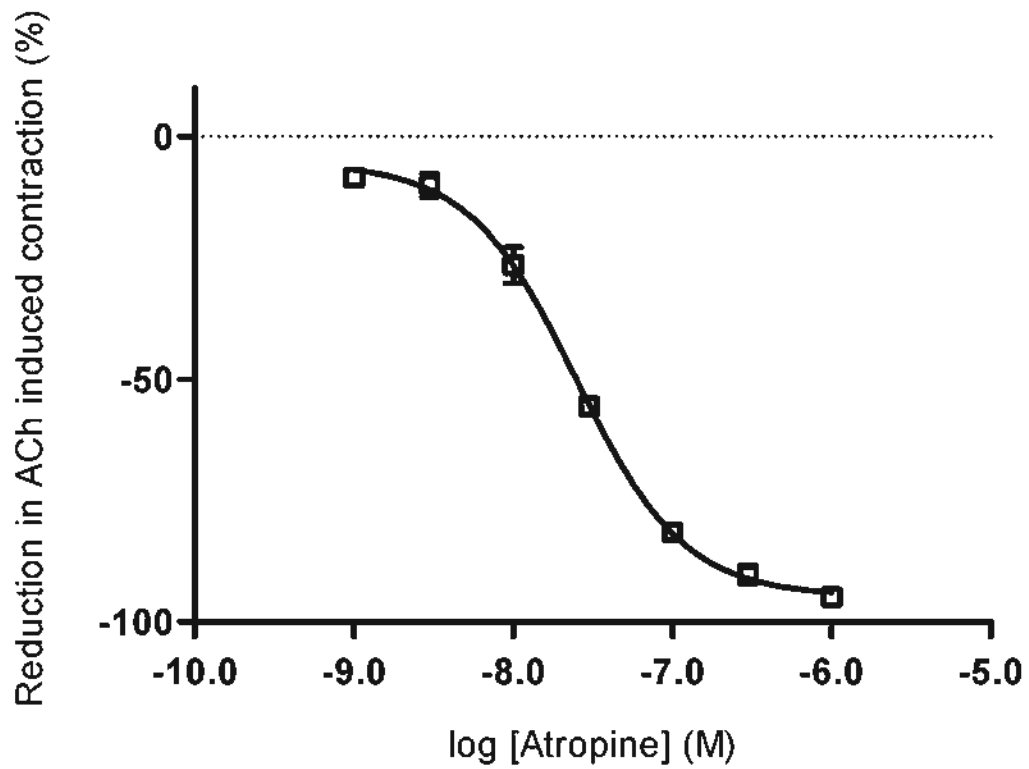


Fig. 4-2 Effects of atropine (a competitive nonselective antagonist for muscarinic receptors) on ACh ($10 \mu\text{M}$) induced contraction in isolated guinea pig ileums. Isolated tissues were pre-incubated with atropine (or vehicle) for 15 min before addition of ACh. Values are expressed as mean \pm S.E.M. ($n = 5$).

4.3.1.2 Binding of Schisandra lignans to cholinergic muscarinic (M3) receptor

To determine the mechanisms of actions of Schisandra lignans, receptor binding assays for cholinergic muscarinic (M3) receptor were performed in M3 CHO-K1 DA cells. Carbachol, an agonist of M receptor, caused concentration-dependent response on fluorescence activation (blue/green), as shown in Fig. 4-3. The antagonism of test drugs was examined by inhibitory response on carbachol induced fluorescence activation. The more inhibition a drug exhibits, the higher affinity and potency of receptor binding it should process. Atropine, a muscarinic receptor (M receptor) antagonist as positive control, inhibited the fluorescence activation ratio induced by carbachol (2 μ M) in a concentration-dependent manner, and abolished it at the concentration of 1 μ M (Fig. 4-4). On the other hand, as shown in Fig. 4-5, SCH-1, SCH-3 and SCH-4 did not cause any inhibitory effects on the fluorescence action at the concentration from 1 μ M to 25 μ M. The inhibitory response of SCH-4 at 100 μ M may be due to the reduction of cell viability or interruption of fluorescence excitation, indicated by the significant decrease of fluorescence signals at both blue and green excitation wavelengths for about 40%.

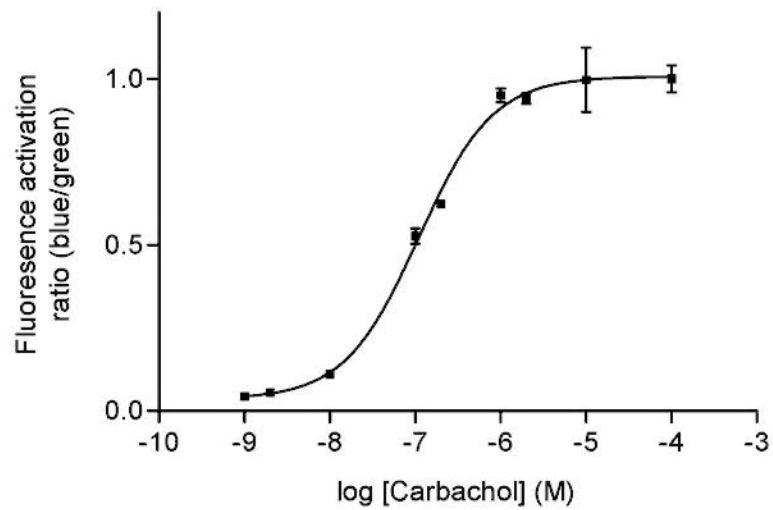


Fig. 4-3 Concentration response of fluorescence ratio (blue/green) in M3 CHO-K1 DA cells to carbachol. Cells were incubated with carbachol for 5 h followed by addition of substrate to produce fluorescence. Values are expressed as mean \pm S.E.M. (n = 3).

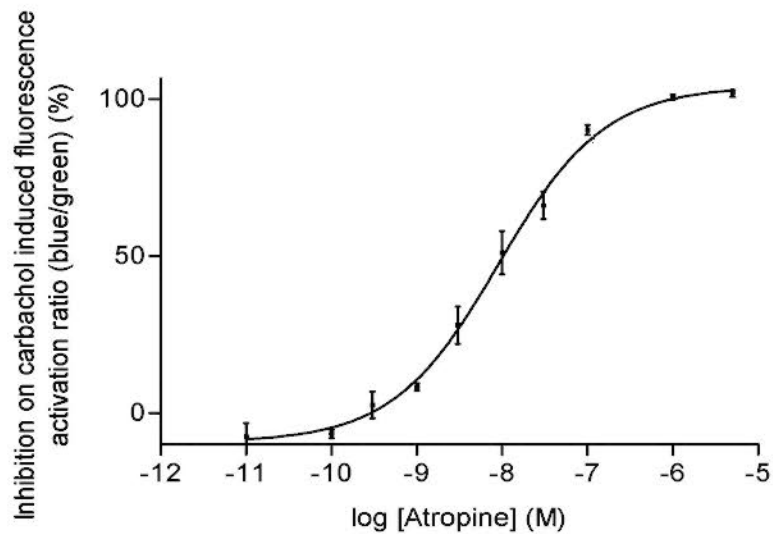


Fig. 4-4 Dose-dependent inhibition of atropine on fluorescent response stimulated by carbachol (2 μ M) in M3 CHO-K1 DA cells. Cells were pre-incubated with atropine for 30 min before addition of carbachol. Values are expressed as mean \pm S.E.M. (n = 3).

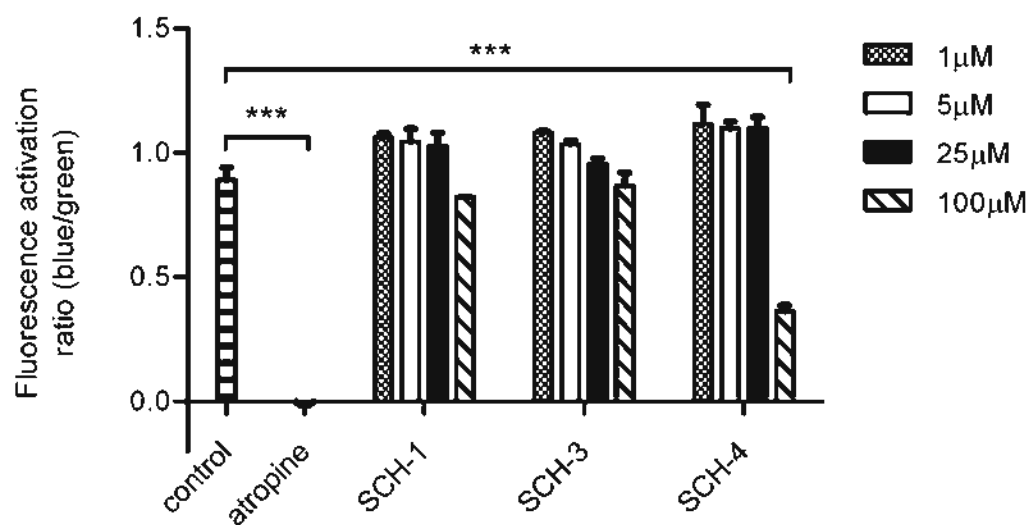


Fig. 4-5 Effects of atropine (1 μM), SCH-1, SCH-3 and SCH-4 on fluorescence responses stimulated by carbachol (2 μM) in M3 CHO-K1 DA cells with DMSO as vehicle control. Cells were pre-incubated with atropine or Schisandra lignans for 30 min before addition of carbachol. Values are expressed as mean \pm S.E.M. ($n = 3$). *** $P < 0.001$ compared to control using unpaired Student's t test or one-way ANOVA.

4.3.2 Inhibition on serotonin (5-HT) induced contraction in guinea pig ileum

Effects of Schisandra extracts and four Schisandra lignans on the intestinal contractility were studied in guinea pig ileum using another contracting agonist, 5-HT. As shown in Fig. 4-6(a), Schisandra ethanol extract caused a concentration-dependent inhibition on 5-HT induced contraction in isolated guinea pig ileums whereas water extract exhibited significant responses at the concentration up to 5 mg/mL, suggesting that potency of ethanol extract was much higher than water extract ($P < 0.001$).

Fig. 4-6(b) showed that all four Schisandra lignans exhibited inhibitory effects on 5-HT induced contraction in a concentration-dependent manner in isolated guinea pig ileums as compared to DMSO (vehicle blank). SCH-3 was the most potent followed by SCH-4, SCH-2 and SCH-1, with their EC_{50} values of 6.6 ± 0.6 , 10.0 ± 0.8 , 24.5 ± 2.2 , 40.7 ± 5.4 μ M and the E_{max} values of -84.1 ± 6.3 %, -83.6 ± 7.2 %, -64.1 ± 6.5 %, -61.0 ± 7.7 %, respectively (Table 4-1). Compared to the vehicle, SCH-3 showed inhibitory response at concentrations from 10 μ M to 100 μ M, but there was no significant difference between SCH-3 and SCH-4. SCH-1 and SCH-2 caused significant inhibition when the concentration was up to 100 μ M and were significantly less potent than the other two.

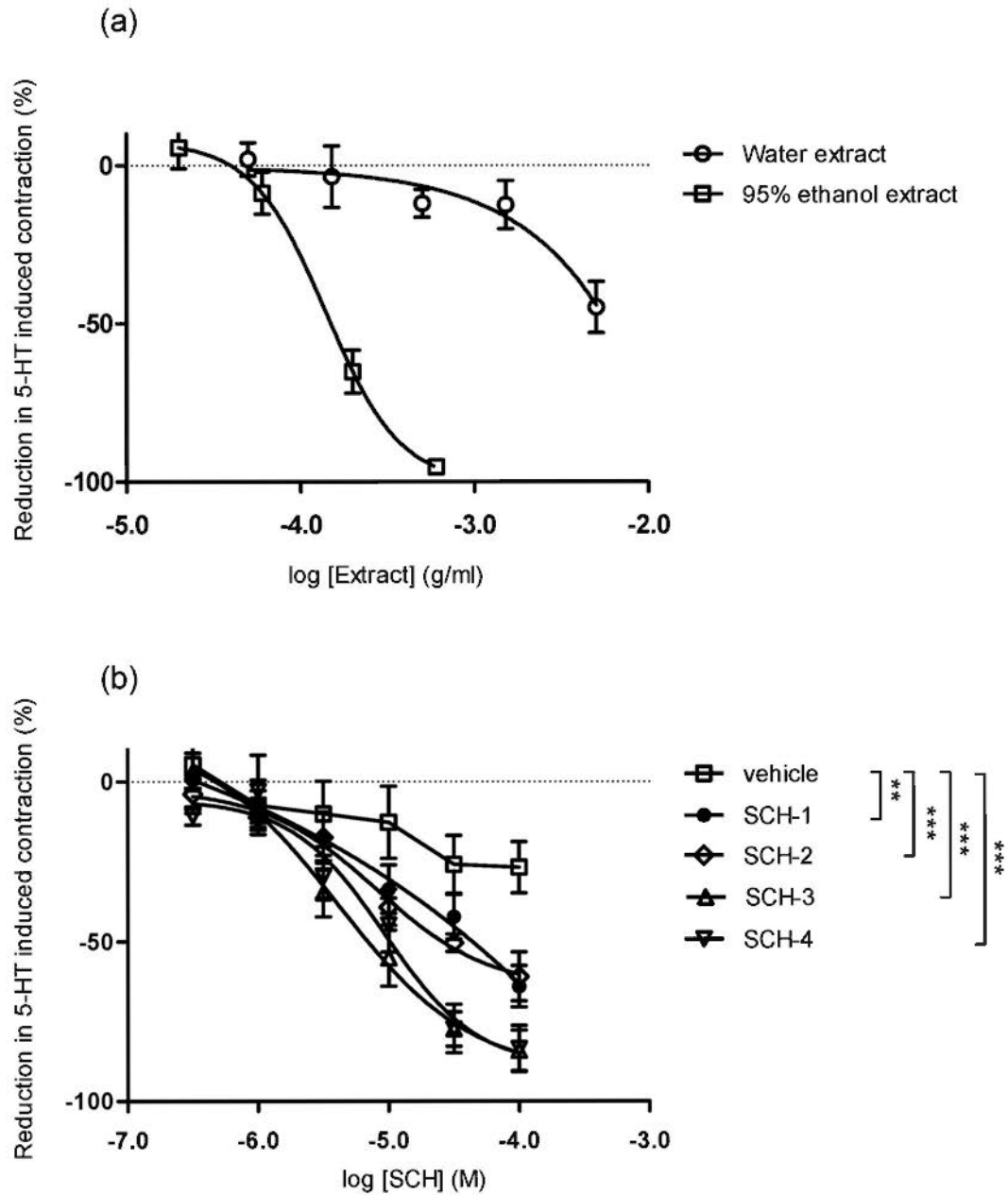


Fig. 4-6 Effects of Schisandra extracts (a) and Schisandra lignans (b) on 5-HT (10 μ M) induced contraction in isolated guinea pig ileums with DMSO as the vehicle blank. Isolated tissues were pre-incubated with drugs (or vehicle) for 15 min before addition of 5-HT. Values are expressed as mean \pm S.E.M. (n = 6). ** P <0.01, *** P <0.001 compared to vehicle using one-way or two-way ANOVA.

The action of 5-HT on intestine is complex due to the various 5-HT receptor subtypes mediating different physiological functions. Considering the important role of 5-HT₃ receptor in irritable bowel syndrome (IBS), the effect of tropisetron (a selective 5-HT₃ receptor antagonist) was tested as a positive control. As presented in Fig. 4-7, tropisetron showed concentration-dependent inhibitory effect on 5-HT induced contraction in guinea pig ileum and reached maximum inhibition of -54.7 ± 6.1 % at the concentration of 1 μ M. The incomplete inhibition of tropisetron indicated the contribution of other subtypes of 5-HT receptors, such as 5-HT₂, to the 5-HT mediated contraction in guinea pig ileum. The EC₅₀ value of tropisetron was 0.18 ± 0.01 μ M, which was about 30-fold lower than the most potent Schisandra lignan SCH-3 (6.6 ± 0.6 μ M).

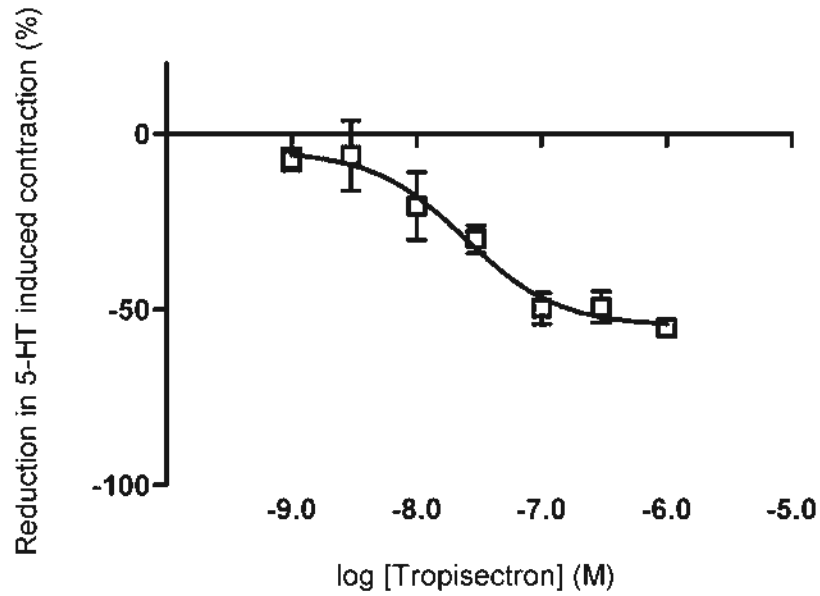


Fig. 4-7 Effects of tropisetron (a selective serotonin 5-HT₃ receptor antagonist) on 5-HT (10 μ M) induced contraction in isolated guinea pig ileums. Isolated tissues were pre-incubated with tropisetron (or vehicle) for 15 min before addition of 5-HT. Values are expressed as mean \pm S.E.M. (n = 6).

4.3.3 Inhibition on electrical field stimulated (EFS) contraction in guinea pig ileum

Electrical field stimulation (EFS) was also employed to elicit contraction in guinea pig ileum. EFS contracted smooth muscle by triggering the release of mediators, such as ACh and substance P, from enteric nerve in isolated intestine. Relaxant effects of Schisandra extracts and Schisandra lignans were evaluated on this neuronal-action involved contractility in isolated guinea pig ileum. Schisandra ethanol extract caused concentration-dependent inhibition on EFS contraction at concentrations from 0.1 mg/mL to 0.7 mg/mL whereas the water extract exhibited less significant response even at high concentration up to 1.5 mg/mL.

All four Schisandra lignans showed concentration-dependent relaxation on EFS contraction in isolated guinea pig ileums as compared to vehicle control as shown in Fig. 4-8 (a). With the comparison of concentration-response curves, there was significant difference among the SCH compounds and SCH-3 was the most potent followed by SCH-4, SCH-2 and SCH-1, with their EC_{20} values of 5.0 ± 0.9 , 8.1 ± 1.9 , 34.7 ± 9.5 , 61.6 ± 11.9 μ M and the E_{max} values of -97.4 ± 0.8 %, -57.7 ± 5.0 %, -35.5 ± 3.6 %, -33.5 ± 3.9 %, respectively.

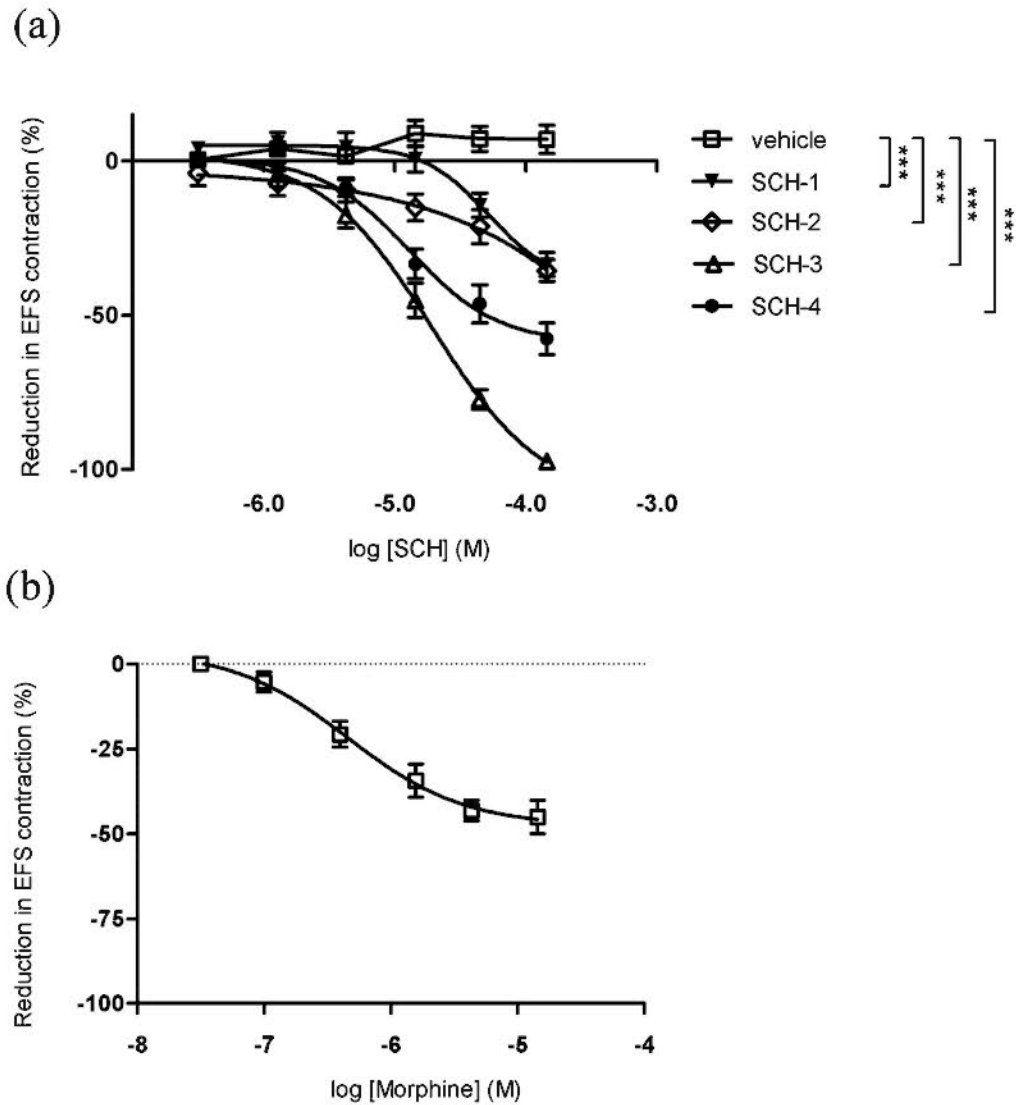


Fig. 4-8 Effects of four Schisandra lignans (a) and morphine (b) on EFS contraction in isolated guinea pig ileums with DMSO as the vehicle blank. Guinea pig ileums were pre-contracted using EFS conditions at 30 V of voltage, 2 ms of duration, and 0.04 TPS of rate. Drugs (or DMSO) were cumulatively added at 5 min intervals. Values are expressed as mean \pm S.E.M. (n = 5-6). *** P <0.001 compared to vehicle using one-way or two-way ANOVA.

Naloxone, a competitive antagonist for opioid receptor, was used to examine whether the relaxant actions of SCH compounds on EFS contraction were related to the opioid receptor. Morphine, a well established opioid receptor agonist as positive control, concentration – dependently inhibited EFS contraction in guinea pig ileum with the EC_{20} and E_{max} values of $0.4 \pm 0.1 \mu\text{M}$ and $-45.2 \pm 4.9 \%$, respectively. Additional dosing of naloxone (200 nM) completely abolished the inhibitory response of morphine (Fig. 4-9). However, as shown in Fig. 4-9, the inhibitory responses of SCH compounds were not reversed by the addition of naloxone, suggesting that these SCH compounds did not act on opioid receptor, and other mechanisms in the downstream pathways might be involved in the actions of SCH compounds.

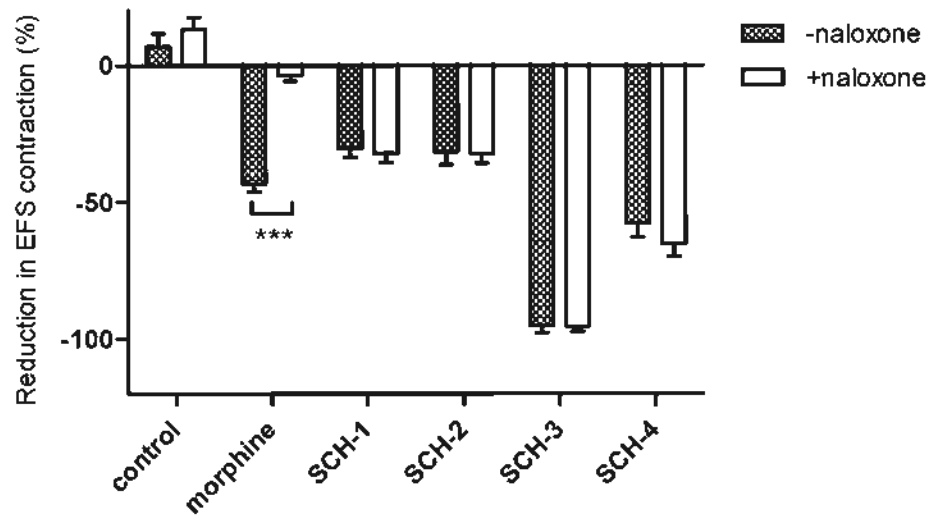


Fig. 4-9 Effects of naloxone (200 nM) on the inhibitory responses of morphine (3 μ M) and four Schisandra lignans (100 μ M) on EFS contraction in isolated guinea pig ileum. Guinea pig ileums were pre-contracted using EFS conditions at 30 V of voltage, 2 ms of duration, and 0.04 TPS of rate. Drugs were cumulatively added at 5 min intervals, and naloxone (200 nM) was added at the end of last dose. Values are expressed as mean \pm S.E.M. (n = 5-6). *** $P < 0.001$ compared to corresponding group using unpaired Student's *t* test or one-way ANOVA.

4.3.4 Inhibition on spontaneous contraction in rat colon

The relaxant effects of Schisandra extracts and lignans were also evaluated on spontaneous contraction in isolated rat colon. As shown in Fig. 4-10(a), both ethanol and water extracts of *S. chinensis* caused concentration-dependent inhibition on the spontaneous contraction in isolated rat colon. Comparing the concentration-response curves, ethanol extract was more potent than water extract ($P < 0.001$) with the EC_{50} values of $38.0 \pm 3.1 \mu\text{g/mL}$ and $263.0 \pm 40.9 \mu\text{g/mL}$, respectively. However, their E_{max} values, $-96.2 \pm 3.2 \%$ and $-89.5 \pm 4.8 \%$ respectively, were comparable.

All the Schisandra lignans caused concentration-dependent relaxation on spontaneous contraction in isolated rat colon as compared to vehicle control as shown in Fig. 4-10(b). With the comparison of concentration-response curves, SCH-3 was more potent than SCH-2 and SCH-4 ($P < 0.001$), but unlike the pattern shown in agonist induced contraction, SCH-1 also exhibited higher potency as compared to SCH-2 and SCH-4 ($P < 0.001$). Furthermore, there was no significant difference between SCH-1 and SCH-3. The potencies of SCH compounds were expressed as $\text{SCH-2} < \text{SCH-4} < \text{SCH-3}$, SCH-1 with their EC_{20} values of 9.77 ± 3.83 , 1.66 ± 0.26 , 0.44 ± 0.23 , $0.24 \pm 0.05 \mu\text{M}$ and E_{max} values of $-34.8 \pm 15.2 \%$, $-75.2 \pm 5.2 \%$, $-85.8 \pm 6.7 \%$, $-92.2 \pm 5.0 \%$, respectively (Table 4-1).

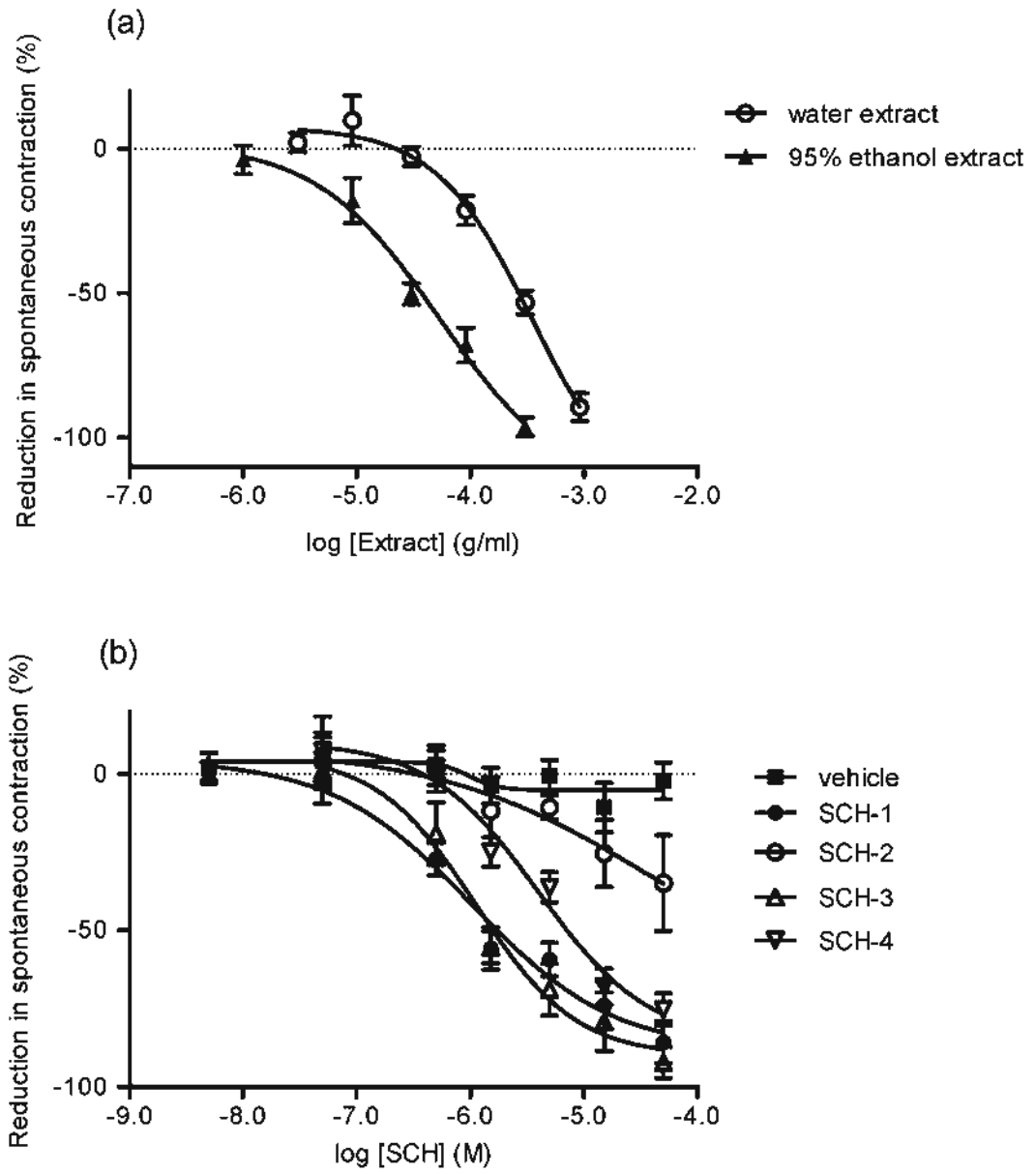


Fig. 4-10 Inhibitory effects of Schisandra extracts (a) and Schisandra lignans (b) on spontaneous contraction in isolated rat colon with DMSO or distilled water as the vehicle blank. Isolated tissues were non-cumulative incubated with drugs (or vehicle) for 5 min. Values are expressed as mean \pm S.E.M. (n = 6).

Table 4-1 EC₂₀ (EC₅₀) and E_{max} of inhibitory effects of Schisandra lignans on intestinal contractility *in vitro*. Values are expressed as mean ± S.E.M.. (n = 5-6).

Compound	ACh induced contraction		5-HT induced contraction		EFS contraction		Spontaneous contraction	
	EC ₂₀ (μM)	E _{max} (%)	EC ₅₀ (μM)	E _{max} (%)	EC ₂₀ (μM)	E _{max} (%)	EC ₂₀ (μM)	E _{max} (%)
SCH-1	13.2 ± 4.7	-34.6 ± 5.1	40.7 ± 5.4	-64.1 ± 6.5	61.6 ± 11.9	-33.5 ± 3.9	0.3 ± 0.1	-85.8 ± 6.7
SCH-2	3.5 ± 0.7	-47.0 ± 3.9	24.5 ± 2.2	-61.0 ± 7.7	34.7 ± 9.5	-35.5 ± 3.6	9.8 ± 3.8	-34.8 ± 15.2
SCH-3	2.2 ± 0.4	-94.5 ± 6.5	6.6 ± 0.6	-84.1 ± 6.3	5.0 ± 0.9	-97.4 ± 0.8	0.4 ± 0.1	-92.2 ± 5.0
SCH-4	3.1 ± 0.6	-98.3 ± 13.6	10.0 ± 0.8	-83.6 ± 7.2	8.1 ± 1.9	-57.7 ± 5.0	1.7 ± 0.3	-75.2 ± 5.2

4.4 Discussion

Schisandra chinensis has been widely used to control excessive loss of essential energy and body fluid in Chinese Medicine (National Committee of Chinese Pharmacopoeia, 2005). This herb is usually prescribed for the patients with serious diarrhea syndromes. In this study, *Schisandra chinensis* extracts and its major active components exhibited relaxant activities on the intestinal contractility, both in isolated guinea pig ileum and rat colon *in vitro*. The modulatory effects of *S. chinensis* on gut motility support its well known clinical application in treating diarrhea. Moreover, the ethanol extract of *Schisandra chinensis* showed significant higher potency than the water extract, which agrees with clinical practice that *Schisandra chinensis* would be soaked in alcohol when used for serious diarrhea syndromes. As determined in Chapter 2, and as reported previously (Halstead et al., 2007), SCH-1, SCH-2, SCH-3 and SCH-4 were the dominant chemical components isolated from *Schisandra chinensis*. Considering the potency of these Schisandra lignans, they could be regarded as the biomarkers representing the relaxant activities of *Schisandra chinensis* on intestinal motility *in vitro*, and the difference of potency between ethanol and water extracts could be explained by the higher content of SCH compounds contained in the ethanol extract than in the water extract approximately in a proportion of 10:1 (Chapter 2).

SCH compounds showed various potencies of relaxant effects, indicating important relationship between their pharmacological activities and chemical structures. In the agonist (ACh, 5-HT) or EFS induced contraction experiments in guinea pig ileum, SCH-3

and SCH-4 showed remarkably higher potency than SCH-1 and SCH-2 while there was non-significant or slight difference between SCH-3 and SCH-4, or SCH-1 and SCH-2. Referring to the chemical structures of these Schisandra lignans (Chapter 2), a 6-hydroxy substitution on the cycloocten-ring is present in SCH-1 and SCH-2, but not in SCH-3 or SCH-4, indicating that the absence of 6-hydroxy group appeared to result in an increase of potency of Schisandra lignans on inhibiting the contractility of guinea pig ileum preparations. Comparatively, the impact of 11, 12-methylenedioxy substitution on the potency appeared not strong and significant. The presence of 11, 12-methylenedioxy substitution in SCH-2 (rather than 11, 12-dimethoxy in SCH-1) could increase potency as compared to SCH-1, whereas there was little difference between SCH-4 and SCH-3, with or without 11, 12-methylenedioxy substitution. Generally, the cycloocten-ring could play a critical role in the molecular binding events than the benzene ring and the 6-hydroxy substitution could increase obstruction in binding interaction between drug and receptor/ion channel.

On the other hand, the impact of substitutions on inhibiting spontaneous contraction in isolated rat colons was different. Substitution of 6-hydroxyl in SCH-2 appeared to decrease its potency as compared to SCH-4 (without 6-hydroxy substitution) while SCH-1 and SCH-3 showed comparable potency irrespective of 6-hydroxy substitution. In contrast, 11, 12-methylenedioxy substituted SCH compounds (SCH-2 and SCH-4) showed remarkably lower potency than 11, 12-dimethyl substituted ones (SCH-1 and SCH-3), indicating the presence of 11, 12-methylenedioxy group rather than dimethyl group appeared to reduce potency of inhibiting spontaneous contraction in rat colon

preparations. These results implied that in the rat colon preparations, substitution on the benzene ring, such as methylenedioxy and dimethyloxy, rather than the cycloocten-ring, could play a more important role in molecular binding events, which are responsible for inducing the short-term relaxant effects. The varied manners of activity-structure relationship in guinea pig ileum preparations and rat colon preparations could be mainly due to the different approaches in producing contractile responses that were measured and the mechanisms of the drugs used. Nevertheless, since coordinated contraction and relaxation of smooth muscle cells are the well known basic of gut motility, Schisandra lignans contributed to the inhibitory effects on gut motility by both short-term and long-term treatments, which could be potentially useful for treating diarrhea.

Inhibition on contraction of smooth muscle cells can be contributed by upstream pathways, such as suppression of nerve stimulation, and downstream pathways, such as antagonism of receptor/ion channel. In this study, the receptor binding assays revealed that SCH compounds were not specifically acting on M3 receptor which is mainly responsible for ACh induced contraction in smooth muscle cells. In EFS experiments, naloxone had no reversal response on the relaxant effects of SCH compounds, demonstrating that the actions of these lignan compounds were not specifically through the opioid receptors in the enteric nerve. In addition, incomplete inhibition of morphine on EFS contraction ($E_{\max} = -45.2 \pm 4.9 \%$) implied that direct membrane depolarization on smooth muscle cells could occurred under the EFS condition. In contrast, the E_{\max} values of SCH-3 and SCH-4 on EFS contraction reached more than 50% ($-97.4 \pm 0.8 \%$ and $-57.7 \pm 5.0 \%$ respectively), suggesting that SCH-3 and SCH-4 inhibited the

intestinal contractility at least partially by antagonizing the ion channel/receptor in smooth muscle cells. Magnolol, a natural substance isolated from *Cortex Magnoliae officinalis*, was reported to inhibit KCl, carbachol and serotonin induced contraction in distal colon of guinea pig *in vitro* (Bian et al., 2006). The mechanistic studies concluded that magnolol may inhibit calcium influx by blocking ion channels (cation channels and calcium channel) and inhibit intracellular calcium release from the sarcolemmal membrane (SR). The results in this study suggested that SCH-3 and SCH-4 may act on the downstream pathways in smooth muscle cells like magnolol and it appeared that more than one pathway would be involved in the actions of SCH compounds, but it is certain that more investigations is needed to clear up the whole picture. Nevertheless, it is more interesting to note that the potency of SCH-1 in rat colon preparations was much higher than that in guinea pig ileum preparations. As an IBS *in vivo* rat model was employed in Chapter 6, preparations from the rat were preferred due to the correlation between *in vivo* and *in vitro* experiments. Furthermore, considering SCH-1 being the most abundant chemical constituent and the most readily absorbable component in *Schisandra chinensis* (Chapter 2 and 3), SCH-1 has been selected in an attempt to elucidate the mechanisms of action *in vitro* (Chapter 5).

Chapter 5

Mechanisms of the Inhibitory Effect of Schisandrin (SCH-1) on Spontaneous Contraction of Isolated Rat Colon

5.1 Introduction

Schisandrin (SCH-1) is one of the major lignan compounds isolated from *Schisandra chinensis*, a famous medicinal herb in East Asia and also a widely used dietary supplement in Western countries. It has been suggested that SCH-1 and a number of analogous lignan compounds have anti-oxidant, neuro-protective and anti-cancer effects (Chapter 1). Schisandra lignans such as gomisin J (Suekawa et al., 1987) and gomisin A (Park et al., 2007) have shown relaxant effect on isolated smooth muscle preparations, including mesenteric artery, trachea, ileum, tenia coli and thoracic aorta. It is conceivable that these lignans and related lignan compounds such as SCH-1 may relax smooth muscles in gastrointestinal tract. Nevertheless, there are only limited investigations on the effects of Schisandra lignans in gastrointestinal system, despite the common use of *Schisandra chinensis* for controlling essential loss of body fluid (National Committee of Chinese Pharmacopoeia, 2005).

In our previous studies, the aqueous and ethanolic extracts of *S. chinensis*, as well as the major Schisandra lignans, have shown relaxant effects on ACh- and 5-HT-induced contraction in isolated guinea-pig ileum (Chapter 4). In addition to the sensorimotor-modulatory effects on upper gastrointestinal tract, the aqueous and

ethanolic extracts also induced concentration-dependent inhibitions on spontaneous contraction in isolated rat colon. The spontaneous activities of colon, regulated by excitatory nerves (i.e. cholinergic nerve) and inhibitory nerves (i.e. non-adrenergic non cholinergic nerve) in the enteric nervous system, is the basis of colonic transit (Foxx-Orenstein and Grider, 1996). Relaxing the spontaneously contracted colon may contribute to attenuating the enhanced intestine motility in gastrointestinal diseases with diarrhea symptom such as inflammatory bowel disease (Collins, 1996) and irritable bowel syndrome (Camilleri, 2001).

As characterized by HPLC-MS, SCH-1 is the main lignan present in both aqueous and ethanolic extracts of the herb (Chapter 2), and one of major absorbable components of *Schisandra chinensis* (Chapter 3). Thus studies on SCH-1 would be of value in the initial studies of the modulatory effects on lower gastrointestinal tract. The present work aims to investigate the inhibitory effect of SCH-1 on spontaneous contraction of isolated rat colon. The mediators involved in the SCH-1 response were identified using ion channel blockers, receptor antagonist and enzyme inhibitor, as well as quantitative determination of the mediators.

5.2 Materials and methods

5.2.1 Chemicals and reagents

Schisandrin (SCH-1) and γ -schisandrin (SCH-4) with purity >98% were obtained from the Control of Pharmaceutical and Biological Products (Beijing, China). Tetrodotoxin (TTX), atropine, propranolol, N^o-nitro-L-arginine methyl ester (L-NAME), 1*H*-[1,2,4]oxadiazolo[4,3- α]-quinoxalin-1-one (ODQ), 8-cyclopentyl-1,3-dipropylxanthine (DPCPX), sodium nitroprusside (SNP), adenosine, cicaprost and α -chymotrypsin were purchased from Sigma Co. (U.S.A.); Ro1138452 from Roche Co. (Swiss); apamin from Research Biochemicals International (U.S.A.). The chemicals for buffer solution were analytical grade for common laboratory use. SCH-1 and SCH-4 were dissolved in 100% DMSO at 100 μ M as stock. A stock solution of TTX (500 μ M) was prepared in saline containing 0.01% acetic acid. ODQ (50 mM) and Ro1138452 (10 mM) were dissolved in DMSO. Other stock solutions were prepared in distilled water and diluted with saline before use. Adenosine solutions were freshly prepared each day. All the stock solutions were stored at -20 °C. Appropriate diluents were prepared before use. Each drug administration was between 0.5 to 30 μ l, and in each experiment, the total volume of drug working solution added to the bath was no more than 0.3% of the bath volume.

5.2.2 Animals

Sprague-Dawley rats (250 – 300 g) were bred and housed by the Laboratory Animal Services Centre of the Chinese University of Hong Kong. All experiments were performed with approval from the Animal Research Ethics Committee, The Chinese University of Hong Kong. The animals were kept in a temperature controlled room (23 ± 2 °C) with a 12-hr light-dark cycle, with free access to food and water.

5.2.3 Isolation of colon preparations

Male Sprague-Dawley rats (250 – 300 g) were fasted overnight and sacrificed by cervical dislocation and exsanguination. A 6 cm length of ascending colon from cecum was removed and placed in Krebs-Henseleit solution: NaCl 118, KCl 4.7, CaCl₂ 2.5, MgSO₄ 1.2, KH₂PO₄ 1.18, NaHCO₃ 25, glucose 10 mM. Subsequently, the colon was flushed with buffer solution, cleaned of mesenteric tissues, and cut into proximal and distal segments of 2 cm length. The colon segments were suspended in 10 ml organ bath filled with Krebs solution maintained at constant temperature 37 °C and aerated with 95%O₂/5%CO₂. Washout of the organ bath was performed by solution upward displacement and overflow. Contractions of the longitudinal muscle of isolated rat colon were measured with Grass FT03 isometric transducers connected to Powerlab data acquisition system (ADInstruments Pty Ltd, Australia). Initially, a basal tension of 0.5 g was applied. On relaxation repeated tension was given until the basal tone remained steady at about 0.3 g.

5.2.4 Experimental protocols

5.2.4.1 Measurement of contractile activity

In all experiments, the proximal and distal segments of rat colon from the same rat were used as matched preparations. After about 1 h equilibration, with frequent washing, a submaximal dose of SCH-1 (10 μ M) was tested on each preparation to ensure stable and acceptable sensitivity that has been reached before the following experiments begun. Concentration-response curve of SCH-1 was obtained by non-cumulative incubation of the inhibitory agonist for 5 min. A standard procedure with washout for 3 min and resting for 10 min was allowed between each drug administration.

5.2.4.2 Effects of blockers/inhibitors on responses to inhibitory agonists

Responses to single doses of SCH-1, cicaprost and SNP were obtained on both proximal and distal colon segments from three different rats, and the effects of blockers or enzyme inhibitors were assessed against the agonist responses by pre-treatment of blockers or enzyme inhibitors for 10 – 15 min at subsequently increasing concentrations (n = 6). Responses to adenosine were obtained from four rats and individually analyzed on proximal and distal segments.

5.2.4.3 Data analysis

Spontaneous contractility of isolated rat colon was measured as the average contractile force (in grams over baseline) for a 4 min period. Relaxant responses to inhibitory agonists were taken as the percentage change from the resting spontaneous contraction before priming with the inhibitory agonists (e.g. -100% corresponds to an abolition of contraction).

5.2.5 Measurement of nitric oxide (NO) production

Isolated colon from the same rat was cut into two proximal and two distal segments that were equilibrated in Krebs solution at 37 °C with aeration of 95%O₂/5%CO₂. After 30 min equilibration, the segments were correspondingly transferred into 2 ml aerated Krebs solution at 37 °C containing 100 µM SCH-1 (or DMSO as vehicle blank) for 5 min incubation. Subsequently, the colon segments were blotted dry, frozen in liquid nitrogen and homogenized in 1 ml distilled water. The supernatant was obtained by centrifugation at 10,000 × g for 20 min, and subsequently passed through a 0.45 µm membrane filter prior to ultrafiltration using a 30 kDa molecular weight cut-off filter (Millipore, U.S.A.) at 2,000 × g for 60 min. The ultrafiltrate was used as assay sample for nitrite + nitrate measurement following the instructions of nitrate/nitrite colorimetric assay kit (Cayman, U.S.A). Generally, nitrate in the sample was converted to nitrite by the nitrate reductase mixture and the total nitrite was reacted with Griess reagent prior to the absorbance

measurement at 540 nm. Nitric oxide production was calculated by the total nitrite and normalized to corresponding proximal or distal segment treated with vehicle blank.

5.2.6 Measurement of cGMP production

Isolated colon segments were prepared as described in Section 5.2.4.2 and incubated with 50 μ M SCH-1 (or DMSO as vehicle blank) for 5 min. After the treatment, the blotted tissues were snap frozen in liquid nitrogen. The frozen tissues were subsequently homogenized in cold 6% (w/v) trichloroacetic acid to give 10% (w/v) homogenates. The supernatants obtained from centrifugation at $2000 \times g$ for 15 min at 4 °C were washed 4 times with five volumes of water saturated diethyl ether prior to lyophilization. The dry residues were then reconstituted in assay buffer prior to analysis using Amersham cGMP enzymeimmunoassay Biotrak (EIA) System (GE Healthcare, U.S.A.). Briefly, it combines the use of a specific cGMP antiserum that can be immobilised on to the pre-coated microplates, a peroxidase-labelled cGMP conjugate, and substrate solution. The optimal density was measured with a 96-well plate at 450 nm. The cGMP level was expressed as fmol per g wet weight of tissue.

5.2.7 Statistical analysis

All values were expressed as mean \pm S.E.M.. Results from the controls and treatments were compared by unpaired Student's *t* test or one-way ANOVA followed by Bonferroni post test, as appropriate. All tests were two-tailed and the significance was set at $P < 0.05$.

5.3 Results

5.3.1 Effects of SCH-1 on spontaneous contraction

In all experiments, responses of the proximal and distal colon to the tested drugs were both investigated. In the case of SCH-1, the inhibitory responses on spontaneous contraction in proximal and distal colon segments were similar in magnitude, and it was decided to combine the data for statistic analysis and graph presentation. As shown in Fig. 5-1, SCH-1 produced a concentration-dependent relaxation on isolated rat colon from the concentration of 0.5 μM . Non-cumulative dosing of SCH-1 resulted in an EC_{50} value of $1.66 \pm 0.31 \mu\text{M}$ and an E_{max} value of $-85.8 \pm 6.7 \%$, whereas the vehicle blank (DMSO) had no effect. In subsequent experiments, the effects of antagonists and enzyme inhibitor were assessed against 10 μM SCH-1 as a submaximal dose. The standard dosing elicited an approximately 60 % inhibition on the spontaneous contraction in isolated rat colon.

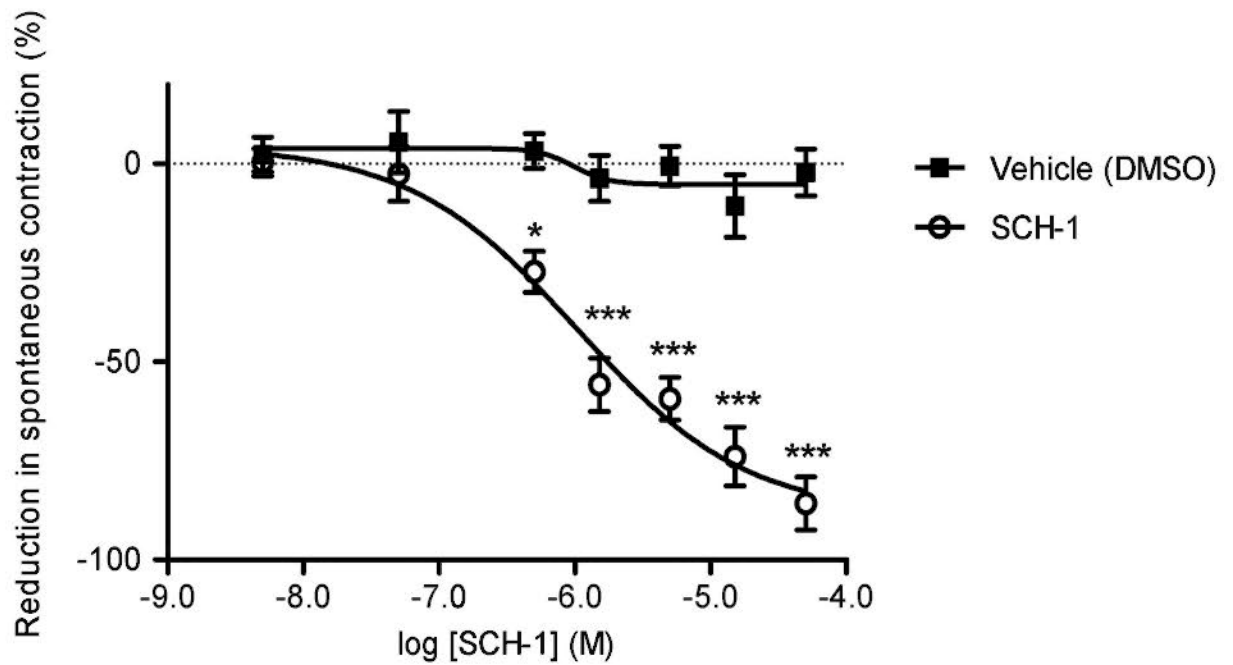


Fig. 5-1 Effects of SCH-1 on spontaneous contraction in isolated rat colon with DMSO as vehicle blank. SCH-1 produced a concentration-dependent relaxation on isolated rat colon from the concentration of 0.5 μ M with the EC_{50} value of $1.66 \pm 0.31 \mu$ M. Values are expressed as mean \pm S.E.M. (n = 6). * $P < 0.05$, *** $P < 0.001$ compared to vehicle using two-way ANOVA with Bonferroni post-tests.

5.3.2 Evidence that SCH-1 activated non-adrenergic non-cholinergic (NANC) enteric nerves

To determine the significance of neuronal mechanisms in the relaxant effects of SCH-1, the rat colon segments were pretreated with tetrodotoxin (TTX), a neuronal Na⁺ channel blocker. TTX (1 μM) slightly increased the amplitude and frequency of spontaneous contractions, and tended to make the contraction pattern more regular. As depicted in Fig. 5-2 and Fig. 5-3, the inhibitory responses of SCH-1 ($-61.2 \pm 7.1\%$, $n = 6$) were abolished by TTX at a concentration of 1 μM ($-1.3 \pm 5.3\%$, $P < 0.001$). Subsequently, propranolol and atropine were used to examine the involvement of adrenergic and cholinergic systems. The adrenergic antagonist, propranolol at 1 μM (which had no significant effect on the base tones and spontaneous contractions), did not affect SCH-1 responses ($P > 0.05$). Since an initial dosing of atropine at 1 μM caused marked reduction in spontaneous contraction for 70-80 %, the colon preparations were initially exposed to 50 nM atropine with subsequent dosing of 0.1-1 μM. As shown in Fig. 5-2, atropine had no effect on inhibitory responses of SCH-1 ($P > 0.05$).

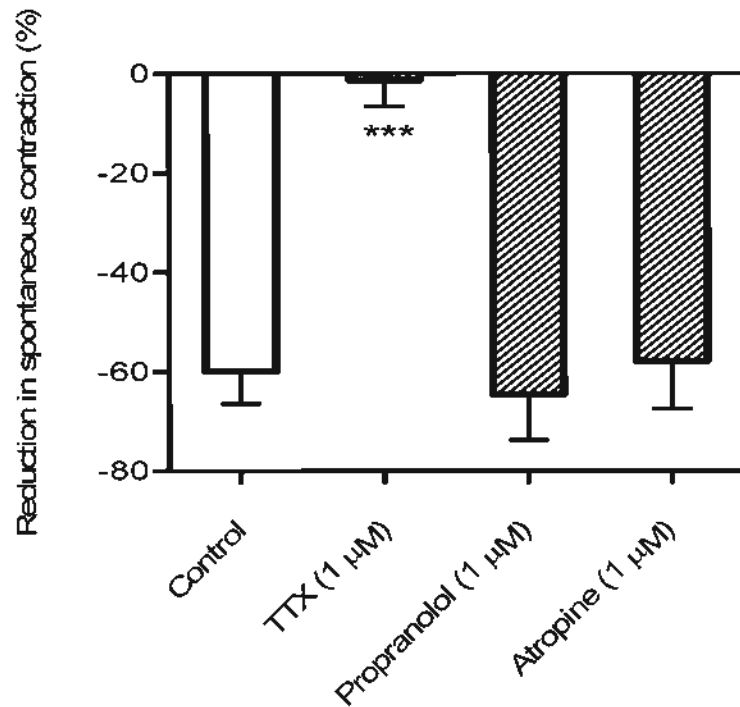


Fig. 5-2 Effects of tetrodotoxin (TTX, 1 μ M), propranolol (1 μ M) and atropine (1 μ M) on the inhibitory responses of SCH-1 (10 μ M) in isolated rat colon. The colon segments were pre-incubated with the antagonists for 10 min before the addition of SCH-1. 1 μ M TTX abolished the SCH-1 responses (***) P <0.001), whereas propranolol and atropine did not affect the relaxant effects of SCH-1 (P >0.05). Values are expressed as mean \pm S.E.M. (n = 6). *** P <0.001 compared to control.

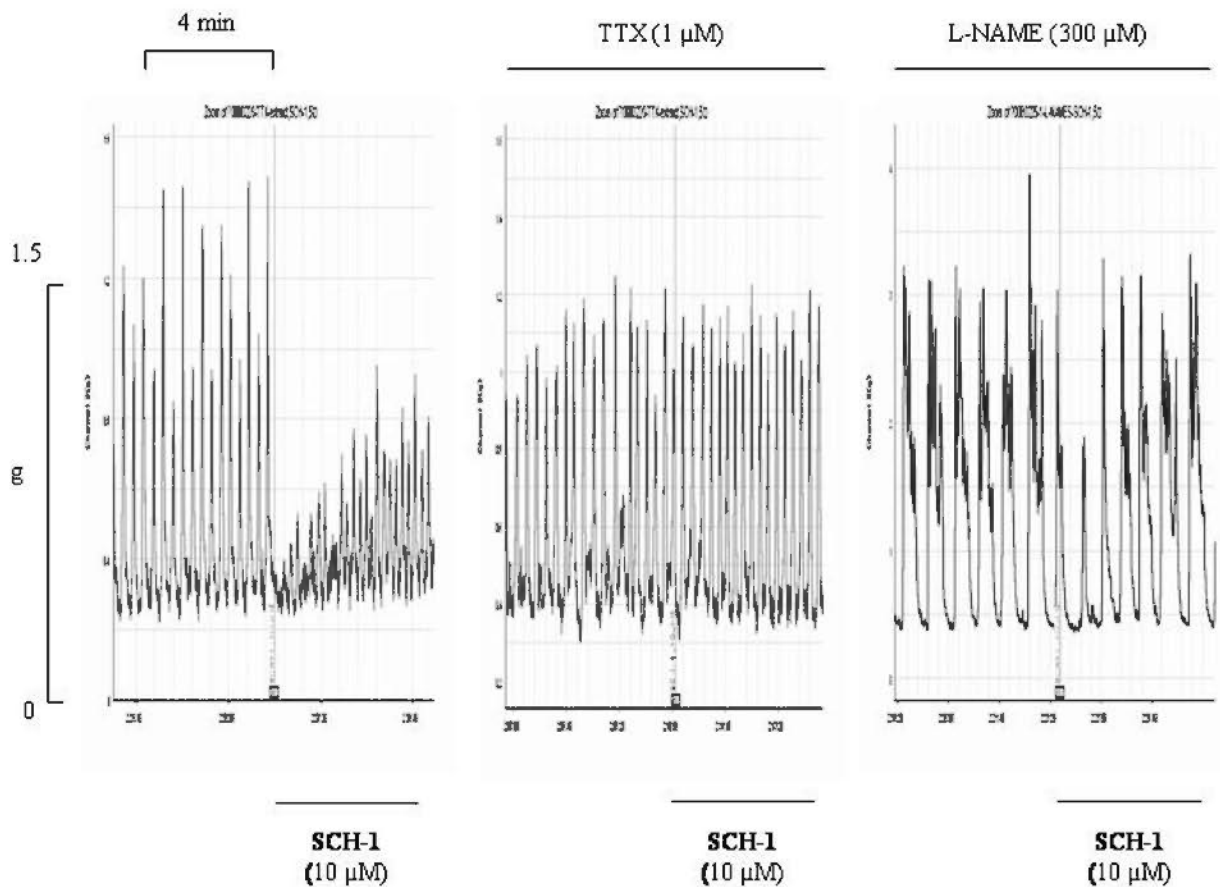


Fig. 5-3 Representative experimental records of spontaneous contraction in rat colon showing that the effects of tetrodotoxin (TTX, 1 μ M) and N^ω-nitro-L-arginine methyl ester (L-NAME, 300 μ M) on the inhibitory responses of SCH-1 (10 μ M). The colon segments were pre-incubated with the antagonists for 10 min before addition of SCH-1. 1 μ M TTX abolished the inhibitory response of SCH-1, whereas 300 μ M L-NAME attenuated but not abolished the response of SCH-1.

The effects of TTX were also assessed against the inhibitory responses of another major lignan isolated from *Schisandra chinensis*, SCH-4, and the aqueous extract and ethanol extract of *S. chinensis*. As presented in Fig 5-4, the SCH-4 responses ($-74.0 \pm 3.0\%$, $n = 6$) were attenuated but not abolished by TTX at $1\ \mu\text{M}$ ($-40.0 \pm 8.4\%$, $P < 0.001$), in contrast to SCH-1. Schisandra water extract at $600\ \mu\text{g/ml}$ (equivalent to $4.11\ \mu\text{M}$ SCH-1 and $0.09\ \mu\text{M}$ SCH-4) and ethanol extract at $100\ \mu\text{g/ml}$ (equivalent to $4.40\ \mu\text{M}$ SCH-1 and $2.89\ \mu\text{M}$ SCH-4) produced comparable relaxation on rat colon ($-78.1 \pm 6.2\%$ and $-78.9 \pm 4.5\%$, respectively). TTX ($1\ \mu\text{M}$) inhibited the responses of water extract ($-8.2 \pm 5.8\%$, $P < 0.001$) and ethanol extract ($-48.8 \pm 5.0\%$, $P < 0.001$).

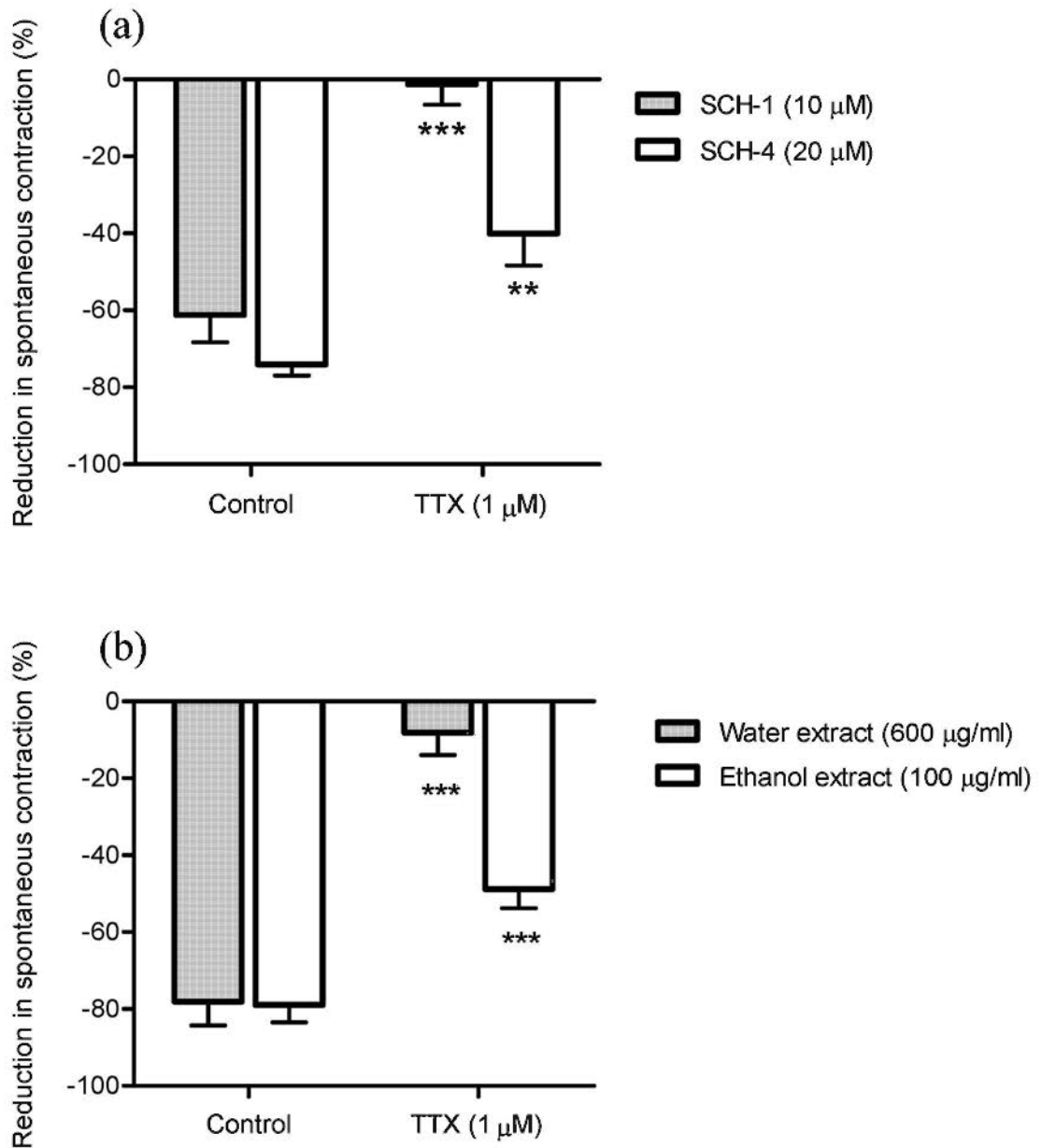


Fig. 5-4 Effects of tetrodotoxin (TTX, 1 μM) on the inhibitory responses of (a) SCH-1 (10 μM) and SCH-4 (20 μM), (b) Schisandra water extract (600 μg/ml) and ethanol extract (100 μg/ml) in isolated rat colon. The colon segments were pre-incubated with ion channel blocker for 10 min before the addition of inhibitory agonists. Values are expressed as mean ± S.E.M. (n = 6). ***P*<0.01, ****P*<0.001 compared to control.

5.3.3 Involvement of nitric oxide synthesis

The nitric oxide synthase (NOS) inhibitor L-NAME slowed the rate of spontaneous contraction. As depicted in Fig. 5-3, 100 μ M L-NAME attenuated but did not abolish the inhibitory response of SCH-1. Fig. 5-4 showed the SCH-1 responses (-64.5 ± 4.1 %, $n = 6$) were partially inhibited by L-NAME at the concentrations of 100 μ M (-20.0 ± 2.6 %, $P < 0.001$) and 300 μ M (-12.3 ± 3.8 %, $P < 0.001$). To further determine the involvement of nitric oxide (NO), the contents of nitric oxide in isolated rat colon (proximal and distal) were measured using nitrite + nitrate colorimetric assays. As presented in Fig. 5-6, the NO production in colon segments, expressed as percentage over vehicle control, markedly increased after incubation with 100 μ M SCH-1 for 5 min (SCH-1: 191.2 ± 23.3 % vs. vehicle control: 100 ± 17.7 %, $P < 0.01$).

In a set of colon preparations, a selective prostacyclin receptor antagonist Ro1138452 was used to test the possible involvement of prostacyclin receptor in the SCH-1-induced response. Cicaprost, a prostacyclin receptor agonist with high selectivity and potency, caused a 73.4 ± 3.6 % inhibition on the spontaneous contraction and Ro1138452 markedly inhibited cicaprost responses in a concentration-dependent manner at concentrations of 0.1 μ M (-37.7 ± 7.9 %, $P < 0.001$), 1 μ M (-18.8 ± 7.5 %, $P < 0.001$), 3 μ M (-9.9 ± 7.7 %, $P < 0.001$), as indicated in Fig. 5-7. The inhibitory responses of SCH-1 (10 μ M) were however not affected by Ro1138452 at the concentrations used ($P > 0.05$).

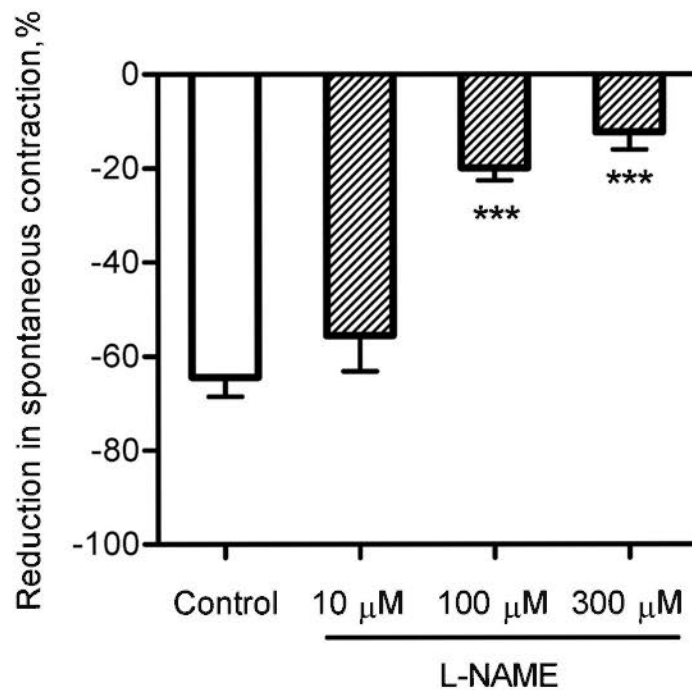


Fig. 5-5 Effects of N^o-nitro-L-arginine methyl ester (L-NAME) at the concentrations of 10 μM, 100 μM and 300 μM on the inhibitory responses of SCH-1 (10 μM) in isolated rat colon. The colon segments were pre-incubated with the enzyme inhibitor for 15 min before the addition of SCH-1. L-NAME attenuated the inhibitory response of SCH-1 in a concentration-dependent manner ($P < 0.001$). Values are expressed as mean \pm S.E.M. (n = 6). *** $P < 0.001$ compared to control.

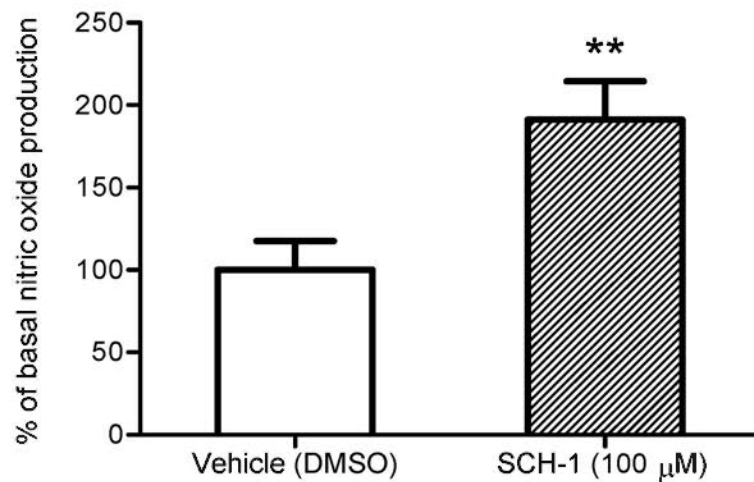


Fig. 5-6 Effects of SCH-1 (100 μM) on the nitric oxide (NO) production in isolated rat colon. The colon segments were incubated with SCH-1 (or DMSO) for 5 min, then frozen in liquid nitrogen and homogenized. The nitric oxide content in supernatant was measured by colorimetric assays. 100 μM SCH-1 markedly increased the nitric oxide production in isolated rat colon ($P < 0.01$). Values are expressed as mean \pm S.E.M. (n = 7). ** $P < 0.01$ compared to vehicle.

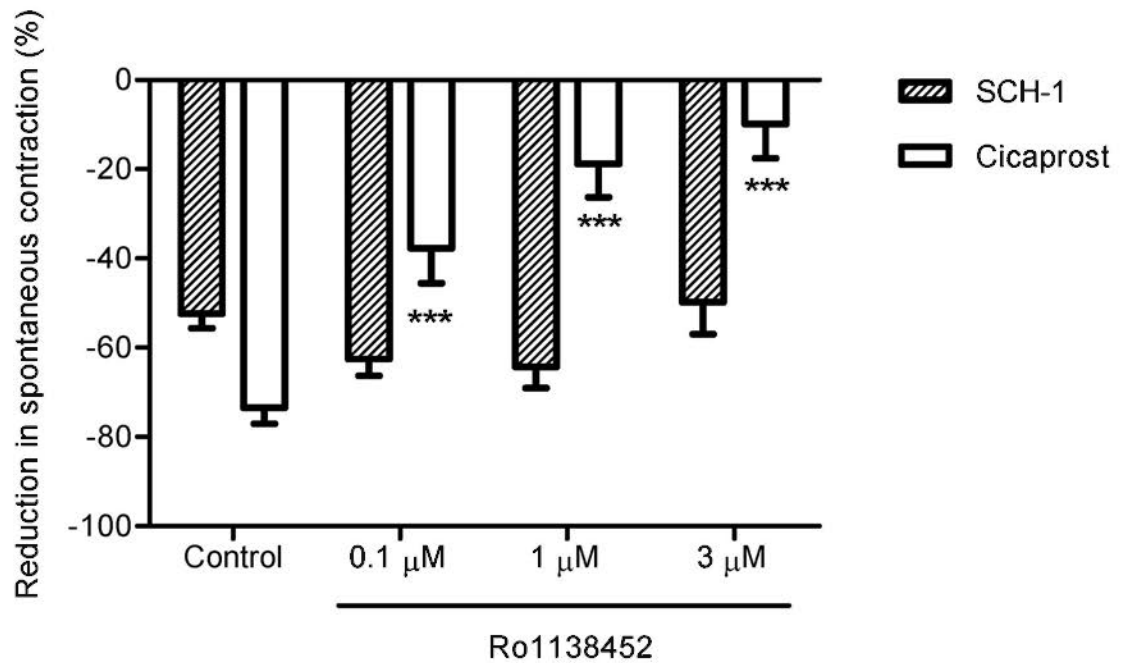


Fig. 5-7 Effects of Ro1138452 at the concentrations of 0.1 μM ($n = 8$), 1 μM ($n = 8$) and 3 μM ($n = 5$) on the inhibitory responses of SCH-1 (10 μM) and cicaprost (10 nM) in isolated rat colon. The colon segments were pre-incubated with the prostacyclin receptor antagonist for 15 min before the addition of SCH-1 or cicaprost. Ro1138452 attenuated the inhibitory response of cicaprost in a concentration-dependent manner ($P < 0.001$) while had no effect on SCH-1 ($P > 0.05$). Values are expressed as mean \pm S.E.M.. * $P < 0.05$, ** $P < 0.01$, *** $P < 0.001$ compared to control.

5.3.4 Effect of cyclic guanosine monophosphate (cGMP)

As shown in Fig. 5-8, a soluble guanylyl cyclase (GC) inhibitor ODQ (which had no significant effect on the rate and amplitude of contraction) was used to test the involvement of GC-dependent pathways in the relaxant effect of SCH-1. The SCH-1 response ($-59.5 \pm 7.4\%$, $n = 6$) was partially inhibited by ODQ at the concentrations of $1\ \mu\text{M}$ ($-25.4 \pm 8.0\%$, $P < 0.05$), $10\ \mu\text{M}$ ($-11.6 \pm 10.7\%$, $P < 0.01$) and $30\ \mu\text{M}$ ($-5.0 \pm 8.6\%$, $P < 0.05$).

To further determine the significance of GC-dependent pathways, the cyclic guanylic acid (cGMP) contents in a set of colon segments were measured using enzyme immunoassay (EIA). As shown in Fig. 5-9, the basal levels of cGMP found in proximal and distal colon segment treated with vehicle blank (DMSO) were 6948 ± 711 and 2296 ± 1079 fmol/g of tissue ($n = 3$), respectively. Incubation with $50\ \mu\text{M}$ SCH-1 tended to decrease cGMP level in proximal colon (3423 ± 1616 fmol/g of tissue, $P = 0.12$), while increase cGMP level in distal colon (5119 ± 569 fmol/g of tissue, $P = 0.08$) although no significant effects were observed. There was little effect found in a combination of proximal and distal ($n = 6$, $P = 0.82$).

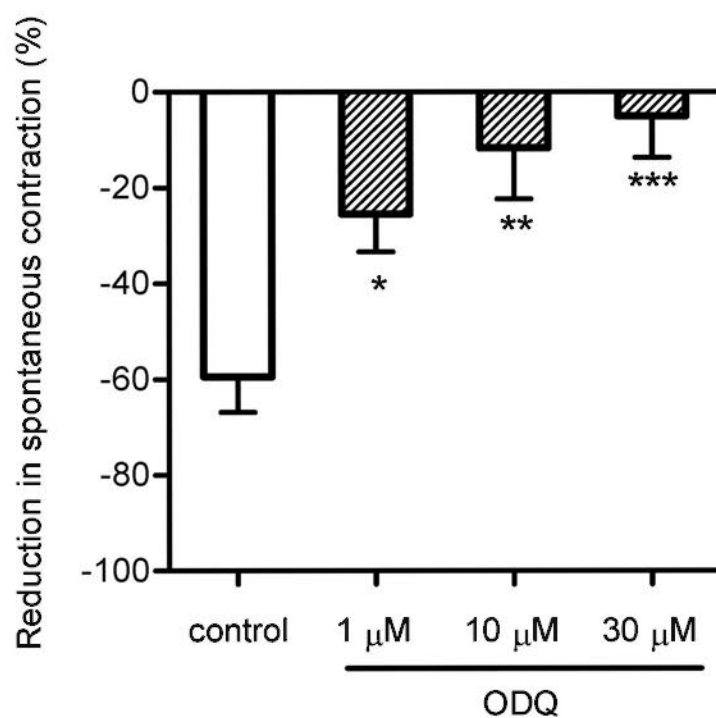


Fig. 5-8 Effects of 1*H*-[1,2,4] oxadiazolo[4,3- α]-quinoxalin-1-one (ODQ) at the concentrations of 10 μ M, 100 μ M and 300 μ M on the inhibitory responses of SCH-1 (10 μ M) in isolated rat colon. The colon segments were pre-incubated with the enzyme inhibitor for 15 min before the addition of SCH-1. ODQ attenuated the inhibitory response of SCH-1 in a concentration-dependent manner ($P < 0.001$). Values are expressed as mean \pm S.E.M. ($n = 6$). * $P < 0.05$, ** $P < 0.01$, *** $P < 0.001$ compared to control.

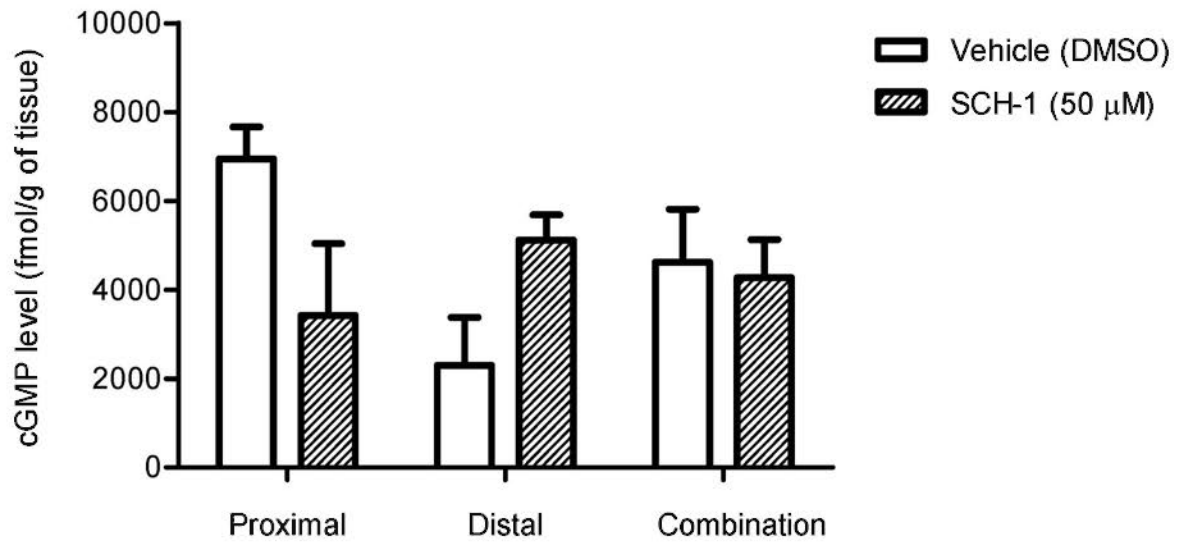


Fig. 5-9 Effects of SCH-1 (50 μ M) on cyclic guanosine monophosphate (cGMP) production in isolated rat colon. The colon segments were incubated with SCH-1 (or DMSO) for 5 min, then frozen in liquid nitrogen and homogenized. The cGMP content in reconstituent was measured using enzyme immunoassay (EIA). 50 μ M SCH-1 tended to decrease cGMP production in proximal colon segments ($n = 3$, $P = 0.12$) while increase cGMP in distal colon ($n = 3$, $P = 0.08$). No effect was observed in a combination of proximal and distal ($n = 6$, $P = 0.82$). Values are expressed as mean \pm S.E.M..

5.3.5 Effects of other non-adrenergic, non-cholinergic (NANC) mediators

These experiments were performed to test whether other non-adrenergic, non-cholinergic transmitters apart from NO were involved in the SCH-1-induced relaxation on rat colon. As presented in Fig. 5-10, the response to 10 μ M SCH-1 (-66.1 ± 6.1 %, $n = 6$) was markedly inhibited by apamin (a specific blocker for calcium-activated K^+ channels in smooth muscle cell) at the concentrations of 25 nM (-45.5 ± 8.9 %, $P < 0.01$) and 50 nM (-31.6 ± 4.6 %, $P < 0.001$). Sodium nitroprusside (SNP), a NO donor, caused a 67.6 ± 8.1 % inhibition on the spontaneous contraction of colon preparations at a concentration of 1 μ M. The responses to SNP were not affected by apamin at the concentrations used ($P > 0.05$).

To determine the possible involvement of adenosine, DPCPX, a potent antagonist for adenosine A_1 receptors was used (5 μ M and 10 μ M). As shown in Fig. 5-11, although adenosine (100 μ M) produced different inhibitory responses in proximal colon preparations (-24.2 ± 5.2 %, $n = 4$) and distal colon preparations (-82.4 ± 2.8 %, $n = 4$), the adenosine responses in both preparations were markedly inhibited by DPCPX (10 μ M, $P < 0.01$). In contrast, DPCPX did not affect the responses to SCH-1 (10 μ M) in colon preparations. Chymotrypsin, a serine endopeptidase, was used to test the interference with the action of vasoactive intestinal peptide (VIP). The SCH-1 responses (-60.0 ± 10.2 %, $n = 5$) were not affected by chymotrypsin at a sufficient concentration of 2 u/ml (-62.2 ± 4.9 %, $P > 0.05$).

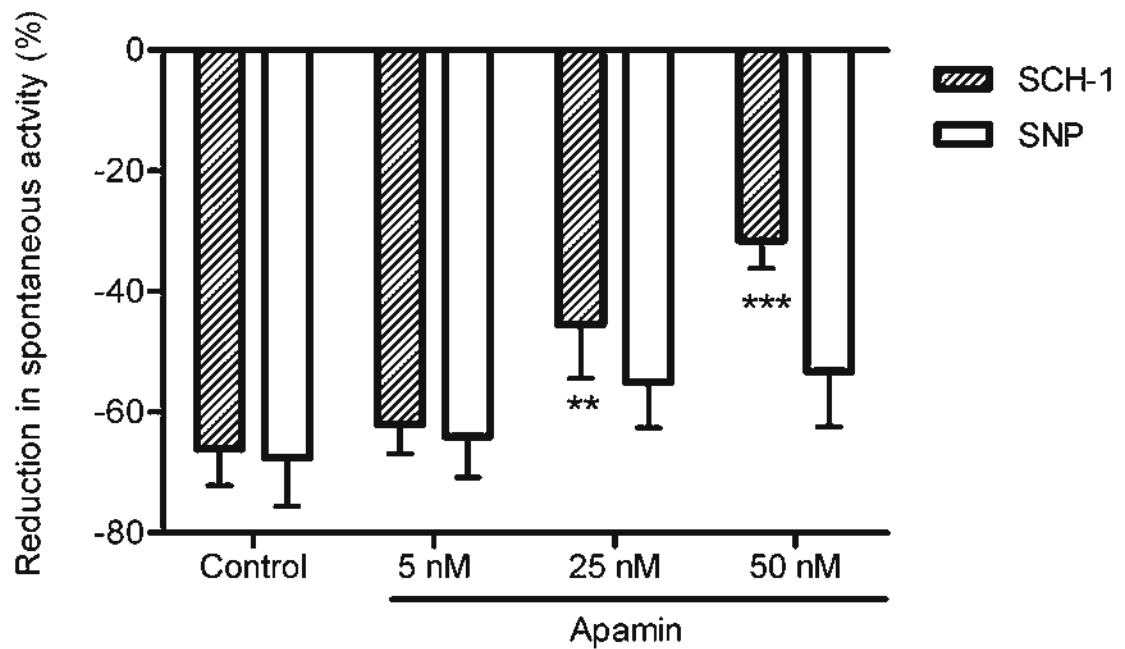


Fig. 5-10 Effects of apamin at the concentrations of 5 nM, 25 nM and 50 nM on the inhibitory responses of SCH-1 (10 μ M) and sodium nitroprusside (SNP, 1 μ M) in isolated rat colon. The colon segments were pre-incubated with apamin for 15 min before the addition of SCH-1 or SNP. Apamin attenuated the inhibitory response of SCH-1 in a concentration-dependent manner ($P < 0.001$) while had no effect on SNP ($P > 0.05$). Values are expressed as mean \pm S.E.M. ($n = 6$). ** $P < 0.01$, *** $P < 0.001$ compared to control.

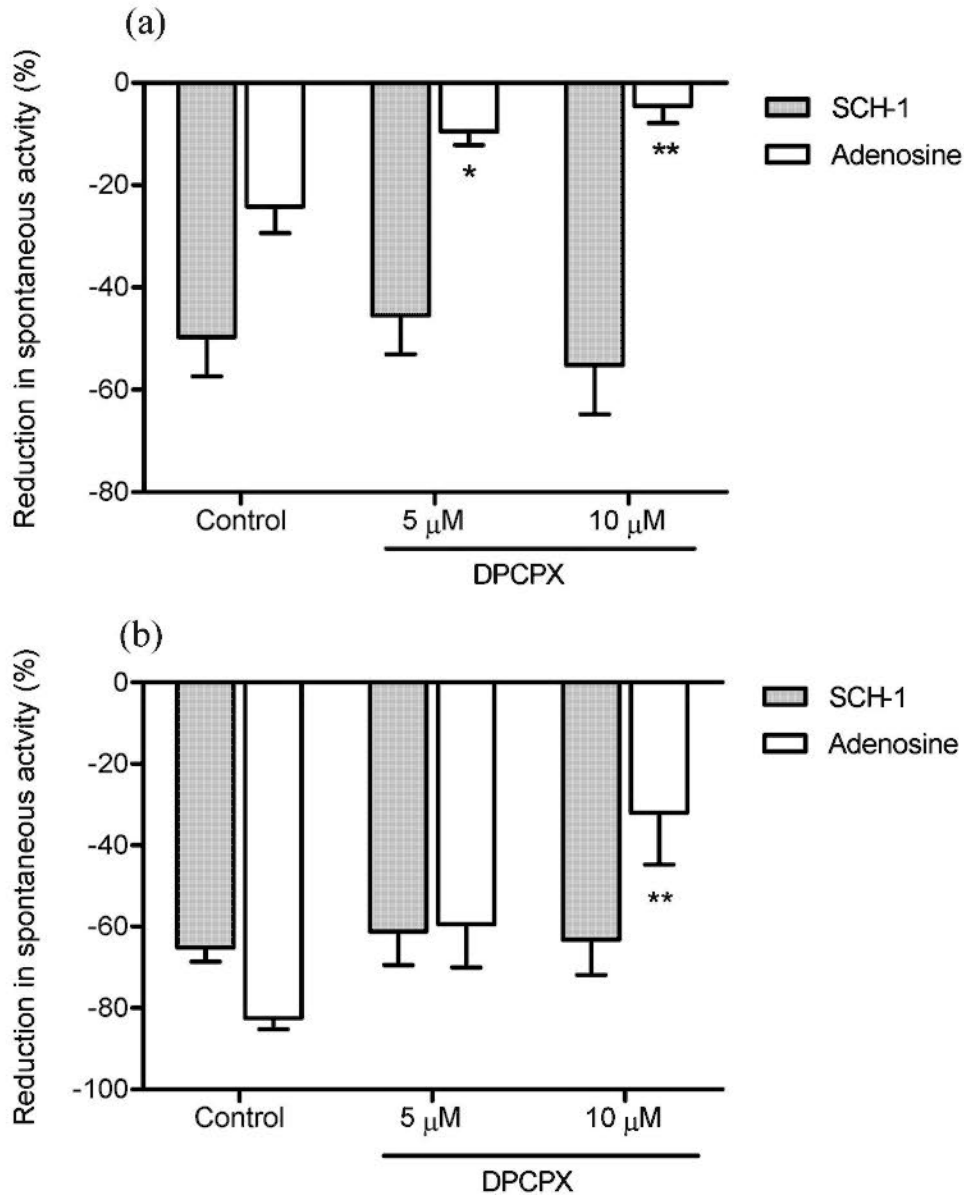


Fig. 5-11 Effects of 8-cyclopentyl-1,3-dipropylxanthine (DPCPX) at the concentrations of 5 μM and 10 μM on the inhibitory responses of SCH-1 (10 μM) and adenosine (100 μM) in (a) proximal (n = 4) and (b) distal isolated rat colon (n = 4). Pre-incubation of DPCPX for 15 min concentration-dependently attenuated the responses of adenosine in both proximal and distal colon ($P < 0.05$), whereas did not affect the responses of SCH-1 ($P > 0.05$). Values are expressed as mean \pm S.E.M.. * $P < 0.05$, ** $P < 0.01$, compared to control.

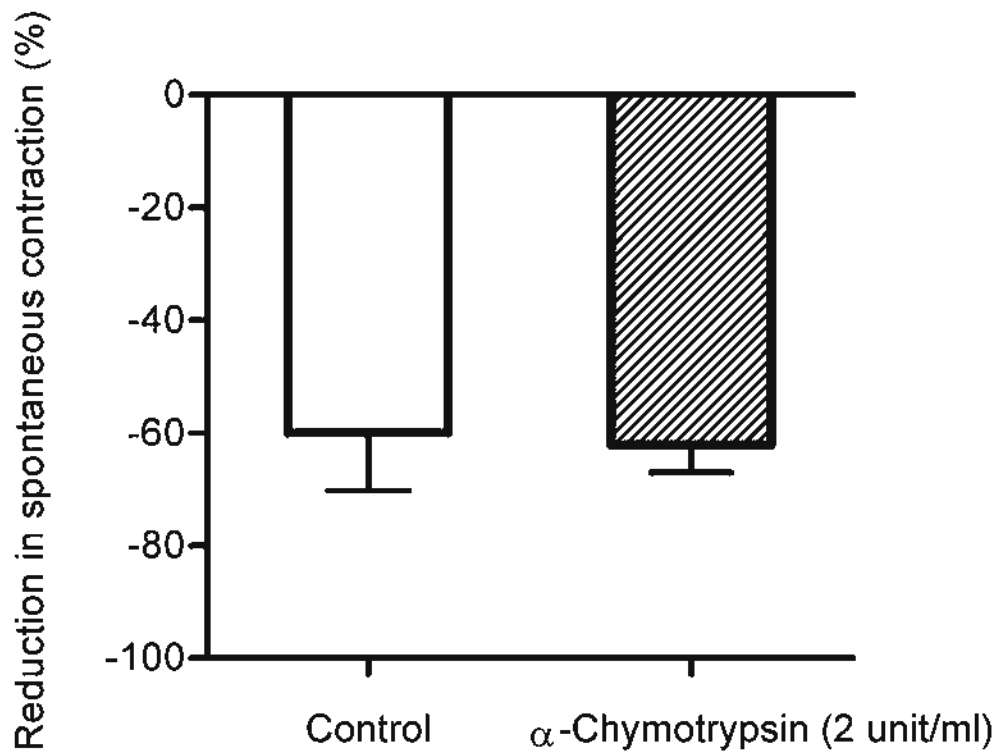


Fig. 5-12 Effects of α -chymotrypsin (2 unit/ml) on the inhibitory responses of SCH-1 (10 μ M) in isolated rat colon. The colon segments were pre-incubated with the serine peptidase for 10 min before the addition of SCH-1. α -Chymotrypsin did not affect the relaxant responses of SCH-1 ($P>0.05$). Values are expressed as mean \pm S.E.M. (n = 5).

5.4 Discussion

Schisandra chinensis, a well-known tonic and astringent agent, has been widely used to control excessive loss of essential energy and body fluid in Chinese Medicine (National Committee of Chinese Pharmacopoeia, 2005). This herb is usually prescribed for the treatment of night sweating and diarrhea syndromes. Schisandrin (SCH-1) is one of the major lignan components isolated and characterized in *Schisandra chinensis*. The present study is our first attempt to study the *in vitro* modulatory effect of SCH-1 on the motility of lower gastrointestinal tract (rat colon). In the previous study (Chapter 4), SCH-1 and other three Schisandra lignans caused concentration-dependent relaxant effects on the spontaneous contraction in rat colon, with SCH-1 displaying the highest potency (EC_{50} value of $1.66 \pm 0.31 \mu\text{M}$). In addition, the colon motility was also inhibited by Schisandra water and ethanol extracts, where SCH-1 was characterized as the major lignan component (Chapter 2), thereby suggesting SCH-1 could play a key role in lower gut motility modulation of *Schisandra chinensis*. The mechanisms of SCH-1-mediated relaxation on spontaneously contracting rat colon were thus investigated to identify the involvement of different receptors, enzymes, ion channels and mediators.

Gastrointestinal tract is in the innervation of autonomic and enteric nerve systems that control the rhythmic activity of gut smooth muscle cells in different regions of gastrointestinal tract (Bult et al., 1990; Bauer et al., 1993). In rat colon, the cyclic episodes of myenteric potential oscillations of circular muscles were associated with spontaneous contractions (Pluja et al., 1999). Anatomical and electrophysiological

investigations on contractility of rat and dog colon preparations have shown that three components are involved in the colonic spontaneous contractions: the smooth muscle cells, a network of interstitial cells of Cajal (which generate pacemaker potentials) located near myenteric plexus, and a largely inhibitory innervation which is concentrated on the interstitial cells of Cajal (Huizinga et al., 1990; Faussone-Pellegrini, 1992.). In this study, the neuronal Na⁺ channel blocker TTX essentially abolished the inhibitory effects of SCH-1 on spontaneous contraction of rat colon, suggesting the involvement of neuronal action in the SCH-1-mediated relaxation. Furthermore, the inability of propranolol and atropine to inhibit the SCH-1 responses suggested that this agent activated the enteric nerves to release inhibitory non-adrenergic non-cholinergic (NANC) transmitters leading to relaxation on rat colon (Burnstock, 1986). Unlike SCH-1, the responses of another well-known lignan SCH-4 were only partially inhibited by TTX (50% inhibition at 1 μM), indicating the SCH-4-mediated relaxation comprised of actions of neuronal and non-neuronal components. As SCH-1 accounted for the dominant proportion (>70%) in lignan components of water extract, TTX tended to abolish the inhibitory responses of water extract like SCH-1, whereas the ethanol extract responses were partially inhibited due to the comparable fractions of different lignans. In spite of the regional difference and variance between species (Suthamnatpong, 1993; Okishio et al., 2000), vasoactive intestinal polypeptide (VIP), nitric oxide and ATP have been recognized as the main NANC inhibitory neurotransmitters. In general, the inhibitory NANC response involves the release of a combination of two or more messengers, but one of them could play a predominant role in the particular section of gastrointestinal tract of some species (Maggi et al., 1993; Furness et al., 1995; Benko et al., 2007).

Nitric oxide is an important NANC inhibitory transmitter in gastrointestinal tract. There has been good agreement that NO plays an important role in colon relaxation elicited by activation of enteric nerves. Huizinga et al. (1992) reported that the neural mediated relaxation of canine colonic smooth muscle was essentially abolished by N^G-nitro-L-arginine (L-NOARG), a NOS inhibitor, and the effect was reversed by a NO precursor L-arginine but not D-arginine. In rat colon, relaxation of circular muscle to distension and longitudinal muscle to electrical field stimulation was blocked by L-NOARG (Suthamnatpong et al., 1993; 1994). In this study, pre-treatment of a NOS inhibitor L-NAME markedly inhibited SCH-1-mediated colonic relaxation (60-80% at 100-300 µM), suggesting the involvement of NO in the action of SCH-1. This was further demonstrated by colorimetric measurement showing that NO was produced in colon segments incubated with SCH-1. Since neuronal NOS (nNOS) has been identified in enteric nerve terminals and concentrated in the longitudinal muscle layer with attached myenteric plexus (Bredt et al., 1990; Huber et al., 1998), the neuronally produced NO is facilitated to diffuse to the adjacent smooth muscle cells to take actions. Thus it would appear that SCH-1-induced inhibition on spontaneous contraction of rat colon was mediated mainly by NO. There remains some discussions on the biosynthesis of NO within the enteric nerves directly activated by SCH-1 or in the smooth muscle cells via induction of another released transmitter such as VIP interplaying with NO in NANC inhibition (Boeckxstaens et al., 1991; Grider, 1992; Murthy, 1995; Van Geldre et al., 2004), the difference of which has not been distinguished in this study. It has been reported that prostacyclin inhibited the spontaneous activity of the isolated rat colon via activating the release of NANC neurotransmitters including nitric oxide (Qian and Jones,

1995). In this study, the potent prostacyclin (IP-) receptor antagonist Ro1138452 (Bley et al., 2006) markedly inhibited the responses of an IP-receptor agonist cicaprost, but did not affect the SCH-1 response, suggesting that IP-receptors were not involved in the SCH-1-mediated colonic relaxation.

In the gastrointestinal tract, the neuronally produced NO diffuses to smooth muscle cells containing soluble guanylyl cyclase (sGC). sGC is an important NO-sensitive mediator in signal transduction of smooth muscle relaxation. The activated sGC catalyzes the conversion of GTP to cyclic GMP (cGMP), which in turn activates the cGMP-dependent protein kinase (PKG). PKG subsequently stimulates the extrusion of intracellular Ca^{2+} by phosphorylating a number of important target proteins including ion channels, ion pumps, receptors and enzymes, thereby decreasing the sensitivity of contractile apparatus to Ca^{2+} , leading to smooth muscle relaxation (Friebe et al., 2003). In this study, pre-treatment of a sGC inhibitor ODQ strongly inhibited the SCH-1-mediated relaxation. The inhibitory responses of ODQ were concentration-dependent, with a comparable inhibition potency with L-NAME (80-90 %) at the highest concentrations, suggesting NO mainly acted through sGC to elicit relaxations on the rat colon. There are a number of reports which have demonstrated that NO-sGC coupled pathways mediate colonic relaxation in different species including rodent, canine and human (Ward et al., 1992; Benko et al., 2007; Dhaese et al., 2008). However, the cGMP levels in response to SCH-1 seemed to be difficult to explain, with a decrease in proximal colon but an increase in distal colon. Nevertheless, it should be noted that the basal cGMP levels observed in this study differed between proximal and distal sections, implying that various components (such as

mucosa) contributing to the cGMP levels could be present in different colon regions. The cGMP levels in response to SCH-1 could thus vary from the interactions between other colon components (apart from enteric nerves) and SCH-1. Nevertheless, it has been reported that the cGMP levels were elevated in colonic smooth muscles exposed to exogenous NO and/or electrical field stimulation (Ward et al., 1992; Dhaese et al., 2008).

A variety of functional and morphological studies have provided evidence that more than one transmitter may be involved in the NANC relaxation in response to stimulation in most regions of gastrointestinal tract (Belai and Burnstock, 1994; Smits and Lefebvre, 1996; Mule and Serio, 2003; El-Mahmoudy et al., 2006). Apamin, a small conductance Ca^{2+} -activated K^{+} channel blocker, is widely used to study the non-nitroergic components of NANC inhibition (Kishi et al., 1996), although some evidences showing the apamin-sensitive components of NO response (Serio et al., 1996; Matsuyama et al., 1999). In this study, apamin markedly inhibited SCH-1-mediated colonic relaxation in a concentration-dependent manner but did not affect the responses of a NO donor sodium nitroprusside (SNP), indicating non-nitroergic, apamin-sensitive transmitter(s) participate(s) in the SCH-1-induced relaxation. In previous studies on colon preparations, purinergic mediators such as ATP and adenosine (Qian and Jones, 1995; Rozsai et al., 2001; Burnstock G., 2008), as well as neuropeptides such as pituitary adenylate cyclase activating peptide (PACAP) but not vasoactive intestinal peptide (VIP), are recognized as apamin-sensitive candidates (Kishi et al., 1996; Zagoradnyuk et al., 1996). In this study, adenosine receptor appeared to mediate relaxation on rat colon, as indicated by the inhibitory effects of adenosine in spite of different inhibition extents observed in

proximal and distal sections. A potent adenosine A₁ receptor antagonist DPCPX (Martinson et al., 1987), used at high concentration to block adenosine A₂ receptor (Collis et al., 1989), markedly attenuated the adenosine-induced relaxation. In contrast, the SCH-1 responses were not influenced by pre-treatment of DPCPX, suggesting the activators of adenosine receptors did not participate in the SCH-1-induced relaxation. The involvement of VIP was also tested in our study using an enzyme α -chymotrypsin that can cleave VIP peptide bonds. The inability of α -chymotrypsin to affect the SCH-1 response indicated VIP and other susceptible peptides appeared to be excluded as a transmitter role in the inhibitory action of SCH-1. Although VIP-like peptides are less evident to be involved in mediating NANC inhibition in colon preparations (Rozsai et al., 2001), the interplay between VIP and NO should be noted. The proposed mechanisms of SCH-1-induced relaxation on rat colon are described in Fig. 5-13.

NANC inhibitory neurotransmitters, particularly NO, play important roles in regulating peristaltic reflex in colon (Foxy-Orenstein and Grider, 1996; Mizuta et al., 1999; Takahashi, 2003). The SCH-1-mediated colonic relaxation by activating the release of NANC transmitters could increase the accommodation of colon, reduce the velocity of colonic propulsion, and thereby moderate the enhanced colonic transit in gastrointestinal diseases with diarrhea symptoms in gastrointestinal disorders, such as diarrhea-predominant irritable bowel syndrome. Given the significance of NANC innervation in the different parts of gastrointestinal tract, SCH-1 is also speculated to be potentially useful in regulating the esophageal motility (Konturek et al, 1997a), gastrin

motility and emptying (Sarna, 1996), although the selectivity of the drug must be systematically addressed.

In conclusion, SCH-1 has been demonstrated to induce NANC relaxation on the rat colon and the response appeared to involve two or more mediators. NO was likely to be one of inhibitory transmitters that acted via cGMP-dependent pathways, whereas neither adenosine nor VIP seemed to participate in the mediating role. Further studies are warranted to identify the transmitter(s) contributing to the non-nitroergic, apamin-sensitive component of SCH-1-mediated response.

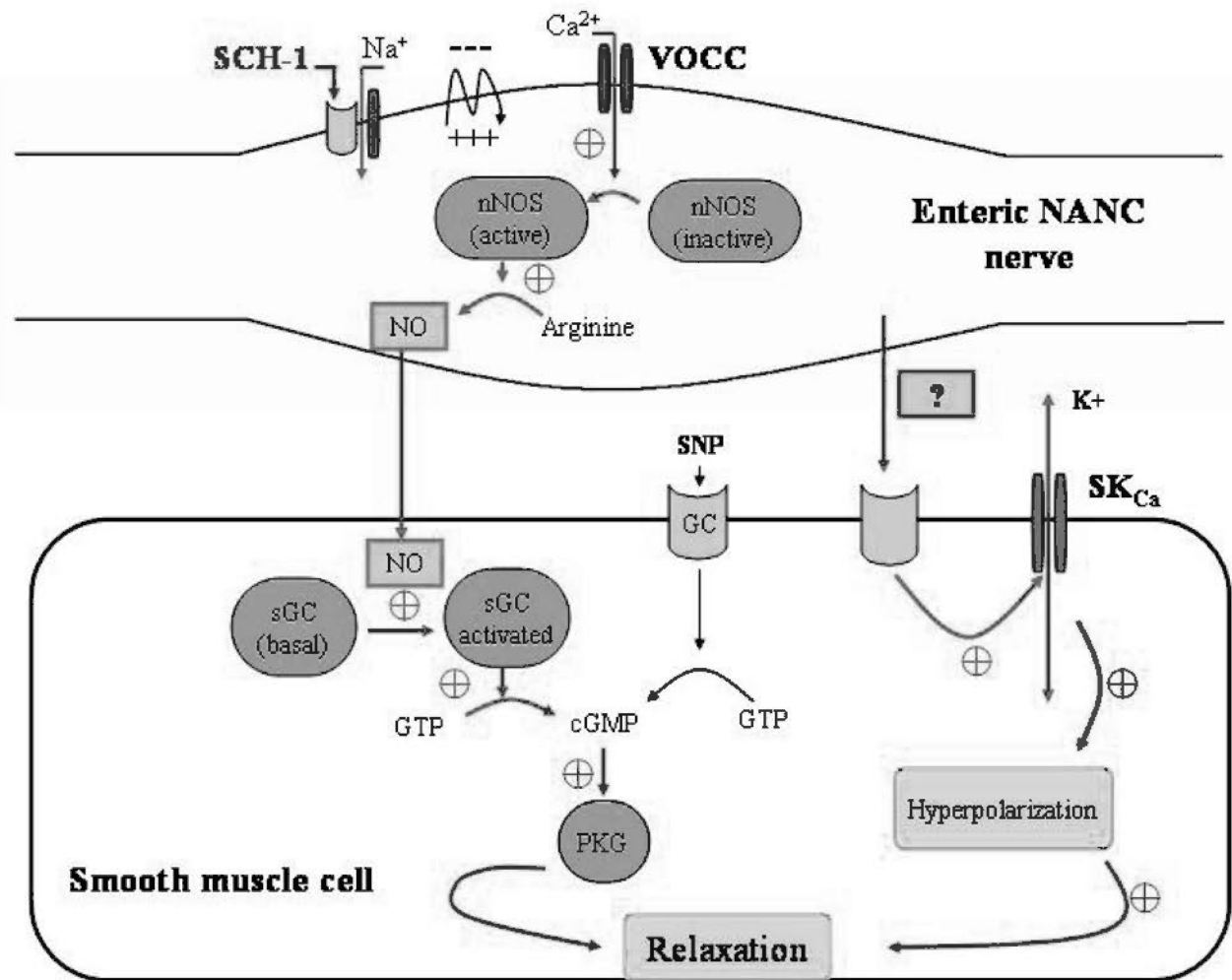


Fig. 5-13 Proposed mechanisms of SCH-1-mediated inhibition on spontaneous contraction of isolated rat colon. There are probably two or more mediators involved in the SCH-1 response. In enteric non-adrenergic non-cholinergic (NANC) nerve, SCH-1 acts on the membrane receptor controlling a sodium channel, thereby initiating plasma membrane depolarization, which subsequently triggers the Ca^{2+} influx through voltage-operated calcium channel (VOCC). The increase of intracellular Ca^{2+} activates the neuronal nitric oxide synthase (nNOS) which catalyzes the conversion of L-arginine to nitric oxide (NO). The neuronally produced NO diffuses to the adjacent smooth muscle, activates the soluble guanylyl cyclase (sGC). The activated sGC catalyzes the conversion

of GTP to cyclic GMP (cGMP), which in turn to activate the cGMP-dependent protein kinase (PKG), leading to smooth muscle relaxation. The right side shows the action(s) of unidentified non-nitroergic transmitter(s) released from enteric NANC nerve. The unidentified transmitter(s) act(s) on the receptor controlling the small conductance Ca^{2+} -activated K^+ channel (SK_{Ca}) on smooth muscle cell, thereby initiates hyperpolarization, resulting in smooth muscle relaxation.

Chapter 6

Schisandra chinensis Reverses Visceral Hypersensitivity in Neonatal Maternal Separated Rats

6.1 Introduction

Schisandra chinensis has been indexed as an astringent, tonic and sedative agent in Chinese medicine. In the extensive pharmacological studies using animals, isolated organs, cultured cells and enzymes, *S. chinensis* extracts and the isolated lignan compounds have been demonstrated to exhibit a wide range of biological activities (Chapter 1). Recently, there is increasing interest in the pharmacological effects of *S. chinensis* acting on central nervous system. Kim et al. (2004) reported that a number of dibenzocyclooctadiene lignans isolated from *S. chinensis* protect cultured rat cortical cells from glutamate-induced toxicity. Besides, both schisandrin and gomisin A have been shown to improve scopolamine-induced memory impairment in rats (Kim et al., 2006; Egashira et al., 2008). In spite of being a well-known sedative agent, the effect of *S. chinensis* on stress-induced pain perception is less understood.

Irritable bowel syndrome (IBS) is a common functional gastrointestinal disorder characterized by abdominal pain and discomfort associated with altered bowel habits in the absence of a demonstrable pathology. Visceral hypersensitivity is one of the most common pathophysiological alterations in IBS patients (Camilleri et al., 2001), and rectal hypersensitivity in patients with IBS has been reported by previous studies (Whitehead et

al., 1990; Bouin et al., 2002). For the pharmacotherapeutic development of IBS, it is essential to construct suitable animal models that mimic the features of IBS patients, in particular the enhanced visceral perception. Recent studies have demonstrated neonatal maternal separation, in a form of early life stress, exaggerates the visceromotor responses to colorectal distension in rats, and stated that visceral hyperalgesia in maternally separated rats is related to enhanced neurochemical responsiveness centrally and peripherally to stimuli (Ren et al., 2007; Chung et al., 2007). Moreover, the early life stressful events are also suggested to increase the colon motility in response to an acute psychological stressor, mimicking the diarrhea symptoms of IBS (Coutinho et al., 2002).

Previously, a Chinese herbal formula prescribed for IBS patients has been demonstrated to relieve the visceral hyperalgesia induced by early life stress and *Schisandra chinensis* is one of the component herbs (Bensoussan et al., 1998). In addition, the findings in previous studies (Chapter 4) have revealed that *S. chinensis* extracts and the major Schisandra lignans exert *in vitro* inhibitory effects on intestinal sensorimotor responses and spontaneous contraction, indicating *S. chinensis* could be used as an antispasmodic agent for relieving diarrhea symptoms in IBS patients. With the aim of evaluating the potential of *S. chinensis* in the treatment for IBS, this study further determines whether *S. chinensis* provides improvement on visceral hypersensitivity induced by neonatal maternal separation in rats. The neurophysiological factors involved in visceral perception were also examined to elucidate the action pathways of *S. chinensis*.

6.2 Methods

6.2.1 Animals

Sprague-Dawley male neonate rats were obtained from Laboratory Animal Service Centre of the Chinese University of Hong Kong on postnatal day 1. Six male pups were randomly assembled for fostering with a lactating mother housed in standard polycarbonate (46×25×20 cm) cages containing 2.5 cm of wood chip bedding material. The dams and their litters were then exposed to 180-min period of daily maternal separation on post-natal day 2-21 inclusive. Manipulation of the pups was initiated at 9:00 am by removal of the dams from the maternity cage and placing them into separate identical cages until the end of the manipulation. The litters were maintained as a group in the maternity cage and further thermoregulated by burrowing into bedding material and by huddling. At the end of the designated daily separation period, the dams were returned to the home cages to reunite with the pups. Approximately 50% of the soiled bedding material in all cages were replaced with clean bedding and mixed well no more than once a week. A separated group of pups maintained in the same conditions were fostered with the lactating mothers without maternal separation. On day 22, all the rats were weaned and litter housed until day 50, at which they were housed in same treatment groups. Animals were maintained in a temperature controlled room (20 °C) with a 12-hr light-dark cycle, with free access to food and water.

6.2.2 Drug preparation and treatment

Ethanol extract (70%) of *Schisandra chinensis* was prepared as described in Section 2.2.4. The neonatal maternal separated (NMS) rats were randomly allocated to NMS control group and SCH-treated group, and the non-separated rats were designated to the normal group. The SCH-treated rats were intragastrically administered with *Schisandra chinensis* extract suspended in 0.5% sodium carboxymethylcellulose (sigma) solution (less than 3 ml per treatment), at low dose (0.3 g/kg) and high dose (1.5 g/kg) for 7 days from day 54 to day 60, respectively. The normal and the NMS control rats were given intragastrical administration of 0.5% sodium carboxymethylcellulose solution as vehicle blank for the same period. Animal manipulation and drug administration of the four animal groups are summarized in Table 6-1.

Table 6-1 Manipulation and drug administration of four animal groups

	Normal	SCH (0)	SCH (0.3)	SCH (1.5)
NMS	No	Yes	Yes	Yes
Drug/Vehicle Administration	0.5% CMC-Na	0.5% CMC-Na	<i>S. chinensis</i> (0.3 g/kg)	<i>S. chinensis</i> (1.5 g/kg)

6.2.3 Behavioral testing

6.2.3.1 Abdominal withdrawal reflex (AWR)

On day 60, colorectal distension (CRD) was given and abdominal withdrawal reflex (AWR) was quantified as scores in the individual rat of all groups. CRD was performed as previously described (Al-Chaer et al., 2000). Rats were first anesthetized with isoflurane. The balloon was constructed from a latex glove finger (6 cm of length) attached to a balloon dilator (2 mm of diameter), connected via a Y connector to a syringe pump and a sphygmomanometer. The balloon was inserted in the distal colon with the distal tip 1 cm from the anal verge and secured to the base of the tail with duct tape. Animals were allowed to recover for 30 min. CRD was applied in graded intensity of 10, 20, 40, 60, 80 mmHg with 20-s inflation and subsequently 4-min interval of deflation. AWR responses were measured by an independent observer (blind to animal handling such as drug administration) assigning scores as follow: 0, no behavioural response to CRD; 1, brief head movement followed by immobility; 2, contraction of abdominal muscles; 3, lifting of abdomen; 4, body arching and lifting of pelvic structures (Fig. 6-1). The threshold pressure (increments of 10 mmHg starting at 10 mmHg) was defined as stimulus intensity that elicited visually definable contraction of abdominal muscles. All the measurements were repeated twice for each intensity level of distension and the data for each animal were averaged for further analysis.



Score 1



Score 2



Score 3



Score 4

Fig. 6-1 Scores of abdominal withdrawal reflex (AWR) response to graded intensity of colorectal distension (CRD). Score 0, no behavioral response to CRD; Score 1, brief head moving followed by immobility; Score 2: contraction of abdominal muscles; Score 3, lifting of abdomen; Score 4, body arching and lifting of pelvic structures.

6.2.3.2 Electromyography (EMG)

The visceralmotor responses to CRD in rats were also quantified by measuring the electromyography (EMG) activities.. Rats were anesthetized by inhalation of isoflurane during the surgery. Electrodes (W3 631 stainless steel wire, W3 Wire international, Las Vegas) were stitched into the external oblique musculature, just superior to the inguinal ligament (Fig. 6-2). With the aid of leads, electrodes were tunnelled subcutaneously and externalized laterally for further EMG recording. Rats were allowed to recover for at least 4 days. Wounds were tested for tenderness to ensure complete recovery before behavioral testing. On day 60, CRD in graded intensity was applied as described in 6.2.3.1. The EMG activity was amplified via a bioamplified (ML132, ADInstruments International, Australia), filtered (50-5000 Hz) and recorded by Powerlab system (ADInstruments International, Australia). The EMG data of 20 s before CRD (baseline) and 20 s during CRD were recorded for calculation. The response was taken as the percentage of EMG amplitude during CRD over baseline using Chart 5 program (ADInstruments international, Australia). All the measurements were conducted twice for each intensity level of CRD and the data for each animal were averaged for analysis.

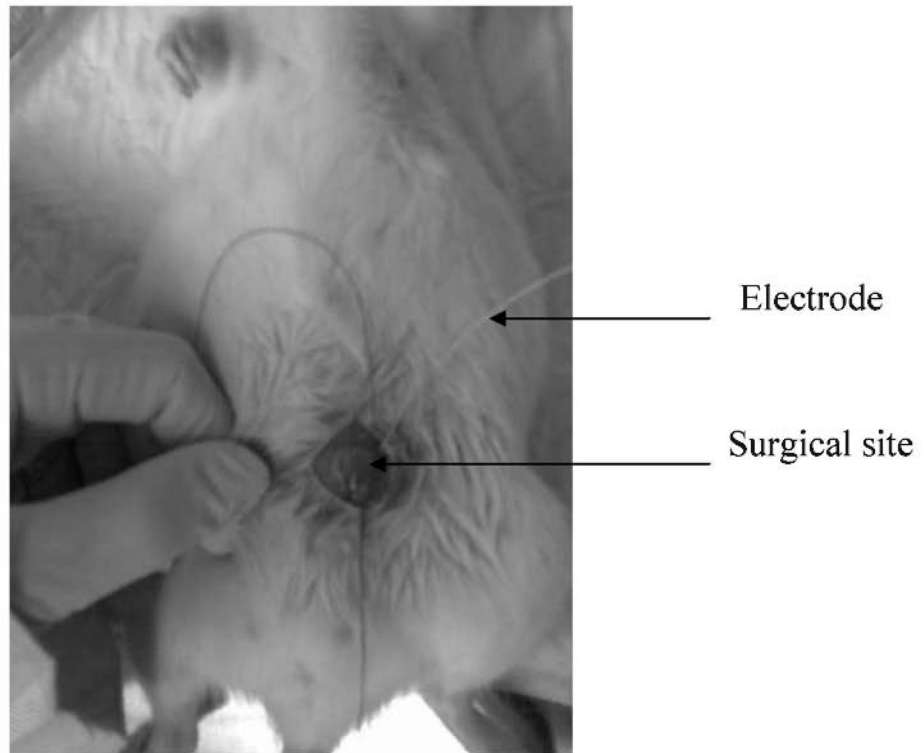


Fig. 6-2 Surgery for the measurement of electromyography (EMG). An electrode was stitched into the external oblique musculature, just superior to the inguinal ligament.

6.2.4 Tissue harvesting

After a series of graded CRD, rats were deeply anesthetized with overdoses of ketamine. Tissues including distal colon (5-6 cm from anus), lumbosacral spinal cord (L6-S1), and brain were dissected and snap frozen in liquid nitrogen. The tissues were stored at -80°C before use.

6.2.5 Measurement of 5-HT content

A segment of distal colon (~0.1 g) was homogenized in 0.2 M perchloric acid, and centrifuged at 10,000 ×g for 5 min. The supernatant was removed, neutralized with an equal volume of 1.0 M borate buffer (pH 9.25) and centrifuged at 10,000 ×g for 1 min. The 5-HT content in the supernatant was quantitatively analyzed using an enzyme immunoassay according to the manufacturer's notes (Beckman Coulter, Fullerton, CA). Briefly, 5-HT in the samples was chemically acylated in the first step. Acylated 5-HT was then incubated in antibody coated wells in presence of acetylcholinesterase-acylated-serotonin conjugate. After washing to remove non-bound components, a chromogenic substrate was added. The absorbance at 405 nm was measured with a 96-well plate. The 5-HT level was expressed as ng per g wet weight of tissue.

6.2.6 Measurement of mRNA encoding 5-HT receptors, 5-HT transporter, and opioid receptors

The amount of mRNA encoding 5-HT_{3A} and 5-HT_{3B} subunits of 5-HT₃ receptor, 5-HT₄ receptor, 5-HT transporter (SERT), κ -, μ - and δ -opioid receptors were quantified by real-time RT-PCR. A segment of distal colon (~0.1 g) was homogenized in 1 ml Trizol reagents (Sigma, St. Louis, MO). Total RNA was obtained by an extraction method using chloroform and isopropanol. The RNA was quantified using the standard OD₂₆₀ method. The absorbance at 260 and 280 nm was measured using spectrophotometer. The OD₂₆₀/OD₂₈₀ ratio for each RNA sample used in the following experiments was in the range of 1.8-2.2. Subsequently, RNA was converted into cDNA using the high-capacity cDNA reverse transcription kit (Applied Biosystems). Taqman assays were performed for the quantification of mRNA with ABI step-one real time PCR system (Applied Biosystems). The Taqman primers and probe for the measurements of 5-HT_{3A} and 5-HT_{3B} subunits of 5-HT₃ receptor, 5-HT₄ receptor, 5-HT transporter (SERT), κ -, μ - and δ -opioid receptors, and the housekeeping gene β -actin were purchased from Applied Biosystems (product codes: Rn00577803_m1, Rn00573408_m1, Rn00563402_m1, Rn00564737_m1, Rn00561699_m1, Rn01448892_m1, Rn01430371_m1, Rn00667869_m1).

6.2.7 Data analysis

All the presented values were expressed as mean \pm S.E.M.. Statistical analysis was performed using Graphpad Prism 5 software. Comparison between groups with two

factors was made by two-way ANOVA. Comparison between groups with one factor was made by unpaired Student's *t* test or one-way ANOVA followed by Bonferroni post test, as appropriate. All tests were two-tailed and the significance was set at $P < 0.05$.

6.3 Results

6.3.1 Effects on pain responses to colorectal distension

6.3.1.1 Body weight

Body weights of animals were monitored daily during the period of drug (vehicle) treatment. Fig. 6-3 shows the body weight changes in normal rats, neonatal maternal separated (NMS) control rats administered with CMC-Na (0.5%) as vehicle, and the rats administered with *Schisandra chinensis* extract at the dosages of 0.3 g/kg and 1.5 g/kg. The average values of body weight changes in all groups were within the range of ± 10 g. No significant reduction in body weight had been observed in the drug treated rats, suggesting *S. chinensis* extract at the used dosages did not cause acute toxicity to the animals.

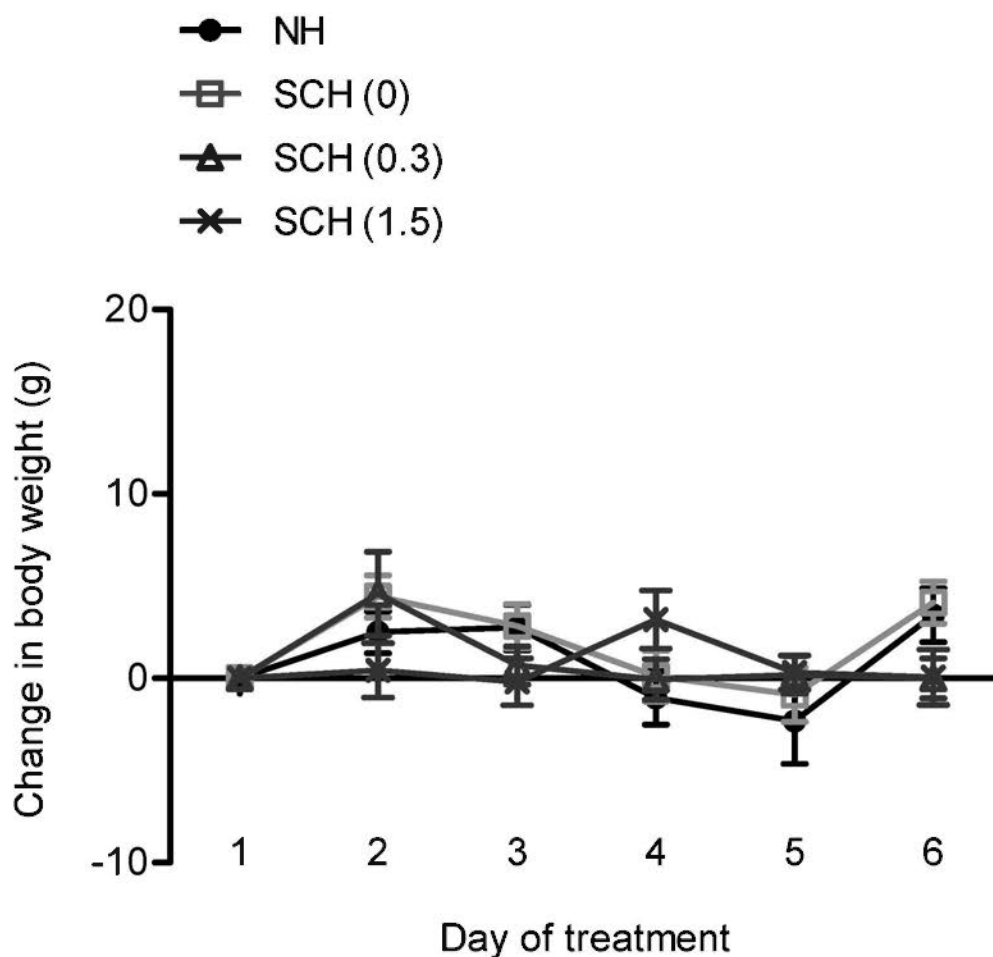


Fig. 6-3 Body weight changes in normal rats (n = 21) and neonatal maternal separated (NMS) rats administered with CMC-Na (0.5%) as vehicle (SCH, 0 g/kg; n = 23) and *Schisandra chinensis* extract at the dosages of 0.3 g/kg (SCH, 0.3 g/kg; n = 21) and 1.5 g/kg (SCH, 1.5 g/kg; n = 20) during the period of drug (vehicle) treatment. The average values of body weight changes in all groups were within the range of ± 10 g. No significant difference was observed between groups as compared by two-way ANOVA ($P > 0.05$). Values are expressed as mean \pm S.E.M..

6.3.1.2 Abdominal withdrawal reflex (AWR)

Abdominal withdrawal reflex (AWR) responses to the graded intensity of colorectal distension (CRD) were scored from normal, neonatal maternal separated (NMS) control rats and SCH-treated rats. As shown in Fig. 6-4, the threshold pressure to elicit abdominal muscle contraction (AWR score is two) in response to CRD was markedly lower in NMS control rats (19.13 ± 1.03 mmHg) than in normal rats (25.71 ± 1.39 mmHg) ($P < 0.001$). Administration of *Schisandra chinensis* extract, at 0.3 g/kg/day (24.76 ± 1.313 mmHg) and 1.5 g/kg/day (25.25 ± 1.80 mmHg) for 7 days, produced significant moderation on the visceral hypersensitivity in NMS rats, respectively ($P < 0.01$).

As depicted in Fig 6-5, a graded AWR response was observed in all animals exposed to CRD with a stepwise increase in balloon pressures from 10 to 80 mmHg. NMS control rats (AUC, 13.04 ± 0.42) showed exaggerated abdominal reflex responses to visceral pain compared with normal rats (AUC, 11.01 ± 0.44 ; $P < 0.01$). The exaggerated responses appeared to be more significant at lower CRD pressures. Administration of *Schisandra chinensis* extract at low (AUC, 10.60 ± 0.37) and high (AUC, 10.71 ± 0.38) dosages both markedly reversed the enhanced abdominal reflex to visceral pain in NMS rats ($P < 0.001$). The effects of *S. chinensis* on abdominal responses were evident at all CRD pressures except for the noxious pressure of 80 mmHg.

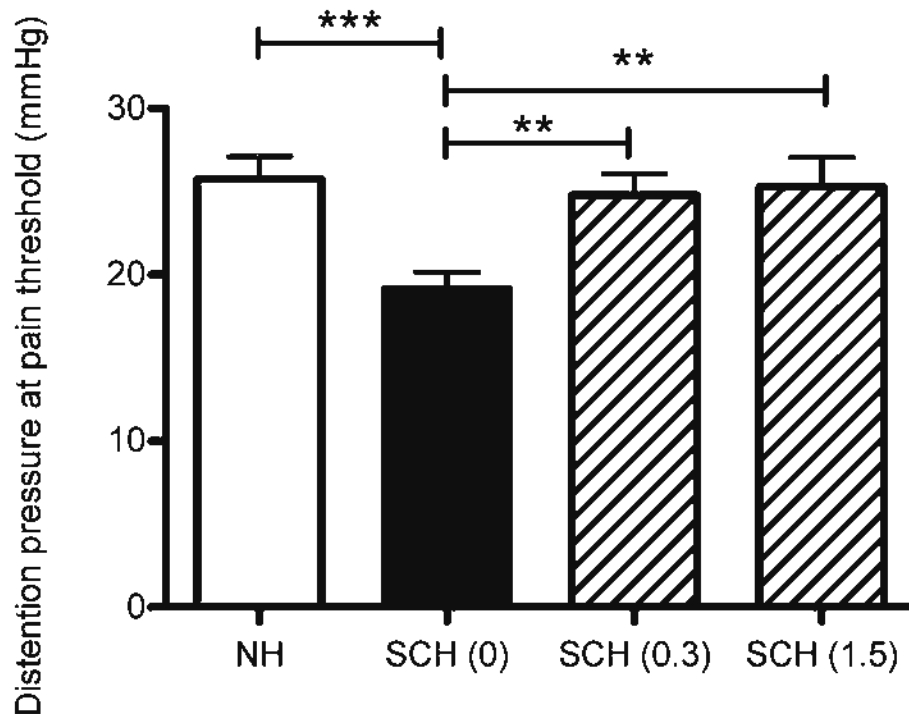


Fig. 6-4 Pain threshold responses to the graded intensity of colorectal distension (CRD) in normal rats ($n = 21$) and neonatal maternal separated (NMS) rats administered with CMC-Na (0.5%) as vehicle (SCH, 0; $n = 23$), and *Schisandra chinensis* extract at the dosages of 0.3 g/kg/day (SCH, 0.3; $n = 21$) and 1.5 g/kg/day (SCH, 1.5; $n = 20$) for 7 days. Pain threshold was set as the CRD pressure to elicit abdominal muscle contraction in rats (AWR score is two). NMS control rats (SCH (0)) showed more sensitive pain threshold than normal rats in response to CRD ($P < 0.001$). *Schisandra chinensis* extract used at two dosages both produced significant attenuation on hypersensitivity of pain threshold in NMS rats ($P < 0.01$). Values are expressed as mean \pm S.E.M.. ** $P < 0.01$, *** $P < 0.001$ compared to NMS control by unpaired Student's t test or one-way ANOVA

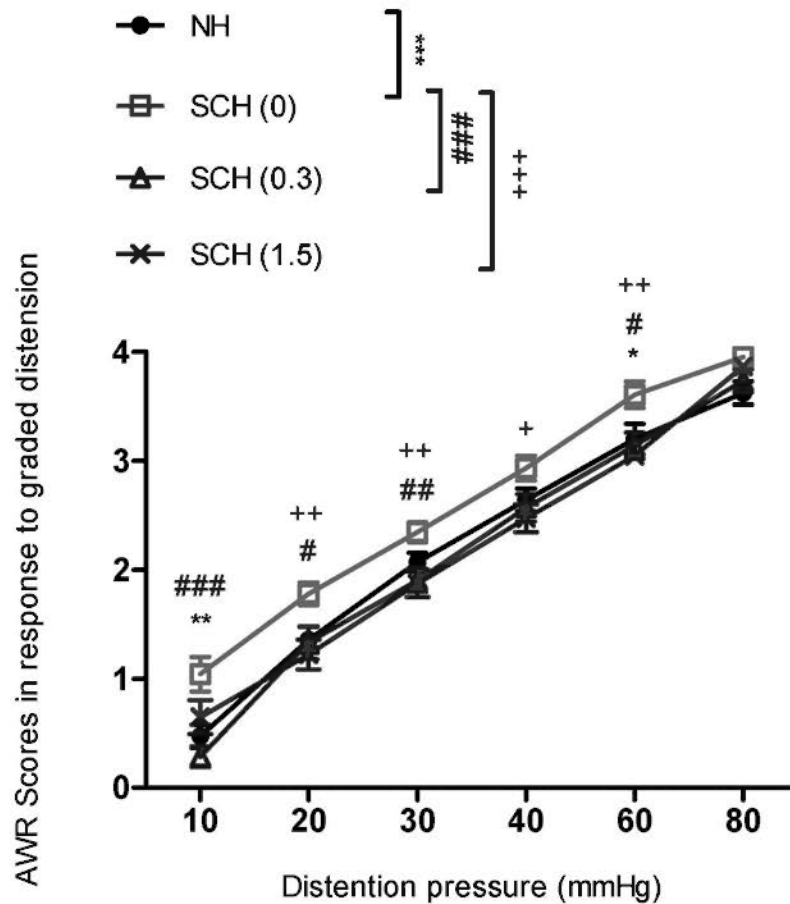


Fig. 6-5 Abdominal withdrawal reflex (AWR) responses to the graded intensity of colorectal distension (CRD) at the pressures from 10 to 80 mmHg in normal rats (n = 21), NMS control rats administered with 0.5% CMC-Na (SCH, 0 g/kg; n = 23) and SCH-treated rats administered with *Schisandra chinensis* extract at the dosages of 0.3 g/kg/day (SCH, 0.3 g/kg; n = 21) and 1.5 g/kg/day (SCH, 1.5 g/kg; n = 20). NMS control rats showed exaggerated abdominal reflex responses to visceral pain compared with normal rats ($P<0.001$). *S. chinensis* extract at two dosages both produced significant reversion on visceral hypersensation in NMS rats ($P<0.001$). Values are expressed as mean \pm S.E.M.. *, #, + $P<0.05$; **, ##, ++ $P<0.01$; ***, ###, +++ $P<0.001$ compared to NMS control by one-way or two-way ANOVA.

6.3.1.3 Electromyography (EMG)

Abdominal muscle electromyography (EMG) in response to the graded intensity of CRD was recorded at the same time while AWR response was scored. An EMG response with higher amplitude represents an exaggerated response to visceral pain. As presented in Fig 6-6, a graded EMG response was observed in all animals exposed to CRD with a stepwise increase in balloon pressures from 10 to 80 mmHg. NMS control rats consistently showed a significant enhancement in EMG responses to visceral pain compared with normal rats ($P < 0.001$). The exaggerated responses remained significant at a noxious pressure of 80 mmHg ($P < 0.05$). Administration of *Schisandra chinensis* extract at low and high dosages both dramatically reversed the enhanced abdominal reflex to visceral pain in NMS rats ($P < 0.001$). The effects of *S. chinensis* on abdominal responses were evident at all CRD pressures including the noxious pressure of 80 mmHg. As summarized in Table 6-2, the AUC value of AWR responses to graded CRD was larger in NMS control rats (1952 ± 202) than in normal rats (1273 ± 146 , $P < 0.05$), whereas values of the rats treated with *S. chinensis* extract at the dosages of 0.3 g/kg (1074 ± 90 , $P < 0.001$) and 1.5 g/kg (1145 ± 92 , $P < 0.001$) dramatically decreased.

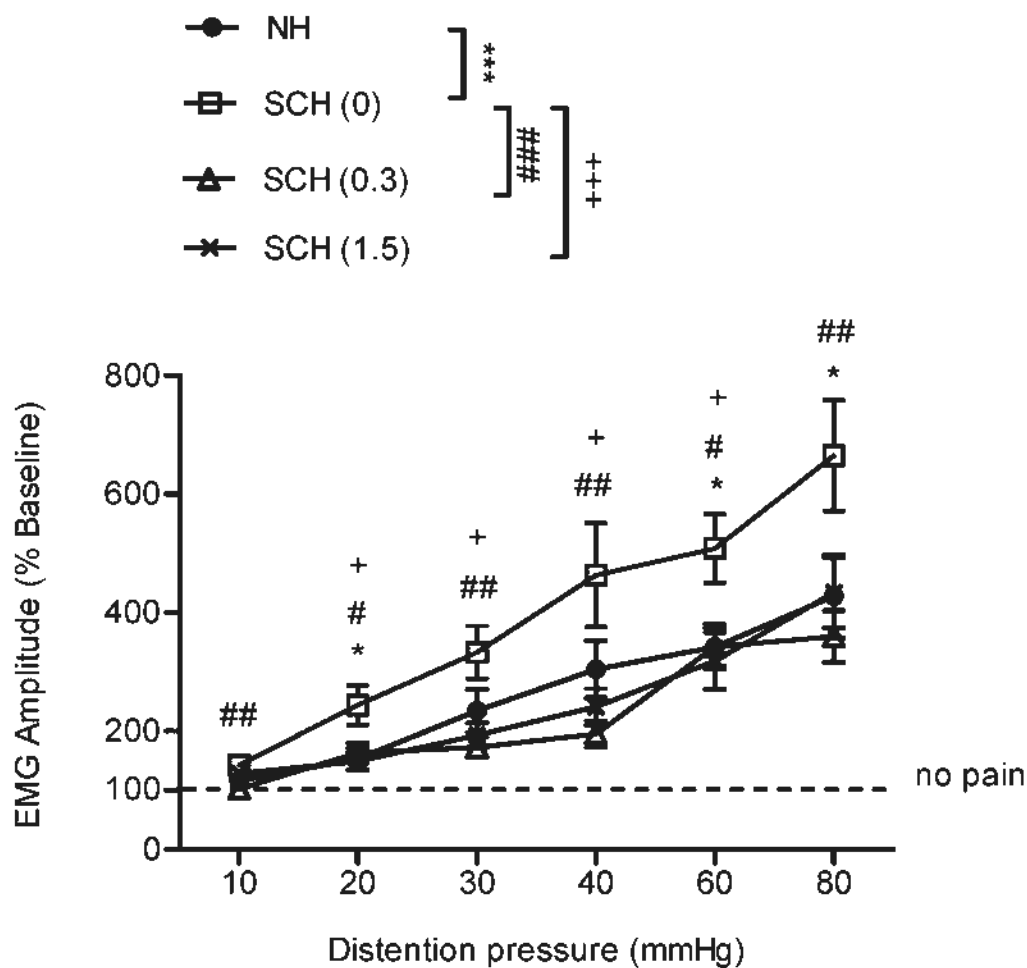


Fig. 6-6 Abdominal electromyographic (EMG) responses to the graded intensity of colorectal distension (CRD) at the distension pressures from 10 to 80 mmHg in normal rats (n = 13), NMS control rats (SCH, 0 g/kg; n = 12) and SCH-treated rats administered with *Schisandra chinensis* extract at the dosages of 0.3 g/kg (SCH, 0.3 g/kg; n = 15) and 1.5 g/kg/day (SCH, 1.5 g/kg; n = 10). NMS control rats showed exaggerated abdominal EMG responses to visceral pain compared with normal rats ($P<0.001$). *S. chinensis* extract at two dosages both significantly reversed the visceral hypersensation in NMS rats ($P<0.001$). Values are expressed as mean \pm S.E.M.. *, #, + $P<0.05$; ## $P<0.01$; ***, ###, +++ $P<0.001$ compared to NMS control by one-way or two-way ANOVA

Table 6-2 AUC (area under curve) of AWR and EMG responses to graded intensity of CRD in normal, NMS control and SCH-treated rats. Values are expressed as mean \pm S.E.M.

	Normal	SCH (0)	SCH (0.3)	SCH (1.5)
AWR	11.01 \pm 0.44	13.04 \pm 0.42	10.60 \pm 0.37	10.71 \pm 0.38
EMG	1273 \pm 146	1952 \pm 202	1074 \pm 90	1145 \pm 92

6.3.2 5-HT content in distal colon

5-HT content in distal colon was measured by immunoenzyme assays from normal, NMS control and SCH-treated rats after CRD. As shown in Fig 6-7, there was a significant increase in colonic 5-HT content in NMS control rats (1122.0 \pm 107.3 ng/g tissue) compared to normal rats (772.7 \pm 102.6 ng/g tissue, $P < 0.05$). The colonic 5-HT content in the rats treated with *S. chinensis* extract at the dosages of 0.3 g/kg (722.6 \pm 47.2 ng/g tissue, $P < 0.01$) and 1.5 g/kg (616.7 \pm 71.68 ng/g tissue, $P < 0.001$) dramatically decreased, even lower than that in normal rats.

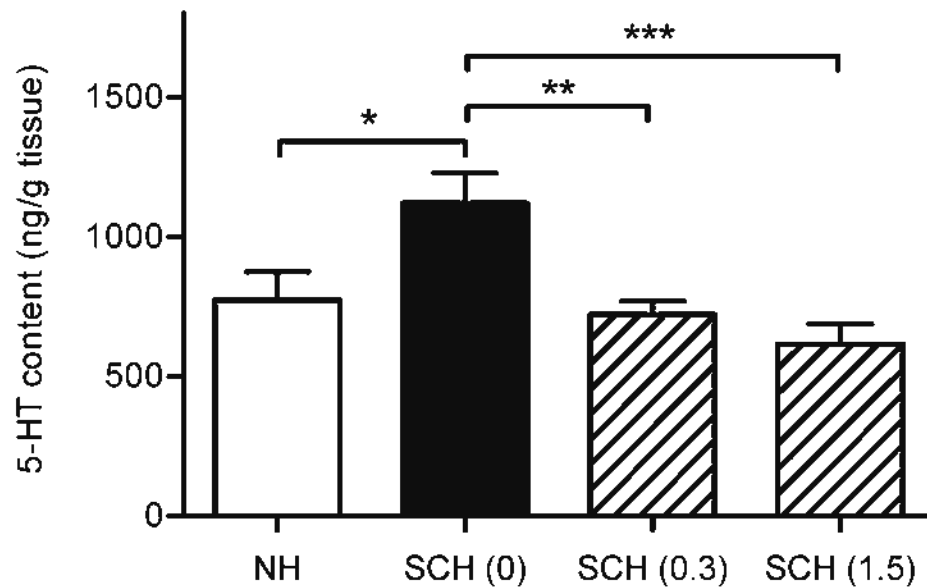


Fig. 6-7 5-HT content in distal colon of normal, NMS control and SCH-treated rats after CRD. 5-HT content in distal colon of NMS control rats significantly increased as compared to normal rats ($P < 0.05$). *Schisandra chinensis* extract at 0.3 g/kg ($P < 0.01$) and 1.5 g/kg ($P < 0.001$) abolished the increase of 5-HT content in distal colon of NMS rats. Values are expressed as mean \pm S.E.M. ($n = 6$). * $P < 0.05$, ** $P < 0.01$, *** $P < 0.001$ compared to NMS control by unpaired Student's *t* test or one-way ANOVA.

6.3.3 mRNA expression of 5-HT receptors and 5-HT transporter in distal colon

Amounts of mRNA encoding 5-HT_{3A} and 5-HT_{3B} subunits of 5-HT₃ receptor, 5-HT₄ receptor and 5-HT transporter (SERT) in distal colon were measured by real-time PCR (RT-PCR) from normal, NMS control and SCH-treated rats after CRD. As presented in Fig 6-8, there was no difference in 5-HT_{3A} and 5-HT_{3B} subunits between normal and NMS control rats ($P>0.05$). 5-HT_{3A} subunit significantly decreased in the NMS rats administered with *S. chinensis* extract at 0.3 g/kg as compared to NMS control rats ($P<0.05$), whereas difference at high dose of 1.5 g/kg approached but did not reach significance. There was also a trend toward decreasing 5-HT_{3B} subunit in the rats treated with *S. chinensis*, although both dosages did not show significant difference compared to NMS control rats. As shown in Fig 6-9, no difference was observed in mRNA expression of 5-HT₄ receptor between normal, NMS control and treated rats ($P>0.05$). No difference in SERT mRNA expression was observed between normal and NMS control rats ($P>0.05$), despite an increasing trend in the rats administered with *S. chinensis* extract at 0.3 g/kg (expression ratio, 1.28 ± 0.32 ; $P = 0.427$) and 1.5 g/kg (expression ratio, 1.97 ± 0.42 ; $P = 0.056$) as compared to NMS control rats (expression ratio, 0.97 ± 0.20). The difference approached, but did not reach significance ($P>0.05$).

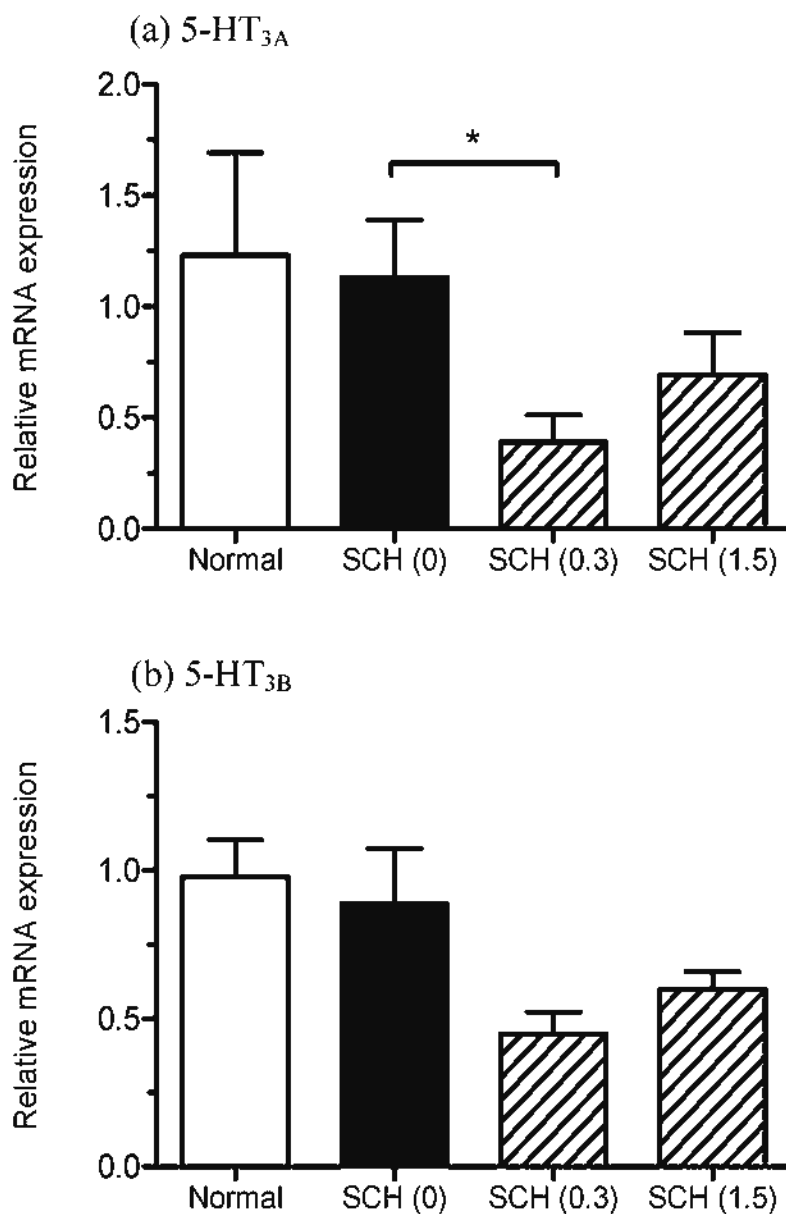


Fig. 6-8 Amount of mRNA encoding 5-HT_{3A} (a) and 5-HT_{3B} (b) subunits of 5-HT₃ receptor in distal colon of normal, NMS control and SCH-treated rats. There was no significant difference in 5-HT_{3A} and 5-HT_{3B} subunits between normal and NMS control rats ($P>0.05$). Treatment of *S. chinensis* tended to decrease 5-HT₃ receptor subunits. Values are expressed as mean \pm S.E.M. ($n = 6-7$). * $P<0.05$ compared to NMS control by unpaired Student's *t* test or one-way ANOVA.

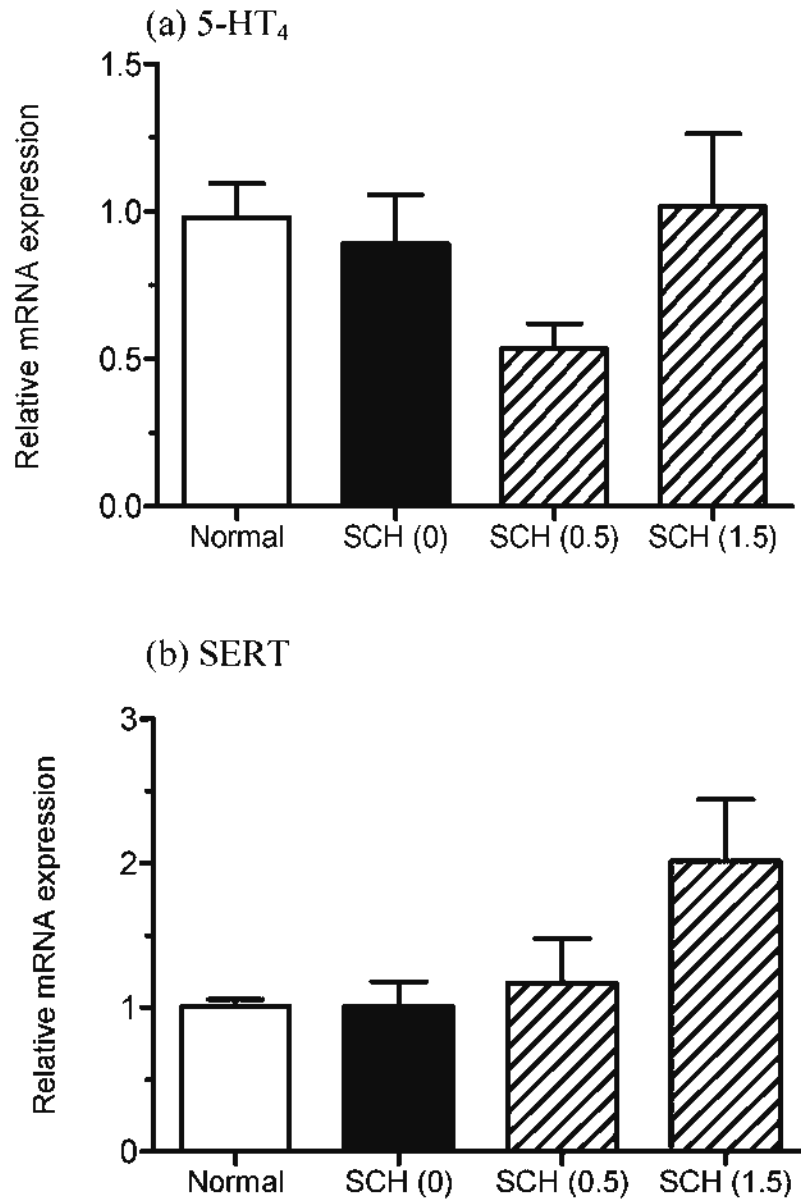


Fig. 6-9 Amount of mRNA encoding 5-HT₄ receptor (a) and 5-HT transporter (SERT; b) in distal colon. There was no difference in 5-HT₄ between normal, NMS control and SCH-treated rats ($P>0.05$). No difference in SERT was observed between normal and NMS control rats, whereas *S. chinensis* extract tended to increase SERT in distal colon but did not show significance ($P>0.05$). Values are expressed as mean \pm S.E.M. (n = 6-7).

6.3.4 mRNA expression of opioid receptors in distal colon

Amounts of mRNA encoding κ -opioid, μ -opioid and δ -opioid receptors in distal colon were also measured by real-time PCR (RT-PCR) from normal, NMS control and SCH-treated rats after CRD. As shown in Fig 6-10 and Fig 6-11, there was no difference in mRNA expression of μ -opioid receptor in distal colon between normal, NMS control and SCH-treated rats ($P>0.05$). κ -Opioid receptor tended to decrease in NMS rats compared to normal control and SCH-treated rats, and there was a significant difference between normal rats and NMS rats administered with *S. chinensis* extract at the dose of 0.3 g/kg/day ($P<0.05$) while it did not show significance in NMS control rats and the NMS rats treated with high dose of *S. chinensis* extract ($P>0.05$).

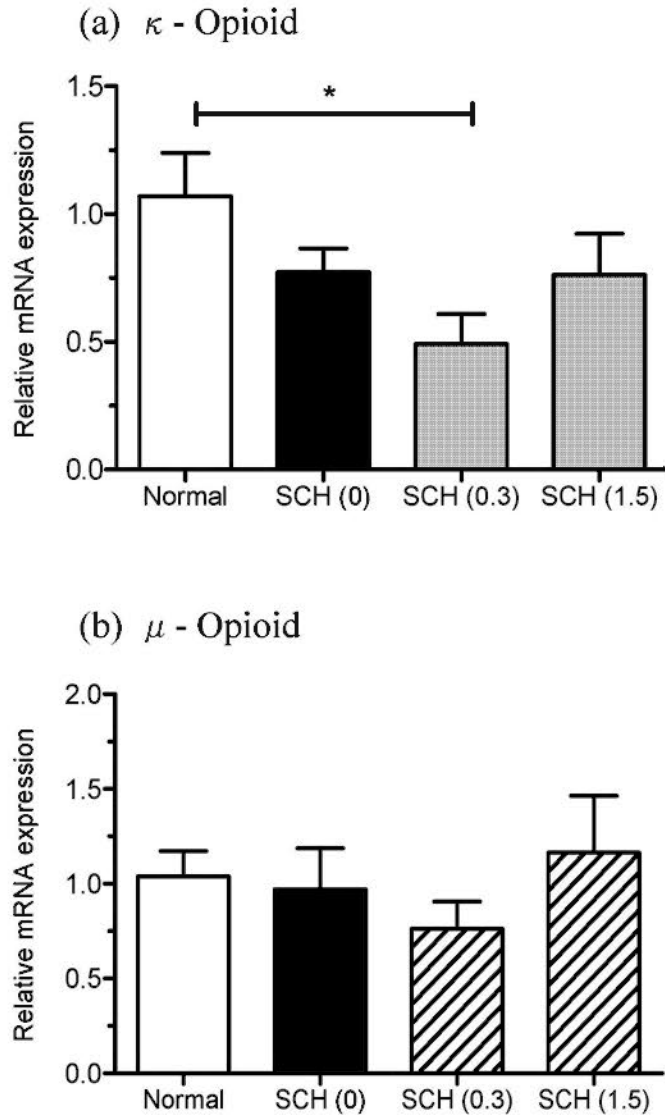


Fig. 6-10 Amount of mRNA encoding κ -opioid receptor (a) and μ -opioid receptor (b) in distal colon. There was no difference in μ -opioid receptor between normal, NMS control and SCH-treated rats ($P>0.05$). κ -Opioid receptor tended to decrease in NMS rats compared to normal rats, and there was a significant difference between normal rats and the rats administered with *S. chinensis* extract at the dose of 0.3 g/kg/day ($P<0.05$). Values are expressed as mean \pm S.E.M. (n = 6). * $P<0.05$ compared to normal or NMS control by unpaired Student's *t* test or one-way ANOVA.

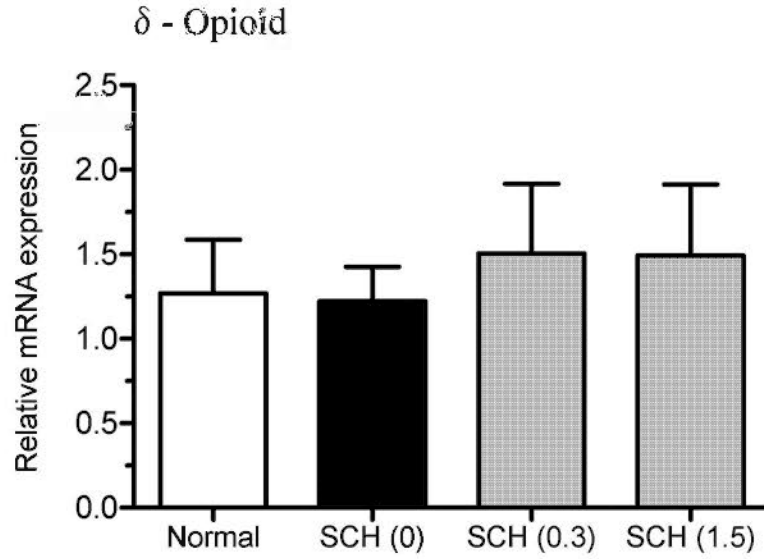


Fig. 6-11 Amount of mRNA encoding δ -opioid receptor in distal colon. There was no difference in δ -opioid receptor between normal, NMS control and SCH-treated rats ($P>0.05$). Values are expressed as mean \pm S.E.M. (n = 6).

6.4 Discussion

Schisandra chinensis is a well-known tonic and sedative agent in Chinese medicine. The lignan components isolated from *S. chinensis* have been recognized as the major active ingredients. A number of these dibenzocyclooctadiene derivatives have been demonstrated to exhibit various neuropharmacological activities, such as protection from glutamate-induced toxicity in cultured cortical cells (Kim et al., 2004), improvement of scopolamine-induced memory impairment (Kim et al., 2006; Egashira et al., 2008). This study represents the first attempt to evaluate the modulatory effect of *S. chinensis* on visceral hypersensitivity in an IBS rat model with neonatal maternal separation, and to further determine the neurophysiological factors involved in the action of *S. chinensis*. The ethanolic extract has been used in this study, since it contains the abundant fraction of Schisandra lignans as determined in Chapter 2 and reported in literature (Halstead et al., 2007).

In rats, neonatal maternal separation (NMS), in a form of early life stress, has been demonstrated to result in permanent alterations in central nervous system, such as unrestrained secretion of corticotrophin-releasing factor and increased expression of its receptors (Owens and Nemeroff, 1993), as well as gastrointestinal tract, for example the induced expression of hypercontractility-related protein (Lopes et al., 2008). Recent studies have shown that the NMS rats display visceral hypersensitivity in response to colorectal distension (CRD) (Coutinho et al., 2002; Ren et al., 2007), enhanced central

5-HT response (O'Mahony et al., 2008), and increased colonic motility in response to acute stressor (Coutinho et al., 2002), which mimic the symptoms of IBS.

In this study, the visceral pain was assessed by visceromotor response to CRD using abdominal withdrawal reflex (AWR) and electromyography (EMG) as complementary quantitative measurements. The induction of visceral hypersensitivity in rats by maternal separation in early life has been confirmed, as indicated by the marked reduction in pain threshold and the exaggerated visceral nociceptive response to graded intensity of CRD in NMS rats compared to normal rats. Treatment with *Schisandra chinensis* can reverse the visceral hypersensitivity in NMS rats. In the NMS rats treated with *S. chinensis* at low and high dosages, the pain threshold was significantly increased as compared with NMS control rats, and there was no difference between normal and SCH-treated rats. Further, as indicated by the AWR and EMG responses to the increasing intensity of CRD, the aggravated visceral nociception has been relieved by *S. chinensis*. Moreover, the graded visceromotor responses in *S. chinensis* treated rats appeared to be lower than those in normal rats, in particular at noxious CRD pressures. Comparison of the AUC values of AWR and EMG responses, which represents overall visceromotor response, has demonstrated that the rats treated with *S. chinensis* seemed to perceive less visceral pain to stimuli as compared with NMS control rats, and even normal rats, although the difference from the latter was not evident. Taken together, it seems that *Schisandra chinensis* can reverse the visceral hypersensitivity in NMS rats, and produce an analgesia effect in normal rats, which may agree with its well-known sedative property in Chinese medicine. Furthermore, treatment with low dose and high dose were both effective, and

the rats didn't show different visceral nociceptive responses in these two groups. In terms of the analgesia effect of *S. chinensis*, the dosages from 0.3 – 1.5 g/kg are likely within the effective dose range, and the lowest effective dose could be lower than 0.3 g/kg.

Serotonin (5-HT) is one of the key neurotransmitters in the gastrointestinal (GI) tract. It plays a critical role in regulating both the motility and sensory events in GI tract by the activation of a number of 5-HT receptors distributed widely on smooth muscle, enteric nerves and sensory afferents (De Ponti and Tonini, 2001). A number of recent studies have demonstrated altered 5-HT availability and signaling in IBS patients. It has been reported that the postprandial 5-HT levels in plasma increased in diarrhea-predominant IBS patients (Bearcroft et al., 1998; Houghton et al., 2003; Atkinson et al., 2006) and patients with post-infectious IBS (Dunlop et al., 2005). In this study, the 5-HT levels in distal colon after CRD significantly increased in NMS control rats compared to normal rats, which was in agreement with previous report (Ren et al., 2007). Treatment with *Schisandra chinensis* abolished this increment. Although there was no significant difference between normal rats and *S. chinensis* treated rats, the colonic 5-HT content tended to be lower in the treated rats as compared with normal rats. Considering the pattern of visceromotor responses to CRD in the four groups of rats, it is thus implied that the visceral pain perception in rats could be related to the changes in colonic 5-HT levels. In fact, it has been demonstrated that 5-HT plays a key role in visceral pain transmission. In brief, the released 5-HT from enterochromaffin cells activates primary afferent nerves in submucosal and myenteric plexus via 5-HT₃ and 5-HT₄ receptors, thereby conveying sensory responses to the central nervous system (Mazzia et al., 2003; Berthoud et al.,

2004). It is thus conceivable that increased colonic 5-HT could cause enhanced nociceptive responses to stimuli. Therefore, the effect of *S. chinensis* to reverse visceral hypersensitivity could be partially attributed to the downregulation of colonic 5-HT level in response to stimuli. In addition to the peripheral action, 5-HT is known to be an important modulator of pain perception in central nervous system (Kim and Camilleri, 2000). In NMS rats, increased expression of 5-HT in spinal cord (Ren et al., 2007) and enhanced central 5-HT response have been demonstrated (O'Mahony et al., 2008), suggesting serotonergic pathways could be involved in the early stress-induced visceral hyperalgesia. The central 5-HT levels have not been determined in this study, but it would need future investigations to examine the modulatory effects of *Schisandra chinensis* on the central serotonergic pathways.

The availability of 5-HT is determined by the synthesis, release and reuptake in a secretive event. The findings in this study have demonstrated that the elevated levels of colonic 5-HT in NMS rats was not associated with changes in mRNA expression of serotonin reuptake transporter (SERT), suggesting that the increased 5-HT could physiologically enhance the 5-HT-mediated effects, such as visceral sensation and gut motility. In contrast, there was a trend towards increasing SERT expression in *S. chinensis* treated rats. The elevated SERT expression could reduce the availability of 5-HT after release, thereby potentiating the inhibition of 5-HT-mediated visceral nociception. This finding could be related to the observation that the rats treated with *S. chinensis* seemed to show slightly lower visceromotor responses to CRD than normal rats.

5-HT₃ and 5-HT₄ receptors are the major receptors responsible for 5-HT-mediated sensory transmission in the gut. They have been found in peripheral nervous system such as myenteric and submucosal neurons (Glatzle et al., 2002; Poole et al., 2006), and central nervous system including spinal cord and brain (Morales et al., 1998). In the present study, mRNA expression of 5-HT_{3A}, 5-HT_{3B} subunits of 5-HT₃ receptor and 5-HT₄ receptor in colon were determined. There was no significant difference in either 5-HT₃ receptor subunits or 5-HT₄ receptor expression between NMS rats and normal rats. On the other hand, administration with *S. chinensis* tended to decrease the mRNA expression of both 5-HT_{3A} and 5-HT_{3B} subunits in NMS rats. 5-HT₃ receptor has been known to play a key role in sensory events in the gut. The released 5-HT in response to stimuli activates the extrinsic nerves in mucosa primarily by 5-HT₃ receptor, thereby conveying nociceptive signals to central nervous system (Mazzia et al., 2003; Berthoud et al., 2004). Reduction in 5-HT₃ receptor expression could result in the attenuation of nociceptive responses functionally triggered by the released 5-HT in response to CRD. Our findings therefore suggested that downregulation of 5-HT₃ receptor expression in the rat colon could be engaged in the capability of *Schisandra chinensis* to reverse visceral hypersensitivity in NMS rats.

Moreover, the attempts to explore the possible involvement of opioid receptors in the action of *S. chinensis* were also performed. Treatment of *S. chinensis* did not show significant effects on the mRNA expression of all types of opioid receptors, including κ -, μ - and δ -opioid receptor. Interestingly, there was a significant decrease in κ -opioid receptor expression between normal rats and the rats treated with low dose of *S. chinensis*.

However, this change could not be involved in the sedative effects of *S. chinensis*, since the κ -opioid receptor expression in the *S. chinensis* treated rats did not differentiate from the NMS control rats.

As determined in Chapter 3, a number of Schisandra lignans, such as schisandrin, gomisin A and deoxyschisandrin, have been identified as the absorbable components of *S. chinensis* in the rat. It has also been reported that schisandrin can cross blood-brain barrier and distributed in different regions of brain in rats (Niu et al., 1983). Thus, after oral administration of *S. chinensis* to the rats in this study, the lignan compounds are likely able to reach and react with the potential targets in the body, including central nervous system (CNS). Schisandra lignans have shown a variety of biological activities in CNS. Zhang and Niu (1991) reported that schisandrin affected the presence of monoamine neurotransmitters and their metabolites in different regions of brain in rats. A recent study has demonstrated that deoxyschisandrin decreases spontaneous and synchronous intracellular calcium oscillations in cultured hippocampal neural networks, and suggested deoxyschisandrin might play a role in maintaining neural networks in homeostasis in case of perturbations caused by pathological events (Fu et al., 2008). It is conceivable that these suggested activities of Schisandra lignans could contribute to the capability of *S. chinensis* to relieve the early stress-induced visceral hypersensitivity. The current findings of peripheral neurophysiological factors involved in the action of *S. chinensis* could be complementary to the studies on the central pathways in terms of sedative effects of *S. chinensis*. Nevertheless, it is certainly valuable to clarify the

centrally acting mechanisms of *S. chinensis* in the early-stress model, and further elucidate the connection between central and peripheral factors.

In conclusion, this study shows that *Schisandra chinensis* reversed the exaggerated visceral nociceptive responses to stimuli induced by early life stress in rats. Relief of visceral hypersensitivity by *S. chinensis* could be related to the normalization of elevated 5-HT level and the reduction in 5-HT₃ receptor expression in colon. *Schisandra chinensis* would be potentially useful for the treatment of relieving visceral pain symptoms in IBS patients.

Chapter 7 General Discussion

The present work is the first report on the modulatory effects of *Schisandra chinensis* fruits and the major lignan components on gut motility and visceral sensation in relation to irritable bowel syndrome (IBS), as well as the *in vitro* and *in vivo* absorption profile and pharmacokinetics of this herb. In the initial studies, quantitative analysis using a validated HPLC method has conformed that Schisandra lignans are the major chemical constituents in *S. chinensis* with four dominant components of schisandrin (SCH-1), gomisin A (SCH-2), deoxyschisandrin (SCH-3) and γ -schisandrin (SCH-4), and ethanolic extract contains higher abundance of lignan components than aqueous extract approximately in the proportion of 10:1.

Despite a number of reports on the pharmacokinetics of single pure compound isolated from *S. chinensis*, absorption and pharmacokinetic of the multiple active ingredients in herbal extract are less understood. With the aid of HPLC-DAD-MS for qualitative and quantitative analysis, the absorption of *Schisandra chinensis* in the rat everted gut sac and human Caco-2 monolayer *in vitro* models have been profiled. On the basis of experimental data, including retention time, UV and MSⁿ spectra, Schisandra lignans have been identified as the major absorbable components in these models, suggesting their high intestinal absorption potentials both in the rat and human. Besides, transport studies on a major absorbable lignan schisandrin (SCH-1) in Caco-2 cell monolayers have shown a passive diffusion pathway with high permeability, which provides quantitative evidence on the intestinal absorption of Schisandra lignans in addition to the

profiling analysis. Compared to the *in vitro* results, Schisandra lignans have been consistently identified in rat plasma after oral administration of *S. chinensis*. While no first-pass metabolism has been observed in the *in vitro* studies, remarkable first-phase metabolites deriving from absorbable components have been found in rat plasma. Interestingly, the ester lignans including angeloylgomisin H, tigloylgomisin H and gomisin G, which were markedly found in the *in vitro* absorption profile, dramatically decreased, or even disappeared in rat plasma, indicating the rapid clearance of these kinds of compounds *in vivo*. The results have thus suggested that *in vivo* studies are indispensable in studying the absorption of herbal medicines, although *in vitro* approaches are efficient in absorption potential evaluation and provide more information on the absorption mechanism. It should also be noted that even though these ester lignans have shown antioxidant and anti-cancer activities according to *in vitro* assays (Choi et al., 2008), they could be inactivated because of their properties susceptible to *in vivo* metabolism. The plasma pharmacokinetics of *S. chinensis* in rats has been further evaluated using simultaneous quantification of four representative Schisandra lignans (SCH-1, -2, -3 and -4), and various pharmacokinetic characteristics have been observed. The highly absorbed components including SCH-1 and SCH-2 exhibited rapid elimination and weak organ distribution, whereas the lipid-soluble components including SCH-3 and SCH-4 were less absorbed, but slowly eliminated and widely distributed in organs. The various pharmacokinetic characteristics of these lignans could enable their complementary contributions to the pharmacological effects of *S. chinensis*.

Further to the studies on chemical constituents and absorbable components of *S. chinensis*, the modulatory effects of both *S. chinensis* extracts and four major lignans on gut motility have been evaluated using *in vitro* intestinal motor assays. All the drugs tested displayed relaxation on guinea pig ileum contracted by acetylcholine, serotonin and electrical field stimulation, as well as on rat colon with spontaneous contractility. Ethanolic extract of *S. chinensis* has shown higher potency than aqueous extract, which could be explained by the higher content of lignan compounds in ethanolic extract as described above. SCH-3 is the most potent in inhibiting sensorimotor response in guinea pig ileum among the four lignans, whereas SCH-1 has been shown the highest potency of inhibition on spontaneous contraction of rat colon. Structure-activity analysis has revealed that 6-hydroxy substitution on the cycloocten-ring appeared to play a key role in (decreasing) the inhibitory effect on sensorimotor response in guinea-pig ileum, whereas methylenedioxy group on benzene ring were likely to more important in (decreasing) the relaxant effect on spontaneous contraction in rat colon. Preliminary studies have demonstrated that these Schisandra lignans did not specifically act on muscarinic 3 receptor or opioid receptors. Downstream pathways in smooth muscle cells, such as blocking ion channels or antagonizing receptors, might be involved in the inhibitory responses of these lignans compounds.

Mechanisms of the relaxant effect on rat colon induced by SCH-1 has been further investigated considering the dominant content of SCH-1 in *S. chinensis*, the high absorption potential and the correlation between *in vivo* and *in vitro* studies. It has been demonstrated that the action of SCH-1 involved two or more non-adrenergic

non-cholinergic (NANC) mediators, which are proposed to release from the activated enteric nerves. NO was likely one of the major inhibitory transmitters, and induced colonic relaxation via cGMP-dependent pathways. The non-nitroergic component was apamin-sensitive, and could induce muscle relaxation by opening the small conductance Ca^{2+} -activated K^+ channel. VIP and adenosine did not seem to participate in the action of SCH-1. Since NANC inhibitory neurotransmitters play important roles in regulating peristaltic reflex in colon, SCH-1-mediated colonic relaxation might modulate the enhanced colonic transit in gastrointestinal diseases with diarrhea symptoms in gastrointestinal disorders, such as diarrhea-predominant IBS.

In addition to modulation on gut motility, the effect of *S. chinensis* on visceral sensation has also been evaluated in an IBS rat model. In this model, early life stress in a form of neonatal maternal separation exaggerated visceral nociceptive response (AWR and EMG) to colorectal distension, whereas treatment with *S. chinensis* extract has reversed the enhanced visceral sensation, suggesting an anti-hypersensitivity effect produced by *S. chinensis*, which may agree with its well-known sedative property in Chinese medicine. Colonic 5-HT-dependent pathways could play a role in visceral hypersensation and the sedative action of *S. chinensis*. 5-HT content in distal colon has been elevated in the maternally separated rats while *S. chinensis* has abolished the increment. Moreover, treatment of *S. chinensis* decreased colonic 5-HT₃ receptor expression, and tended to increase 5-HT transporter expression, which might attenuate 5-HT-mediated nociceptive response to stimuli. Since SCH-1 can activate the release of enteric NANC transmitter, it is conceivable that the expression of receptors present in myenteric plexus, such as 5-HT₃

receptor, could be regulated by long-term exposure to the released transmitter, such as NO. Moreover, Schisandra lignans, which have been demonstrated as absorbable components in this study, have shown a variety of activities in central nervous system in literatures, such as affecting the presence of monoamine neurotransmitters in brain (Zhang and Niu, 1991), indicating the lignan components could contribute to the capability of *S. chinensis* to relieve the early stress-induced visceral hypersensitivity. It is valuable to further clarify the peripherally and centrally acting mechanisms of *S. chinensis* in the early-stress model.

In summary, *Schisandra chinensis* has shown relaxant effects on sensorimotor responses in guinea pig ileum as well as spontaneous contraction in rat colon, and this herb also exhibits reversal effects on visceral hypersensitivity in an early-stress rat model. Thus, *S. chinensis* would be potentially useful for the treatment of relieving diarrhea and visceral pain symptoms in IBS patients. Schisandra lignans, the major absorbable components, can be regarded as the active ingredients in *S. chinensis* for the potential treatment of IBS.

References

- Accarino A.M., Azpiroz F., & Malagelada J.R. (1995). Selective dysfunction of mechanosensitive intestinal afferents in irritable bowel syndrome. *Gastroenterology*, 108, 636–643.
- Al-Chaer E.D., Kawasaki M., & Pasricha P.J. (2000). A new model of chronic visceral hypersensitivity in adult rats induced by colon irritation during postnatal development. *Gastroenterology*, 119, 1276-1285.
- Arellano C., Philibert C., Vachoux C., Woodley J., & Houin G. (2005). Validation of a liquid chromatography–mass spectrometry method to assess the metabolism of bupropion in rat everted gut sacs. *Journal of Chromatography, B*, 829, 50-55.
- Artursson P., Palm K., & Luthman K. (2001). Caco-2 monolayers in experimental and theoretical predictions of drug transport. *Advanced Drug Delivery Reviews*, 46, 27-43.
- Artursson P., Ungell A.L., & Lofroth J.E. (1993). Selective paracellular permeability in two models of intestinal absorption: cultured layers of human intestinal epithelial cells and rat intestinal segments. *Pharmaceutical Research*, 10, 1123-1129.
- Atkinson W., Lockhart S., Whorwell P.J., Keevil B., & Houghton L.A. (2006). Altered 5-hydroxytryptamine signalling in patients with constipation and diarrhea-predominant irritable bowel syndrome. *Gastroenterology*, 130, 34–43.
- Avula B., Choi Y.W., Srinivas P.V., & Khan I.A. (2005). Quantitative determination of lignan constituents from *Schisandra chinensis* by liquid chromatography. *Chromatographia*, 61, 515-518.
- Azpiroz F. (2002). Hypersensitivity in functional gastrointestinal disorders. *Gut*. 51 (Suppl. 1), i22-i28.
- Baker E. H. and Sandle, G. I. (1996). Complications of laxative abuse. *Annual Review of Medicine*, 47, 127–134.
- Barbara G., De Giorgio R., Stanghellini V., Cremon C., & Corinaldesi R. (2002). A role for inflammation in irritable bowel syndrome? *Gut*, 51 (Suppl. 1), 41–44.
- Barbara G., Stanghellini V., De Giorgio R., Cremon C., Cottrell G.S., Santini D., Pasquinelli G., Morselli-Labate A.M., Grady E.F., Bunnett N.W., Collins S.M., & Corinaldesi R. (2004). Activated mast cells in proximity to colonic nerves correlate with abdominal pain in irritable bowel syndrome. *Gastroenterology*, 126, 693–702.
- Barthe L., Bessouet M., Woodley J.F., & Houin G. (1998). The improved everted gut sac: a simple method to study intestinal P-glycoprotein. *International Journal of Pharmaceutics*, 173, 255-258.

Barthe L., Woodley J., & Houin G. (1999). Gastrointestinal absorption of drugs: methods and studies. *Fundamental & Clinical Pharmacology*, 13, 154-168.

Barthe L., Woodley J.F., Kenworthy S., & Houin G. (1998). An improved everted gut sac as a simple and accurate technique to measure paracellular transport across the small intestine. *European Journal of Drug Metabolism and Pharmacokinetics*, 23, 313-323.

Bauer V. (1993). NANC transmission in intestines and its pharmacological modulation. *Acta Neurobiologiae Experimentalis*, 53, 65-77.

Bearcroft C.P., Perrett D., & Farthing M.J. (1998). Postprandial plasma 5-hydroxytryptamine in diarrhoea predominant irritable bowel syndrome: a pilot study. *Gut*, 42, 42-46.

Belai A. & Burnstock G. (1994). Evidence for coexistence of ATP and nitric oxide in non-adrenergic, non-cholinergic (NANC) inhibitory neurons in the rat ileum, colon and anococcygeus muscle. *Cell and Tissue Research*, 278, 197-200.

Benko R., Undi S., Wolf M., Vereczkei A., Illenyi L., Kassai M., Cseke L., Kelemen D., Horvath O.P., Antal A., Magyar K., & Bartho L. (2007). P2 purinoceptor antagonists inhibit the non-adrenergic, non-cholinergic relaxation of the human colon in vitro. *Neuroscience*, 147, 146-152

Bensoussan A., Talley N.J., Hing M., Menzies R., Guo A., & Ngu M. (1998). Treatment of irritable bowel syndrome with Chinese herbal medicine: a randomized controlled trial. *The Journal of the American Medical Association*, 280, 1585-1589.

Berthoud H.R., Blackshaw L.A., Brookes S.J., & Grundy D. (2004). Neuroanatomy of extrinsic afferents supplying the gastrointestinal tract. *Neurogastroenterology and Motility*, 16 (Suppl. 1), 28-33.

Bian Z.X., Zhang G.S., Wong K.L., Hu X.G., Liu L., Yang Z.J., & Li M. (2006). Inhibitory Effects of Magnolol on Distal Colon of Guinea Pig in Vitro. *Biological and Pharmaceutical Bulletin*. 29, 790-795.

Bley K.R., Bhattacharya A., Daniels D.V., Gever J., Jahangir A., O'Yang C., Smith S., Srinivasan D., Ford Anthony P.D.W., & Jett M.F. (2006). RO1138452 and RO3244794: characterization of structurally distinct, potent and selective prostacyclin receptor antagonists. *British Journal of Pharmacology*, 147, 335-345.

Boeckxstaens G.E., Pelckmans P.A., Ruytjens I.F., Bult H., De man J.G., Herman A.G., & Van Maercke Y.M. (1991). Bioassay of nitric oxide released upon stimulation of non-adrenergic non-cholinergic nerves in the canine ileocolonic junction. *British Journal of Pharmacology*, 103, 1085-1091.

Boisset M., Botham R.P., Haegele K.D., Lenfant B., & Pachot J.I. (2000). Absorption of

angiotensin II antagonists in Ussing chambers, Caco-2, perfused jejunum loop and in vivo: Importance of drug ionisation in the in vitro prediction of in vivo absorption. *European Journal of Pharmaceutical Sciences*, 10, 215-224.

Bouin M., Plourde V., Boivin M., Riberdy M., Lupien F., & Laganier M. (2002). Rectal distention testing in patients with irritable bowel syndrome: sensitivity, specificity, and predictive values of pain sensory thresholds. *Gastroenterology*, 122, 1771–1777.

Bradesi S., Lao L., McLean P.G., Winchester W.J., Lee K., Hicks G.A., & Mayer E.A. (2007). Dual role of 5-HT₃ receptors in a rat model of delayed stress-induced visceral hyperalgesia. *Pain*, 130, 56–65.

Bredt D.S., Hwang P.M., & Snyder S.H. (1990). Localization of nitric oxide synthase indicating a neural role for nitric oxide. *Nature*, 347, 768-770.

Bridges J.F., Millard P.C., & Woodley J.F. (1978). The uptake of liposome entrapped 125I-labelled polyvinylpyrrolidone by the rat jejunum in vitro. *Biochimica et Biophysica Acta*, 544, 448-451.

Bueno L. (2005). Gastrointestinal pharmacology: irritable bowel syndrome. *Current Opinion in Pharmacology*, 5, 583–588.

Bult H., Boeckxstaens G.E., Pelckmans P.A., Jordaens F.H., Van Maercke Y.M., & Herman A.G. (1990). Nitric oxide as an inhibitory non-adrenergic non-cholinergic neurotransmitter. *Nature*, 345, 346-347.

Burnstock G. (1986). The non-adrenergic, non-cholinergic nervous system. *Archives Internationales de Pharmacodynamie et de Therapie*, 280, 1-15.

Burnstock G. (2008). The journey to establish purinergic signalling in the gut. *Neurogastroenterology and Motility*, *European Journal of Pharmacology*, 20, 8-19.

Caldarella M.P., Serra J., Azpiroz F., & Malagelada J.R. (2002). Prokinetic effects in patients with intestinal gas retention. *Gastroenterology*, 122, 1748–1755.

Camilleri M. & Choi M. G. (1997). Review article: irritable bowel syndrome. *Alimentary Pharmacology & Therapeutics*, 11, 3-15.

Camilleri M. (2001). Novel medications for the irritable bowel syndrome: motility and sensation. *Journal of Pediatric Gastroenterology and Nutrition*, 32 (Suppl. 1), S35-37.

Camilleri M. (2001). Review article: tegaserod. *Alimentary Pharmacology & Therapeutics*, 15, 277-289.

Camilleri M. (2002). Serotonergic modulation of visceral sensation: lower gut. *Gut*. 51 (Suppl. 1), i81-i86.

Camilleri M., Atanasova E., Carlson P.J., Ahmad U., Kim H.J., Viramontes B.E., McKinzie S., & Urrutia R (2002). Serotonin transporter polymorphism pharmacogenetics in diarrheapredominant irritable bowel syndrome. *Gastroenterology*, 123, 425–432.

Camilleri M., Chey W.Y., & Mayer E.A. (2001). A randomized controlled clinical trial of the serotonin type 3 receptor antagonist alosetron in women with diarrhea-predominant irritable bowel syndrome. *Archives Internal Medicine*, 161, 1733-1740.

Camilleri M., Coulie B., & Tack J.F. (2001). Visceral hypersensitivity: facts, speculations, and challenges. *Gut*, 48, 125-131.

Camilleri M. & Ford M.J. (1998). Colonic sensorimotor physiology in health, and its alteration in constipation and diarrhoeal disorders. *Alimentary Pharmacology & Therapeutics*, 12, 287-302.

Capiello M., Guiliani L., & Pacifici G.M. (1991). Distribution of UDP-glucuronosyl transferase and its endogenous substrate uridine 5-diphosphoglucuronic acid in human tissues. *European Journal of Clinical Pharmacology*, 41, 345-350.

Chadwick V.S., Chen W., Shu D., Paulus B., Bethwaite P., Tie A., & Wilsion I. (2002). Activation of the mucosal immune system in irritable bowel syndrome. *Gastroenterology*, 122, 1778–1783.

Chan K. , Liu Z. Q., Jiang Z.H., Zhou H., Wong Y.F., Xu H.X., & Liu L (2006). The effects of sinomenine on intestinal absorption of paeoniflorin by the everted rat gut sac model. *Journal of Ethnopharmacology*, 103, 425-432.

Chen N., Chiu P.Y., & Ko K.M. (2008). Schisandrin B enhances cerebral mitochondrial antioxidant status and structural integrity, and protects against cerebral ischemia/reperfusion injury in rats. *Biological & Pharmaceutical Bulletin*, 31, 1387-1391.

Chen W., Li H., Luo W., Cai S., & Wen B. (2007). Rapid determination of Schisandrin B by liquid chromatography mass spectrometry and analysis of plasma pharmacokinetics in rat. *Zhongguo Xiandai Yixue Zazhi*, 17, 1665-1669.

Chey W.Y., Jin H.O., Lee M.H., Sun S.W., & Lee K.Y. (2001). Colonic motility abnormality in patients with irritable bowel syndrome exhibiting abdominal pain and diarrhea. *American Journal of Gastroenterology*, 96, 1499–1506.

Chiu P.Y., Leung H.Y., & Ko K.M. (2008). Schisandrin B enhances renal mitochondrial antioxidant status, functional and structural integrity, and protects against gentamicin-induced nephrotoxicity in rats. *Biological & Pharmaceutical Bulletin*, 31, 602-605.

Chung E.K., Zhang X., Li Z., Zhang H., Xu H., & Bian Z. (2007). Neonatal maternal separation enhances central sensitivity to noxious colorectal distention in rat. *Brain*

Research, 1153, 68–77.

Clemens C.H., Samsom M., Roelofs J.M., Van Berge Henegouwen G.P., & Smout A.J., (2003). Association between pain episodes and high amplitude propagated pressure waves in patients with irritable bowel syndrome. *American Journal of Gastroenterology*, 98, 1838–18.

Coates M.D., Mahoney C.R., Linden D.R., Sampson J.E., Chen J., & Blaszyk H. (2004). Molecular defects in mucosal serotonin content and decreased serotonin reuptake transporter in ulcerative colitis and irritable bowel syndrome. *Gastroenterology*, 126, 1657–16.

Collins, S.M. (1996). The immunomodulation of enteric neuromuscular function: Implications for motility and inflammatory disorders. *Gastroenterology*, 111, 1683-1699.

Collis M.G., Stoggall S.M., & Marthin F.M. (1989). Apparent affinity of 1,3-dipropyl-8-cyclopentylxanthine for adenosine A₁ and A₂ receptors in isolated tissues from guinea-pigs. *European Journal of Pharmacology*, 97, 1274-1278.

Corsetti M., Cesana B., Bhoori S., & Basilisco G. (2004). Rectal hyperreactivity to distention in patients with irritable bowel syndrome: role of distention rate. *Clinical Gastroenterology and Hepatology*, 2, 49–56.

Corsetti M., Ogliari C., Marino B., & Basilisco G. (2005). Perceptual sensitivity and response bias during rectal distension in patients with irritable bowel syndrome. *Neurogastroenterology and Motility*, 17, 541–547.

Coutinho S.V., Plotsky P.M., Sablad M., Miller J.C., Zhou H., Bayati A.I., McRoberts J.A., & Mayer E.A. (2002). Neonatal maternal separation alters stress-induced responses to viscerosomatic nociceptive stimuli in rat. *American Journal of Physiology – Gastrointestinal and Liver Physiology*, 282, G307–G316.

Crowell M.D. (2004). Role of serotonin in the pathophysiology of the irritable bowel syndrome. *British Journal of Pharmacology*, 141, 1285–1293.

Cui Y.Y. & Wang M.Z. (1992). Metabolic transformation of schizandrin. *Acta Pharmacologica Sinica*, 27, 57-63.

Cummins C.L., Mangravite L.M., & Benet L.Z. (2001). Characterizing the expression of CYP3A4 and efflux transporters (P-gp, MRP1, and MRP2) in CYP3A4-transfected Caco-2 cells after induction with sodium butyrate and the phorbol ester 12-O-tetradecanoylphorbol-13-acetate. *Pharmaceutical Research*, 18, 1102–1109.

Dainese R., Serra J., Azpiroz F., & Malagelada J.R. (2003). Influence of body posture on intestinal transit of gas. *Gut*, 52, 971–974.

- Dainese R., Serra J., Azpiroz F., & Malagelada J.R. (2004). Effects of physical activity on intestinal gas transit and evacuation in healthy subjects. *American Journal of Medicine*, 116, 536–539.
- D'Amato M., Curro D., Montuschi P., & Curro' D. (1992). Evidence for dual components in the non-adrenergic non-cholinergic relaxation in the rat gastric fundus: role of endogenous nitric oxide and vasoactive intestinal polypeptide. *Journal of the Autonomic Nervous System*, 37, 175-186.
- De Ponti F. & Malagelada J.R. (1998). Functional gut disorders: from motility to sensitivity disorders. A review of current and investigational drugs for their management. *Pharmacology & Therapeutics*, 80, 49-88.
- De Ponti F. & Tonini M. (2001). Irritable bowel syndrome: new agents targeting serotonin receptor subtypes. *Drugs*, 61, 317–332.
- Degen L., Matzinger D., Merz M., Appel-dingemans S., Osborne, S., Luchinger S., Bertold R., Maecke H., & Beglinger C. (2001). Tegaserod, a 5-HT₄ receptor partial agonist, accelerates gastric emptying and gastrointestinal transit in healthy male subjects. *Alimentary Pharmacology & Therapeutics*, 15, 1745–1751.
- Delgado-Aros S., Chial H.J., Camilleri M., Szarka L.A., Weber F.T., Jacob J., Ferber I., McKinzie S., Burton D.D., & Zinsmeister A.R. (2003). Effects of a kappa-opioid agonist, asimadoline, on satiation and GI motor and sensory functions in humans. *American Journal of Physiology – Gastrointestinal and Liver Physiology*, 284, G558-G566.
- Delie F. & Rubas W. (1997). A human colonic cell line sharing similarities with enterocytes as a model to examine oral absorption: advantages and limitations of the Caco-2 model. *Critical Reviews in Therapeutic Drug Carrier Systems*, 14, 221-286.
- Deng X., Chen X., Cheng W., Shen Z., & Bi K. (2008). Simultaneous LC–MS quantification of 15 lignans in *Schisandra chinensis* (Turcz.) Baill. *Fruit. Chromatography*, 67, 559-566.
- Dhaese I., Vanneste G., Sips P., Buys E., Brouckaert P., & Lefebvre R.A. (2008). Involvement of soluble guanylate cyclase $\alpha 1$ and $\alpha 2$, and SKCa channels in NANC relaxation of mouse distal colon. *European Journal of Pharmacology*, 589, 251-259.
- Dickhaus B., Mayer E.A., Firooz N., Stains J., Conde F., & Olivas T.I. (2003). Irritable bowel syndrome patients show enhanced modulation of visceral perception by auditory stress. *American Journal of Gastroenterology*, 98, 135–143.
- Distrutti E., Hauer S.K., Fiorucci S., Pensi M.O., & Morelli A. (2000). Intraduodenal lipids increase perception of rectal distension in IBS patients. *Gastroenterology*, 118 (Suppl. 2), 138.

- Drossman D.A., Li Z., Leserman J., Toomey T.C., & Hu Y.J. (1996). Health status by gastrointestinal diagnosis and abuse history. *Gastroenterology*, 110, 999–1007.
- Dunlop S.P., Coleman N.S., Blackshaw E., Perkins A.C., Singh G., Marsden C.A., & Spiller R.C. (2005). Abnormalities of 5-hydroxytryptamine metabolism in irritable bowel syndrome. *Clinical Gastroenterology and Hepatology*, 3, 349–357.
- Dunlop S.P., Jenkins D., Neal K.R., Naesdal J., Borgaonker M., Collins S.M., & Spiller R.C. (2003). Randomized, double-blind, placebo-controlled trial of prednisolone in post-infectious irritable bowel syndrome. *Alimentary Pharmacology & Therapeutics*, 18, 77-84.
- Dunlop S.P., Jenkins D., Neal K.R., & Spiller R.C. (2003). Relative importance of enterochromaffin cell hyperplasia, anxiety, and depression in postinfectious IBS. *Gastroenterology*, 125, 1651–1659.
- Dunphy R.C., Bridgewater L., Price D.D., Robinson M.E., Zeilman C.J., & Verne G.N. (2003). Visceral and cutaneous hypersensitivity in Persian Gulf war veterans with chronic gastrointestinal symptoms. *Pain*, 102, 79–85.
- Egashira N., Kurauchi K., Iwasaki K., Mishima K., Orito K., Oishi R., & Fujiwara M. (2008). Schizandrin reverses memory impairment in rats. *Phytotherapy Research*, 22, 49–52.
- El-Mahmoudy A., Khalifa M., Draid M., Shiina T., Shimizu Y., El-Sayed M., & Takewaki T. (2006). NANC inhibitory neuromuscular transmission in the hamster distal colon. *Pharmacological Research*, 54, 452-460.
- Eutamene H., Theodorou V., Fioramonti J., & Bueno L. (2003). Acute stress modulates the histamine content of mast cells in the gastrointestinal tract through interleukin-1 and corticotropin-releasing factor release in rats. *Journal of Physiology*, 553, 959–96.
- Faure C., Bouin M., & Poitras P. (2007). Visceral hypersensitivity in irritable bowel syndrome: does it really normalize over time? *Gastroenterology*, 132, 464-465.
- Faussone-Pellegrini M.S. (1992). Histogenesis, structure and relationships of interstitial cells of Cajal (ICC): from morphology to functional interpretation. *European Journal of Morphology*, 30, 137-148.
- Fioramonti J. & Buéno L. (1995). Toxicity of laxatives: how to discriminate between myth and fact. *European Journal of Gastroenterology & Hepatology*, 7, 5–7.
- Foxx-Orenstein A.E. & Grider J.R. (1996). Regulation of colonic propulsion by enteric excitatory and inhibitory neurotransmitters. *American Journal of Physiology*, 271, G433-G437.

Friebe A. & Koesling D. (2003). Regulation of nitric oxide-sensitive guanylyl cyclase. *Circulation Research*, 93, 96-105.

Fu M., Sun Z.H., Zong M., He X.P., Zuo H.C., & Xie Z.P. (2008). Deoxyschisandrin modulates synchronized Ca^{2+} oscillations and spontaneous synaptic transmission of cultured hippocampal neurons I. *Acta Pharmaceutica Sinica*, 29, 891–898.

Furness J.B., Young H.M., Pompolo, S., Bornstein, J.C., Kunze, W.A.A., & McConalogue, K. (1995). Plurichemical transmission and chemical coding of neurons in the digestive tract. *Gastroenterology*, 108, 554-563.

Gattuso J.M. & Kamm M.A. (1994). Adverse effects of drugs used in the management of constipation and diarrhoea. *Drug Safety*, 10, 47–65.

Gershon M.D. (2005). Nerves, reflexes, and the enteric nervous system: pathogenesis of the irritable bowel syndrome. *Journal of Clinical Gastroenterology*, 39, S184–S193.

Giorgio R.D., Barbara G., Furness J.B., & Tonini M. (2007). Novel therapeutic targets for enteric nervous system disorders. *Trends in Pharmacological Sciences*, 28, 453-481.

Glatzle J., Sternini C., Robin C., Zittel T.T., Wong H., Reeve Jr J.R., & Raybould H.E. (2002). Expression of 5-HT₃ receptors in the rat gastrointestinal tract. *Gastroenterology*, 123, 217-226.

Gonsalkorale W.M., Perrey C., Pravica V., Whorwell P.J., & Hutchinson I.V. (2003). Interleukin 10 genotypes in irritable bowel syndrome: evidence for an inflammatory component? *Gut*, 52, 91–93.

Grider J.R., Murthy K.S., Jin J.G., & Makhlof G.M. (1992). Stimulation of nitric oxide from muscle cells by VIP: prejunctional enhancement of VIP release. *American Journal of Physiology*, 262, 774-778.

Grundy D. (2002). Towards a reduction of rectal pain? *Neurogastroenterology and Motility*, 14, 217–219.

Guo L.Y., Hung T.M., Bae K.H., Shin E.M., Zhou H.Y., Hong Y.N., Kang S.S., Kim H.P., & Kim Y.S. (2008). Anti-inflammatory effects of schisandrin isolated from the fruit of *Schisandra chinensis* Baill. *European Journal of Pharmacology*, 591, 293-299.

Gwee KA, Collins SM, Read NW, Rajnakova A., Deng Y., Graham J.C., McKendrick M.W., & Moolhala S.M. (2003). Increased rectal mucosal expression of interleukin 1beta in recently acquired post-infectious irritable bowel syndrome. *Gut*, 52, 523–526.

Halstead C.W., Lee S., Khoo C.S., Hennell J.R., & Bensoussan A. (2007). Validation of a method for the simultaneous determination of four schisandra lignans in the raw herb and commercial dried aqueous extracts of *Schisandra chinensis* (Wu Wei Zi) by RP-LC with

DAD. *Journal of Pharmaceutical and Biomedical Analysis*, 45, 30-37.

Hammer J., Phillips S.F., Talley N.J., & Camilleri M. (1993). Effect of a 5-HT₃ antagonist (ondansetron) on rectal sensitivity and compliance in health and the irritable bowel syndrome. *Alimentary Pharmacology & Therapeutics*, 7, 543-551.

He X., Lian L., & Lin L. (1997). Analysis of lignan constituents from *Schisandra chinensis* by liquid chromatography-electrospray mass spectrometry. *Journal of Chromatography, A*, 757, 81-87.

Hirohashi T., Suzuki H., Chu X.Y., Tamai I., Tsuji A. & Sugiyama Y. (2000). Function and expression of multidrug resistance-associated protein family in human colon adenocarcinoma cells (Caco-2). *The Journal of Pharmacology and Experimental Therapeutics*, 292, 265–270.

Houghton L.A., Atkinson W., Whitaker R.P., Whorwell P.J., & Rimmer M.J. (2003). Increased platelet depleted plasma 5-hydroxytryptamine concentration following meal ingestion in symptomatic female subjects with diarrhoea predominant irritable bowel syndrome. *Gut*, 52, 663–670.

Houghton L.A., Foster J.M., & Whorwell P.J. (2000). Alosetron, a 5-HT₃ receptor antagonist, delays colonic transit in patients with irritable bowel syndrome and healthy volunteers. *Alimentary Pharmacology & Therapeutics*, 14, 775–782.

Houghton L.A. & Whorwell P.J. (2005). Towards a better understanding of abdominal bloating and distension in functional gastrointestinal disorders. *Neurogastroenterology and Motility*, 17, 500–511.

Huang M., Jin J., Sun H., & Liu G.T. (2008). Reversal of P-glycoprotein-mediated multidrug resistance of cancer cells by five schizandrins isolated from the Chinese herb *Fructus Schizandrae*. *Cancer Chemotherapy and Pharmacology*, 62, 1015–1026.

Huang T., Shen Y., & Shen P. (2005). Preparative separation and purification of schisandrin and schisantherin from *Schisandra chinensis* (Turcz.) Baill by high speed countercurrent chromatography. *Journal of Liquid Chromatography & Related Technologies*, 27, 2383-2390.

Huang X., Song F., Liu Z., & Liu S. (2007). Studies on lignan constituents from *Schisandra chinensis* (Turcz.) Baill. fruits using high-performance liquid chromatography/ electrospray ionization multiple-stage tandem mass spectrometry. *Journal of Mass Spectrometry*, 42, 1148-1161.

Huang X., Song F., Liu Z., & Liu S. (2008a). Lignans from different processed products of *Schisandra chinensis* fruits. *Yaoxue Xuebao*, 43, 630-633.

Huang X., Song F., Liu Z., & Liu S. (2008b). Structural characterization and

identification of dibenzocyclooctadiene lignans in Fructus Schisandrae using electrospray ionization ion trap multiple-stage tandem mass spectrometry and electrospray ionization Fourier transform ion cyclotron resonance multiple-stage tandem mass spectrometry. *Analytica Chimica Acta*, 615, 124-135.

Huizinga J.D., Berezin I., Daniel E.E., & Chow E. (1990). Inhibitory innervation of colonic smooth muscle cells and interstitial cells of Cajal. *Canadian Journal of Physiology and Pharmacology*, 68, 447-454.

Hung T.M., Na M., Min B.S., Ngoc T.M., Lee I., Zhang X., & Bae K. (2007). Acetylcholinesterase inhibitory effect of lignans isolated from *Schizandra chinensis*. *Archives of Pharmacal Research*, 30, 685-690.

Hungin A.P., Whorwell P.J., Tack J., & Mearin F. (2003). The prevalence, pattern and impact of irritable bowel syndrome: an international survey of 40,000 subjects. *Alimentary Pharmacology & Therapeutics*, 17, 643-650.

Hunter J., Jepson M.A., Tsuruo T., Simmons N.L. & Hirst B.H. (1993). Functional expression of P-glycoprotein in apical membranes of human intestinal caco-2 cells. kinetics of vinblastine secretion and interaction with modulators. *Journal of Biological Chemistry*, 268, 14991-14997.

Ikeya Y., Taguchi H., Yosioka I., & Kobayashi H. (1979). The constituents of *Schizandra chinensis* Baill. I. Isolation and structure determination of five new lignans, gomisin A, B, C, F and G, and the absolute structure of schizandrin. *Chemical & Pharmaceutic Bulletin*, 27, 1383-1394.

Ip S.P., Mak D.H., Li P.C., Poon M.K., & Ko K.M. (1996). Effect of a lignan-enriched extract of *Schizandra chinensis* on aflatoxin B1 and cadmium chloride-induced hepatotoxicity in rat. *Pharmacology and Toxicology*, 78, 413-416.

Ip, S.P., Poom, M.K.T., Wu, S.S., Che, C.T., Ng, K.H., Kong, Y.C., & Ko, K.M. (1995). Effect on schizandrin b on hepatic glutathione antioxidant system in mice: protection against carbon tetrachloride toxicity. *Planta Medica*, 61, 398-401.

Irwin C., Falsetti S.A., Lydiard R.B., Ballenger J.C., Brock C.D., & Brener W. (1996). Comorbidity of posttraumatic stress disorder and irritable bowel syndrome. *Journal of Clinical Psychiatry*, 57, 576-578.

Kalantar J.S., Locke 3rd G.R., Zinsmeister A.R., Beighley C.M., & Talley N.J. (2003). Familial aggregation of irritable bowel syndrome: a prospective study. *Gut*, 52, 1703-1707

Kanazawa M., Endo Y., Whitehead W.E., Kano M., Hongo M., & Fukudo S. (2004). Patients and nonconsulters with irritable bowel syndrome reporting a parental history of bowel problems have more impaired psychological distress. *Digestive Diseases and*

Sciences, 49, 1046–1053.

Kim D.H., Hung T.M., Bae K.H., Jung J.W., Lee S., Yoon B.H., Cheong J.H., Ko K.H., & Ryu J.H. (2006). Gomisin A improves scopolamine-induced memory impairment in mice. *European Journal of Pharmacology*, 542, 129–135.

Kim D.Y. & Camilleri M. (2000). Serotonin: a mediator of the brain-gut connection. *The American Journal of Gastroenterology*, 95, 2698-2709.

Kim J.H., Lee J.H., Jeong S.M., Lee B.H., Yoon I.S., Lee J.H., Choi S.H., & Nah S.Y. (2005). Effect of Ginseng Saponins on a Rat Visceral Hypersensitivity Model. *Biological & Pharmaceutical Bulletin*, 28, 2120-2124.

Kim S.R., Lee M.K., Koo K.A., Kim S.H., Sung S.H., Lee N.G., Markelonis G.J., Oh T.H., Yang J.H., & Kim Y.C. (2004). Dibenzocyclooctadiene lignans from *Schisandra chinensis* protect primary cultures of rat cortical cells from glutamate-induced toxicity. *Journal of Neuroscience Research*, 76, 397-405.

Kishi M., Takeuchi T., Suthamnatpong N., Ishii T., Nishio H., Hata F., & Takewaki T. (1996). VIP- and PACAP-mediated nonadrenergic, noncholinergic inhibition in longitudinal muscle of rat distal colon: involvement of activation of charybdotoxin- and apamin-sensitive K⁺ channels. *British Journal of Pharmacology*, 119, 623-630.

Ko K.M. & Yiu H.Y. (2001). Schisandrin B modulates the ischemia-reperfusion induced changes in non-enzymatic antioxidant levels in isolated-perfused rat hearts. *Molecular and Cellular Biochemistry*, 220, 141-147.

Konturek J. W., Thor P., Lukaszuk A., Gabryelewicz A., Konturek S. J., & Domschke W., (1997). Endogenous nitric oxide in the control of esophageal motility in humans. *Journal of Physiology and Pharmacology*, 48, 201-209.

Kozlowski C.M., Green A., Grundy D., Boissonade F.M., & Bountra C. (2000). The 5-HT₃ receptor antagonist alosetron inhibits the colorectal distention induced depressor response and spinal c-fos expression in the anaesthetised rat. *Gut*, 46, 474–480.

Kvasnickova L., Glatz Z., Sterbova H., Kahle V., Slanina J., & Musil, P. (2001). Application of capillary electrochromatography using macroporous polyacrylamide columns for the analysis of lignans from seeds of *Schisandra chinensis*. *Journal of Chromatography, A*, 916, 265-271.

La J.H., Kim T.W., Sung T.S., Kang J.W., Kim H.J., & Yang I.S. (2003). Visceral hypersensitivity and altered colonic motility after subsidence of inflammation in a rat model of colitis. *World Journal of Gastroenterology*, 9, 2791-2795.

La J.H., Kim T.W., Sung T.S., Kim H.J., Kim J.Y., & Yang I.S. (2004). Role of mucosal mast cells in visceral hypersensitivity in a rat model of irritable bowel syndrome. *Journal*

of Veterinary Science, 5, 319–324.

Lampen A., Bader A., Bestmann T., Winkler M., Witte L., & Borlak J.T. (1998). Catalytic activities, protein- and mRNA-expression of cytochrome P450 isoenzymes in intestinal cell lines. *Xenobiotica*, 28, 429–441.

Lee Y.J., Cho J.Y., Kim J.H., Park W.K., Kim D.K., & Rhyu M.R. (2004). Extracts from *Schizandra chinensis* fruit activate estrogen receptors: a possible clue to its effects on nitric oxide-mediated vasorelaxation. *Biological & Pharmaceutical Bulletin*, 27, 1066-1069.

Leung, P.H. H., Zhang L., Zuo Z., & Lin G. (2006). Intestinal absorption of *Stemona* alkaloids in a Caco-2 cell model. *Planta Medica*, 72, 211-216.

Levy R.L., Jones K.R., Whitehead W.E., Feld S.I., Talley N.J., & Corey L.A. (2001). Irritable bowel syndrome in twins: heredity and social learning both contribute to etiology. *Gastroenterology*, 121, 799–804.

Li L., Lu Q., & Hu X. (2006). Schisandrin B enhances doxorubicin-induced apoptosis of cancer cells but not normal cells. *Biochemical Pharmacology*, 71, 584-595.

Li L., Pan Q., Sun M., Lu Q., & Hu X. (2007). Dibenzocyclooctadiene lignans - A class of novel inhibitors of multidrug resistance-associated protein 1. *Life Sciences*, 80, 741-748.

Li M.J. & Xiao J. (2007). TLC identification of *Schizandra chinensis* and pilose deerhorn in Qianglinaoqingsu tablets. *Zhongguo Yaoye*, 16, 30-31.

Liang L.X., Zhang Q., Qian W., & Hou X.H. (2005). Antinociceptive property of tegaserod in a rat model of chronic visceral hypersensitivity. *Chinese Journal of Digestive Diseases* 2005, 6, 21–25.

Liu G.T. (1977) World health organization regional office for the western pacific, final report, pp. 101-112.

Liu G.T. (1989). Clinical uses and pharmacology of biphenyl dimethyl carboxylate (DDB). A new drug for chronic viral hepatitis B, Chinese Academy of Medical Science Press, Beijing.

Liu, G.T. (1992). Antioxidant activity of dibenzocyclooctene lignans isolated from Chinese herbs. *International Congress Series*, 998, 805-808.

Liu, K.T. & Lesca, P. (1982). Pharmacological properties of dibenzo[a,c]cyclooctene derivatives isolated from fructus *Schizandrae chinensis*. III. Inhibitory effects on carbon tetrachloride-induced lipid peroxidation, metabolism and covalent binding of carbon tetrachloride to lipids. *Chemico-Biological Interactions*, 41, 39-47.

- Lopes L.V., Marvin-Guy L.F., Fuerholz A., Affolter M., Ramadan Z., Kussmann M., Fay L.B., & Bergonzelli G.E. (2008). Maternal deprivation affects the neuromuscular protein profile of the rat colon in response to an acute stressor later in life. *Journal of Proteomics*, 71, 80-88.
- Lu H. & Liu G.T. (1992). Antioxidant activity of dibenzocyclooctene lignans isolated from Schisandraceae. *Planta Medica*, 58, 311-313.
- Lu Y. & Chen D.F. (2009). Analysis of *Schisandra chinensis* and *Schisandra sphenanthera*. *Journal of Chromatography, A*, 1216, 1980-1990.
- Madgula V.L., Avula B., Choi Y.W., Pullela S.V., Khan I.A., Walker L.A., & Khan S.I. (2008). Transport of *Schisandra chinensis* extract and its biologically-active constituents across Caco-2 cell monolayers - an in-vitro model of intestinal transport. *Journal of Pharmacy and Pharmacology*, 60, 363-370.
- Maggi C.A. & Giulani S. (1993). Multiple inhibitory mechanisms mediate non-adrenergic non-cholinergic relaxation in the circular muscle of the guinea-pig colon. *Naunyn-Schmiedebergs Archives of Pharmacology*, 347, 630-634.
- Mamoru S., Takashi S., Hideko S., Yukinobu I., Heihachiro T., Masaki A., & Eikichi H. (1987). Effects of gomisins J and analogous lignan compounds in schisandra fruits on isolated smooth muscles. *Yakugaku Zasshi*. 107, 720-726.
- Martinson E.A., Johnson R.A., & Wells J.N. (1987). Potent adenosine receptor antagonists that are selective for the A₁ receptor subtype. *Molecular Pharmacology*, 31, 247-252.
- Matsuyama H., Thapaliya S., & Takewaki T. (1999). Cyclic GMP-associated apamin-sensitive nitrenergic slow inhibitory junction potential in the hamster ileum. *British Journal of Pharmacology*, 128, 830-836.
- Mawe G.M., Coates M.D., & Moses P.L. (2006). Review article: intestinal serotonin signaling in irritable bowel syndrome. *Alimentary Pharmacology & Therapeutics*, 23, 1067-1076.
- Mayer E.A., Naliboff B.D., Chang L., & Coutinho S.V.V. (2001). Stress and irritable bowel syndrome. *American Journal of Physiology – Gastrointestinal and Liver Physiology*, 280, G519-G524.
- Mazzia C., Hicks G.A., & Clerc N. (2003). Neuronal location of 5-hydroxytryptamine₃ receptor-like immunoreactivity in the rat colon. *Neuroscience*, 116, 1033-1041.
- McLean P.G., Borman R.A., & Lee K. (2006). 5-HT in the enteric nervous system: gut function and neuropharmacology. *Trends in Neurosciences*, 30, 9-13.

- Mertz H., Naliboff B., Munakata J., Niazi N., & Mayer E.A. (1995). Altered rectal perception is a biological marker of patients with irritable bowel syndrome. *Gastroenterology*, 109, 40–52.
- Min H.Y., Park E.J., Hong J.Y., Kang Y.J., Kim S.J., Chung H.J., Woo E.R., Hung T.M., Youn U.J., Kim Y.S., Kang S.S., Bae K., & Lee S.K. (2008). Antiproliferative effects of dibenzocyclooctadiene lignans isolated from *Schisandra chinensis* in human cancer cells. *Bioorganic & Medicinal Chemistry Letters*, 18, 523-526.
- Miranda A., Peles S., McLean P.G., & Sengupta J.N. (2006). Effects of the 5-HT₃ receptor antagonist, alosetron, in a rat model of somatic and visceral hyperalgesia. *Pain*, 126, 54–63.
- Mizuta Y., Takahashi T., & Owyang C. (1999). Nitroergic regulation of colonic transit in rats. *American Journal of Physiology*, 277, G275-G279.
- Morales M., Battenberg E., & Bloom F.E. (1998). Distribution of neurons expressing immunoreactivity for the 5-HT₃ receptor subtype in the rat brain and spinal cord. *Journal of Comparative Neurology*, 402, 385-401.
- Morris-Yates A., Talley N.J., Boyce P.M., Nandurkar S., & Andrews G. (1998). Evidence of a genetic contribution to functional bowel disorder. *American Journal of Gastroenterology*, 93, 1311–1317.
- Mu F.Y., Jin M.H., & Liu R.J. (2005). Components and contents of *Schisandra chinensis* Baill fruit, rattan and fruit stem. *Yanbian Daxue Yixue Xuebao*, 28, 28-30.
- Mule F. & Serio R. (2003). NANC inhibitory neurotransmission in mouse isolated stomach: Involvement of nitric oxide, ATP and vasoactive intestinal polypeptide. *British Journal of Pharmacology*, 140, 31-437.
- Munzel, P.A., Schmohl, S., Heel, H., Kalberer, K., Bock-Hennig, B.S., & Bock, K.W. (1999). Induction of human UDP glucuronosyltransferases (UGT1A6, UGT1A9, and UGT2B7) by t-butylhydroquinone and 2,3,7,8-tetrachlorodibenzo-p-dioxin in Caco-2 cells. *Drug Metabolism and Disposition*, 27, 569–573.
- Murray C.D., Flynn J., Ratcliffe L., Jacyna M.R., Kamm M.A., & Emmanuel A.V. (2004). Effect of acute physical and psychological stress on gut autonomic innervation in irritable bowel syndrome. *Gastroenterology*, 127, 1695–1703.
- Murthy K.S., Grider J.R., Jin J.G., & Makhlof G.M. (1995). Interplay of VIP and nitric oxide in the regulation of neuromuscular activity in the gut. *Internationales de Pharmacodynamie et de Therapie*, 329, 27-38.
- Naliboff B.D., Munakata J., & Fullerton S. (1997). Evidence for two distinct perceptual alterations in irritable bowel syndrome. *Gut*, 41, 505–512.

National Committee of Chinese Pharmacopoeia (2005). Pharmacopoeia of the People's Republic of China. Chemical Industry Press, Beijing, pp, 44-45.

Nicholas M.B. & Trevor S. (1999). A review of central 5-HT receptors and their function. *Neuropharmacology*, 38, 1083–1152.

Niu X.Y., Bian Z.J., & Ren Z.H. (1983). The metabolic fate of schizandrol A and its distribution in brain in rats determined by TLC method. *Acta Pharmaceutica Sinica*, 18, 491-495.

North C.S., Downs D., Clouse R.E., Alrakawi A., Dokucu M.E., & Cox J. (2004). The presentation of irritable bowel syndrome in the context of somatisation disorder. *Clinical Gastroenterology and Hepatology*, 2, 787–795.

O'Mahony S., Chua A.S.B., Quigley E.M.M., Clarke G., Shanahan F., Keeling P.W.N., & Dinan T.G. (2008). Evidence of an enhanced central 5HT response in irritable bowel syndrome and in the rat maternal separation model. *Neurogastroenterology and Motility*, 20, 680–688.

O'Sullivan M., Clayton N., Breslin N.P., Harman I., Bountra C., McLaren A., & O'Morain C.A. (2000). Increased mast cells in the irritable bowel syndrome. *Neurogastroenterology and Motility*, 12, 449–457.

Okishio Y., Niioka S., Takeuchi T., Nishio H., Hata F., & Takatsuji K. (2000). Differences in mediator of non-adrenergic, non-cholinergic relaxation of the distal colon between Wistar-ST and Sprague-Dawley strains of rats. *European Journal of Pharmacology*, 388, 97–105.

Okuwaki M., Takada T., Iwayanagi Y., Koh S., Kariya Y., Fujii H., & Suzuki H. (2007). LXR alpha transactivates mouse organic solute transporter alpha and beta via IR-1 elements shared with FXR. *Pharmaceutical Research*, 24, 390–398.

O'Mahony S., Chua A.S., Quigley E.M., Clarke G., Shanahan F., Keeling P.W., & Dinan T.G. (2008). Evidence of an enhanced central 5-HT response in irritable bowel syndrome and in the rat maternal separation model. *Neurogastroenterology and Motility*, 20, 680–688.

Ono H., Matsuzaki Y., Wakui Y., Takeda S., Ikeya Y., Amagaya S., & Maruno M. (1995). Determination of schizandrin in human plasma by gas chromatography-mass spectrometry. *Journal of Chromatography, B*, 674, 293-297.

Opletal L., Sovová H., & Bártlová M. (2004). Dibenzo[a,c]cyclooctadiene lignans of the genus *Schisandra*: importance, isolation and determination. *Journal of Chromatography, B*, 812, 357-371.

Palmgrén J.J., Töyräs A., Mauriala T., Mönkkönen J., & Auriola S. (2005). Quantitative

determination of cholesterol, sitosterol, and sitostanol in cultured Caco-2 cells by liquid chromatography–atmospheric pressure chemical ionization mass spectrometry. *Journal of Chromatography, B*, 821, 144-152.

Pan H. & Gershon M.D. (2000). Activation of intrinsic afferent pathways in submucosal ganglia of the guinea pig small intestine. *Journal Neuroscience*, 20, 3295–3309.

Panossian A. & Wikman G. (2008). Pharmacology of *Schisandra chinensis* Bail.: An overview of Russian research and uses in medicine. *Journal of Ethnopharmacology*, 118, 183-212.

Park J.Y., Lee S.J., Yun M.R., Seo K.W., Bae S.S., Park J.W., Lee Y.J., Shin W.J., Choi Y.W. & Kim C.D. (2007). Gomisins A from *Schisandra chinensis* induces endothelium-dependent and direct relaxation in rat thoracic aorta. *Planta Medica*, 73, 1537-1542.

Park J.Y., Shin H.K., Lee Y.J., Choi Y.W., Bae S.S., & Kim C.D. (2009). The mechanism of vasorelaxation induced by *Schisandra chinensis* extract in rat thoracic aorta. *Journal of Ethnopharmacology*, 121, 69-73.

Parry S.D., Stansfield R., Jelley D., Gregory W., Phillips E., & Barton J.R. (2003). Is irritable bowel syndrome more common in patients presenting with bacterial gastroenteritis? A community-based, case-control study. *American Journal of Gastroenterology*, 98, 327-331.

Parsons M.E. & Garner A.G. (1995). Review article. Drug development in gastroenterology – the changing view of industry. *Alimentary Pharmacology & Therapeutics*, 9, 457-463.

Peters W.H. & Kremers P.G. (1989). Cytochromes P450 in the intestinal mucosa of man. *Biochemical Pharmacology*, 38, 1535-1538.

Peters W.H. & Roelofs H.M. (1989). Time-dependent activity and expression of glutathione S-transferases in the human colon adenocarcinoma cell line Caco-2. *Biochemical Journal*, 264, 613–616.

Pluja L., Fernandez E., & Jimenez M. (1999). Neural modulation of the cyclic electrical and mechanical activity in the rat colonic circular muscle: putative role of ATP and NO. *British Journal of Pharmacology*, 126, 883-892.

Plumb J.A., Burston D., Baker T.G., & Gardner M.L.G. (1987). A comparison of the structural integrity of several commonly used preparations of rat small intestine in vitro. *Clinical Science*, 73, 53–59.

Poole D.P., Xu B., Koh S.L., Hunne B., Coupar I.M., Irving H.R., Shinjo K., & Furness J.B. (2006). Identification of neurons that express 5-hydroxytryptamine₄ receptors in

intestine. *Cell and Tissue Research*, 325, 413-422.

Portincasa P., Moschetta A., Baldassarre G., Altomare D.F., & Palasciano G. (2003). Pan-enteric dysmotility, impaired quality of life and alexithymia in a large group of patients meeting ROME II criteria for irritable bowel syndrome. *World Journal of Gastroenterology*, 9, 2293–2299.

Posserud I., Agerforz P., Ekman R., Bjornsson E.S., Abrahamsson H., & Simren M., (2004). Altered visceral perceptual and neuroendocrine response in patients with irritable bowel syndrome during mental stress. *Gut*, 53, 1102–1108.

Prueksaritonont T., Gorham L.M., Hochman J.H., Tran L.O., & Vyas K.P. (1996). Comparative studies of drug metabolizing enzymes in dog, monkey and human small intestines and in Caco-2 cells. *Drug Metabolism and Disposition*, 24, 634-642.

Prueksaritonont T., Deluna P., Gorham L.M., Ma B., Cohn D., Pang J., Xu X., Leung K., & Lin J.H. (1998). In vitro and in vivo evaluation of intestinal barriers for the zwitterions L-767,679 and its carboxyl ester prodrug L-775,318. *Drug Metabolism and Disposition*, 26, 520-527.

Qiangrong P., Wang T., Lu Q., & Hu X. (2005). Schisandrin B – a novel inhibitor of P-glycoprotein. *Biochemical and Biophysical Research Communications*, 335, 406-411.

Ragnarsson G. & Bodemar G. (1999). Division of the irritable bowel syndrome into subgroups on the basis of daily recorded symptoms in two outpatients samples. *Scandinavian Journal of Gastroenterology*, 34, 993-1000.

Ren T.H., Wu J., Yew D., Ziea E., Lao L., Leung W.K., Berman B., Hu P.J., & Sung J.J. (2007). Effects of neonatal maternal separation on neurochemical and sensory response to colonic distension in a rat model of irritable bowel syndrome. *American Journal of Physiology – Gastrointestinal and Liver Physiology*, 292, G849–G856.

Rhyu M.R., Kim E.Y, Yoon B.K., Lee Y.J., & Chen S.N. (2006). Aqueous extract of *Schizandra chinensis* fruit causes endothelium-dependent and -independent relaxation of isolated rat thoracic aorta. *Phytomedicine*, 13, 651-657.

Ringel Y., Whitehead W.E., Toner B.B., Diamant N.E., Hu Y., & Jia H. (2004). Sexual and physical abuse are not associated with rectal hypersensitivity in patients with irritable bowel syndrome. *Gut*, 53, 838–842.

Rowland R.N. & Woodley J.F. (1981). The uptake of distearyphosphatidylcholine /cholesterol liposomes by rat intestinal sac in vitro. *Biochimica et Biophysica Acta*, 673, 217-223.

Rozsai B., Lazar Z., Benko R., & Bartho L. (2001). Inhibition of the NANC relaxation of the Guinea-pig proximal colon longitudinal muscle by the purinoceptor antagonist

PPADS, inhibition of nitric oxide synthase, but not by a PACAP/VIP antagonist. *Pharmacological Research*, 43, 83-87.

Saito Y.A., Petersen G.M., Locke 3rd G.R., & Talley N.J. (2005). The genetics of irritable bowel syndrome. *Clinical Gastroenterology and Hepatology*, 3, 1057–1065.

Salmon P., Skaife K., & Rhodes J. (2003). Abuse, dissociation, and somatisation in irritable bowel syndrome: towards an explanatory model. *Journal of Behavioral Medicine*, 26, 1–18.

Sarna S.K. (1996). Nitroergic regulation of gastric motility and emptying. *Current Opinion in Gastroenterology*, 12, 512-516.

Schikowski, A., Thewissen, M., Mathis, C., Ross, H.G., & Enck, P. (2002). Serotonin type-4 receptors modulate the sensitivity of intramural mechanoreceptive afferents of the cat rectum. *Neurogastroenterology and Motility*, 14, 221–227.

Schwarzinger C. & Kranawetter H. (2004). Analysis of the active compounds in different parts of the *Schisandra chinensis* plant by means of pyrolysis – GC/MS. *Monatshefte fuer Chemie*, 135, 1201-1208.

Serio R., Mule F., Postorino A., Vetri T., & Bonvissuto F. (1996). Apamin-sensitive and -insensitive components of inhibitory junction potentials in rat cecum: role of nitric oxide. *Journal of Autonomic Pharmacology*, 16, 183-189.

Serra J., Azpiroz F., & Malagelada J.R. (1998). Intestinal gas dynamics and tolerance in humans. *Gastroenterology*, 115, 542–550.

Serra J., Azpiroz F., & Malagelada J.R. (2001). Impaired transit and tolerance of intestinal gas in the irritable bowel syndrome. *Gut*, 48, 14–19.

Serra J., Salvioli B., Azpiroz F., & Malagelada J.R. (2002). Lipid-induced intestinal gas retention in irritable bowel syndrome. *Gastroenterology*, 123, 700–706.

Simrén M., Abrahamsson H., & Björnsson E.S. (2001a). An exaggerated sensory component of the gastrocolonic response in patients with irritable bowel syndrome. *Gut*, 48, 20–27.

Simrén M., Abrahamsson H., & Björnsson E.S. (2007a). Lipid-induced colonic hypersensitivity in the irritable bowel syndrome: the role of bowel habit, sex, and psychologic factors. *Clinical Gastroenterology and Hepatology*, 5, 201-208.

Simrén M., Agerforz P., Björnsson E.S., & Abrahamsson H. (2007b). Nutrientdependent enhancement of rectal sensitivity in irritable bowel syndrome (IBS). *Neurogastroenterology and Motility*, 19, 20-29.

Simrén M., Axelsson J., Gillberg R., Abrahamsson H., Svedlund J., & Björnsson E. (2002). Quality of life in inflammatory bowel disease in remission: The impact of IBS-like symptoms and associated psychological factors. *American Journal of Gastroenterology*, 97, 389–396.

Simrén M., Månsson A., Langkilde A.M., Svedlund J., Abrahamsson H., & Bengtsson U. (2001b). Food-related gastrointestinal symptoms in the irritable bowel syndrome. *Digestion*, 63, 108–115.

Simrén M., Simms L., D'Souza D., Abrahamsson H., & Björnsson E.S. (2003). Lipid-induced colonic hypersensitivity in irritable bowel syndrome: the role of 5HT₃-receptors. *Alimentary Pharmacology & Therapeutics*, 17, 279-287.

Smits G.J.M. & Lefebvre R.A. (1996). ATP and nitric oxide: inhibitory NANC neurotransmitters in the longitudinal muscle-myenteric plexus preparation of the rat ileum. *British Journal of Pharmacology*, 118, 695–703.

Sneddon P. & Graham A. (1992). Role of nitric oxide in the autonomic innervation of smooth muscle. *Journal of Autonomic Pharmacology*, 12, 445-456.

Spiegel B.M., Kanwal F., Naliboff B., & Mayer E. (2005). The impact of somatisation on the use of gastrointestinal health-care resources in patients with irritable bowel syndrome. *American Journal of Gastroenterology*, 100, 2262–2273.

State Administration of Traditional Chinese Medicine of China & Editorial Committee of Chinese Materia Medica (1999). *Chinese Materia Medica (Zhong Hua Ben Cao)*. Shanghai Scientific and Technical Publisher, China, pp 1558.

Sterbova H., Sevcikova P., Kvasnickova L., Glatz Z., & Slanina J. (2002). Determination of lignans in *Schisandra chinensis* using micellar electrokinetic capillary chromatography. *Electrophoresis*, 23, 253-258.

Sun D., Lennernas H., Welage S.L., Barnett J.L., Landowski C.P., Foster D., Fleisher D., Lee K.D., & Amidon G.L. (2002). Comparison of human duodenum and Caco-2 gene expression profiles for 12,000 gene sequences tags and correlation with permeability of 26 drugs. *Pharmaceutical Research*, 19, 1400–1416.

Sun H.D. & Pang K.S. (2008). Permeability, Transport, and Metabolism of Solutes in Caco-2 Cell Monolayers: A Theoretical Study. *Drug Metabolism and Disposition*, 36, 102-123.

Sun M., Xu X., Lu Q., Pan Q., & Hu X. (2007). Schisandrin B: A dual inhibitor of P-glycoprotein and multidrug resistance-associated protein 1. *Cancer Letters*, 246, 300–307.

Suthamnatpong N., Hata F., Kanada A., Takeuchi T., & Yagasaki O. (1993). Mediators of

nonadrenergic, noncholinergic inhibition in the proximal, middle and distal regions of rat colon. *British Journal of Pharmacology*, 108, 348-355.

Suthamnatpong N., Hosokawa M., Takeuchi T., Tata F., & Takewaki T. (1994). Nitric oxide-mediated inhibitory response of rat proximal colon: independence from changes in membrane potential. *British Journal of Pharmacology*, 112, 676-682.

Swain M.G., Agro A., Blennerhassett P., Stanisiz A., & Collins S.M. (1992). Increased levels of substance P in the myenteric plexus of *Trichinella*-infected rats. *Gastroenterology*, 102, 1913-1919.

Takahashi T. (2003). Pathophysiological significance of neuronal nitric oxide synthase in the gastrointestinal tract. *Journal of Gastroenterology*, 38, 421-430.

Takashi M., Sayaka S., & Masahiro H. (2005). Simultaneous HPLC assay of lenampicillin (ampicillin prodrug), ampicillin, and marker compound for high-throughput *in vitro* assessment of intestinal absorption and metabolism using Caco-2 cells *Journal of Liquid Chromatography & Related Technologies*, 28, 1531-1537.

Thompson W.G., Longstreth G.F., Drossman D.A., Heaton K.W., & Irvine E.J. (1999). Muller-Lissner S.A., Functional bowel disorders and functional abdominal pain. *Gut*, 45 (Suppl. 2), 43-47.

Tian Q.G., Failla M.L., Bohn T., & Schwartz S.J. (2006). High-performance liquid chromatography/atmospheric pressure chemical ionization tandem mass spectrometry determination of cholesterol uptake by Caco-2 cells. *Rapid Communications in Mass Spectrometry*, 20, 3056-3060.

Tornblom H., Lindberg G., Nyberg B., & Veress B. (2002). Full-thickness biopsy of the jejunum reveals inflammation and enteric neuropathy in irritable bowel syndrome. *Gastroenterology*, 123, 1972-1979.

Trimble K.C., Farouk R., Pryde A., Douglas S., & Heading R.C. (1995). Heightened visceral sensation in functional gastrointestinal disease is not site-specific. Evidence for a generalized disorder of gut sensitivity. *Digestive Diseases and Sciences*, 40, 1607-1613.

Vallance B.A. & Collins S.M. (1998). The effect of nematode infection upon intestinal smooth muscle function. *Parasite Immunology*, 20, 249-253.

Van Geldre L.A. & Lefebvre R. A. (2004). Interaction of NO and VIP in Gastrointestinal Smooth Muscle Relaxation. *Current Pharmaceutical Design*, 10, pp, 2483-2497.

Wang B.L., Hu J.P., Tan W., Sheng L., Chen H., & Li Y. (2008). Simultaneous quantification of four active schisandra lignans from a traditional Chinese medicine *Schisandra chinensis* (Wuweizi) in rat plasma using liquid chromatography/mass spectrometry. *Journal of Chromatography, B*, 865, 114-120.

- Wang Z., Hop C.E.C.A., Leung K.H., & Pang J.M. (2000). Determination of in vitro permeability of drug candidates through a Caco-2 cell monolayer by liquid chromatography/tandem mass spectrometry. *Journal of Mass Spectrometry*, 35, 71-76.
- Ward S.M., Dalziel H.H., Bradley M.E., Buxton I.L.O., Keef K., Westfall D.P., & Sanders K.M. (1992). Involvement of cyclic GMP in non-adrenergic, non-cholinergic inhibitory neurotransmission in dog proximal colon. *British Journal of Pharmacology*, 107, 1075-1082.
- Watkins P.B., Wrighton S.A., Schuetz E.G., Molowa D.T., & Guzelian P.S. (1997). Identification of glucocorticoid cytochrome P450 in the intestinal mucosa of rats and man. *Journal of Clinical Investigation*, 80, 1029-1036.
- Weinryb R.M., Osterberg E., Blomquist L., Hulcrantz R., Krakau I., & Asberg M. (2003). Psychological factors in irritable bowel syndrome: a population-based study of patients, non-patients and controls. *Scand Journal of Gastroenterology*, 38, 503-510.
- Welgan P., Meshkinpour H., & Beeler M. (1988). Effect of anger on colon motor and myoelectric activity in irritable bowel syndrome. *Gastroenterology*, 94, 1150-1156.
- Whitehead W.E., Holtkotter B., & Enck P. (1990). Tolerance for rectosigmoid distention in irritable bowel syndrome. *Gastroenterology*, 98, 1187-1192.
- Wilson T.H. & Wiseman G. (1954). The use of sacs of everted small intestine for the study of the transference of substances from the mucosal to the serosal surface. *The Journal of Physiology*, 123, 116-125.
- Xu J.R., Luo J.Y., Shang L., & Kong W.M. (2006). Effect of change in an inhibitory neurotransmitter of the myenteric plexus on the pathogenetic mechanism of irritable bowel syndrome subgroups in rat models. *Chinese Journal of Digestive Diseases*, 7, 89-96.
- Xu M., Wang G., Xie H., Huang Q., Wang W., & Jia Y. (2008). Pharmacokinetic comparisons of schizandrin after oral administration of schizandrin monomer, Fructus Schisandrae aqueous extract and Sheng-Mai-San to rats. *Journal of Ethnopharmacology*, 115, 483-488.
- Xu M., Wang G., Xie H., Wang R., Wang W., Li X., Li H., Zhu D., & Yue L. (2005). Determination of schizandrin in rat plasma by high-performance liquid chromatography-mass spectrometry and its application in rat pharmacokinetic studies. *Journal of Chromatography, B*, 828, 55-61.
- Yoo H.H., Lee M., Lee M.W., Lim S.Y., Shin J., & Kim D.H. (2007). Effects of Schisandra lignans on P-glycoprotein-mediated drug efflux in human intestinal Caco-2 cells. *Planta Medica*, 73, 444-450.

Yu C., Zhang D., & Yin D. (2007). Differentiation of Fructus Schisandrae chinensis and Fructus Schisandrae sphenantherae. *Zhongguo Yiyuan Yaoxue Zazhi*, 27, 681-682.

Yu L.H., Liu G.T., Sun Y.M., & Zhang H.Y. (2004). Antioxidant effect of schisanhenol on human low density lipoprotein and its quantum chemical calculation. *Acta Pharmacologica Sinica*, 25, 1038-1044.

Zagoradnyuk V., Santicioli P., Maggi C.A., & Giachetti A. (1996). The possible role of ATP and PACAP as mediators of apamin-sensitive NANC inhibitory junction potentials in circular muscle of guinea pig colon. *British Journal of Pharmacology*, 119, 779-786.

Zhang H., Zhang G.Q., Zhu Z.Y., Zhao L., Fei Y., Jing J., & Chai Y.F. (2009). Determination of six lignans in *Schisandra chinensis* (Turcz.) Baill. Fruits and related Chinese multiherb remedies by HPLC. *Food Chemistry*, 115, 735-739.

Zhang L.K. & Niu X.Y. (1991). Effects of schizandrol A on monoamine neurotransmitters in the central nervous system. *Acta Academiae Medicinae Sinicae*, 13, 13-16.

Zhang Y., Dan M., Wu J., Yang H., Huang H., Qi Y., Wei S., Okuyama T., & Nakajima K. (2008). Study on the chromatographic fingerprinting of *Schisandra chinensis* (Turcz.) Baill. by LC coupled with principal component analysis. *Chromatographia*, 68, 101-104.

Zhao H., Xu J.R., & Liu R.L. (1995). Determination of γ -schisandrin in traditional Chinese medicine Wuweizi (*Schisandra chinensis*) and its preparation Sanlingdan by TLC -densitometry. *Yaowu Fenxi Zazhi*, 15, 33-35.

Zhou S.F., Feng X., Kestell P., Paxton J.W., Baguley B.C., & Chan E. (2005). Transport of the investigational anti-cancer drug 5,6-dimethylxanthenone-4-acetic acid and its acyl glucuronide by human intestinal Caco-2 cells. *European Journal of Pharmaceutical Sciences*, 24, 513-524.

Zhu M., Chen X.S., & Wang K.X. (2007). Variation of the lignan content of *Schisandra chinensis* (Turcz.) Baill. and *Schisandra sphenanthera* Rehd. et Wils.. *Chromatographia*, 66, 125-128.

Zhu M., Lin K.F., Yeung R.Y., & Li R.C. (1999). Evaluation of the protective effects of *Schisandra chinensis* on Phase I drug metabolism using a CCl₄ intoxication model. *Journal of Ethnopharmacology*, 67, 61-68.

Zou N., Lv H., Li J., Yang N., Xue H., Zhu J., & Qian J. (2008). Changes in brain G proteins and colonic sympathetic neural signaling in chronic-acute combined stress rat model of irritable bowel syndrome (IBS). *Translational Research*, 152, 283-289.